Ovine Bone Marrow Mesenchymal Stem Cells: Isolation, Characterisation, and Developmental Potential for Application in Growth Plate Cartilage Regeneration

Rosa Clare McCarty

B.Sc. (Hons)

Discipline of Paediatrics
Faculty of Health Sciences
University of Adelaide
Adelaide, South Australia

Department of Orthopaedic Surgery
Women's & Children's Hospital
Adelaide, South Australia

Division of Haematology
Institute of Medical & Veterinary Science
Adelaide, South Australia

A thesis submitted for the degree of Doctor of Philosophy (Medicine)

December 2007

TABLE OF CONTENTS

CHAPTER 2
MATERIALS & METHODS

ABSTRACT

The growth plate is a cartilaginous structure located at the proximal and distal ends of immature long bones, which contributes to longitudinal growth through the process of endochondral ossification. Cartilage has a limited ability to regenerate and in children, injury to the growth plate can result in limb length discrepancies and angular deformity, due to formation of a bone bridge at the damaged site which disturbs structure and function of the growth plate. Current treatments of the abnormalities arising from growth plate arrest involve surgical correction once the deformities have manifested. To date, there is no biological based therapy for the repair of injured/damaged growth plate cartilage.

Mesenchymal stem cells (MSC) are self renewable multipotential progenitor cells with the capacity to differentiate toward the chondrogenic lineage. Since their discovery, significant interest has been generated in the potential application of these cells for cartilage regeneration. The therapeutic potential of MSCs for the repair of growth plate cartilage has not been thoroughly investigated and has been restricted to small animal models. In this study, the ability of autologous BM MSC to regenerate growth plate cartilage in a sheep model was examined. Due to the limited amount of information available regarding ovine MSC, sheep BM derived MSC were characterised both in vitro and in vivo prior to application in a model of growth plate injury repair.

Ovine MSC were isolated from BM aspirates and exhibited a fibroblast-like morphology. Supplementation with human PDGF, EGF, IGF-1, FGF-2, and particularly TGFα, induced significant proliferation in vitro negating the requirement of serum in the media. Evaluation of the multipotential capability of sheep MSC revealed these cells can be induced to differentiate toward cells of an osteogenic, adipogenic, or chondrogenic lineage.

The cell surface expression profile of ovine BM MSC, chondrocytes and cultured chondrocytes was analysed. Immunoselection of MSC directly from processed ovine BM aspirates with the panel of novel antibodies resulted in enrichment of CFU-F in all instances. Characterisation of the antigenic specificity of two of the novel antibodies (Hybridoma B and H) by immunoprecipitation revealed proteins with high homology to integrin beta 1 subunit (CD29) and the Heat Shock Protein-90β (HSP-90β) molecule respectively.

In vivo, transplantation of sheep MSC into immunocompromised mice resulted in the formation of ectopic bone and cartilage-like tissue, which was dependent on and exclusive to the delivery scaffold employed. Application of autologous BM MSC within a gelatin sponge to a lamb model of growth plate injury did not accelerate osteogenesis but inhibited bone bridge formation. Interposition of scaffold alone also hindered the establishment of bone.

In conclusion, the characterisation of sheep MSC is beneficial for translational studies using MSC for eventual therapeutic benefit. Ovine MSC can be isolated from bone marrow aspirates and exhibit morphological and multipotential characteristics similar to those observed in human MSC, in vitro and in vivo. Preliminary analysis of the application of autologous MSC to growth plate injury suggests that although further investigation is necessary, MSC may offer a viable therapeutic option for the biological regeneration of the growth plate.

DECLARATION

This work contains no material which has been accepted for the award of any other degree or diploma in any university or other tertiary institution and, to the best of my knowledge and belief, contains no material previously published or written by another person, except where due reference has been made in the text.

I give consent to this copy of my thesis, when deposited in the University Library, being made available for loan and photocopying.

Rosa McCarty

December 2007

ACKNOWLEDGEMENTS

Firstly, I wish to thank my exceptional supervisors Associate Professor Cory Xian and Associate Professor Bruce Foster at the Women's & Children's Hospital, and Associate Professor Stan Gronthos at the Institute of Medical & Veterinary Science. Thank you for the patience, guidance, motivation and wisdom you have provided throughout my PhD candidature. I greatly appreciate the insightful comments, advice and help provided by Associate Professor Andrew Zannettino.

I am extremely grateful to the Bone Growth Foundation for financial support provided by the John Fitzgerald/Bone Growth Foundation PhD Scholarship.

Thank you to all the past and present members of the Bone Growth Laboratory (WCH) and Matthew Roberts Laboratory (IMVS) for your friendship, help and advice over the years. In the scope of this thesis I would particularly like to acknowledge Mr Kris Mrozik for his collaboration in protein characterisation, and Ms Jo Cool for her extensive knowledge and assistance in sheep surgery and tissue processing.

I particularly wish to thank Dr Tim Kuchel, Ms Glenda Summersides and Ms Jodi Dier from IMVS Animal Services Division for their help and assistance in bone marrow collection and lamb selection, and Ms Lynn Scarman at the WCH Animal House for guidance, support and assistance during surgery.

I would like to acknowledge the Medical Staff Specialist Fund (IMVS), Division of Paediatrics, and the Bone Growth Foundation for financial support giving me the opportunity to visit laboratories within Europe and attend the ECTS/IBMS conference in Geneva, Switzerland.

Thank you to all my friends for their continual support, encouragement and laughs over the years. Thank you music for the joy it brings. Finally, I wish to thank my incredible parents, Clare and Douglas, for their unconditional patience, encouragement, financial, and emotional support. Most importantly, thankyou for believing in me – I dedicate this thesis to you both, with much love.

ABBREVIATIONS

αMEM	Alpha-modified Minium Essential Medium
A_{260}	Absorbance at 260 nm
ABC	Avidin-Biotin Conjugate
AP	Alkaline Phosphatase
ASC-2-P	L-ascorbic acid 2-phosphate
BM	Bone Marrow
BMP	Bone Morphogenic Protein
bp, kb	Base Pair, Kilobase Pair
BSA	Bovine Serum Albumin
cbfa-1	Core Binding Factor α-1
CD	Cluster Designation or Cluster of Differentiation
cDNA	Complimentary DNA
CFU-F	Colony Forming Unit-Fibroblast
cm, mm, μm, nm	Centimetre, Millimetre, Micrometre, Nanometre
CO_2	Carbon dioxide
Col	Collagen
D0, D1, D2…	Day0, Day1, Day2…
DAB	3'3'-diamino-benzidine tetrachloride
DEPC	Diethyl Pyrocarbonate
DEX	Dexamethasone Sodium Phosphate
dH_20	Deionised Water
DNA	Deoxyribonucleic Acid
DTT	Dithiothreitol
ECL	Enhanced Chemiluminescence
ECM	Extracellular Matrix
EDTA	Ethylenediamine tetra acetic acid
EGF	Epidermal Growth Factor
FACS	Fluorescence Activated Cell Sorting
FCS	Foetal Calf Serum
FGF	Fibroblast Growth Factor
GAG	Glycosaminoglycan
H & E	Haematoxylin & Eosin
H_2O_2	Hydrogen Peroxide

HA	Hydroxyapatite
HCl	Hydrogen Chloride
hr, min, sec	hour, minute, second
HRP	Horse-Radish Peroxidase
HSC	Hematopoietic Stem Cell
IGF	Insulin-like Growth Factor
Ihh	Indian hedgehog
IL	Interleukin
K-Wires	Kirschner Wires
kDa	Kilodalton
kg, g, mg, µg, ng	kilogram, gram, milligram, microgram, nanogram
l, ml, µl	Litre, Millilitre, Microlitre
lg	Immunoglobulin
lgG_1	Immunoglobulin gamma-1 isotype
lgG_{2a}	Immunoglobulin gamma-2a isotype
lgM	Immunoglobulin M
LPL	Lipoprotein Lipase
M, mM, µM, nM	Molar, millimolar, micromolar, nanomolar
MMP	Matrix Metalloproteinase
MNC	Mononuclear Cells
mRNA	Messenger Ribonucleic Acid
MSC	Mesenchymal Stromal Cell
NaCl	Sodium Chloride
NaOH	Sodium Hydroxide
NHBC	Normal Human Bone Cells
NP-40	Nonidet P40
O/N	Overnight
°C	Degrees Celsius
OCN	Osteocalcin
OD	Optical Density
ON	Osteonectin
OP	Osteopontin
OPG	Osteoprotegerin
PAGE	Poly Acrylamide Gel Electrophoresis
PBS	Phosphate Buffered Saline

PCR	Polymerase Chain Reaction
PDGF	Platelet Derived Growth Factor
pH	Hydrogen Ion Concentration
PO_{4i}	Inorganic Phosphate
PTH	Parathyroid Hormone
PTH-R	Parathyroid Hormone Receptor
PTHrP	Parathyroid Hormone Related Peptide
RANK	Receptor Activated Nuclear factor Kappa B
RANK-L	Receptor Activated Nuclear factor Kappa B-Ligand
RT	Reverse Transcription
RT-PCR	Reverse Transcription-Polymerase Chain Reaction
SCID	Severe Combined Immunodeficient
SDS	Sodium Dodecyl Sulphate
SEM	Standard Error of Mean
Sox	Sex reversal Y-related high-mobility group box protein
SSC	Side Light Scatter
TGF-β	Transforming Growth Factor-β
TNF	Tumour Necrosis Factor
Tris	Tris (hydroxymethyl) Amino Methane
U	Units
UV	Ultra Violet
V	Volts
v/v	Volume Per Volume
VCAM-1	Vascular Cell Adhesion Molecule-1
VEGF	Vascular Endothelial Growth Factor
w/v	Weight Per Volume

CHAPTER 1

GENERAL INTRODUCTION AND AIMS OF THIS STUDY

1.1. Project Summary

The growth plate is a unique cartilaginous tissue located at the proximal and distal ends of the long bones of children, and is responsible for longitudinal bone growth until closure at skeletal maturity. The growth plate is a complex and tightly regulated tissue that elongates bone through a sequential process of chondrocyte proliferation, maturation and hypertrophy known as endochondral ossification.

Due to the avascular and alymphatic nature of cartilage, once damaged, cartilage has poor repair capacity and rarely regenerates. Injury to growth plate cartilage results in an undesirable repair response mechanism at the site of injury, where ossification of the damaged tissue may occur leading to formation a bone bridge. Establishment of a bone bridge across the growth plate can have serious consequences in children, and may lead to limb length discrepancies and angular deformity. Current treatments of limb abnormalities include surgical correction of angulation or length discrepancy after manifestation of the deformity. To date, there is no biological based therapy to prevent bone bridge formation and regenerate the damaged growth plate cartilage.

The discovery of a population of self renewable multipotential progenitor cells (termed mesenchymal stem cells (MSC)) from bone marrow with the capacity to differentiate into cells of the chondrogenic lineage has stimulated considerable interest in the application of these cells for cartilage tissue engineering. Significant effort has been invested into cartilage regeneration using chondrocytes and growth factors. Coupled with the ease of harvest and rapid expansion in vitro, MSC offer an attractive alternative to traditional therapies of cartilage regeneration. Whilst the majority of research to date has focussed on articular cartilage repair, relatively little information exists on the repair of growth plate cartilage. In this study, the potential of autologous ovine MSC to promote regeneration of growth plate cartilage in a lamb model was investigated. However, as the characteristics of ovine MSC are poorly understood, these cells were initially examined for their properties and developmental potential in vitro and in vivo.

1.2. The Vertebrate Skeleton

The vertebrate skeleton is a complex and essential organ which serves as a scaffold to both support and protect the soft tissues and organs within the body and is comprised of two tissue types, bone and cartilage. Bone intrinsically provides the strength and mechanical support for the musculature and soft tissues, whereas growth plate cartilage is required for longitudinal growth of the long bones at the growth plate prior to skeletal maturity, and articular cartilage throughout life at the joint surfaces to lubricate for smooth movement and absorb compressive forces during locomotion for minimal trauma to the more rigid bony skeleton (Price et al., 1994; Recker, 1992).

1.3. Anatomy of the Developing Long Bone

The long bones of growing children can be divided into four separate and functionally distinct regions, the epiphysis, growth plate or physis, the metaphysis and the diaphysis (Figure 1.1). These four regions originate by the process of endochondral ossification during skeletal development, which continues at the growth plate until skeletal maturity (Kerr, 1999).

1.3.1. Epiphysis

The epiphysis is located at the distal ends of the long bones and is covered by a thin layer of articular cartilage. In combination with lubrication from synovial fluid, articular cartilage provides the joint with continuous sliding motion (Mankin et al., 1994). Articular cartilage additionally absorbs mechanical shock and distributes applied load evenly to the bone. The sides of the epiphysis are flanked by the perichondrium. Muscle fibres, tendons and ligaments attach to the perichondrium, which additionally contributes to enlargement of the epiphysis. The perichondrium blends undetectably with the periosteum, contributing to biomechanical strength of the epiphyseal-metaphyseal junction at the groove of Ranvier. The epiphysis also includes the secondary ossification centre, which functions to determine the shape and form of the joint surface, and to impart mechanical rigidity (Iannotti et al., 1994).

Figure 1.1: The major anatomical regions of a long bone. From the articular surface the long bone consists of an epiphysis, physis (growth plate), metaphysis and diaphysis. The cartilage growth plate is located between the epiphysis and metaphysis. Bone marrow is localised within a cavity of cortical bone in the metaphysis. Photo kindly provided by A/Prof. C.J. Xian.

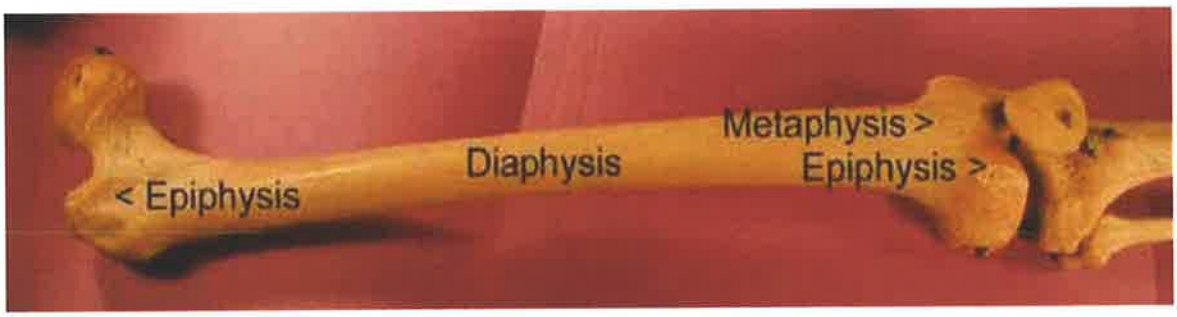
< Epiphysis
Diaphysis
Metaphysis >
Epiphysis >

1.3.2. Growth Plate

The growth plate or physis is a complex cartilage structure adjacent to the epiphysis and is fundamental for longitudinal growth of the long bones. Chondrocytes of the growth plate are tightly regulated to sequentially proliferate, mature and synthesise a cartilage extracellular matrix which is eventually calcified (Brighton, 1978; Brighton, 1987a; Brighton, 1987b; Buckwalter et al., 1985). This calcified matrix acts as an intermediary scaffold, and is subsequently remodelled and resorbed to allow deposition of bone, by the process of endochondral ossification.

Encircling the growth plate is the perichondrial ring of LaCroix and the groove of Ranvier. The perichondrial ring limits lateral growth of the physis and contributes to mechanical strength at the bone-cartilage junction, thereby resisting compressive forces experienced across the growth plate (Iannotti et al., 1994). The groove of Ranvier merges with the growth plate resting zone and aids in latitudinal physeal growth.

1.3.3. Metaphysis

At the primary spongiosa of the metaphysis immediately below the growth plate, the calcified cartilage matrix is remodelled by osteoclasts to form calcified cartilage trabeculae, onto which osteoblasts deposit a bony matrix (Kaplan et al., 1994; Kerr, 1999). Synchronously, osteoclasts resorb the calcified matrix while osteoblasts synthesise new bone extracellular matrix. Further remodelling of the primary spongiosa (where the trabeculae are more prevalent and thinner) produces the more mature secondary spongiosa (where the trabeculae are fewer in number and larger in size), characterised by an increase of bone content. Compared with other regions of the long bone, the metaphysis has a significantly elevated level of osteoclast and osteoblast activity (Iannotti et al., 1994).

1.3.4. Diaphysis

The diaphysis comprises the majority of the long bone, which is comprised of dense cortical bone surrounding the cavity within which bone marrow forms. During skeletal development, cells of the diaphysis differentiate into osteoblasts, to form a collar of bone surrounding the diaphysis, known as the periosteum. Vascularisation of the internal calcified cartilage rudiment allows infiltration of mesenchymal progenitor cells, osteoclasts

and the marrow forming elements. The bone marrow primarily serves as an active site of haematopoiesis.

1.4. Mechanisms of Bone Formation

The process by which mineralised bone is formed through the establishment of a cartilage scaffold is known as endochondral ossification. Most of the skeleton during embryonic development occurs through this process with progenitor cells originating from the mesoderm. However, some craniofacial bones develop through an alternate mechanism of bone formation termed intramembranous ossification. In this instance, mesenchymal progenitors of neural crest origin differentiate directly into osteoblasts, without the requirement of a cartilage template. Endochondral ossification is not restricted to embryogenesis; this mechanism is used at the growth plate for elongation of the long bones during skeletal development post utero, until growth plate closure at skeletal maturity. Intramembranous ossification is also important for the periosteal cortical bone formation during longitudinal bone growth of long bones, in which the cortical bone is formed directly from osteoblasts differentiated from osteoprogenitor cells located in the inner layer of the periosteum.

1.5. Bone

In addition to providing mechanical support and protection for the soft tissues, bone also serves as a lever for muscle action, and is responsible for maintaining blood calcium levels and supporting haematopoiesis within the bone marrow. The tensile strength of bone is due to its composition of calcified connective tissue matrix (hydroxyapatite). In addition to the mineralised phase, bone also consists of cells, water and an organic matrix including collagenous and non-collagenous proteins (Recker, 1992).

Bone is an extremely well organised tissue that can be loosely grouped into two categories based upon structural and functional differences: cortical and trabecular bone. Cortical bone is denser and mechanically stronger than trabecular bone, but has a slower remodelling rate as it possesses less surface area (Buckwalter et al., 1996; Price et al., 1994).

Trabecular bone is found primarily in the metaphysis and diaphysis of the long bones and within the cuboid bones of the vertebrae. The spicules of trabecular bone form a three-dimensional lattice aligned along areas of biomechanical loading within the hollow cavities of the cortical bone. Trabecular bone is therefore porous and spongy. Cortical bone acts as a dense envelope surrounding most of the bones of the body including the diaphysis of the long bones. This type of bone provides the strength against bending, torsional and compressive forces encountered during movement. Cortical bone is made up of layers of mature organised lamellar bone and non-uniform woven bone. Vascularisation of cortical bone is predominantly found in the woven component.

1.6. Cells of Bone

Based on the location within the bone, there are generally three major types of bone cells: osteoblasts, osteocytes and osteoclasts. Osteoblasts and osteocytes are responsible for the synthesis of bone, and are located at the surface or within the mineralised matrix of bone respectively. Both osteoblasts and osteocytes originate from the mesenchymal osteoprogenitor cells, whereas osteoclasts are haematopoietic in origin.

1.6.1. Osteoblasts

Osteoblasts are the cells directly responsible for deposition and organisation of the extracellular matrix, and mineralisation of bone tissue. Lining the surface of bone, osteoblasts synthesise and secrete the organic extracellular matrix of new bone (Buckwalter et al., 1996). At the junction between the osteoblast cell membrane and mineralised bone matrix, there is a seam of newly formed unmineralised bone matrix (osteoid). Histochemically osteoblasts are characterised by cell surface expression of alkaline phosphatase. Osteoblasts synthesise a multitude of bone extracellular matrix components such as collagen-1, osteocalcin, bone sialoprotein, osteonectin and osteopontin (Xian and Foster, 2006a). Each of these molecules plays a significant role in the mineralisation of bone. At the conclusion of bone formation, osteoblasts either decrease synthetic activity, flatten and elongate to become bone lining cells, or become surrounded by mineralised matrix and become osteocytes, or migrate to other sites (Kaplan et al., 1994).

1.6.2. Osteocytes

When an osteoblast becomes enveloped by bone matrix, which is subsequently mineralised, this cell is now termed an osteocyte. Osteocytes are considered to be terminally differentiated osteoblasts and are the most predominant type of bone cells. Unlike osteoblasts, osteocytes have extensive cellular processes, which project and establish contact with adjacent osteocytes, blood vessels and bone lining cells, through canals (canaliculi) in the bone matrix. This osteocyte process network enables the osteocytes to monitor their environment for mechanical stress and maintain the bone matrix in which they reside (Buckwalter et al., 1996; Reinholt et al., 1990). Interstitial fluid flows through the osteocyte canaliculi network from regions of high strain to low strain thus modulating the production of signalling factors to regulate bone formation and resorption. Osteocytes have been reported to positively express bone matrix proteins collagen-1, osteopontin and osteonectin, but not alkaline phosphatase, bone sialoprotein, and osteocalcin (Aubin and Turksen, 1996; van der Plas et al., 1994).

1.6.3. Bone Lining Cells

Bone lining cells are commonly referred to as resting osteoblasts or surface osteocytes. These cells are flattened and elongated and are found lying directly against the majority of inert bone surfaces, neither undergoing bone deposition nor resorption. Bone lining cells have long cytoplasmic extensions that penetrate the bone matrix to connect with the cellular processes of osteocytes. These cells are sensitive to parathyroid hormone (PTH) and exposure to PTH stimulates the bone lining cells to secrete collagenases in order to remove the thin layer of osteoid sheathing the mineralised matrix (McSheehy and Chambers, 1986a; McSheehy and Chambers, 1986b). This initial degradation of the osteoid is the first sequence of events to allow osteoclasts to bind to the bone surface and begin resorption (Buckwalter et al., 1996). Therefore, bone lining cells play a significant role in attracting and stimulating osteoclasts for the remodelling process.

1.6.4. Osteoclasts

Osteoclasts are large mobile multinucleated cells derived from haematopoietic progenitor cells of monocyte/macrophage origin (Suda et al., 1997; Vaananen, 1996). These cells have irregular cytoplasmic branches and are the main cell type responsible for the

resorption of bone during remodelling. Osteoclasts are characterised by production of tartrate-resistant acid phosphatase (TRAP). Initially, differentiated osteoclasts attach to the target site via protein integrins and develop a ruffled border through extensive infolding of the cell membrane adjacent to the resorptive surface. The ruffled border is completely surrounded by the clear zone – a region where the osteoclast is smooth and lies directly against the underlying bone (Blair and Zaidi, 2006; Vaananen, 1996; Zaidi et al., 2003). Following attachment to the bone surface, osteoclasts release lysosomal enzymes and acids into the spaces within the ruffled border, which lowers the local environment pH to aid the solubility of the hydroxyapatite and digest the organic collagen component, culminating in the breakdown and removal of the calcified extracellular matrix.

1.6.5. Bone Marrow

The bone marrow organ is a soft connective tissue located within the hollow cavity of bone, and is an active site of haematopoiesis. The development of haematopoietic cells in vivo is dependent on the close association between haematopoietic stem cells (HSC), mesenchymal stem cells (MSC), and the bone marrow microenvironment (Allen et al., 1990; Dexter et al., 1984; Lichtman, 1981; Tavassoli and Friedenstein, 1983; Weiss, 1976). Regulation of haematopoiesis by stromal cells is also mediated by the production of a repertoire of cytokines and the expression of a broad range of cell adhesion molecules to facilitate specific cell-cell and cell-matrix interactions (Dorshkind, 1990; Gronthos et al., 2001b; Gronthos et al., 1997; Simmons et al., 1994; Verfaillie, 1998). In addition to the progenitors cells described here, the bone marrow microenvironment also contains many other cell types including reticular cells, smooth muscle cells, adipocytes, endothelial cells, macrophages and immature haematopoietic cells (Allen et al., 1990; Dexter et al., 1984; Lichtman, 1981; Tavassoli and Friedenstein, 1983; Weiss, 1976). The long term culture of BM aspirates in vitro gives rise to an adherent population of stromal cells with the ability to support the growth of myeloid and lymphoid progenitor cells (Dexter et al., 1977; Johnson and Dorshkind, 1986; Whitlock and Witte, 1982). Further analysis of the adherent cellular fraction of BM aspirates has revealed a minor population of self renewable progenitor cells with the capacity to differentiate into a variety of connective tissue types. These cells are commonly termed mesenchymal stem cells, mesenchymal stromal cells and stromal precursor cells. This discovery has stimulated much interest in the application of these cells for musculoskeletal repair, and will be discussed in more detail in section 1.19.

1.7. Bone Remodelling

Bone is continually turned over and remodelled by osteoblasts and osteoclasts in order to repair sites of microdamage, and to respond to changes in mechanical loading. Osteocytes mediate the entire remodelling process, by sensing bone damage or stress via the mechanosensory network of cellular processes and canaliculi which is then transmitted to the bone lining cells (Nijweide et al., 1996; van der Plas and Nijweide, 1992; Xian and Foster, 2006a). Bone lining cells then degrade the osteoid lining of bone to allow attachment of osteoclasts, which ruffle and secrete acids and enzymes to erode the underlying bone. Osteoclastogenesis is entirely dependent on the combined presence of NF-κB ligand (RANKL) and macrophage colony stimulating factor (M-CSF), which are provided by cell of the osteoblast lineage (Anderson et al., 1997; Lacey et al., 1998; Yasuda et al., 1998). The acidic pH and proteases liberate sequestered signalling molecules from the bone matrix such as growth factors IGF-1 and TGF-β. The released growth factors subsequently stimulate the recruitment, proliferation, differentiation and/or activation of osteoprogenitor cells to become active osteoblasts. These metabolically active osteoblasts begin to synthesise new bone matrix, which is later mineralised to become bone.

1.8. Cartilage

Cartilage is specialised connective tissue containing chondrocytes within a unique extracellular matrix. The extracellular matrix of cartilage consists of collagens, water, and proteoglycans which impart the tissue with tensile strength, structural support and flexibility without distortion. Cartilage tissue is avascular, aneural and alymphatic, and as a consequence nutrients and metabolites perfuse the tissue through the matrix by diffusion (Mankin et al., 1994).

Based upon the types and amount of fibres present in the matrix, there are three types of cartilage in the body: hyaline, elastic and fibrocartilage. Hyaline cartilage is the most common form of cartilage and during embryogenesis acts as the scaffold for bone formation. In adults, hyaline cartilage functions in a structural and flexible manner at the articular joint surfaces and in the nose, ribs, larynx, trachea and bronchi. Elastic cartilage contains elastic fibres within the extracellular matrix to provide increased flexibility. For example, the external ear contains elastic cartilage which is surrounded by a layer of

perichondrium. Fibrocartilage is characterised by the presence of irregular thick bundles of collagen fibres. This cartilage type is located at sites where durability, tensile strength and resistance to compression are necessary such as in the invertebral discs and certain joints (Mankin et al., 1994). Damage to articular cartilage joint surfaces is often endogenously repaired with fibrocartilage.

1.8.1. Articular Cartilage

Articular cartilage is a type of hyaline cartilage, and is the resilient load bearing surface of the joint which allows for minimal friction, lubrication and wear characteristics required for continuous gliding motion. In addition, articular cartilage absorbs mechanical shock to spread the load on the underlying supporting bone structures. Characterised by sparsely populated chondrocytes distributed within a large extracellular matrix, the structure and composition of articular cartilage varies throughout its depth. Biochemically, articular cartilage consists of approximately 65% to 80% water, 10% to 20% collagen-II, 4% to 7% aggrecan proteoglycan, with the remainder a cocktail of proteoglycan, collagen, link protein, hyaluronan, and fibronectin (Mankin et al., 1994). Cell shape and volume, collagen fibril diameter and proteoglycan concentration alter from the articular surface to the subchondral bone.

1.8.2. Chondrocytes

The fundamental role of the chondrocyte is the synthesis and maintenance of the cartilage extracellular matrix. Chondrocytes originate from mesenchymal progenitor cells, which differentiate to exhibit the chondrocyte phenotype. Within articular cartilage tissue, chondrocytes occupy less than 10% of the total tissue volume. These cells are metabolically active and respond to a variety of soluble mediators including growth factors, cytokines, matrix constituents, mechanical loads and hydrostatic pressure changes (Lin et al., 2006).

1.9. Growth Plate Structure

In children, longitudinal growth of the long bones occurs at either end of the bone, at the cartilaginous growth plate through the process of endochondral ossification. At the growth plate there is a continual establishment of new prechondrocytic cells which are stimulated

to proliferate and differentiate into chondrocytes, the specific resident cells of cartilage that synthesise and eventually mineralise the cartilage extracellular matrix. Following differentiation and cell division, chondrocytes synthesise molecules to contribute to the cartilage matrix and undergo maturation and hypertrophy (Wilsman et al., 1996). In response to molecular and microenvironment cues the hypertrophic chondrocytes apoptose, stimulating vascular invasion and degradation of the cartilage extracellular matrix. Although not directly contributing to the formation of bone, the growth plate chondrocytes generate a calcified cartilage scaffold upon which bone can be deposited. Longitudinal growth continues in this fashion until growth plate closure at skeletal maturity. The growth plate can be subdivided according to histological and biochemical characteristics into three distinct zones: the resting zone, proliferative zone and hypertrophic zone (Figure 1.2). Polarity of the growth plate is absolute, as partial removal and reversal maintains both cellular orientation and maturation pattern, in comparison to the original growth plate (Abad et al., 1999).

1.9.1. Resting Zone

The resting or reserve zone of the growth plate is located distally to the secondary centre of ossification. Histologically, the resting zone contains sparsely distributed round prechondrocytic cells in a large extracellular matrix. Cartilage specific matrix molecule collagen-II is highest in the resting zone, and associates in aggregate form to inhibit matrix mineralisation (Buckwalter and Rosenberg, 1988; Sandberg and Vuorio, 1987). Another major cartilage matrix molecule aggrecan is present in the resting zone, at a level comparable to those in other zones of the growth plate. These cells undergo sporadic cellular proliferation, and are relatively inactive in matrix turnover (Iannotti, 1990). The resting zone chondrocytes do not contribute to longitudinal growth, and their function is unclear, as they do not actively participate in proliferation, matrix synthesis or calcification. However, functional studies of the resting zone indicate calls of the resting zone are progenitor cells that give rise to cells of the proliferative zone (Abad et al., 2002).

1.9.2. Proliferative Zone

The proliferative zone is located immediately distally from the resting zone of the growth plate. Proliferative chondrocytes in the upper regions of the proliferative zone rapidly divide, flatten and align into longitudinal columns in response to molecular activation

Figure 1.2: The growth plate from the proximal tibia of sheep contains three morphologically distinct zones. The resting zone is located immediately below epiphyseal plate and is characterised by sparsely distributed chondrocytes within an abundant extracellular matrix. The proliferative zone is comprised of chondrocytes aligned into vertical columns. Cells of the hypertrophic zone enlarge in size, apoptose and are subsequently mineralised following vascular invasion from the metaphysis.

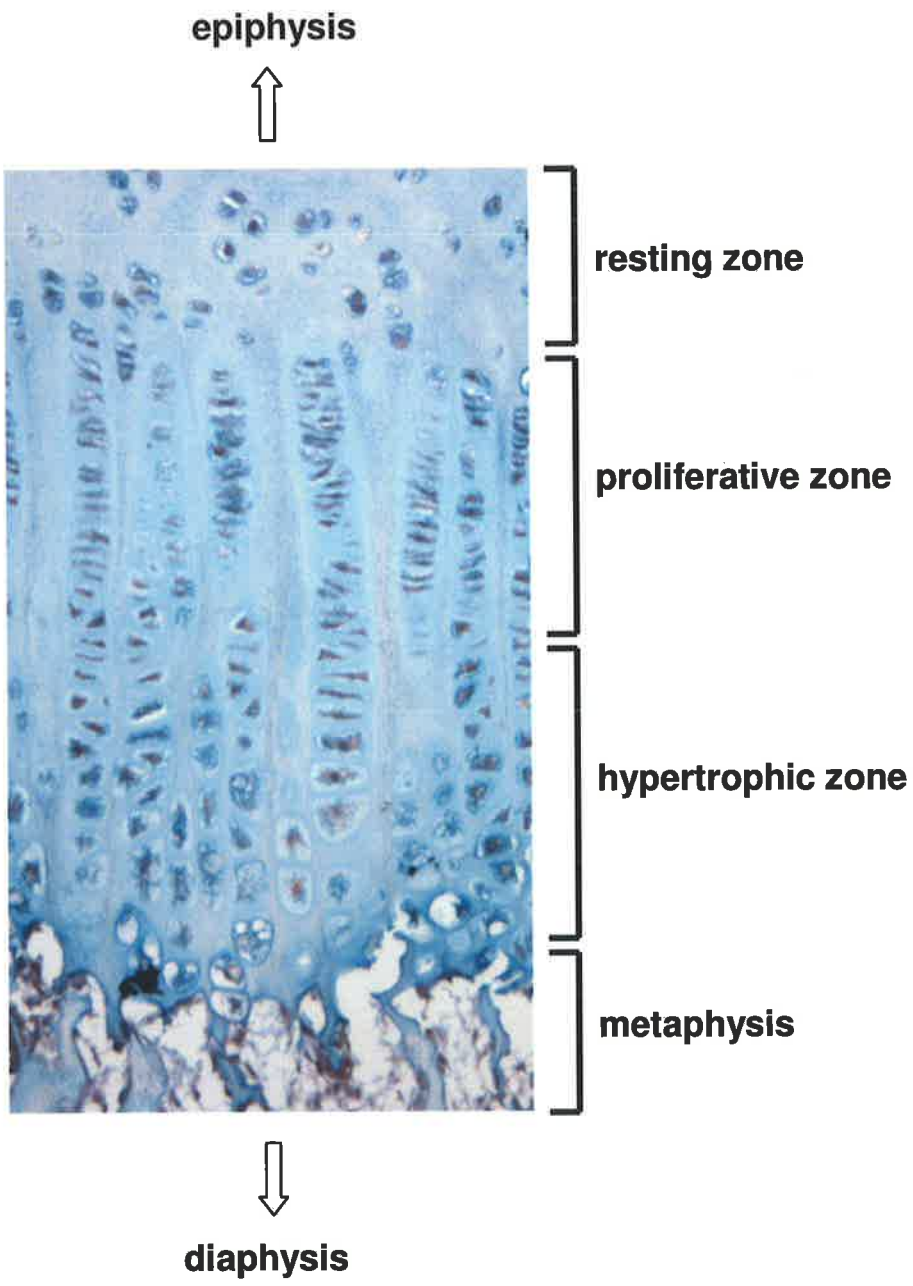
epiphysis
resting zone
proliferative zone
hypertrophic zone
metaphysis
diaphysis

signals. The uppermost cell of each column is the progenitor cell for longitudinal growth of each column. In the lower region of the proliferative zone, these chondrocytes exit the cell cycle and terminally differentiate. The rate of cellular proliferation is sufficient to balance the cellular loss at the chondro-osseous junction (Iannotti et al., 1994). An excellent blood supply via the epiphyseal artery, in combination with high oxygen tension, provides nutrients and oxygen essential for aerobic metabolism within cells of the proliferative zone (Brighton, 1978). Proteoglycan synthesis and turnover is highest within this zone and is deposited in aggregates to inhibit mineralisation. Prior to entry into the hypertrophic zone, the cells distal to those undergoing cell division and proximal to the cell hypertrophy seen in the hypertrophic zone, experience a transitory phase between the two. The rate of terminal differentiation is tightly regulated by Indian hedgehog (Ihh) and parathyroid hormone related protein (PTHrP) signalling loop (Lee et al., 1996; Vortkamp et al., 1996). Overall, the proliferative zone chondrocytes contribute to longitudinal growth by matrix production and cell proliferation.

1.9.3. Hypertrophic Zone

The hypertrophic zone is characterised histologically by the presence of large cells five to ten times the size of proliferative chondrocytes (Buckwalter and Rosenberg, 1983; Hunziker, 1994; Iannotti, 1990). These cells are responsible for the synthesis of alternate matrix molecules and for the preparation and calcification of the extracellular matrix. The hypertrophic chondrocyte is metabolically active and synthesises alkaline phosphatase, neutral proteases and collagen-10, which is the principal collagenous protein of the hypertrophic zone. Diffusion of nutrients and oxygen from the epiphyseal blood supply in the proliferative zone is poor, resulting in a progressive decrease proximally to distally of energy stores and oxygen tension. The presence of mineralised matrix in the lower hypertrophic zone additionally acts as a barrier of oxygen and nutrient supply from the metaphysis. Collectively, the lack of nutrient and oxygen supply, and the depletion of endogenous energy stores within the cell required for accumulation, storage and release of calcium into the extracellular environment, result in the apoptosis of hypertrophic chondrocytes (Gibson, 1998; Roach et al., 2004; Zenmyo et al., 1996).

1.9.4. Mineralisation

Mineralisation of the growth plate extracellular matrix is restricted to the final layers of the hypertrophic zone. The exact mechanism of mineralisation is unknown; however it is likely that changes within the organisation and composition of the extracellular matrix are responsible. It has been suggested that growth plate chondrocytes may play a significant role in the mineralisation of the matrix, through intracellular calcium transport and the synthesis, secretion and modification of extracellular matrix molecules such as collagen-10, and biogenesis of matrix vesicles essential for the mineralisation process (D'Angelo et al., 2001; Schmid and Linsenmayer, 1985). Matrix vesicles are produced by the chondrocyte plasma membrane and are alkaline phosphatase, neutral protease, and matrix metalloproteinase-enriched extracellular membrane bodies (Anderson, 1995). Interestingly, matrix vesicle biogenesis in the growth plate is linked to programmed chondrocyte apoptosis (Anderson, 1995). Located within the ECM, matrix vesicles generate the initial crystals of hydroxyapatite bone mineral during the instigation of mineralisation. The neutral proteases assist degradation of proteoglycans, and as previously mentioned, disaggregated proteoglycans promote mineralisation (Anderson, 2003). Disaggregated proteoglycans have been observed within the hypertrophic zone, and are thought to bind and localise calcium to the matrix, in contrast to the proliferative and resting zones where aggregated proteoglycans resist mineralisation. Disaggregation is believed to be the result of enzymatic digestion by lysozyme, neutral proteases, and matrix metalloproteinases (MMP) (Anderson, 1995; Malemud, 2006).

1.10. Blood supply to the growth plate

Although cartilage by nature is avascular, a blood supply is essential for the maintenance and regulation of the growth plate. The main arteries of the growth plate are the epiphyseal artery, the main nutrient artery, and the perichondrial arteries (Figure 1.3).

The epiphyseal artery enters the bone at the secondary centre of ossification. The terminal branches feed through the growth plate resting zone and terminate in the proximal-most cells of the proliferative zone. There is no penetration and nutrient delivery to the more distal proliferative zone chondrocytes or to cells in the hypertrophic zone (Trueta and Little, 1960). Furthermore, the capillaries never traverse from the epiphyseal to metaphyseal sides of the growth plate. Transient or permanent interruption of the epiphyseal blood supply affects only the cells in the uppermost proliferative zone (Iannotti et al., 1994; Peterson, 1984). These cells fail to proliferate appropriately and growth is

Figure 1.3: Schematic representation of the arterial blood supply to the growth plate. The epiphyseal artery enters at the secondary site of ossification and feed chondrocytes within the proliferative zone. The main nutrient artery enters from the metaphysis and supplies nutrients to the interface of the hypertrophic zone and the last transverse septae of the metaphysis. The perichondral arteries feed the perichondrial ring of LaCroix. Chondrocytes of the resting zone receive blood supply from transphyseal vessels which traverse the growth plate from the metaphysis to the epiphysis. Illustration adapted from Wirth et al. (2002).

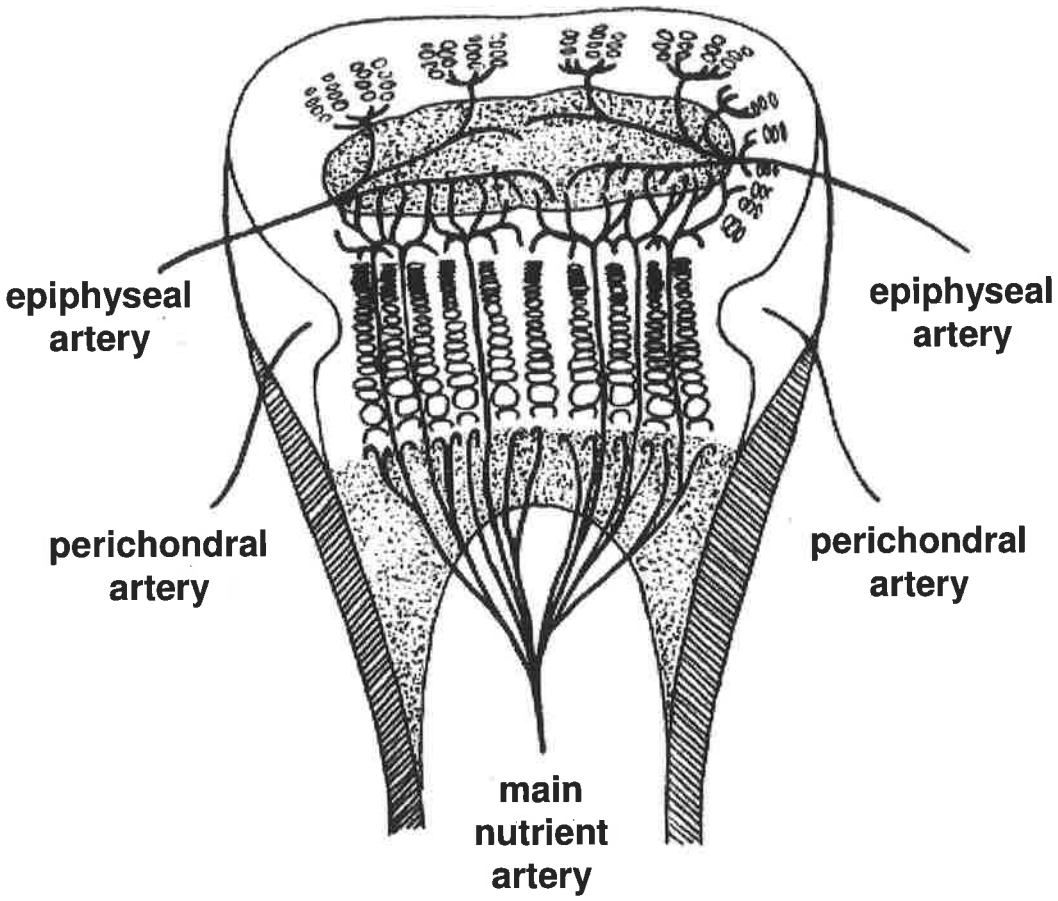
epiphyseal artery
epiphyseal artery
perichondral artery
perichondral artery
main nutrient artery

partially or completely prevented. Interestingly, cells independent of the epiphyseal artery supply will continue to grow longitudinally and laterally, leaving the affected region behind. This differential growth can result in growth deformity.

The main nutrient artery of the long bone enters from the metaphysis and branches to reach the last transverse septae at the bone-cartilage interface (Trueta and Amato, 1960). If the metaphyseal artery is compromised, there is no consequence on the proliferation and maturation of the growth plate chondrocytes. However, remodelling of cartilage scaffold to bone at the primary spongiosa is ablated. Consequently, the growth plate widens at the affected site due to the accumulation of cartilage tissue. Restoration of blood supply to the metaphysis rapidly penetrates and ossifies the cartilage build-up, thus restoring normal growth plate width (Trueta and Amato, 1960). The perichondrial arteries provide oxygen and nutrients to the perichondrial ring of LaCroix (Iannotti, 1990; Trueta and Little, 1960).

1.11. Molecular and Genetic Regulation of the Growth Plate

Endochondral ossification is a tightly controlled mechanism of bone formation regulated by a complex array of signalling systems and factors. In addition to the constituents of the extracellular matrix, soluble messenger molecules such as growth factors play a fundamental role in the transition of chondrocytes within each zone of the growth plate, and subsequent formation of bone. Significant progresses in the understanding of the molecular mechanisms controlling growth plate differentiation have been elucidated through genetic manipulation of animal models. Many hormones, vitamins, morphogens, growth factors, cytokines, transcription factors, and binding proteins have been demonstrated to be important in coordinating the process of endochondral ossification (Xian and Foster, 2006a).

1.11.1. Indian Hedgehog

Indian Hedgehog (Ihh) is considered the master regulator of endochondral bone development, controlling chondrocyte proliferation and maturation (Kronenberg, 2003). Ihh is a member of the hedgehog family of structurally conserved secreted proteins known to provide key signals in embryonic pattering. In the developing long bones, Ihh is highly expressed in the transitional region from proliferating to hypertrophic chondrocytes, and in the upper hypertrophic chondrocytes. The ablation of Ihh in transgenic mice severely

reduced skeletal growth (St-Jacques et al., 1999), which was associated with markedly reduced chondrocyte proliferation, extensive hypertrophy, and abolished expression of parathyroid hormone-related protein (PTHrP). Conversely, overexpression of Ihh was characterised by cartilage elements lacking hypertrophic chondrocytes, accompanied by upregulation of PTHrP (Vortkamp et al., 1996).

1.11.2. Parathyroid Hormone Related Protein

PTHrP is a paracrine hormone synthesised by multiple tissues, with structurally homology to parathyroid hormone (PTH). Both these molecules bind to the same PTH/PTHrP receptor. In the growth plate, PTHrP is expressed by perichondrial cells and proliferating chondrocytes, whereas the receptor is distributed at low levels within the columnar proliferative zone and at high levels in the prehypertrophic and hypertrophic chondrocytes (Kronenberg et al., 1998). The targeted disruption of PTHrP or the PTH/PTHrP receptor gave rise to homozygous mice with a highly similar phenotype. Progeny died shortly after birth from abnormalities caused as a result of diminished proliferation, premature maturation, and mineralisation of chondrocytes (Karaplis et al., 1994). Forced expression of PTHrP dramatically inhibited cartilage maturation and bone formation (Schipani et al., 1997). A direct interaction between Ihh and PTHrP has been demonstrated (Vortkamp et al., 1996). While supplementation of Ihh blocked hypertrophy of wildtype mouse limb explants in vitro, it had no effect on chondrocyte differentiation in PTHrP or PTH/PTHrP receptor knockout animals, suggesting that Ihh acts through PTHrP to inhibit chondrocyte hypertrophy and maintain cells within a proliferative state. Thus, the hypothesis that chondrocyte proliferation and maturation in the growth plate is regulated by a negative feedback loop of intercellular communication, mediated by the secreted signalling molecules PTHrP and Ihh was established (Vortkamp et al., 1996).

1.11.3. Fibroblast Growth Factor

Recent genetic studies have established that fibroblast growth factor (FGF) signalling crucially regulates chondrocyte proliferation and differentiation. The FGF family of proteins consist of at least 23 structurally related polypeptides and contain four tyrosine kinase receptors that bind the FGF ligands with variable affinity. Proliferating chondrocytes express FGFR3 and prehypertrophic chondrocytes express FGFR1. The former is most understood. Knockout of FGFR3 in mice leads to an increased rate of

proliferation of chondrocytes and an elongation of the proliferative columns (Colvin et al., 1996; Deng et al., 1996). Thus it appears that FGF signalling through FGFR3 inhibits chondrocyte proliferation. Gain of function mutations of FGFR3 lead to constitutively active FGFR3 signalling and present with achondroplasia (dwarfism) (Shiang et al., 1994). The FGF-1, 2, 4, 8, 9, and 18 ligands, bind and activate FGFR3 with high affinity (Provot and Schipani, 2005). Binding of the FGF ligands to FGFR3 requires the heparan-sulfate proteoglycan. Furthermore, knockout of the FGFR3 gene increases Ihh expression, and conversely, activation of FGFR3 decreases Ihh expression (Naski and Ornitz, 1998).

FGF-2 is a potent ligand for FGFR3, and is located in the proliferative and upper hypertrophic zones of growth plate chondrocytes (Jingushi et al., 1995; Leach et al., 1997). Transgenic mice overexpressing FGF-2 have shortened bones with a large reserve and proliferative zone, while the size of the hypertrophic zone is greatly reduced (Coffin et al., 1995). Systemic administration of FGF-2 in growing rats found that a low concentration FGF-2 increased proliferation and longitudinal growth, whereas at high concentration, the effect was reversed (Nagai et al., 1995). Interestingly, in vitro studies of the effect of FGF-2 on growth plate chondrocyte proliferation and matrix synthesis have been conflicting. Most investigations have reported that FGF-2 is a potent mitogen for cultured growth plate chondrocytes (Trippel et al., 1993), which is inconsistent with in vivo observations. The use of an organ culture system maintains cells in a normal spatial relationship within the growth plate. Employing this technique, the addition of FGF-2 to intact growth plates inhibited longitudinal growth (Mancilla et al., 1998). Moreover, the concentration of FGF-2 applied inversely affected cartilage matrix production. Additionally, there is some evidence that FGF-2 also plays a role in angiogenesis. Direct infusion of FGF-2 into a rabbit growth plate accelerated vascular invasion, cartilage remodelling and ossification of the growth plate (Baron et al., 1994).

1.11.4. Bone Morphogenic Protein

Bone morphogenic proteins (BMPs) are a subfamily of related proteins within the TGF-β superfamily of secreted growth factors. These molecules were first identified for their ability to induce endochondral bone formation at ectopic sites in rats (Urist, 1965). BMPs impart function by cell surface receptor binding, and have multiple roles during bone formation. In the long bones, BMP-2, 3, 4, 5, and 7 are expressed in the perichondrium, with BMP-2 and 6 expressed in the hypertrophic chondrocytes and BMP-7 in the

proliferative chondrocytes of the growth plate (Anderson et al., 2000). Analysis of the effect of single mutations in BMPs in mutant mice has not elucidated significant insight into their roles in skeletal development. While mutations of BMP-4 led to early embryonic lethality (Winnier et al., 1995), mutations of BMP-6 (Solloway et al., 1998) or 7 (Dudley et al., 1995; Luo et al., 1995) exhibited a mild skeletal phenotype suggesting the existence of a compensatory mechanism and a high level of redundancy between the BMP genes in regulating skeletal development.

The actions of BMPs have been somewhat established using various overexpression systems or by recombinant proteins or antagonists. Supplementation with BMP-2 delays terminal differentiation of hypertrophic chondrocytes, to which Noggin accelerates (Minina et al., 2002; Minina et al., 2001). In contrast to the FGF molecules, various overexpression systems have shown that BMPs are positive modulators of chondrocyte proliferation and negatively regulate terminal differentiation (Minina et al., 2002; Minina et al., 2001). Therefore, it appears that BMPs oppose the effects of FGF signalling at several levels, namely chondrocyte proliferation and differentiation (Minina et al., 2002). The molecular mechanisms of BMP/FGF antagonism are currently unknown.

1.11.5. Growth Hormone/Insulin-like Growth Factor

Growth hormone (GH) and insulin-like growth factor (IGF-1) are considered to be two fundamental systemic regulators of developmental and childhood growth. IGF-1, IGF receptor (IGFR) and GH receptor (GHR) are expressed at all stages of growth plate chondrocyte differentiation (Hunziker et al., 1994; Olney and Mougey, 1999; Werther et al., 1990). Additionally, IGF-1 is also found sequestered within the ECM (Robson et al., 2002). Genetically modified mice deficient for GHR exhibit severe growth retardation, dwarfism, markedly diminished IGF-1, and elevated GH plasma concentrations (Sjogren et al., 2000; Zhou et al., 1997). Chondrocyte proliferation and hypertrophy are reduced and consequently, the growth plate is narrower (Sjogren et al., 2000). Treatment with IGF-1 in GHR mutant mice almost completely restores growth, suggesting that most of the effects of GH on growth are mediated by actions of IGF-1 (Sims et al., 2000). Similarly, IGF-1 knockout mice exhibit growth retardation with delayed bone development (Wang et al., 2006).

A considerable body of evidence has concluded that the actions of GH are mediated predominantly via IGF-1 but also by IGF-1-independent direct effects (Hunziker et al., 1994). Termed the "dual effector theory", it is proposed that GH acts selectively on reserve zone cells, but also promotes chondrocyte proliferation via local IGF-1 production (Green et al., 1985). IGF-1 subsequently stimulates proliferative chondrocyte expansion in an autocrine/paracrine manner. A comparison of knockout mouse models indicates a dual role for GH in promoting longitudinal growth: an IGF-1-independent role in growth plate chondrocyte generation, and an IGF-1-dependent role in promoting chondrocyte proliferation and hypertrophy (Wang et al., 2004).

1.11.6. Transforming Growth Factor-β

The transforming growth factor-beta (TGF-β) superfamily is comprised of more than 30 members (Miyazono et al., 2004). With a diverse array of biological activities, TGF-β members are critical during skeletal development, maintenance, and repair. TGF-β1 and TGF-β2 are highly expressed in bone, and are sequestered within the ECM associated with molecules such as biglycan, decorin, and fibromodulin (Hildebrand et al., 1994). Furthermore, TGF-β receptor 3 is a membrane bound proteoglycan known as betaglycan, and is thought to act as a TGF-β cell surface reservoir (Rosado et al., 2002). Within the growth plate TGF-β1, TGF-β2, and TGF-β3 are expressed differentially in the resting, proliferative and hypertrophic zones (Matsunaga et al., 1999). Both genetic manipulation and organ culture explants have indicated a function for TGF-β in limiting terminal differentiation. The supplementation of limb explants with TGF-β1 demonstrated inhibition of hypertrophic differentiation and matrix mineralisation (Serra et al., 1999). Moreover, PTHrP mRNA expression was stimulated in response to TGF-β suggesting that TGF-β action in the growth plate may be partially mediated by PTHrP.

1.11.7. Angiogenic factors

The establishment of a vascular supply is fundamental for the formation of bone during endochondral and intramembranous ossification, and fracture repair. Angiogenic factors are an integral part of this process and promote neovascularisation by endothelial cells and localised proteolytic modification of the ECM. During endochondral ossification at the growth plate, the process of mineralisation is dependent on the establishment of a vascular supply. Previous studies have demonstrated the essential mediator of angiogenesis is

vascular endothelial growth factor (VEGF). VEGF is an endothelial specific mitogen, which is highly expressed by hypertrophic chondrocytes in the growth plate, osteoblasts, and is stimulated by hypoxic conditions in the growth plate (Ferrara and Davis-Smyth, 1997; Horner et al., 1999). VEGF is indispensable for embryonic development, with both homozygous and heterozygote progeny presenting with embryonic lethality (Carmeliet et al., 1996; Ferrara et al., 1996). Beyond embryogenesis, VEGF and is also necessary for growth and survival during post-natal life. The early embryonic lethality observed in classic knockout experiments precluded analysis of the contribution of VEGF in the vascularisation of long bones. The inactivation of VEGF by systemic administration of a soluble receptor in juvenile mouse growth plates suppressed blood vessel invasion and trabecular bone formation (Gerber et al., 1999). This was coupled with substantial expansion of the hypertrophic zone, and the inhibition of resorption of terminally differentiated chondrocytes. Thus VEGF is essential for blood vessel invasion, subsequent cartilage remodelling and bone formation during endochondral bone lengthening. Another important angiogenic factor is hypoxia inducible factor (HIF)-1α, a key transcription factor which regulates VEGF expression and is upregulated in hypoxic hypertrophic chondrocytes (Schipani et al., 2001). In addition, the pro-angiogenic factors matrix metalloproteinase (MMP) are expressed by and around developing blood vessels and hypertrophic chondrocyte matrix vesicles, and are integral in the proteolysis of the cartilage extracellular matrix

Apart from VEGF, HIF-1α, and MMPs, several other molecules appear to play an important role in regulating angiogenesis at the growth plate. TGF-β, PDGF, and FGF-2 have been shown to accelerate differentiation, vascular invasion, and ossification when infused into the growth plate (De Luca and Baron, 1999; Mitlak et al., 1996; Zerath et al., 1997). Factors such as FGF-2 and TGF-β are sequestered within the ECM, and once liberated may promote vascularisation either directly or indirectly. The presence of a blood supply not only provides essential nutrients for the mineralisation process, but permits migration of osteoblasts, osteoclasts and other cell types to degrade the mineralised cartilage ECM, and deposit new bone.

1.11.8. Transcription Factors Central to Endochondral Ossification

There are a number of transcription factors known to regulate endochondral ossification during bone growth. Sox-9 is a member of the Sox family of transcription factors that are

characterised by a high-mobility-group (HMG)-box DNA binding domain with high sequence similarity to the sex determining factor SRY (Foster et al., 1994; Wagner et al., 1994). Sox-9 is now known to be the key transcription factor controlling chondrogenesis (Wright et al., 1995). Expression of Sox-9 is found in mesenchymal cells undergoing chondrogenic differentiation and in proliferating chondrocytes, but not in hypertrophic chondrocytes or osteoblasts. Sox-9 acts early in chondrogenesis and can activate other transcription factors that promote overt chondrocyte differentiation such as Sox5 and Sox6 (Bi et al., 1999; Lefebvre et al., 2001). Sox-9 stimulates expression of cartilage specific matrix genes including Col-2a1, Col-11a2, and aggrecan, which contain Sox-9 binding sites (Bi et al., 1999).

The essential role of Sox-9 was demonstrated by the analysis of human genetic diseases and genetically manipulated mice. In humans, haploinsufficiency of Sox-9 leads to campomelic dysplasia (CD) which is characterised by hypoplasia of virtually all endochondral skeletal elements (Foster et al., 1994; Wagner et al., 1994), accompanied by an increase in the length of hypertrophic chondrocyte zones premature mineralisation (Bi et al., 2001). Sox-9 deficient mouse chimera cells failed to form chondrogenic condensations expression of Col-2, Col-9, Col-11 and aggrecan molecules were absent (Bi et al., 1999). This suggests Sox-9 may play two roles; in the formation of mesenchymal cartilage condensations which is the earliest step in chondrocyte differentiation and cartilage formation, and in the regulation of the rate of chondrocyte differentiation to hypertrophy.

Signalling by PTHrP, BMP, Shh and FGF all markedly upregulate the expression and maintenance of Sox-9 in vitro (Huang et al., 2001; Murakami et al., 2000; Semba et al., 2000). In contrast, tumour necrosis factor-α (TNF-α) and interleukin-1 (IL-1) potently inhibit Sox-9 expression (Murakami et al., 2000).

The importance of Sox-9 in chondrocyte differentiation and cartilage formation is equivalent to the significance of Cbfa-1 in osteogenesis and bone formation. Core binding factor alpha-1 (Cbfa-1 or Runx2) is a member of the Runt domain family of transcription factors, and is expressed by all osteoblasts (Ducy et al., 1997) and hypertrophic chondrocytes (Inada et al., 1999). Expression and activity of Cbfa-1 is upregulated by BMP-2, BMP-4, BMP-7, FGF-2, and FGF-8 and downregulated by glucocorticoid, vitamin D, and TGF-β (Alliston et al., 2001; Chang et al., 1998; Ducy et al., 1997; Gori et al.,

1999; Zhou et al., 2000). Cbfa-1 is able to induce both early and late markers of osteoblast differentiation including alkaline phosphatase, Col-1, osteopontin, bone sialoprotein and osteocalcin (Ducy et al., 1997).

Haploinsufficiency of Cbfa-1 in humans leads to severe skeletal dysplasia (Lee et al., 1997; Mundlos et al., 1997). Genetic experiments in mice have demonstrated that Cbfa-1 is required for osteoblast differentiation, chondrocyte maturation and angiogenesis. In Cbfa-1 null mice, no endochondral or intramembranous bone formation occurs, due to the absence of mature osteoblasts, bone matrix, and osteoclasts (Komori et al., 1997; Otto et al., 1997). Chondrocyte maturation was also disturbed, with an inhibition of chondrocyte hypertrophy in most of the skeleton. Additionally, knockout mice displayed no vascular invasion of cartilage or degradation of the cartilage ECM, and lack expression of many osteoblastic ECM markers. Conversely, the overexpression of Cbfa-1 in Col-2 expressing chondrocytes of transgenic mice accelerated endochondral ossification and partially rescued the anomalies observed in Cbfa-1 deficient embryos (Takeda et al., 2001). This rescue returned hypertrophic chondrocyte differentiation, VEGF expression by hypertrophic chondrocytes, vascular invasion, and the presence of osteoclasts/chondroclasts in the hypertrophic cartilage matrix, all which were defective in Cbfa-1 null mice. However, osteoblast differentiation and bone formation were not restored. The overexpression of a dominant negative form of Cbfa-1 in chondrocytes suppressed maturation and delayed endochondral ossification (Ueta et al., 2001). Collectively, these studies indicate Cbfa-1 has two distinct functions, in the differentiation of mesenchymal progenitors to osteoblasts, and the stimulation of hypertrophic chondrocyte differentiation; both of which affect intramembranous and endochondral ossification.

Cbfa-1 also appears to mediate the vascular invasion of cartilage (Hoshi et al., 1999; Inada et al., 1999; Kim et al., 1999; Komori et al., 1997; Otto et al., 1997). Knockout mice lack vascular invasion and the expression of angiogenic factor VEGF, which is normally expressed by hypertrophic chondrocytes. Coupled with the observation that Cbfa-1 activates the VEGF promoter in vitro (Zelzer et al., 2001), it appears that the Cbfa-1 dependent regulation of blood vessel invasion is mediated by VEGF.

1.12. Extracellular Matrix Molecules of Bone and Cartilage

The biological function and structural properties of cartilage and bone are largely dependent on the characteristics of the extracellular matrix (Table 1.1). The cartilage extracellular matrix is synthesised and maintained by chondrocytes, and predominantly consists of cartilage specific collagen-2 and sulfated proteoglycans. Collagen provides structural strength, whereas the proteoglycans are bifunctional, interacting with collagen to contribute to strength, and playing a regulatory role on the cartilage microenvironment through interaction with growth factors and cell-matrix connections. Bone is a composite material consisting of minerals, proteins, water, cells and other macromolecules. Although the bone cells are the primary mediators of metabolism, the acellular components are also involved in the control of cellular processes (Robey, 1996). The mineral and inorganic components account for 60-70% of bone tissue, water 5-8%, and the organic components makes up for the remainder (Kaplan et al., 1994). The inorganic component of bone is the calcium phosphate mineral similar to crystalline calcium hydroxyapatite. Apatite is a small plate-like crystal which imparts bone its physical strength. The organic extracellular matrix of bone has roles in determining the bone structure, and both mechanical and biomechanical properties.

1.12.1. Collagen-1

Collagen-1 is a member of the fibrillar collagen family which are encoded by at least 32 identified genes. Collagens are characterised by a triple helix structure of approximately 1,000 amino acids each. Cross linking of the collagen chains produces a rigid linear molecule, which is further aligned in a staggered parallel fashion in a quartet to form a collagen fibril. The collagen fibrils subsequently group in bundles to produce the collagen fibre. The aggregation of collagen fibrils and fibres impart the tensile strength to the bone and bone marrow connective tissues.

Type-1 collagen is the most abundant collagen in bone, contributing to 90% of total bone collagen (Kaplan et al., 1994). Collagen-1 is synthesised by bone-forming cells (osteoblasts) during bone formation. The collagen fibres act as sites for initial mineralisation and provide a scaffold for the bone extracellular matrix, which imparts tensile strength to the bone (Mundlos et al., 1990).

Table 1.1. Extracellular matrix molecules associated with bone and cartilage.

Molecule	Site/Cellular Expression	Function
Bone sialoprotein	10-15% of non collagenous protein in bone. Mineralised bone and calcified cartilage	High binding affinity for hydroxyapatite crystals and collagen - potential role in early mineralisation (Bianco et al., 1991; Chen et al., 1991)
Collagen-1	Major organic component of bone. Synthesised by osteoblasts.	Provides scaffold for the bone extracellular matrix to impart skeletal strength (Mundlos et al., 1990; Sandberg and Vuorio, 1987).
Osteocalcin	10-20% of non collagenous protein in bone. Synthesised by osteoblasts and hypertrophic chondrocytes.	Calcium and mineral binding protein (binds hydroxyapatite) – regulates rate of mineralisation and recruits osteoclasts (Boskey et al., 1998; Ducy et al., 1996).
Osteonectin	5-10% of non collagenous protein in bone. Secreted by osteoblasts. Rich at sites of remodelling.	Binds hydroxyapatite and collagen – regulates mineralisation, bone formation and remodelling (Delany et al., 2000; Lane and Sage, 1994; Young et al., 1992).
Osteopontin	Wide distribution throughout body. Secreted by osteoblasts, osteocytes and hypertrophic chondrocytes.	Anchor osteoclasts to resorptive sites, promotes angiogenesis, and negatively regulates hydroxyapatite mineral formation (Boskey et al., 1993; McKee et al., 1992; Reinholt et al., 1990).

Table 1.1. Extracellular matrix molecules associated with bone and cartilage continued.

Molecule	Site/Cellular Expression	Function
Aggrecan	80-90% of glycosaminoglycan content of cartilage.	Imparts resistance to compression by water retention. Forms complex with hyaluronan and link protein (Muir, 1995; Perkins et al., 1992; Rittenhouse et al., 1978; Watanabe et al., 1994; Watanabe et al., 1998).
Biglycan	Expressed in cartilage, subchondral cartilage and periosteum.	Binds collagen during extracellular matrix assembly and regulates TGFβ activity. Regulates bone formation (Bianco et al., 1990; Fisher et al., 1989; Hildebrand et al., 1994; Xu et al., 1998)
Collagen-10	Hypertrophic zone of growth plate. Expressed by hypertrophic chondrocytes.	Mediates matrix mineralisation and vascular invasion (Kielty et al., 1985; Kirsch and von der Mark, 1990; Paschalis et al., 1996).
Collagen-2	Unique and major macromolecule of cartilage. Synthesised by chondrocytes.	Provides tensile strength (Aszodi et al., 1998; Li et al., 1995; Mundlos et al., 1990; Sandberg and Vuorio, 1987; Talts et al., 1998).
Decorin	Found at surface of collagen fibrils.	Mediates collagen fibril formation and assembly. Negatively regulates TGFβ activity (Danielson et al., 1997; Schonherr et al., 1995; Weber et al., 1996; Yamaguchi et al., 1990).
Matrix Gla	Expressed by proliferative and late hypertrophic chondrocytes.	Inhibits calcification of ECM (Luo et al., 1997).

1.12.2. Collagen-2

Collagen-2 is the major structural macromolecule of the extracellular matrix in the resting and proliferative zones of the growth plate, and in articular cartilage. Expression of collagen-2 is unique and exclusive to cartilage tissue, and indicative of chondrocyte differentiation (Mankin et al., 1994; Muir, 1995). The main function of collagen-2 is to provide tensile strength and to immobilise proteoglycans within the matrix. Structurally similar to other members of the collagen family, collagen-2 is a triple helical molecule comprised of three identical α1(II) polypeptide subunits encoded by the COL2A1 gene (Cheah et al., 1985). Mutant mice display dwarfism, with shortened long bones and disorganisation of the endochondral bones. In addition there is a complete lack of an organised growth plate (Li et al., 1995). Although chondrocyte differentiation, maturation and hypertrophy are not affected by the lack of the collagen-2 expression, it appears the collagen-2 matrix is critical for cartilage organisation and function.

1.12.3. Collagen-10

Type 10 collagen is expressed in the hypertrophic zone of the growth plate and is indicative of cartilage undergoing endochondral ossification (Chan and Jacenko, 1998; Jacenko et al., 1993; LuValle et al., 1992). In articular cartilage, expression is restricted to a thin layer at the interface of calcified cartilage and bone (Eyre, 2002). Collagen-10 is also expressed by mesenchymal progenitor cells cultured in vitro (Gronthos et al., 2003). The function of collagen-10 is unknown but spacio-temporal location at the site of endochondral ossification in the growth plate suggests a role in regulating matrix mineralisation, matrix stabilisation and remodelling, or vascular invasion (Price et al., 1994; Schmid et al., 1990; Wu et al., 1989). Genetic manipulation of Col-10 in mouse models exhibited a mild skeletal abnormality with similarities to the phenotype observed in mutated human Col-10 (Chan and Jacenko, 1998; Gress and Jacenko, 2000; Kwan et al., 1997). Although phenotypic discrepancies exist between transgenic and knockout mice, taken together, these studies indicate the role of Col-10 in endochondral ossification and establishment of the bone marrow.

1.12.4. Proteoglycans and Glycosaminoglycans

Proteoglycans are complex macromolecules found within all connective tissues. Gaps at the ends and between sides of parallel collagen molecules are filled by deposits of noncollagenous matrix molecules such as proteoglycans and structural glycoproteins. By definition proteoglycans consist of a protein core to which one or a number of different extended polysaccharide (glycosaminoglycan) chains are linked. Hyaluronate, heparin, heparin sulfate, chondroitin sulfate, dermatan sulfate and keratan sulfate are all polysaccharide glycosaminoglycans (GAGs). Hyaluronate is an unsulfated GAG, and as it is not bound to a protein core it is essentially not considered to be a proteoglycan. The glycosaminoglycans differ in their disaccharide structure, and can combine with other extracellular matrix molecules to produce macromolecular structures. GAGs are long-chain, unbranched repeating disaccharide units differing according to their constituent structures. The primary function of proteoglycans is maintaining structural integrity by interaction with collagen fibrils, or due to their high viscosity, providing a lubricating function in connective tissue (Jackson et al., 1991; Knudson and Knudson, 2001).

1.12.5. Aggrecan

Approximately 80% to 90% of proteoglycans in cartilage are of the large aggregating type called aggrecan. Aggrecan has a large protein core, with chondroitin sulfate and keratan sulfate GAG side chains, which is anchored via the link protein at the N-terminal end to hyaluronate (Watanabe et al., 1997; Watanabe et al., 1998). The hyaluronate molecule serves to anchor aggrecan. As each hyaluronate chain is long and unbranched; many aggrecan molecules can bind to a single chain of hyaluronate to form a large aggregate. This aggregation is thought to immobilise the proteoglycan within the cartilage collagen network. The aggrecan molecule contributes to water retention and resistance to compression (Muir, 1995; Watanabe et al., 1998).

Cartilage matrix deficient mice have a naturally occurring knockout of the aggrecan gene. Homozygous animals die shortly after birth due to respiratory failure and are characterised by dwarfism, a shortened snout and cleft palate (Rittenhouse et al., 1978; Watanabe et al., 1994). Tightly packed chondrocytes within little cartilage extracellular matrix is observed in these aggrecan deficient mice. Thus the interaction between aggrecan, link protein and

hyaluronate is essential for the development, organisation and maintenance of cartilage architecture (Kimata et al., 1981; Wai et al., 1998).

1.13. Fracture Repair

Following fracture of the developing skeleton, there is a complex cascade of molecular and cellular events to regenerate the damaged tissue. Injury to both cartilage and bone stimulates sequential phases of events, which can be divided into the inflammatory phase, reparative phase and remodelling phase (Ogden, 2000).

1.13.1. Inflammatory Phase

Bleeding from the damaged soft tissue, bone or periosteum initiates the repair process through the release of stimulatory growth factors, cytokines, and prostaglandins. There is formation of a haematoma at the injury site. Coagulation and platelet activation functionally ablate bleeding, and synthesise inflammatory mediators and angiogenic factors. The angiogenic stimulants recruit endothelial cells to the fracture site to promote neovascularisation, which in turn allow the migration of leukocytes, monocytes and macrophages of the immune system into the injury (Xian and Foster, 2006a).

Disruption of the blood supply either side of the fracture site leads to local necrosis, releasing sequestered growth factors to stimulate inflammatory cell-mediated debris removal and osteoblastic differentiation of surrounding mesenchymal progenitors (Bolander, 1992; Sandberg et al., 1993; Xian and Foster, 2006a). In parallel there is modification of the extracellular matrix by fibroblast like cells to assist new bone formation. Vascularised fibrous tissue replaces the blood clot with deposits of ground substances and matrix proteins including collagens and proteoglycans. This initial matrix supports endochondral or intramembranous bone formation (Sandberg et al., 1993; Szczesny, 2002). Eventually there is mineralisation of the matrix and formation of a provisional fracture callus, which is dependent on the presence of a functional vascular supply. The primary callus is gradually remodelled to mature bone from the immediate fracture site outwards.

1.13.2. Reparative Phase

The inflammatory phase initiates the repair of bone fracture through the formation a soft callus. Following haematoma, in the reparative phase, osteogenic cells proliferate from the periosteum and endosteum to instigate deposition of an external (surrounding) and internal (within) bone callus around the fracture site (Ogden, 2000; Xian and Foster, 2006a). This new bone is randomly organised and cannot withstand general mechanical stress, so must be immobile to permit the entire repair process. Mesenchymal progenitors are recruited through the release of growth factors and cytokines, and differentiate within the haematoma in response to TGFβ and BMP molecules (Xian and Foster, 2006a). At this point bone formation can proceed either via the endochondral or intramembranous mechanisms, as mesenchymal progenitors can be modulated to differentiate to chondrocytes or osteoblasts (Bruder et al., 1994; Owen, 1988; Xian and Foster, 2006a). In mechanically unstable fractures, mesenchymal cells may become chondrogenic to produce bone via the endochondral pathway in a transitional fashion. Alternately, in stable fractures, these progenitors directly differentiate into osteoblasts to form a hard callus by intramembranous ossification. Microvascular invasion in the fracture callus originates from the periosteal, nutrient, and endosteal blood vessels for the delivery of nutrients and reparative cells.

1.13.3. Remodelling Phase

The final and longest phase of fracture repair is the remodelling phase. The fundamental step in the reparative/remodelling transition is the formation of an intact bony bridge between the fragments. The osseous callus undergoes extensive remodelling involving actions of osteoclasts and osteoblasts, similar to the normal bone maturation process (Gerstenfeld et al., 2003). Mechanically unnecessary portions of the callus are removed. As the bone grows, the immature bony fracture callus is gradually incorporated into the pre-existing cortical bone and replaced by the remodelling process.

1.14. Current Treatment of Articular Cartilage Repair

Articular cartilage is remarkably durable, however once damaged has a poor capacity to repair. Although metabolically active, cartilage is avascular and alymphatic and due to cellular entrapment within the dense ECM limiting cell movement, articular cartilage is

unable to elicit any inflammatory or reparative response, and as a consequence has a limited capacity for repair. Trauma, chronic or progressive disease at the articular cartilage surface can lead to degradation of the cartilage tissue and destruction of the articular surface. Due to the lack of repair, surface damage is frequently associated with disability and symptoms such as joint pain, locking phenomena, and disturbed function (Mankin et al., 1994). Moreover, damage to the articular surface can lead to rapid degeneration of the entire joint surface, as characterised by osteoarthritis. Surgical interventions attempt to relieve joint pain, joint functionality, and to delay progression of severe joint destruction. Partial thickness defects do not self heal, because the defect is confined to the articular surface and devoid of a vascular supply. In contrast, spontaneous healing of articular cartilage is associated with defects that penetrate the subchondral bone, and are termed full thickness defects. This observation prompted the surgical practice of drilling or microfracture, where penetration of the subchondral bone permits progenitor cells from the marrow to infiltrate the injury site to remove necrotic tissue and endogenously repair the joint surface (Hunziker, 2002). However, the repair tissue is a poorly integrating fibrocartilage with inferior mechanical properties and durability.

1.14.1. Autologous Chondrocytes for the Repair of Articular Cartilage

The potential of autologous chondrocytes to repair full thickness articular cartilage defects has been under extensive investigation. The initial experiment investigating the potential of expanded chondrocytes to regenerate articular cartilage defects was undertaken by Grande et al (1989) in rabbits (Grande et al., 1989). Chondrocytes were isolated from surgically created patella defects, cultured in vitro, and autotransplanted by injection under a periosteal flap secured over the chondral defect. The failure of repair in the absence of chondrocytes suggests a direct requirement of chondrocytes for proper repair (Grande et al., 1989). Autologous chondrocyte implantation (ACI) is now the preferred method for joint resurfacing and is in clinical use (Brittberg et al., 1994). Whilst autologous chondrocyte transplantation shows promise, the quality of new repair tissue is often poor (Redman et al., 2005). As a consequence, more sophisticated tissue engineering techniques are required for the establishment of durable, high quality repair cartilage.

To date, the repair of articular cartilage defects has been assessed using numerous delivery vehicles. Implantation of chondrocytes embedded in collagen gels (Wakitani et al., 1998), fibrin (Hendrickson et al., 1994), agarose (Rahfoth et al., 1998), alginate (Fragonas et al.,

2000), hyaluronan (Grigolo et al., 2001) and synthetic polymers polylactic acid (Chu et al., 1997), polyglycolic acid (Liu et al., 2002) and composites (Niederauer et al., 2000) have all produced positive preliminary results. Nevertheless, the application of autologous chondrocytes for cartilage regeneration is still limited by the availability of hyaline cartilage sites for tissue harvest, and inherent risk of damage to previously healthy cartilage.

1.14.2. Growth Factor Repair of Articular Cartilage

Recent studies have approached the regeneration of full thickness cartilage defects using the local administration of growth factors. In theory, the application of specific growth factors would recruit progenitor cells to the injury site and subsequently signal differentiation and endogenous regeneration of the injured tissue. Furthermore, growth factor therapy obviates the requirement for the cultivation of cells or tissue.

The application of BMP-2 within a collagen sponge demonstrated improved healing of a full thickness defect in rabbit, with improved histological appearance when compared with untreated defects (Sellers et al., 2000). Similarly, the direct stimulatory effect of BMP-7 on the repair of full and partial thickness articular cartilage lesions has been established by studies in rabbit, dog, goat and sheep (Cook et al., 2003; Grgic et al., 1997; Jelic et al., 2001; Louwerse et al., 2000). Partial thickness defects were repaired at both high and low concentration BMP-7 administration.

Administration of FGF-2 within a collagen sponge to repair full thickness articular defects was initially reported in rabbits (Fujimoto et al., 1999). Local administration of FGF-2 resulted in successful resurfacing of large full thickness defects with hyaline cartilage (Hiraki et al., 2001). In contrast, defects receiving a neutralising monoclonal antibody against FGF-2 were clearly impeded, and filled with fibrous tissue. The mechanism by which FGF-2 successfully resurfaces a large articular defect may be due to targeting of mesenchymal progenitor cells to form cartilage by selective expansion of chondroprogenitor cells.

Two studies have demonstrated the potential of IGF-1 therapy to repair osteochondral articular damage. Tuncel et al. (2005) employed an IGF-1 laden collagen sponge in rabbits, and Nixon et al. (1999) administered IGF-1 to horse joint surfaces using a slow

release fibrin clot (Nixon et al., 1999; Tuncel et al., 2005). In both circumstances, the repair of the subchondral bone and articular cartilage surface were enhanced by addition of IGF-1, in comparison to controls (Nixon et al., 1999; Tuncel et al., 2005).

To investigate whether partial thickness defects of articular cartilage could be repaired by the introduction of a variety of different growth factors, a comprehensive study was undertaken in miniature pigs (Hunziker et al., 2001). A free chemotactic/mitogenic factor (TGF-β1, TGF-β2, IGF-1, or FGF-2) at low concentration and liposome-encapsulated TGF-β1 at high concentration were administered in combination within a fibrin matrix into partial thickness defects. All defects containing liposome-encapsulated TGF-β1 became filled with cartilage like tissue positive for major cartilage ECM components and the additional presence of a mitogenic factor increased cellularity of the repair tissue. Similarly regeneration of rabbit full thickness defects has been achieved using TGF-β1 delivered within alginate (Perka et al., 2000a). Taken together, these studies detail importance of growth factors in promotion of intrinsic healing of partial thickness articular defects.

1.15. Scaffolds

As opposed to the differentiation of progenitor cells in vitro to a specific cell type, the formation of stable tissue of desired function in vivo is often dependent on the transplantation of cells within some type of supportive scaffold. Biological scaffolds for tissue engineering must ideally provide a non-immunogenic three-dimensional structure that can permit high seeding densities, be porous to allow perfusion of nutrients to maintain cell survival, and degrade at a rate matching that of cellular deposition of an extracellular matrix. The engineering of a specific tissue often requires the selection of a scaffold that is biomechanically and functionally suitable for that purpose (Frenkel and Di Cesare, 2004; Luyten et al., 2001; Xian and Foster, 2006b).

In order for chondrogenesis and maintenance of the chondrocyte phenotype to occur, progenitor cells or chondrocytes require a three dimensional arrangement. It has been well documented that once cultured in monolayer, primary chondrocytes dedifferentiate, become more fibroblastic, and lose expression of molecules unique to chondrocytes (Benya et al., 1978; Grundmann et al., 1980; Haudenschild et al., 2001; Schnabel et al., 2002). The standard procedures for chondrogenic differentiation of progenitor cells in

vitro include the pellet culture or micromass techniques vitro (Benya and Shaffer, 1982; Schulze-Tanzil et al., 2002; Solursh, 1991; Thorogood and Hinchliffe, 1975). Both provide an aggregate three dimensional spatial arrangement for maintenance of phenotype.

Differentiation of MSC to chondrocytes in vitro has been demonstrated using naturally occurring seaweed extracts agarose (Awad et al., 2004; Huang et al., 2004)and alginate (Erickson et al., 2002; Majumdar et al., 2000), gelatin (Awad et al., 2004; Ponticiello et al., 2000), silk (Wang et al., 2005) and hyaluronic acid (Kavalkovich et al., 2002; Lisignoli et al., 2005). More recently the manufacture of synthetic polymers, including polycaprolactone (PCL) (Li et al., 2005a), polyvinyl resin (PVF) (Aung et al., 2002), polylactic acid (PLA) (Caterson et al., 2001), polylactic-polyglycolic acid (PGLA) copolymer (Fan et al., 2006; Uematsu et al., 2005), and PGLA-collagen hybrids (Chen et al., 2004) have also shown to be chondrogenic supportive biomaterials.

In addition to supporting differentiation of chondroprogenitors, the aforementioned biomaterials also maintain primary chondrocytes of various species in a differentiated phenotype in vitro. Alginate (Wong et al., 2001), alginate-fibrin composites (Perka et al., 2000b), hyaluronic acid (Aigner et al., 1998), collagen (Veilleux and Spector, 2005), and polyglycolic acid (PGA) (Freed et al., 1993), are all potential carriers for tissue engineering with chondrocytes, as they maintain phenotype and encourage deposition of a cartilage ECM. Furthermore, dedifferentiated chondrocytes cultured in monolayer can be redifferentiated when cultured in vitro in a PGLA-collagen hybrid mesh (Chen et al., 2003b).

Many bioscaffolds have shown promise in vitro as cell carriers for MSC or chondrocytes in cell transplantation or tissue engineering. Considerable interest lies in the use of cartilage engineering not only for joint resurfacing but for the treatment of craniofacial implants. In vivo, subcutaneous formation of cartilage like tissue by chondrocyte seeded in biomaterials including alginate (Chang et al., 2003; Paige et al., 1996), PCL-fibrin glue (Hutmacher et al., 2003), hyaluronate (Aigner et al., 1998), and PGLA (Kaps et al., 2006; Marijnissen et al., 2002) have been reported. Three separated studies have applied the PGLA (Ethisorb) scaffold, using fibrin glue (Haisch et al., 2002), alginate (Marijnissen et al., 2002), or agarose (Rotter et al., 1998) as the chondrocyte delivery substance to incorporate cells within the non woven fleece. Tissue engineering applications to regenerate articular and growth plate cartilage are discussed in the sections 1.14, 1.18, and 1.20.

1.16. Growth Plate Fracture Repair

Although there has been extensive research of the cellular and molecular events following fracture and subsequent repair of bone, there is minimal understanding about growth plate fracture repair.

The growth plate is the weakest structure in the developing long bone, and is a common region of failure in children. Injury or trauma to the growth plate can be inflicted by fracture, radiation, tumour, infection, metabolic abnormality, and extremes of hot and cold (frostbite and burn). Fractures through the growth plate may be as a result of physiological or mechanical reasons, with mechanical failure often giving rise to physiological failure. This is the case for instance when the mechanical demands placed upon the bone outweigh the strength of the epiphysis-growth plate-metaphysis complex. It is important to assess and classify the type of growth plate fracture accurately, as the location of damage often defines the outcome of proliferative cell activity and epiphyseal blood supply, and consequently further growth.

The incidence of growth plate facture has been reported to range from 18% (Mizuta et al., 1987; Worlock et al., 1986) to 30% (Mann and Rajmaira, 1990). Epidemiologically, males present with fractures twice as often as females. The majority of fractures were sustained through sporting and recreational activities, with an equal distribution on the left and right sides (Peterson et al., 1994). Of the growth plate injuries up to 30% undergo undesirable bony repair at the injury site.

There is currently no universal classification system for growth plate injury; however the most recognised is that of Salter and Harris, which encompasses five types of fracture (Salter and Harris, 1963). The Salter-Harris classification system was proposed to relate the mechanisms, characteristics and prognoses of growth plate fractures (Figure 1.4).

Owing to its avascular and alymphatic nature, both articular and growth plate cartilage have a poor reparative response to injury. The type of repair initiated by trauma to the growth plate is dependent on the injury sustained. If a fracture occurs in a plane within the growth plate, there is minimal disorganisation of the growth plate, and healing occurs without major disruption to the growth plate (Iannotti et al., 1994; Peterson, 1996; Xian and Foster, 2006a).

Figure 1.4: Schematic illustration of the classification of growth plate injuries according to Salter and Harris. This classification system was based on the mechanism of injury, relationship of the fracture line to the cellular layers of the growth plate, and prognosis following disturbance to growth. Illustration taken from Young et al. (2005).

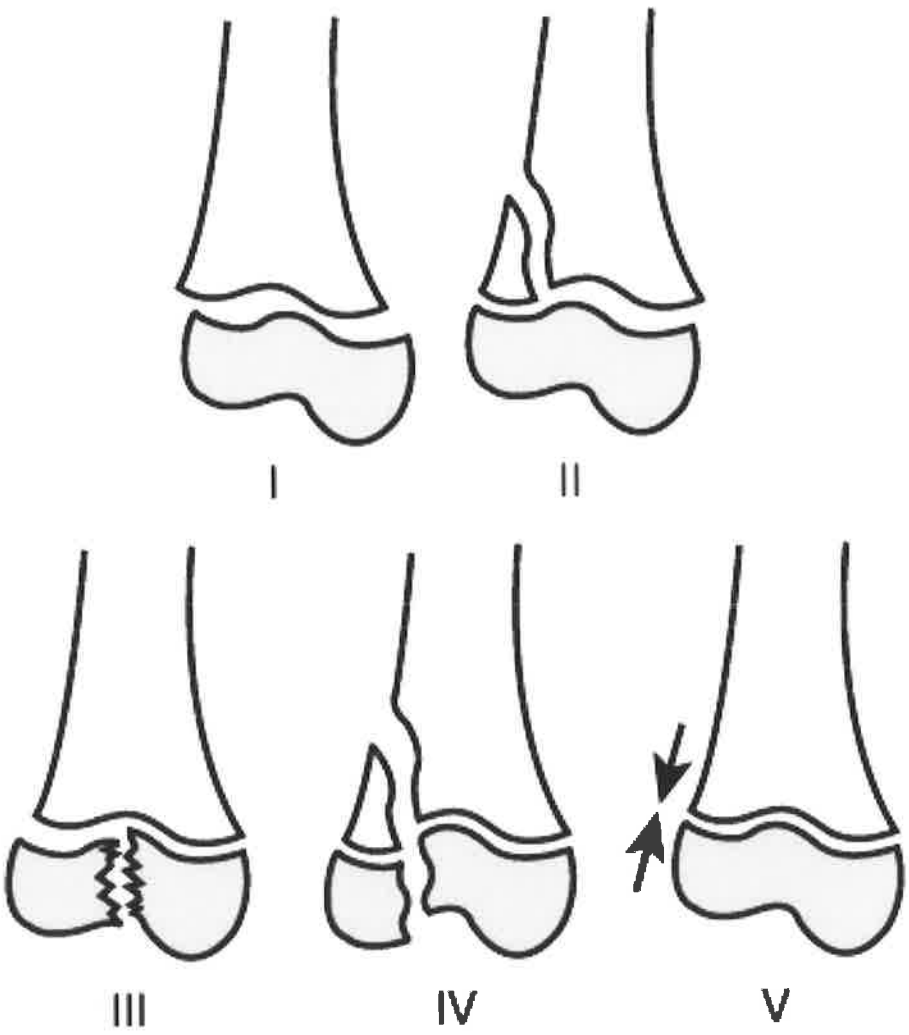
I
II
III
IV
V

However, in the instance of injury extending across all layers of the growth plate, from the epiphysis to the metaphysis (such as in Salter's type 3 and type 4 injuries), cellular debris, growth plate disorganisation and formation of a bone bridge can be observed (Iannotti et al., 1994; Xian and Foster, 2006a). Communication of the epiphysis, metaphysis and corresponding blood supply is believed to be the major causative factor for bone bridge formation (Foster, 1989a). Animal studies exploring the response of the growth plate to partial ablation, have shed some light on the sequence of events leading to bone bridge formation (Foster, 1989a; Lee et al., 2000; Thomas et al., 2005; Wirth et al., 1994; Xian et al., 2004). Initially, there is formation of fibrous tissue within the separated physeal components and an infiltration of mesenchymal cells. If the gap is small, minimal fibrous tissue is necessary and the defect can be slowly replaced by diametric expansion of the adjacent growth plate chondrocytes. Conversely, a larger gap often displays irregular healing firstly characterised by a loss of normal cell architecture. The growth plate adjacent to the injury site degenerates and grows in the direction of the metaphysis. Diametric expansion of the adjacent chondrocytes is minimal, and as a result there is non-union of the growth plate. These larger defects also increase the potential for vascularity. The presence of a blood supply amplifies the propensity for ossification of the fibrous tissue containing mesenchymal progenitor cells which potentially can differentiate into bone cells. If this occurs, small trabeculae develop within the defect which expand and mature, leading to a complete replacement of the fibrous fissure with bone (Xian and Foster, 2006a).

The substitution of damaged growth plate cartilage with osseous tissue is known as a bone bridge (Figure 1.5). Consequently, the functionally undesirable repair of growth plate cartilage following injury can have serious repercussions on growth plate structure and biomechanics. Impairment of growth plate physiology can lead to growth arrest and consequently, limb abnormalities. When the entire growth plate is obstructed, often through the formation of a bone bridge, this can manifest in a limb length discrepancy. This can be further complicated if only a portion of the growth plate is damaged. In addition to limb length discrepancy, presence of a bone bridge can result in angular deformity of the limb (Moseley, 1987).

Figure 1.5: Formation of an osseus bridge following growth plate injury. Under Magnetic Resonance Imaging (MRI), the growth plate appears transparent as the tissue is comprised of cartilage. In this instance a bone bridge has developed through the central portion of the tibial growth plate as indicated by an arrow. Development of a large bone bridge can disrupt growth plate function and may result in limb abnormalities.

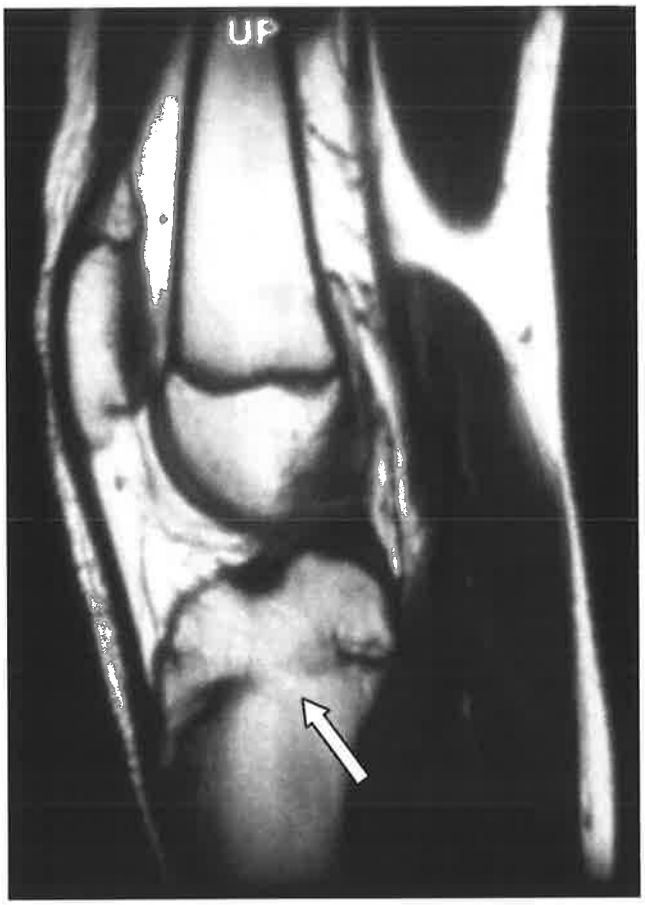
UP

1.17. Current Treatments for Growth Arrest

The clinical intervention of growth plate fractures to minimise abnormal growth is largely dependent on the age of the patient and type of injury sustained. For example, a patient approaching skeletal maturity may not require surgical management as the deformity will not significantly affect growth. In contrast, a young patient with significant pending growth may require surgery in order to maximise growth potential and prevent abnormality.

Currently, there are several modes of therapy to correct both limb length and angular deformity (Foster et al., 2000; Hasler and Foster, 2002; Ilizarov, 1990; Ilizarov and Frankel, 1988; Langenskiold, 1975). The surgical approach is appropriate to the severity of the irregularity. A slight limb length discrepancy can be corrected with the use of a shoe lift. Occasionally the use of a shoe lift needs to be coupled with arrest of the remaining limb growth, to prevent angular deformity from occurring. Established angular deformity can be rectified by wedge osteotomy, where the bone is cut at an angle so as to open one side. Substantial limb length divergence is most commonly approached by bone lengthening or shortening procedures. Current surgical interventions either correct established growth discrepancies through limb lengthening, or minimise potential inconsistencies by resection of the bone bridge and insertion of interpositional materials. These interpositional materials attempt to permit regeneration of the cartilage peripheral to the injury site, and include fat, silicone, bone wax, and cement.

There are two common methods in practice for the correction of large limb length differences, the Ilizarov and Langenskiöld procedures. The Ilizarov technique employs lengthening of the shortened limb to equal that of the contralateral limb (Ilizarov and Frankel, 1988) by a process of distractional osteogenesis and was developed by in 1951 (Figure 1.6). A large frame is placed externally around the affected bone and anchored to the proximal and distal ends by wires. The shortened bone is broken in the diaphyseal region and distracted in increments using screws on the external frame. This strategy is highly invasive, time consuming and painful, and often leads to complications including pin site infection, fracture, dislocation, and more seriously compartment syndrome (increase in internal pressure). As the extent of lengthening is restricted, the procedure often needs to be repeated several times throughout adolescence until skeletal maturity in order to achieve the desired length.

Figure 1.6: Correction of large limb length discrepancies using the Ilizarov frame. The Ilizarov frame is commonly used to resolve discrepancies between limbs by lengthening the affected limb to match that of the contralateral limb (A). The bone is broken within the diaphysis and the frame is attached to the bone through a series of pins. Screws on the outside of the frame are used to elongate the frame which subsequently lengthens the bone (B). This method of distraction is highly invasive and painful, and is often accompanied by infection due to the pins which penetrate the skin. Photos kindly provided by Assoc. Prof. B.K. Foster.

A

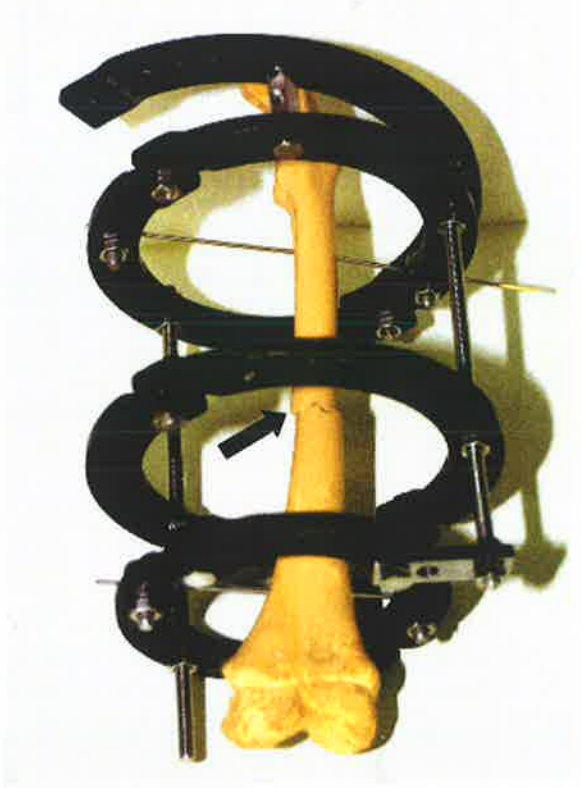

B

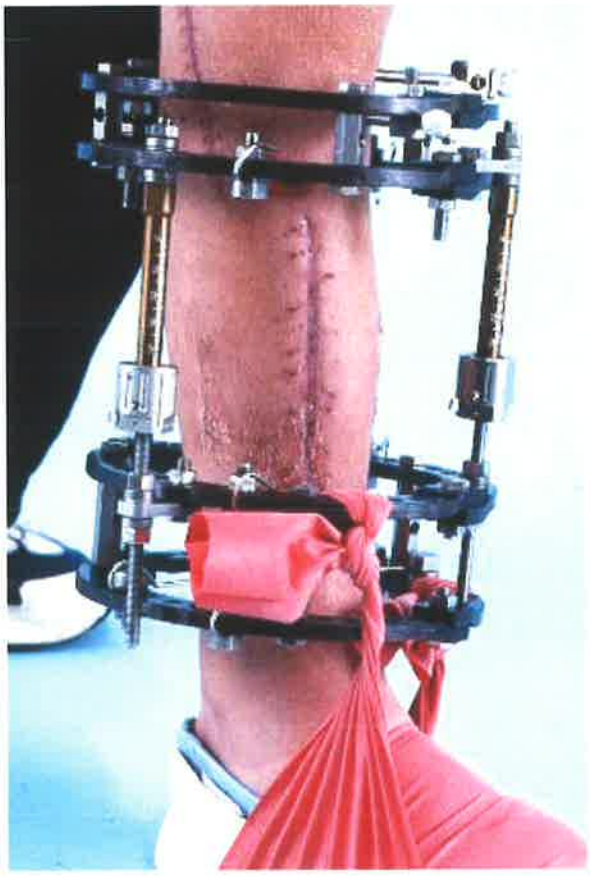

The Langenskiöld procedure involves the excision of an established bone bridge and substitution with autologous fat as an interpositional graft, to prevent reformation of a bone bridge and thereby prevent the progression of deformity by the correction of future growth (Foster et al., 2000; Langenskiold, 1981). However, although the improvement of angular deformity of patients has been documented (Langenskiold and Osterman, 1979), there are variable results in regard to longitudinal growth. Often some additional growth was achieved following removal of the bone bridge, but was not sufficient to restore limb length discrepancy. Despite the improvement of preoperative imaging methods, predictive factors, and continual review of criteria for Langenskiöld procedure, fair and poor results are still observed in 15% to 43% of patients who undergo the technique (Hasler and Foster, 2002). The most common causes of failure were incomplete resection or reformation of the bone bridge due to fat displacement or necrosis (Hasler and Foster, 2002).

A novel and recent technique for the restoration of unequal limb length is the use of internal distraction (FitBone) (Baumgart et al., 2005; Singh et al., 2006). This device is an intramedullary pin with telescopic action that is wirelessly triggered to extend by one millimetre per day in response to a transmitter. As there are no external pins or frame, pain is lessened, and the incidence of misalignment, infection and associated complications is greatly minimised. Hospitalisation time is reduced and weight bearing is possible at an earlier stage. However, the intramedullary pin is inserted from the epiphysis and thus through the growth plate, so is only a suitable therapy for the management of growth discrepancies in children approaching skeletal maturity.

Current treatment of growth plate injury attempts to correct the skeletal manifestation of damage incurred by the growth plate. Nonetheless, currently there is no biological based therapy to assist endogenous repair of the growth plate, in order to prevent the formation of a bone bridge and thus eradicate the requirement for corrective surgery.

1.18. Growth Plate Repair Using Chondrocyte and/or Growth Factors

Injury to the growth plate can lead to growth arrest and/or deformity depending on the size and location of the transphyseal bone bridge. The development of a biological based therapy is now under close investigation, with guidance from the more extensively studied field of articular cartilage regeneration. Research has incorporated the use of tissue grafts,

growth factor therapy and chondrocyte transplantation to reconstitute the damaged growth plate cartilage.

The administration of growth factors to growth plate defects has been investigated previously. Using a sheep model, BMP-7 was delivered to a peripheral growth plate injury in combination with a collagen-1 paste (Johnstone et al., 2002). BMP-7 has previously been shown to not only stimulate ectopic bone formation, but have an essential role in cartilage ECM synthesis, and used in the repair of full thickness articular defects in multiple species (Cook et al., 2003; Hidaka et al., 2003; Kuo et al., 2006; Louwerse et al., 2000). At the growth plate, BMP-7 promoted outgrowth of the physeal cartilage adjacent to the defect site. However, this expansion was eventually blocked by formation of a bone bridge within the defect. Therefore, this suggests a potential role for BMP-7 in growth plate cartilage repair, but, it appears that the collagen-1 paste is not a suitable interpositional material, as it may mediate or act as a template for bone formation. More recently, BMP-7 was administered in conjunction with the Langenskiöld procedure of an interpositional fat graft (Thomas et al., 2005). Although formation of a bone bridge was prevented, histological and molecular evidence indicated that BMP-7 application stimulated expression of both chondrogenic and osteogenic markers. The failure of BMP-7 to induce chondrogenesis may be due to the temporary delivery BMP-7 in a single dose. The sustained delivery of growth factors within microcapsules may be a more advantageous strategy.

The feasibility of an autologous muscle interposition in combination with adenoviral mediated gene transfer of IGF-1 or BMP-2 to repair rabbit growth plate injury was investigated by Lee et al. (2002). Tibial shortening and bone bridge formation was observed in the untreated and muscle graft/adBMP-2 treatment groups. Conversely, autologous muscle interposition alone or combined with adIGF-1 enabled the growth plate to remain open, suggesting that IGF-1 has a supportive effect on physeal chondrocytes, while BMP-2 increases osteogenic activity within the injured growth plate (Lee et al., 2002).

The implantation of allogeneic foetal growth plate chondrocytes into injured lamb growth plates has also been examined (Foster et al., 1990). Following transplantation, the chondrocyte cultures survived, proliferated and produced a cartilage like ECM. In addition, at 2-3 months, cells organised into longitudinal columns, underwent hypertrophy

and integrated well to the process of endochondral ossification. Cell survival was variable and occasionally resulted in a cartilage matrix devoid of chondrocytes, possibly due to a local inflammatory reaction in response to the allogeneic transplant (Foster et al., 1990). Furthermore, the implantation of a cartilage disc always prevented formation of a bone bridge (Foster et al., 1990). A similar technique using canine new born epiphyseal chondrocytes to regenerate growth plate cartilage has been reported (Park et al., 1994). Although cell survival and immunological response were not illustrated, gross findings indicate the implantation of a chondrocytic disc reduced both angular deformity and limb length discrepancy compared to cell free controls (Park et al., 1994). However, a major limitation of these studies is the impracticality of using growth plate chondrocytes harvested from human tissue, especially from foetal or post natal tissues.

Two studies have approached the use of allogeneic chondrocytes sourced from articular surfaces in rabbits (Lee et al., 1998; Tobita et al., 2002). Both employed the use of a cell carrier to deliver cultured chondrocytes to a large (50%) growth plate defect. In the first study, chondrocytes were embedded within agarose and transplanted to a growth plate defect immediately post-injury, and following resection of a previously established bone bridge. Growth arrest and angular deformation were prevented in the case of cell transplantation immediately following injury. Conversely, implantation following excision of a bone bridge reversed growth arrest, but did not restore full longitudinal growth. Labelling of cells confirmed viability within the new host physis, and in most instances columnar arrangement was observed. However, the presence of agarose alone did not prevent bone bridge formation, and is therefore not suitable as an interpositional graft. As the clinical safety of agarose is unknown, in the second study, articular chondrocytes were implanted within type-1 collagen gel (atelocollagen) (Tobita et al., 2002). A reduction in angular deformity and length discrepancy following transplantation of cells in atelocollagen was observed. Additionally, chondrocyte transfer was superior to that of a fat interpositional graft.

The collection of chondrocytes from the human body is not ideal. Isolation of human foetal chondrocytes is not ethically possible and the harvest of autologous articular chondrocytes is invasive and requires damage to an otherwise healthy joint surface. Since the identification of chondrocyte progenitor cells in adult tissues, interest has swung to the application of mesenchymal stem cells for growth plate regeneration. The application of MSC to growth plate defects will be discussed in section 1.20.2.

1.19. Mesenchymal Stem Cells

The possibility of the existence of progenitor cells within the bone marrow became apparent through studies where ablated bone marrow (BM) by various mechanisms spontaneously regenerated, and the development of a BM organ following transplantation of BM to an ectopic site (Friedenstein, 1980; Knospe et al., 1966; Patt and Maloney, 1975; Simmons et al., 1987; Tavassoli and Crosby, 1968; Tavassoli and Khademi, 1980). Pioneering studies by Friedenstein directly demonstrated the presence of bone marrow mesenchymal stem cells (MSC) from BM explants, by growth of plastic-adherent colonies of cells with a fibroblast-like morphology, termed colony forming unit-fibroblastic (CFU-F) (Friedenstein et al., 1976; Knospe et al., 1972; Owen, 1988; Simmons et al., 1991). Although initially identified in rat, subsequent studies have isolated bone marrow MSC from humans (Castro-Malaspina et al., 1980), goat (Fischer et al., 2003; Murphy et al., 2003), rat (Lennon and Caplan, 2006; Yoshimura et al., 2007), rabbit (Awad et al., 1999), mouse (Tropel et al., 2004), horse (Fortier et al., 1998), cow (Bosnakovski et al., 2005), dog (Kadiyala et al., 1997), cat (Martin et al., 2002), sheep (Jessop et al., 1994; Rhodes et al., 2004; Zhang et al., 2004), pig (Ringe, 2002; Vacanti, 2005; Moscoso, 2005) and non-human primates (Devine et al., 2003). A consistent feature of bone marrow derived colonies across all species is the heterogeneity in size, morphology, proliferation, enzyme histochemistry, and developmental potential (Owen, 1988). Various techniques have established that the CFU-Fs observed are clonal in origin, supporting the hypothesis that the bone marrow contains a small population of self-renewable, pluripotent progenitor cells (Figure 1.7). MSC share similarity to haematopoietic stem cells (HSC) in that they are found endogenously in a non-cycling state and are quiescent within the body (Castro-Malaspina et al., 1980; Castro-Malaspina et al., 1981). Numerous studies have demonstrated the multilineage differentiation capacity of MSC, which has stimulated significant research in the potential use of these cells for therapeutic application and will be discussed further in section 1.20.

Since the identification of bone marrow MSC, the isolation and characterisation of MSC from connective tissues other than the bone marrow have been investigated. To date, progenitor cells demonstrating morphological, histochemical, and multilineage similarities to bone marrow-derived MSC have been isolated from fat (Gronthos et al., 2001a; Zannettino et al., 2008; Zuk et al., 2001), muscle (Bosch et al., 2000), synovial membrane (De Bari et al., 2001b), periosteum (De Bari et al., 2001a; Nakahara et al., 1991), bone

Figure 1.7: Schematic illustration of the hypothetical hierarchy of mesenchymal stem cell differentiation. The mesenchymal stem cell (MSC) is capable of self renewal and has the potential to differentiate into one or more of the many connective cell types shown in vitro and in vivo. The MSC and committed progenitors are capable of forming clonogenic clusters (CFU-F) in vitro. Adapted illustration kindly provided by A/Prof. S. Gronthos.

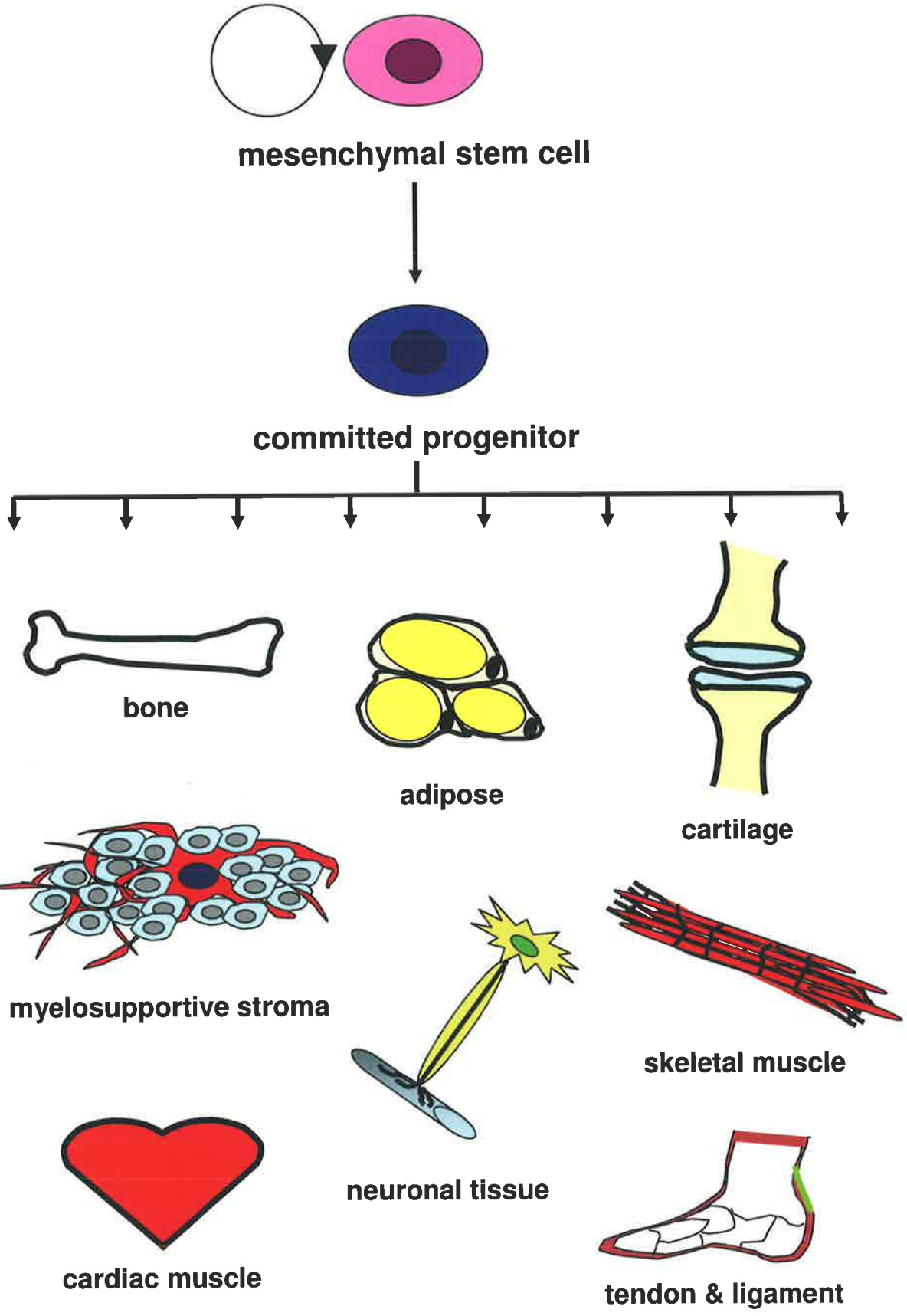
mesenchymal stem cell
committed progenitor
bone
adipose
cartilage
myelosupportive stroma
neuronal tissue
skeletal muscle
cardiac muscle
tendon & ligament

(Noth et al., 2002; Osyczka et al., 2002; Tuli et al., 2003), dental tissues (Gronthos et al., 2000; Miura et al., 2003; Seo et al., 2004), blood (Kuznetsov et al., 2001; Zvaifler et al., 2000), umbilical cord blood (Hou et al., 2003; Korbling et al., 2005), pericytes (Brighton et al., 1992; Reilly et al., 1998), and skin (Young et al., 2001).

1.19.1. Comparison of MSC from Different Sources

In the past it has been assumed that irrespective of the site of origin MSC are relatively comparable, given they all exhibit proliferative potential, multipotential differentiation capability, and express similar extracellular matrix molecules. More recently, a series of comparative studies have been undertaken to define discrepancies between MSC harvested from different sources, specifically pertaining to selection of a suitable harvest site for tissue regeneration. The characteristics of bone marrow and adipose derived MSC have been examined in several cases using human patient matched samples (Afizah et al., 2007; De Ugarte et al., 2003; Huang et al., 2005). In one study, the yield, growth rate and differentiation potential were reported to be equivalent (De Ugarte et al., 2003), whereas other studies demonstrated in vitro chondrogenesis was superior with BM derived progenitor cells (Afizah et al., 2007; Huang et al., 2005). A comparison of rat MSC derived from bone marrow, synovium, periosteum, adipose tissue and muscle revealed the synovium as an optimal source of progenitor cells (Yoshimura et al., 2007). The yield of CFU-F, growth rate, and chondrogenic potential exceeded that of other tissues, a finding supported by similar comparison between BM and synovial MSC (Shirasawa et al., 2006). Adipogenic potential was equivalent between synovial and adipose tissues, whereas osteogenic potential was greatest in cells derived from the periosteum and muscle. A parallel study in patient matched humans reported some discrepancies to the rat study (Sakaguchi et al., 2005). The growth rate and chondrogenic capacity of bone marrow, synovial, and periosteal MSCs were determined to be equivalent. Optimal adipogenesis was observed by synovial and adipose tissue MSC, with superior osteogenic differentiation in bone marrow, synovial, and periosteal MSC. Rabbit MSC obtained from BM, periosteum, and adipose tissue displayed equivalent proliferation rates, osteogenic and chondrogenic potential in vitro, however upon transplantation to a growth plate cartilage defect, only BM and periosteal derived cells were capable of correction of physeal arrest (Hui et al., 2005). Taken together, although these studies are not entirely consistent, they do suggest that the local environment at the site of the harvest tissue may influence the developmental potential of MSC.

1.19.2. MSC Isolation and Enrichment

The incidence of clonogenic MSC in human bone marrow is reported to range from 1 to 20 per 10^5 mononuclear cells plated (Castro-Malaspina et al., 1980; Falla et al., 1993; Simmons and Torok-Storb, 1991b; Walker, 1995). The low frequency of progenitor cells is a major limitation to the application of these cells in a therapeutic setting. The initial technique for isolating MSC based upon their adherence to tissue culture plastic and rapid proliferation results in a heterogeneous pool of BM cells, of which only a minor proportion are multipotent BM derived MSCs (Castro-Malaspina et al., 1980; Friedenstein, 1980; Simmons and Torok-Storb, 1991b). One technique to facilitate isolation and enrichment is the selection of MSC according to the expression of specific cell surface antigens, which has been somewhat hampered due to the paucity of antibodies that can identify and enrich for MSC. One of the first antibodies demonstrated to enrich MSC from human bone marrow aspirates was STRO-1. STRO-1 is expressed by approximately 10% of the bone marrow mononuclear cell population (Simmons and Torok-Storb, 1991b). Essentially, all detectable clonogenic CFU-Fs are included within the STRO-1^+ bright population (Gronthos et al., 2003; Simmons and Torok-Storb, 1991b). The CFU-F can be further restricted to cells that have an absence of glycophorin A expression (Simmons and Torok-Storb, 1991b; Zannettino et al., 2007).

Vascular cell adhesion molecule (VCAM-1; CD106) is a cell surface marker constitutively expressed by cells of the bone marrow in vitro and in vivo, and cultured MSC (Simmons, 1992). The combined selection of bone marrow cells with both STRO-1 and VCAM-1 antibodies enabled the resolution of a discrete population of cells with a cloning efficiency for CFU-F approaching 50% (Gronthos et al., 2003). The degree of enrichment of CFU-F within this fraction is approximately 5,000 fold relative to that of unfractionated bone marrow. Furthermore, the selected population of MSC exhibits extensive proliferation and retains the capacity for multilineage differentiation.

Immunoselection of MSC has been undertaken using various other antibodies, but not with the same enrichment potential as STRO-1/VCAM-1. The SB-10 antigen identified as CD166 (activated leukocyte adhesion molecule; ALCAM) appears to be a marker of pluripotency as its expression is down regulated following osteogenic differentiation (Bruder et al., 1997). The SH-2 antibody is reactive for an epitope present on the TGF-β receptor, endoglin (CD105) is predominantly associated with endothelial cells

(Haynesworth et al., 1992a). Both the SH3 and SH4 antibodies recognise distinct epitopes of the membrane bound ecto-5'-nucleotidase (CD73) (Haynesworth et al., 1992a). All the aforementioned antibodies do not recognise osteocytes or haematopoietic cells.

Supplementary to STRO-1, VCAM-1, ALCAM, Endoglin, and CD73, the cell surface expression profile of MSC also includes receptor molecules for Muc-18 (CD146), ICAM-1 (CD54), hyaluronate (HCAM/CD44), EGF, PDGF (CD140a), IGF-1, TGFβ, FGF-2 and a multitude of integrin subunits (Filshie et al., 1998; Gronthos and Simmons, 1995; Haynesworth et al., 1992a; Simmons et al., 1994). Integrins are a large family of cell surface receptors which mediate adhesion interactions between cells and the surrounding ECM. These molecules are transmembrane bound heterodimers comprised of an α and β subunit. The connection between integrin receptors and corresponding ligands has been linked to many cell proliferation, differentiation, survival, motility and embryogenesis (Gronthos et al., 2001b; Simmons et al., 1994). It is presumed that the expression of integrins allow MSCs to home to sites of injury, to bind to specific matrix molecules, and to regulate cellular processes. MSCs express integrin α1 (CD49a), α2 (CD49b), α5 (CD49e), α6 (CD49f), αv (CD51), β1 (CD29), β3 (CD61), and β5 subunits in an assortment of combinations with variable intensities (Gronthos et al., 2001b; Majumdar et al., 2003).

Cultured MSC express various fibroblastic and osteoblastic related markers including alkaline phosphatase, collagen types 1, 3, and 10, osteopontin, osteonectin, smooth muscle actin, and adipogenic marker LPL (Gronthos et al., 2003). MSC have the capacity to produce a spectrum of cytokines, and constitutively secrete IL-6, IL-7, IL-8, IL-11, IL-12, IL-14, IL-15, LIF, SCF, M-CSF, and Flt-3 ligand (Azizi et al., 1998; Haynesworth et al., 1996; Majumdar et al., 1998). These cytokines and growth factors regulate proliferation, differentiation and maintenance of surrounding cells, especially in regard to the maintenance of haematopoiesis within the bone marrow microenvironment.

Until recently, the anatomical distribution of MSC within the bone marrow has been unknown. Current evidence points towards pericytes of the blood vessel wall. Gronthos et al. (2003) reported that 70% of STRO-1/VCAM-1 bright selected MSC expressed α-smooth muscle actin (α-SMA) (Gronthos et al., 2003). As over 50% of these cells give rise to CFU-F, a significant proportion must express α-SMA. Within the bone marrow microenvironment α-SMA is observed in a pattern restricted to the vascular smooth muscle

cells of arteries, and in the pericytes lining the capillaries (Bianco et al., 2001). Furthermore, MSC in culture exhibit phenotypic similarities characteristic of vascular pericytes (Doherty et al., 1998; Galmiche et al., 1993). Cultured pericytes and MSC synthesise a comparable selection of extracellular matrix proteins comprising basal lamina and interstitial collagens. The responses of MSC and pericytes to PDGF-B demonstrate a close association; PDGF-B is essential for pericyte recruitment and maintaining viability in vivo, and MSC proliferate in response to supplementation under serum free conditions (Gronthos and Simmons, 1995; Hellstrom et al., 1999). These observations advocate the interpretation that MSC are vascular pericytes that reside within the perivascular niche.

1.19.3. In Vitro Expansion of MSC

Due to the limited number of MSCs that can be isolated, MSCs need to be expanded in tissue culture to a sufficient quantity for therapeutic application. Standard expansion of MSC requires supplementation with foetal calf serum; however the components of serum may interfere with and modify the response of exogenously added factors. The growth factor requirement for bone marrow derived STRO-1 positive MSC was investigated by Gronthos et al. (1995). Growth factors were examined for their ability to initiate and support clonogenic growth of CFU-F under serum free conditions. It was demonstrated that clonogenic growth was dependent on the presence of a mitogenic growth factor (Gronthos and Simmons, 1995). Platelet derived growth factor (PDGF) and epidermal growth factor (EGF) exhibited the greatest stimulation of growth in a dose dependent manner. In addition, it was demonstrated that cells of the CFU-F constitutively express receptors for PDGF and EGF. Although MSC also express receptors for IGF-1 and NGF, these factors did not support colony growth. The glucocorticoid dexamethasone and L-ascorbate were also found to be essential for colony development in serum deprived conditions (Gronthos and Simmons, 1995).

In contrast to the study conducted by Gronthos and colleagues (1995), there are many reports documenting the mitogenic effect of FGF-2 supplementation on MSC proliferation (Baddoo et al., 2003; Bianchi et al., 2003; Locklin et al., 1995; Mastrogiacomo et al., 2001; Solchaga et al., 2005; Sotiropoulou et al., 2006). Multipotential capacity was retained following expansion with FGF-2 and in some cases chondrogenesis and osteogenesis were enhanced. However, a proportion did not perform expansion under serum deprived

conditions, therefore it is unknown if the presence of FCS enhanced or inhibited the effect of the added growth factors observed

1.19.4. In Vitro Differentiation of MSC

The potential of human MSC to differentiate in vitro into cells of the osteogenic, adipogenic and chondrogenic lineages has been well established (Gimble, 1998; Gronthos et al., 2003; Johnstone et al., 1998; Mackay et al., 1998; Pittenger et al., 1999). Osteogenic differentiation of MSCs in vitro requires the presence of inorganic phosphate, the glucocorticoid dexamethasone, ascorbate, and β-glycerophosphate. When cultured in monolayer for several weeks with appropriate supplementation, osteogenic differentiation is characterised by the expression of bone related markers bone sialoprotein and osteocalcin, and accompanied by formation of small mineralised nodules throughout the monolayer culture. These nodules are positive for Von Kossa staining and are composed of hydroxyapatite crystals identical to that observed in bone.

The induction to that of a chondrocytic phenotype was initially performed using rabbit culture expanded CFU-F. Single cell suspensions were grown in aggregate cultures, in the presence of ascorbate and TGF-β1 (Johnstone et al., 1998; Yoo et al., 1998). Generally, among a variety of species, chondrogenesis is dependent on a three dimensional culture format, serum free conditions and the presence of a member of the TGFβ superfamily. TGF-β1, 2 (Barry et al., 2001b; Bosnakovski et al., 2005; Worster et al., 2000)and TGF-β3 (Mackay et al., 1998; Majumdar et al., 2000; Pittenger et al., 1999) are all capable of chondrogenic induction, but appear to have differing levels of efficacy depending on the species. Under these conditions the MSC lose their fibroblastic morphology, become rounded, and initiate expression of a number of cartilage specific extracellular matrix components. Differentiation to a chondrogenic phenotype is inferred by the down regulation of collagen-1 expression, and upregulation of cartilage specific markers collagen-2, collagen-10 and aggrecan, and rapid synthesis of sulfated proteoglycans. Human MSC stimulated by TGF-β3 appear to express versican, fibromodulin and decorin to form the earliest extracellular matrix components, with aggrecan and biglycan incorporated at a later stage (Barry et al., 2001b).

Although MSC chondrogenesis was initially demonstrated using members of the TGF-β family, many other growth factors have been revealed to induce chondrogenic

differentiation of both primary and cultivated (cell line) mesenchymal progenitors. Members of the BMP subfamily, including BMP-2, BMP-6, and BMP-9, all stimulate morphological changes and expression of cartilage specific markers (Denker et al., 1999; Majumdar et al., 2001; Sekiya et al., 2001). The combinatorial addition of BMP and TGFβ appear to accelerate and intensify the differentiation process (Schmitt et al., 2003; Sekiya et al., 2001; Sekiya et al., 2005; Toh et al., 2005). Several studies have also established a synergistic effect on chondrogenesis using IGF-1 with TGF-β1 or TGF-β3 (Fukumoto et al., 2003; Indrawattana et al., 2004; Worster et al., 2001). It should be noted that many of the growth factors mentioned above can also induce osteogenesis under different conditions, so caution is warranted for the application of 'chondrogenic' growth factors for cartilage regeneration.

Adipogenic differentiation of MSC in monolayer can be achieved by supplementation with isobutylmethylxanthine, hydrocortisone and indomethacin (Gimble, 1998). This process can be morphologically characterised by the production of large lipid filled vacuoles and genetic upregulation of transcription factor peroxisome proliferator-activated receptor-gamma (PPAR-γ), as well as leptin.

Although the differentiation of MSC to cells of bone, fat and cartilage tissue have been the most frequently documented, parallel studies have also presented evidence that MSC can differentiate beyond that of the connective and supportive tissues. It has now been demonstrated that MSCs also exhibit plasticity and a capable of differentiation into neuronal-like cells including astrocytes and neurons, cardiomyocytes, hepatocytes, mesangial cells, and myocytes (Bianco et al., 2001; Jiang et al., 2003b; Kopen et al., 1999; Ong et al., 2006; Pittenger et al., 1999; Verfaillie et al., 2003; Woodbury et al., 2000; Zhao et al., 2002).

1.20. The Application of MSC to Repair Musculoskeletal Defects

Due to the potential of ex vivo expansion and differentiation into a variety of connective tissues, in the last 15 years, the use of MSCs to repair musculoskeletal defects has increasingly been investigated for potential therapeutic application. MSC have been demonstrated to have the potential in the repair of cardiovascular tissue (Orlic et al., 2001b; Stamm et al., 2003), spinal fusion (Muschler et al., 2005), segmental bone defects (Bruder et al., 1998a; De Kok et al., 2003; Petite et al., 2000; Quarto et al., 2001),

craniotomy defects (Krebsbach et al., 1998), articular cartilage defects (Murphy et al., 2003; Ponticiello et al., 2000; Solchaga et al., 2002; Wakitani et al., 1994), and growth plate injury (Chen et al., 2003a; Hui et al., 2005; Li et al., 2004). Attempts at cartilage tissue engineering using MSC will be discussed in greater detail.

1.20.1. Articular Cartilage Repair Using MSC

The initial study of the potential of MSC to repair articular cartilage was performed by Wakitani and colleagues (1994). Osteoprogenitor cells of rabbit bone marrow and periosteum were isolated by plastic adherence and dispersed within a collagen-1 gel. These constructs were transplanted into large full thickness articular defects of rabbits. Two weeks post transplantation, MSC had uniformly differentiated into chondrocytes throughout the defect and in addition the subchondral bone was repaired (Wakitani et al., 1994). It was hypothesised that full thickness repair occurs via an endochondral process. Transplanted cells initially differentiate within the defect site into chondrocytes, and at the subchondral bone zone cells progress to a hypertrophic state, at which point are targeted for erosion, vascular invasion and subsequent mineralisation to regenerate the subchondral bone. Furthermore, there appeared to be no difference in the repair response between the progenitor cells derived from bone marrow or periosteum. Continuing on from this work, autologous BM MSC have been clinically assessed for application to articular defects in patients with osteoarthritic knee joints (Wakitani et al., 2002). Expanded cells embedded within a collagen gel were transplanted into articular defects and covered with autologous periosteum. Ten months after surgery, the defects were covered with a white soft tissue resembling hyaline cartilage. Arthroscopic and histological evaluations showed better repair outcomes in the cell transplanted group than in the cell free group.

Successful regeneration of meniscal-like tissue in a caprine model of osteoarthritis has recently been documented, without the use of a solid biomatrix (Murphy et al., 2003). Autologous MSCs suspended in a dilute solution of sodium hyaluronate were locally injected into the knee joint six weeks after total medial meniscectomy. In cell treated joints, implanted cells contributed to repair of the damaged tissue, as inferred by detection within the neomeniscal tissue. Degeneration of the articular cartilage and subchondral bone was also reduced; suggesting that local delivery of MSC can stimulate regeneration of the meniscus and retard the progressive destruction of the joint surface, both of which are characteristic of osteoarthritis.

The direct injection of BM MSC to full thickness articular defects in rabbits reported partial regeneration of cartilage tissue (Im et al., 2001). Spontaneous repair of the articular surface within members of the control group highlights the individual differences in ability to self-repair. In addition, some variability between samples was observed, which may be attributed to leakage of cells from the sutured defect.

As hyaluronan is a major component of the cartilage ECM, the use of hyaluronan as a scaffold for cartilage regeneration has been explored. MSC were seeded within a hyaluronan based scaffold, and transplanted into rabbit full thickness articular lesions (Gao et al., 2002; Kayakabe et al., 2006; Radice et al., 2000; Solchaga et al., 2002). Healing and integration of the subchondral bone and articular surface were observed, with neocartilage morphology and matrix expression comparable to that of the adjacent cartilage. Interestingly, transplantation of MSC seeded hyaluronan sponge did not exert a significant advantage in comparison to the scaffold alone, suggesting that hyaluronan itself can elicit a positive biological effect on osteochondral repair.

Repair of full thickness defects by transplantation of MSC has also been documented using polylactic acid (Yan and Yu, 2007), polyglycolic acid (Yan and Yu, 2007), gelatin (Ponticiello et al., 2000; Quintavalla et al., 2002) and a hyaluronic acid- gelatin composite (Liu et al., 2006).

1.20.2. Growth Plate Cartilage Repair Using MSC

The application of MSC in growth plate cartilage repair has not been extensively investigated. Nonetheless two similar studies have approached the repair of large growth plate defects in rabbits using allogenic periosteal derived MSC (Chen et al., 2003a; Li et al., 2004). Both studies used MSC derived from the periosteum, the former transplanted cells within agarose gel, while the latter employed a natural polymer chitin. In each instance, following excision of an established bone bridge, the transplanted MSC-scaffolds corrected growth arrest and angular deformity. The transplanted MSC differentiated into chondrocytes, which integrated, aligned into columns, and closely resembled native growth plate cartilage. Moreover, whereas the transfer of agarose alone did not prevent bone bridge formation, the interposition of chitin did correct deformity, almost to that of MSC, indicating a potential role as an interpositional material.

Ahn and colleagues investigated the use autologous rabbit bone marrow derived MSC in conjunction with gelatin scaffold and growth factor TGF-β3 (Ahn et al., 2004). The application of MSC within the Gelfoam resorbable sponge, in media containing chondrogenic factor TGF-β3, lead to no significant varus deformity or limb length discrepancy. The presence of MSC alone promotes but does not guarantee cartilage healing; the addition of TGF-β3 provides an appropriate external signal for chondrogenesis. Labelling of transplanted cells revealed differentiation of MSC into a chondrogenic phenotype and maintenance within the repair tissue for three weeks. Histological examination showed a predominance of irregularly arranged chondrocytes within a sulfated GAG rich matrix (Ahn et al., 2004). More recently, a comparison between the regenerative potential of MSC derived from bone marrow, periosteum and adipose tissue for growth plate cartilage repair, found that limb angularity and length discrepancies in rabbits were only corrected using MSC harvested from the BM and periosteum, and not adipose tissue (Hui et al., 2005).

Although the aforementioned studies have demonstrated the potential of MSC in growth plate regeneration, in order to translate this research into clinical application, characterisation of the similarities and differences between animal and human MSC needs to be elucidated. To date, the use of MSC in growth plate repair has only been explored in a rabbit model, which has an exceptional inherent ability to regenerate cartilage. Therefore it would be advantageous to undertake further studies of growth plate regeneration using a larger animal model, to gather information that may eventually be applicable to human studies.

Overall, insights into the critical factors that regulate MSC migration, proliferation and differentiation will augment the development of techniques for the engineering of cartilage tissue, and therapeutic application in articular and growth plate cartilage regeneration. As MSC are multipotential, directed differentiation of these cells to the desired (and not undesired) lineage is paramount for regeneration of specific tissue. Eventual success will also be dependent on the characterisation of growth factors and culture conditions that facilitate chondrogenesis of either introduced or endogenous progenitor cells, and the identification or manufacture of biological or synthetic matrix scaffolds, to act as the delivery vehicle for cells and growth factors. Although considerable progress has been achieved to date, there are still many questions remaining, especially in the field of growth plate cartilage repair.

1.21. Rationale, Hypothesis and Aims of the Current Study

Injury to the growth plate in children can give rise to limb length discrepancy and angular deformities. Current treatments of the deformities arising from damage to the growth plate are of a surgical nature, and involve correction of the deformity rather than prevention. Additionally, restoration of normal function of the growth plate is never achieved. As yet, there is no biological based therapy for regeneration of growth plate cartilage. Bone marrow MSCs offer a promising alternative to traditional therapies due to ease of harvest from the body, high proliferative capacity in vitro, and chondrogenic potential. Although there have been some recent investigations in rabbit or rodent models examining potential applications of MSCs in repairing injured growth plate with some success (Ahn et al., 2004; Chen et al., 2003a; Hui et al., 2005; Lui et al., 1995), the therapeutic potential of MSCs in growth plate regeneration remains to be investigated in a large animal model. This project is interested in the repair response initiated by the application of autologous MSC to a growth plate injury using an immature sheep model. However, the characteristics of sheep MSC have been poorly described, so initial research will attempt to characterise the properties of these cells in vitro and in vivo.

Hypothesis:

It is hypothesised that sheep BM MSC will share many characteristics with human MSC in vitro and in vivo, and that delivery of MSC to the site of the growth plate will augment the repair of growth plate cartilage. Furthermore it is hypothesised that transplantation of a scaffold alone will inhibit bone bridge formation.

Project Aims:

1. Determine the characteristics of ovine BM derived MSC in vitro, in regard to incidence, morphology, proliferative response to mitogens, and multipotential differentiation capacity, specifically the optimal growth factors for chondrogenesis.
2. Define the cell surface expression profile of ovine BM MSC, cultured chondrocytes and articular chondrocytes, examine the potential enrichment of BM MSC using these antibodies, and elucidate the antigenic target of two novel anti-sheep MSC antibodies.
3. Examine the differentiation potential of ovine BM MSC in vivo, and determine the optimal delivery scaffold for chondrogenic differentiation of these cells.
4. Investigate the tissue repair response following application of autologous MSC to a growth plate injury using a lamb model.

CHAPTER 2

MATERIALS & METHODS

2.1. Cell Culture

All tissue culture was performed in Class 2 'biohazard' laminar flow hoods (BioAir Instruments, Siziano, Italy). Cell cultures were incubated at 37°C (Forma Scientific air incubator), in the presence of 5% CO_2 to maintain a pH of 7.0 and relative humidity of 97%.

Cell densities and viabilities were determined using a haemocytometer and Trypan blue dye exclusion. Cells were incubated briefly in 0.4% (w/v) Trypan blue solution (Sigma-Aldrich, St Louis, MO, USA) and counted using a light microscope.

2.1.1. Solutions and Buffers

2.1.1.1. β-Mercaptoethanol (β-ME)

1 M stock solution of β-ME was prepared by diluting 0.7 ml of 14.27 M β-mercaptoethanol (Sigma-Aldrich) into 9.3 ml Hank's Balanced Salt Solution (HBSS, SAFC Biosciences, Lenexa, KS, USA) and was stored at -20°C.

2.1.1.2. 10% (w/v) Bovine Serum Albumin (BSA)

To prepare 10% (w/v) BSA, 20g BSA (JRH Biosciences, Lenexa, KS, USA) was gently overlayed on the surface of 88.4 ml of Milli-Q water, and was allowed to sit at 4°C for 24 hours. Once dissolved, 3 g of AG® 501-X8 (D) Resin (Bio-Rad Laboratories, Hercules, CA, USA) was used to deionise the BSA and remove trace elements and contaminants. The beads were removed by filtration through Whatman No. 1 paper (Whatman, Maidstone, Kent, UK) when beads had changed colour from green to yellow. This procedure was then repeated 3 times. An equal volume (100ml) of 2 x DMEM (SAFC Biosciences)or 2 x PBS (JRH Biosciences) was added to the BSA solution, sterilised by filtration through a 0.22 µm bottle filter (Nalgene Nunc International, Rochester, NY, USA), and stored at -20°C.

2.1.1.3. Standard Wash Buffer for Cell Culture and Immuno Analysis (HHF)

To prepare HHF, HBSS was supplemented with 5% (v/v) foetal calf serum (FCS; Hyclone, South Logan, UT, USA or JRH Biosciences), sterilised by filtration through a 0.22 μm bottle filter, and stored at 4°C.

2.1.1.4. White Cell Fluid

To prepare white cell fluid, 2 ml acetic acid (BDH AnalaR®, Merck), was slowly added to 98 ml of MilliQ water. A few crystals of methyl violet (BDH Gurr®, Merck, Darmstadt, Germany) were added the solution and mixed well to ensure crystals were completely dissolved. The solution was subsequently filtered through a 0.22 μM minisart filter (Sartorius, Goettingen, Germany) and stored at room temperature.

2.1.2. Media

2.1.2.1. Alpha Minimal Essential Media-10 (α-MEM-10)

To prepare, alpha minimal essential media (α-MEM; JRH Biosciences) was supplemented with penicillin (50 i.u./ml)/streptomycin sulphate (50 μg/ml), 10% (v/v) FCS, 2 mM L-glutamine (SAFC Biosciences), 1 mM sodium pyruvate (SAFC Biosciences), and 100 μM L-ascorbate-2-phosphate (Asc-2-P, WAKO Pure Chemical Industries Ltd, Osaka, Japan). The medium was subsequently filter sterilised and stored at 4°C.

2.1.2.2. Alpha Minimal Essential Media-20 (α-MEM-20) for BM CFU-F Culture

This media is essentially as described for α-MEM-10, with 20% (v/v) FCS. To prepare, α-MEM was supplemented with penicillin (50 i.u./ml)/streptomycin sulphate (50 μg/ml), 20% foetal calf serum (FCS), 2 mM L-glutamine, 1 mM sodium pyruvate, and 100 μM ASC-2P. The medium was subsequently filter sterilised and stored at 4°C.

2.1.2.3. Dulbecco's Modified Eagles Medium-10 (DMEM-10)

To prepare 500 ml of DMEM-10, Dulbecco's Modified Eagles Medium (JRH Biosciences) was supplemented with penicillin (50 i.u./ml)/streptomycin sulphate (50 μg/ml), 10% (v/v)

FCS, 2 mM L-glutamine, 1 mM sodium pyruvate, 15 mM of N-2-Hydroxyethylpiperazine N'-2-ehtaneslphonic acid pH 7.2 (HEPES; JRH Biosciences), and buffered with 1 g sodium bicarbonate (Infectious Disease Laboratories, IMVS). The medium was subsequently filter sterilised and stored at 4°C. The media was replenished with 2 mM L-glutamine at weekly intervals.

2.1.3. Specimens

2.1.3.1. Isolation of Bone Marrow Samples

Fresh bone marrow (BM) aspirates were obtained from the iliac crest of adult sheep (approximately 1-4 years old) under general anaesthesia at Animal Services, IMVS. Coagulation of the bone marrow was minimised by rinsing of equipment used with 1000 Units/ml heparin (David Bull Laboratories, DBL, part of Mayne Pharma, Lake Forest, IL, USA). After dilution (approximately 1:2) in HHF, a white cell estimation was performed using white cell fluid to determine a pre-processing cell count. Small clots and bone chips were removed using a 70 μm cell strainer (Becton Dickinson, BD Biosciences, Franklin Lakes, NJ, USA). Bone marrow mononuclear cells (BM MNC) were isolated by gentle overlay in 14ml polystyrene round bottom tubes (Falcon, BD Biosciences) on a Lymphoprep™ density gradient (S.G. 1.077 g/ml) (Axis Shield or Nycomed, Oslo, Norway) and centrifugation at 1,400 rpm for 30 mins. Mononuclear cells at the interface were carefully removed and washed twice in HHF, by centrifugation at 1,400 rpm for 5 mins at 4°C. The cell pellet was resuspended in fresh HHF, and a post processing count was performed. BM MNC were then used for cell culture, immunological studies, or cryopreserved (at 2×10^7 cells per ampoule) for future use.

2.1.3.2. Sheep Primary Mesenchymal Stem Cell Cultures

Primary ovine MSC were isolated and expanded according to their plastic adhering ability. Briefly, single cell suspensions of BM MNC were plated in $75cm^2$ polypropylene flasks (Cellstar, Griener Bio-One) at a density of 7 to 13×10^4 cells per cm^2 (5×10^6 to 10×10^6 cells per flask) in α-MEM-10 media and subsequently incubated at 37°C in the presence of 5% CO_2. After 3 days, non adherent cells were removed by a quick rinse with HHF and fresh media was replaced. From that point, fresh media was exchanged twice weekly until

adherent cells were confluent, at which point cells were routinely detached by trypsin-EDTA digestion and passaged at lower density.

2.1.3.3. Sheep Chondrocytes

Single cell chondrocyte suspensions were obtained from euthanised adult sheep (Animals Services, IMVS) by enzymatic digestion. Briefly, using a scalpel, sterile scrapings of cartilage from the articular surface were collected under sterile conditions and suspended in α-MEM-10 media. Following gentle centrifugation at 1400 rpm for 5 minutes, shavings were washed twice in PBS and then digested in 10 ml solution containing collagenase type II (3 mg/ml working concentration, Worthington Biochemical Corporation, Lakewood, NJ, USA) and dispase (4 mg/ml working concentration, Roche, Basel, Switzerland) overnight at 37°C. The suspension was occasionally vortexed to facilitate disaggregation of the cartilage extracellular matrix. The suspension was then washed with HHF, spun at 1400 rpm for 10 mins, resuspended in α-MEM-10, strained using a 70 μm cell strainer (Falcon, BD Biosciences), and a cell count performed. These cells were then used for flow cytometry, RNA extraction, or cryopreserved.

2.1.3.4. Dedifferentiated chondrocytes

Regression of chondrocyte phenotype in vitro is initiated upon attachment of cells to plastic, and culture in monolayer. To generate dedifferentiated chondrocytes, single cell suspensions of sheep chondrocytes liberated from the native cartilage were transferred to $25cm^2$ or $75cm^2$ polypropylene flasks (Cellstar, Griener Bio-One) and cultured in α-MEM-10 at 37°C in the presence of 5% CO_2. On approaching confluence, cells were harvested by trypsin-EDTA detachment and repassaged at lower density, or used for in vitro assays, transplantation studies or cryopreservation.

2.1.3.5. Adherent Stromal Cell Lines

Human osteosarcoma cell lines MG63 and SAOS were provided by Dr. Karina Stewart (Bath Institute of Rheumatic Diseases, Bath, UK). Both cell lines were maintained in filter sterilised α-MEM-10 media, and harvested by detachment using trypsin digestion.

2.1.3.6. Human Normal Osteoblast Donor

Normal osteoblast like cells were obtained from young healthy donors according to the institutional ethics approved Normal Bone Marrow Donor Program. In summary, bone marrow donations were strained with a 70 μm cell strainer to isolate small bone chips. These were subsequently washed in HHF and cultured in α-MEM-10 supplemented with 100 μM L-ascorbate-2-phosphate at 37°C in the presence of 5% CO_2. Media was exchange twice weekly for 5 to 6 weeks until confluent. NOD cells were liberated and harvested by digestion with collagenase/dispase solution.

2.1.3.7. Human Mesenchymal Stem Cells

Bone marrow derived human MSC were similarly isolated from aspirates according to the protocol outlined above for sheep. Briefly, single cell suspensions of BM MNC collected by density gradient centrifugation were plated in polypropylene 75cm^2 flasks containing α-MEM-10 media and adherent cells were allowed to attach. After several days, the non-adherent cells were removed by media replacement, and adherent cells were cultured until confluent. Cells were enzymatically detached using trypsin.

2.1.4. Enzymatic Digestion of Adherent Cell Types

2.1.4.1. Trypsin-EDTA Digestion

Trypsin digestion solution was prepared by the addition of 0.05% (w/v) trypsin (Gibco, Invitrogen, Carlsbad, CA, USA) and 0.5 mM EDTA (BDH AnalaR®, Merck) in sterile PBS. To detach cells using this method, trypsin was warmed to 37°C in a water bath, and concurrently, the medium from adherent cultures was removed and cells rinsed with PBS. Following removal of the PBS, 1ml per 25 cm^2 flask surface area of trypsin solution was added to the cells and placed in a 37°C incubator for 5 mins to detach the cells. The trypsin reaction was inactivated by the addition of HHF, and cells were further washed in HHF prior to use.

2.1.4.2. Collagenase/Dispase Digestion

Adherent cell cultures were washed in PBS and incubated in a prewarmed solution of Type II collagenase (3 mg/ml working concentration, Worthington Biochemical Corporation) and dispase (4 mg/ml working concentration, Roche) (1 ml per 25 cm^2 flask surface area) for 60 mins in a 37°C incubator. Single cell suspensions were subsequently washed twice in HHF to neutralise the enzymatic digestion process.

2.1.5. Cryopreservation

2.1.5.1. Cryopreservation of Cells

Cells were cryopreserved in FCS containing 10% (v/v) of the cryoprotectant, dimethyl sulphoxide (DMSO, BDH AnalaR®, Merck) to prevent crystallisation and fracturing of the cell membranes. Immediately prior to freezing, 0.5 ml of pre cooled sterile freeze mix (20% (v/v) DMSO in FCS) was added dropwise with mixing, to cells suspended in 0.5ml of FCS. The cell mixture was kept on ice and immediately transferred to cryovials (Greiner Bio-One Labortechnik, Frickenhausen, Germany). Ampoules were placed in a Cryo 1°C Freezing Container (Mr Frosty, Nalgene, Rochester, NY, USA) to chill cells at a rate of -1°C per minute, and eventually stored at -196°C in liquid nitrogen.

2.1.5.2. Thawing Cryopreserved Samples

Following removal from liquid nitrogen storage, cryoampoules were rapidly thawed at 37°C. Cells were transferred dropwise to a 50 ml polypropylene conical tube (Falcon, BD Biosciences) containing 40-50 ml of HHF, and pelleted by centrifugation at 1400 rpm for 5 mins. The cells were then washed again in HHF to remove residual DMSO, resuspended in appropriate growth medium, and cultured in 75cm^2 flasks at 37°C in the presence of 5% CO_2.

2.1.6. BM CFU-F Clonogenic Assay

Details of this procedure have been well documented elsewhere (Gronthos & Simmons, 1995; Gronthos et al, 1998). BM MNC or immunoselected BM MNC were cultured in 6 well plates (Nunclon, Nalgene Nunc International) with filter sterilised single strength α-

MEM supplemented with 20% FCS. Cells were seeded at two densities, 2 x 10^5 and 5 x 10^5 cells per well, in triplicate and incubated at 37°C in the presence of 5% CO_2 for 10 to 14 days. Cultures were stopped whilst distinct colonies could still be observed, before confluence occurred. When ready to be scored, cultures were rinsed three times with PBS and incubated for 3 hours in 0.1% (w/v) Toluidine blue (Aldrich, Sigma-Aldrich) in 1% paraformaldehyde in PBS. Once fixed and stained the cultures were rinsed well in tap water. Aggregates of greater than 50 cells were scored as CFU-F using a dissecting light microscope (Olympus SZ-PT, Olympus Optical Co., Tokyo, Japan).

2.1.7. Proliferation Assay

2.1.7.1. Serum Free Media for Proliferation Assay

This serum free media is a modification of the serum deprived media developed for growth of haematopoietic progenitors (Lansdorp, 1995; Migliaccio et al., 1988) and adapted for the growth of stromal progenitors (Gronthos and Simmons, 1995). Single strength α-MEM was supplemented with 2 mM L-glutamine, 100 μM L- ASC-2P, 10^{-5} M dexamethasone sodium phosphate (Dex, DBL), penicillin (50 i.u./ml)/streptomycin sulphate (50 μg/ml), 10 mM HEPES (JRH Biosciences), 200 μg/ml iron saturated human transferrin (Sigma-Aldrich), 10 μg/ml bovine pancreas derived insulin (Royal Adelaide Hospital Pharmacy, Adelaide, Australia), 50 μg/ml human low density lipoprotein (LDL, Sigma-Aldrich), 5 x 10^{-5} M β-mercaptoethanol, and 2% (v/v) BSA in DMEM. SDM without growth factors was prepared fresh as required and filter sterilised prior to use.

2.1.7.2. WST-1 Proliferation Assay

Sheep MSC derived from different donors were seeded in 96-well plates (Nunclon, Nalgene Nunc International), at a density of 2 x 10^3 cells per well in 200 μl of α-MEM-10 media and allowed to attach overnight at 37°C. The following day, the media was removed, and wells were washed twice in PBS, prior to the addition of 150 μl of serum free media containing various growth factors. Cells were incubated with growth factors for 5 days. Using the colorimetric assay reagent WST-1 (Roche Molecular Biochemicals, Mannheim, Germany), the relative number of viable cells in each well was determined at day 5. Briefly, 100 μl of WST-1 diluted 1:10 in PBS was added to each well, and incubated for 3 hours at 37°C protected from light. Diluted WST-1 solution was also

added to three wells containing only medium, to enable background subtraction. WST-1 is a tetrazolium salt that is cleaved to formazan by cellular enzymes. An expansion in the number of viable cells results in an increase in the overall activity of mitochondrial dehydrogenase in the sample that leads to an increase in the amount of formazan dye formed, which directly correlates to the number of metabolically active cells in the culture. Following incubation in the dark, the colour of the medium turned to orange, proportionate to the extent of cell viability and cell number. The absorbance of dye solution was measured directly with a plate reader (BIO-RAD Model 3550 microplate reader) at a wavelength of 450 nm. Each treatment group was performed in triplicate and the results were compared against controls using a paired t-test. Statistical significance was confirmed where $p<0.05$.

Table 2.1: Cytokines Used In This Study

Growth Factor	Specificity	Company
BMP-2	Recombinant human	Cytolab/Peprotech, Israel Cat. No. 120-02
BMP-7	OP-1®	Stryker Biotech, St Leonards, NSW, Australia
IGF-1	Recombinant human IGF-1 analogue	Gropep, Thebarton, SA, Australia
FGF-2	Recombinant human	Cytolab/Peprotech, Israel Cat. No. 100-18B
TGF-β1	Recombinant human	Cytolab/Peprotech, Israel Cat. No. 100-21R
TGF-β3	Recombinant human	Cytolab/Peprotech, Israel Cat. No. 100-36
TGFα	Recombinant human	Peprotech, Rocky Hill, NJ, USA Cat. No. 100-16A

2.1.8. In Vitro Osteogenesis Assay

The conditions required for the induction of human bone marrow stromal cells to deposit mineralised bone matrix in vitro has previously been established (Gronthos et al., 1994). Sheep MSC were seeded in 25cm^2 tissue culture flasks (2 x 10^5 cells per flask, Cellstar, Griener Bio-One), and cultured overnight in α-MEM-10 to facilitate attachment. On the following day, the media was exchanged for osteo-inductive medium which consists of single strength α-MEM supplemented with 10% FCS, penicillin (50 i.u./ml)/streptomycin sulphate (50 μg/ml), 2 mM L-glutamine, 10^{-7} M dexamethasone, 100 μg/ml ASC-2P, 1.8 mM KH_2PO_4 (BDH Chemicals, Merck), and 10 mM HEPES. This media was filter sterilised and stored at 4°C. Fresh media was replaced twice weekly and incubated at 37°C in the presence of 5% CO_2. Samples were collected at three time points for gene expression and histological evaluation.

2.1.8.1. Alizarin Red Staining

To prepare Alizarin Red solution, 1% (w/v) Alizarin Red powder (BDH GURR®, Merck) was added to a solution of 2% (v/v) ethanol in water/PBS. The pH was adjusted to 4.1 to 4.3 or 6.5 with concentrated (6M) ammonium hydroxide (BDH AnalaR®, Merck). The solution changed to red upon reaching the desired pH. To perform staining on cell culture flasks, media was aspirated, cells were rinsed in PBS, and fixed for 1 hour at RT in 4% formaldehyde in PBS. Following fixation, flasks were rinsed in distilled water and stained for approximately 5 mins in Alizarin Red solution to reveal mineral. Loosely bound stain was removed by 5 rinses in distilled water, and allowed to air dry at RT.

2.1.9. In Vitro Adipogenesis Assay

The optimal conditions for adipogenic differentiation of human BM MSC to produce lipid laden fat cells, has been described previously (Gimble, 1998). Sheep MSC were seeded in 25cm^2 tissue culture flasks (2 x 10^5 cells per flask), and cultured overnight in α-MEM-10 to facilitate attachment. On the following day, the media was exchanged for adipogenic medium which consisted of single strength α-MEM supplemented with 0.5 mM isobutylmethylxanthine (Sigma-Aldrich), 0.5 μM hydrocortisone (Sigma-Aldrich), 60 μM indomethacin (Sigma-Aldrich), penicillin (50 i.u./ml)/streptomycin sulphate (50 μg/ml), 100 μg/ml ASC-2P and 10% FCS. This media was filter sterilised and stored at 4°C.

Cultures were fed three times a week and incubated at 37°C in the presence of 5% CO_2. Samples were collected at three time points for gene expression and histological evaluation.

2.1.9.1 Oil Red O Staining

Oil Red O stock solution (ICN Biomedicals, Seven Hills, Australia) was prepared by dissolving 0.5 g in 100 ml isopropanol (BDH AnalaR®, Merck). A working solution of stain was prepared by mixing 6ml of stock Oil Red O solution with 4ml of water, allowed to stand for 10 mins, and was then filtered through No. 46 Whatman filter paper (Whatman). Adherent cell cultures exhibiting adipocytic clusters were rinsed gently twice with PBS and fixed in 4% (v/v) formaldehyde in PBS for 10 mins at room temperature. Cell cultures were subsequently stained by immersion in the Oil Red O working solution for approximately 1 hour. Finally, cells were washed three times in distilled water and counterstained with Mayer's Haematoxylin (Sigma).

2.1.10. In Vitro Chondrogenesis Assay

The conditions for differentiation of stromal progenitor cells towards a chondrogenic phenotype have been established (Johnstone et al., 1998; Mackay et al., 1998; Yoo et al., 1998). Employing this technique, 2.5×10^5 cells were added to 10ml polypropylene screw cap conical tubes (Sarstedt, Nümbrecht, Germany), and aggregated by centrifugation at 1400 rpm for 10 mins. The supernatant was gently aspirated and 300 µl of serum deprived media containing growth factors was gently overlayed. Samples were centrifuged again at 1,400 rpm for 5 mins. Cells at the bottom of the tube formed spherical aggregates overnight. Cultures were incubated at 37°C in the presence of 5% CO_2 with lids loosened to allow the diffusion of oxygen. Media was replaced three times a week for 21 days. At this point, for each duplicate culture, RNA was isolated from one sample for gene expression analysis, whereas the other sample was processed in preparation for paraffin embedding, for assessment by histological and immunohistochemical methods.

2.1.10.1. Serum Deprived Chondrogenic Media

Chondroinductive media devoid of growth factors consisted of single strength DMEM (high) supplemented with ITS+ Premix (BD Biosciences), penicillin (50

i.u./ml)/streptomycin sulphate (50 µg/ml), 2 mM L-glutamine, 100 µM L-ascorbate-2-phosphate, 10^{-7} M dexamethasone, 1% BSA in DMEM, and 0.5 mM β-ME. The solution was filter sterilised prior to use and stored at 4°C. Several growth factors and combinations were utilised in this assay including BMP-2 (50ng/ml), BMP-7 (100ng/ml), FGF-2 (10 ng/ml), TGF-β1 (10 ng/ml), TGF-β3 (10 ng/ml), combinatorial factors BMP-2/TGF-β3 (50 and 10 ng/ml respectively) and BMP-7/TGF-β1 (100 and 10 ng/ml respectively). Cytokines were added at appropriate concentration to the serum free chondrogenic media. Manufacturer and specific details are provided in Table 2.1.

2.1.10.2. Pellet Processing for RNA Isolation

Each pellet was rinsed once gently with 1 ml PBS. The PBS was aspirated and cultures were incubated in 400 µl collagenase/dispase solution for 3 hours in a 37°C water bath. Enzymatic activity was neutralised by the addition of 1 ml HHF. This solution was then transferred to a 1.7 ml microcentrifuge tube, spun at 1,400 rpm for 5 mins, rinsed in cold PBS before another spin as above. 200 µl of TRIzol™ was added, the sample was vortexed and frozen at -80°C until required. The subsequent process of RNA extraction, cDNA synthesis and RT-PCR is outlined in Section 2.2.1-2.2.3.

2.1.10.3. Pellet Processing for Paraffin Embedding

Pellet aggregates were rinsed gently once in PBS before fixation overnight in 4% (v/v) formaldehyde in PBS at 4°C. Fixative was then replaced with 70% (v/v) ethanol, and samples were dehydrated ready for paraffin embedding. Following paraffin embedding 5 µM cross sections were histologically stained with H&E and Alcian Blue, and immunohistochemical analysis of Col-2 and Col-10 were performed as described in Section 2.8.

2.2. Gene Expression Analysis

2.2.1. TRIzol™ Isolation of Total RNA

Total RNA was extracted from 0.5-5 x 10^6 cells by adding 1ml (per 5-10 x 10^6 cells) of TRIzol™ (Invitrogen, Mount Waverley, Victoria, Australia). Prior washing of cells before addition of TRIzol reagent was avoided as this increases the possibility of mRNA

degradation. RNA was solubilised by passing the lysate through a pipette several times. The homogenised samples were incubated at room temperature to permit the complete dissociation of nucleoprotein complexes. To each tube, 0.2 ml of chloroform (APS Finechem, Seven Hills, NSW, Australia) was added per 1 ml of TRIzol reagent. The tubes were vortexed or shaken vigorously by hand for 15 seconds and incubated at room temperature for 3 mins. Samples were centrifuged at 12000 x g for 15 mins at 4°C to separate the mixture into a lower red phenol-chloroform phase, an interphase, and a colourless aqueous upper phase. RNA that remained exclusively in the aqueous upper phase was carefully removed and transferred to a fresh 1.7 ml copolymer microcentrifuge tube (Scientific Specialties Incorporated, Lodi, CA, USA). The total RNA was then precipitated by the addition of 0.5 ml isopropanol (BDH Chemicals, Merck) per 1ml of TRIzol reagent used for the initial homogenisation. The sample was mixed gently and incubated for 10 mins at room temperature, prior to centrifugation at 12000 x g for 10 mins at 4°C to pellet the RNA. Once the supernatant was removed, the RNA pellet was washed once with a volume of 75% (v/v) ethanol (Univar, Ajax Finechem, Taren Point, NSW, Australia) equal to the amount of TRIzol reagent used initially. The samples were mixed by vortexing and were centrifuged at 7500 x g for 5 mins at 4°C. Finally, the RNA pellet was briefly air dried at 37°C for 5-10 mins. RNA was resupended in 12 µl RNase free diethylpyrocarbonate (DEPC, Sigma-Aldrich Ltd) treated Milli-Q water, and to facilitate RNA solubility, the samples were incubated for 10 mins at 55°C. The concentration of RNA was determined by spectrophotometry, and either used immediately for cDNA synthesis, or stored at -80°C.

2.2.2. Determination of RNA Concentration

The concentration of RNA in solution was determined by measuring the absorption at 260 nm on a Beckman UV spectrophotometer (Beckman Instruments, Mount Waverley, Victoria, Australia), assuming that an A_{260} of 1.0 represents 40 µg/ml of RNA. The ratio of RNA (A_{260}) to protein (A_{280}) provided some indication of the quality and integrity of RNA isolation.

2.2.3. Reverse Transcription (RT) Polymerase Chain Reaction (PCR) Amplification of DNA

2.2.3.1. Synthesis of Complementary DNA (cDNA)

Total cellular RNA from cells or tissues was prepared with TRIzol, as described previously. The following components were added to a nuclease-free 1.7 ml microcentrifuge tube: 1 µl of 500 ng/µl random hexamers (Oligo-dT, Geneworks, Hindmarsh, SA, Australia), 2 µg total RNA, and RNase free DEPC treated Milli-Q water up to 12 µl. The mixture was heated at 70°C for 10 mins and quickly chilled on ice. The contents of the tube were collected by brief centrifugation and then added to a mixture containing 4 µl of 5 x first strand buffer, 2 µl of 0.1 M DTT, and 1 µl of 10 mM dNTP mix (5 mM each of dATP, dGTP, dCTP, and dTTP at neutral pH) (all Fisher Biotec, Wembley, WA, Australia). The contents of the tube were mixed gently and incubated at 42°C for 5 mins. One µl (200 units) of SuperScript II RT (Gibco, Invitrogen, Carlsbad, CA, USA) was added, and mixed by gentle pipetting before incubation at 42°C for 1 hour. The reaction was inactivated by heating at 70°C for 10 mins. The sample was rapidly cooled on ice for 5 mins and collected by brief centrifugation. In order to remove the RNA from the reaction, and leave cDNA only, 1 µl of 2 Units/µl RNase H (Invitrogen) was added, mixed, and incubated at 37°C for 20 mins. Finally 80 µl of nuclease free DEPC treated Milli-Q water was added for a final volume of 100 µl. The cDNA was then used as a template for amplification by PCR.

2.2.3.2. Polymerase Chain Reaction (PCR) Amplification of cDNA

cDNA was amplified by PCR to generate products corresponding to mRNA encoding the gene products. Two µl of each cDNA synthesis reaction was utilised as template DNA in each PCR reaction. Routinely, the cDNA mixture was added to a 0.2 ml flat cap microcentrifuge PCR tube (Scientific Specialties Incorporated), to which 2 µl of 10 x PCR amplification buffer (10x PCR buffer: 670 mM Tris HCl pH 8.8, 166 mM $(NH_4)_2SO_4$, 4.5% Triton-X 100, 2 mg/ml gelatin, Applied Biosystems, Foster City, CA, USA), 1.2 µl of 25 mM $MgCl_2$ (Applied Biosystems), 2 µl of 2 mM dNTP mixture (Applied Biosystems), 100 ng (1 µl of 100 ng/µl) of each of the appropriate sense and antisense primers, 0.2 µl (1 Unit) of AmpliTaq® DNA Polymerase (Applied Biosystems), and DEPC-treated water were added to a final volume of 20 µl. Amplitaq Gold is a 'hot start' DNA polymerase that has an inactivating protein modification which only permits the enzyme to become active at high temperatures. Amplification was achieved using a Corbett Research thermal cycler or Eppendorf Mastercycler. DNA was amplified under

the following typical cycle conditions: long denaturation at 95°C for 10 mins (once only prior to repeating cycle), denaturation at 94°C for 1 min, annealing at the temperature appropriate for each different primer set for 1 min, and extension at 72°C for 1 min. These three steps were repeated for 22-40 cycles, with a final 10 min extension at 72°C such that all products were assayed in the exponential phase of the amplification curve. Following the amplification, PCR products (10 µl of each reaction) were separated on a 2% (w/v) Type I agarose (Sigma-Aldrich) gel according to molecular weight, and visualised by 1) staining in 0.5 µg/ml ethidium bromide solution (Sigma-Aldrich) and UV exposure, or 2) for quantitation SYBR Gold (Molecular Probes, Invitrogen, Eugene, OR, USA) staining and exposure under UV light at 570nm.

2.2.3.3. Primers

All primers used in the study are displayed in Table 2.2. Where ovine sequences of particular genes were unavailable, multiple alignments of various species were performed. Primers were designed to the consensus sequence within regions of high homology. Multiple sequence alignments are presented in the Appendix with primer site indicated by bold typeface. The cycle numbers were determined by cycle course analysis, and annealing temperatures were determined empirically using AmpliTaq Gold in a gradient thermal cycler.

Table 2.2: RT-PCR Primers Used In This Study, Product Size, and Manufacturer.

Gene Name	Forward Sequence (5' to 3') Reverse Sequence (5' to 3')	Product Size (bp)	Species and Accession Number
Aggrecan	TGGGAGTGAGGACCGTCTAC	445	Appendix A
	GCTAAGGTCACCTGCACGAC		
Cbfa-1	GGACGAGGCAAGAGTTTCAC	465	Appendix B
	GGTGGCAGTGTCATCATCTG		
Collagen-1	CCAGTCACCTGCGTACAGAA	456	Sheep
	GAGACCACGAGGACCAGAAG		AF129287
Collagen-10	AGCCAGGGTTGCCAGGACCA	386	Human[#^]
	TTTTCCCACTCCAGGAGGGC		NM_000493
Collagen-2	GAGGTGGATGCCACGCTCAA	337	Appendix C
	CAGGTTCTCATCGCCGTAGCT		
GAPDH	GACCTCCACTACATGGCCTACA	454	Sheep
	CCATCCACAGTCTTCTGGGT		AF035421
Leptin	TTGGATGGCCTAGGAATCTG	446	Sheep
	TTGCTTCCTGCAAGTGATTG		AY278244
LPL	TGGACGGTGACAGGAATGTA	486	Sheep
	ACATCCTGGTTGGAAAGTGC		X68308
PPARγ	CATCTTCCAGGGGTGTCAGT	487	Sheep
	GAGGTCCGTCATTTTCTGGA		AY137204
Sox-9	GGAGAGCGAGGAGGACAAGTT	439	Appendix D
	CCTGCAGCGCCTTGAAGAT		

[#] As published by Gronthos et al (2003)

[^] All primers manufactured by Invitrogen (Mount Waverley, Victoria, Australia), except for Collagen-10, which was manufactured by Geneworks (Hindmarsh, SA, Australia).

2.3. Immunofluorescence Staining and Flow Cytometry

Flow cytometry was performed using an Epics®-XL-MCL analyser (Beckman Coulter, Fullerton, CA, USA). Cells to be analysed were immunostained with primary antibodies that recognise specific antigens of interest. Cell populations were analysed on the basis of the forward and side scatter, which is indicative of cell size and granularity respectively.

2.3.1. Solutions and Buffers

2.3.1.1. Blocking Buffer for Flow Cytometric Analysis

HBSS was supplemented with 0.4% (w/v) bovine serum albumin, 4% (v/v) normal human serum (NHS; Red Cross, South Australia), 5% (v/v) FCS and penicillin (50 i.u./ml)/streptomycin sulphate (50 µg/ml) (JRH Biosciences). The buffer was filter sterilised through a 0.22 µM bottle filter and stored at 4°C.

2.3.1.2. Flow Cytometry Fixative (FACS Fix)

Single strength PBS was supplemented with 0.4% (v/v) formaldehyde (40% (v/v) stock, BDH AnalaR®, Merck, Darmstadt, Germany), 2% (w/v) D-glucose (BDH AnalaR®, Merck), and 0.02% (w/v) sodium azide (Sigma-Aldrich).

2.3.2. One Colour Flow Cytometric Analysis

Cells to be analysed were harvested from culture (2×10^5 cells per condition tested) and pelleted by centrifugation at 1400 rpm for 5 mins at 4°C. Prior to immunolabelling, cells were incubated in blocking buffer at a concentration of 5×10^6 cells/ml, on ice, for at least 30 mins, to prevent non specific binding to Fc receptors. For each condition, 2×10^5 cells were incubated with 200 µl of antibody, either diluted purified monoclonal antibodies or neat culture supernatant both at a final concentration of 10 µg/ml, or isotype-matched control. After 45 min incubation at 4°C, the cells were washed twice in chilled HHF to remove unbound primary antibody, and pellets were resuspended in 200 µl HHF containing 1:50 dilution of fluorescein isothiocyanate (FITC)-conjugated goat anti mouse Ig G or M (Southern Biotechnology Associates Inc., Birmingham, AL, USA). Following incubation with secondary antibody for 45 mins at 4°C, cells were washed twice in chilled

HHF before fixation in FACS fix. Typically, for each sample 10000 events were analysed on the flow cytometer and stored as list mode data for further analysis using WinMDI software (Windows Multiple Document Interface Flow Cytometry Application, 1993-1998 Joseph Trotter).

2.3.3. Fluorescence Activated Cell Sorting (FACS)

Following thawing of sheep bone marrow mononuclear cells, approximately 1 x 10^7 cells were pelleted in 14 ml polypropylene round bottom tubes (Falcon, BD Biosciences) and resuspended in HHF. These cells were then passed through a 70 μm cell strainer to obtain a single cell suspension, spun again and incubated in 10ml of blocking buffer for at least 30 mins at 4°C. At this point a viable cell count was performed using Trypan blue exclusion. Cells were then distributed into the required number of 5 ml polypropylene round bottom tubes (Falcon, BD Biosciences), and incubated with the appropriate primary antibody (purified at 10 μg/ml or neat supernatant) or isotype matched control (diluted in blocking buffer) for at least 45 mins at 4°C. Samples were washed twice in HHF and incubated with 200-500 μl HHF containing 1:50 dilution of fluorescein isothiocyanate (FITC)-conjugated goat anti mouse Ig G of M (Southern Biotechnology Associates Inc., Birmingham, AL, USA) at 4°C for approximately 45 mins. After secondary antibody incubation, cells were again washed twice in HHF, and resuspended in 3 ml HHF. Suspensions were analysed using FACStarPLUS flow cytometer (Becton Dickinson). Positive fluorescence was defined as the level of fluorescence greater than 99% of the corresponding isotype matched control antibody. Positive and negative cells were collected in 5 ml polypropylene round bottom tubes containing 3 ml of α-MEM-20 and cultured in 6 well plates.

Table 2.3: Antibodies Used In This Study

Antibody	Alternate Names & Specificity	Isotype	Source
1A6.12	Isotype-matched negative control/α-Salmonella	mIgM	[5]Dr. L. Ashman
1B5	Isotype-matched negative control/α-Giardia	$mIgG_1$	[8]Dr. G. Mayrhofer
1D4.5	Isotype-matched negative control/α-Salmonella	$mIgG_{2a}$	[5]Dr. L. Ashman
3G5	microvascular pericytes	mIgM	[1]ATCC
AA6	Glycophorin-A, CD235a, erythrocytes	$mIgG_1$	[5]Dr. L. Ashman
AB11	Endoglin, CD105, endothelial cells, activated monocytes, macrophages, stromal cells	$mIgG_1$	[6]Dr. S. Gronthos
AC11	Integrin CD49b/CD29	$mIgG_1$	[1]ATCC
AC9	CD13, granulocytes, monocytes, endothelial cells, BM stroma, osteoclasts	IgG_1	[6]Dr. S. Gronthos
B478	α human bone/liver/kidney isoform of ALP	$mIgG_1$	[3]DSHB
CC9	MUC-18, CD146, endothelial cells, smooth muscle, stromal cells	$mIgG_{2a}$	[6]Dr. S. Gronthos
CD14	α ovine CD14, monocytes/macrophages	mIgG	[4]Serotec
CD166	ALCAM, activated monocytes, epithelial cells, fibroblasts, stromal cells, endothelial cells	$mIgG_1$	[2]BD Biosciences
CD31	α ovine CD31, PECAM-1, endothelial cells, platelets, leukocytes	mIgG	[4]Serotec
CD45	α ovine CD45, Leukocyte Common Antigen, lymphocytes, macrophage, granulocytes	mIgG	[4]Serotec
CD90	Thy-1, HSC, neurons, connective tissue, fibroblasts, stromal cells	mIgG	[2]BD Biosciences
EB4	MUC-18, CD146, endothelial cells, smooth muscle, stromal cells	$mIgG_1$	[6]Dr. S. Gronthos
H9H11	Phagocytic glycoprotein-1 (Pgp-1), H-CAM, CD44, most cell types, stromal cells	$mIgG_1$	[9]Dr. P. Simmons
Hyb A	F3.F8.B6	mIgM	[10]Dr. A. Zannettino
Hyb B	F11.F8.E4	$mIgG_1$	[10]Dr. A. Zannettino
Hyb E	C11.G6.A12	mIgM	[10]Dr. A. Zannettino
Hyb H	B4.H8.G6	$mIgG_1$	[10]Dr. A. Zannettino
Hyb I	F4.D10.H8	mIgM	[10]Dr. A. Zannettino

Table 2.3: Antibodies Used In This Study Continued

Antibody	Alternate Names & Specificity	Isotype	Source
QE4G9	α ovine VCAM-1, CD106, endothelial cells, myeloid cells, stromal cells	mIgG	[7]Dr. R. Krishnan
STRO-1	Erythroid, stromal cells, CFU-F, endothelial cells	mIgM	[9]Dr. P. Simmons
XB1	Endoglin, CD105, endothelial cells, activated monocytes, macrophages, stromal cells	IgG_1	[6]Dr. S. Gronthos

[1]ATCC American Type Culture Collection, Manasas, VA, USA

[2]BD Biosciences, Becton Dickinson, Franklin Lakes, NJ, USA

[3]DSHB, Developmental Studies Hybridoma Bank, University of Iowa, IA, USA

[4]Serotec, Oxford, England

[5]Dr. L. Ashman, University of Newcastle, NSW, Australia

[6]Dr. S. Gronthos, Institute of Medical and Veterinary Science, Adelaide, Australia

[7]Dr. R. Krishnan, Queen Elizabeth Hospital, Adelaide, Australia

[8]Dr. G. Mayrhofer, University of Adelaide, Australia

[9]Dr. P. Simmons, Peter MacCallum Cancer Institute, Melbourne, Australia

[10]Dr. A. Zannettino, Institute of Medical and Veterinary Science, Adelaide, Australia

2.4. Analysis of Cell Surface Antigens by Immunoprecipitation with Monoclonal Antibodies

2.4.1. Solutions and Buffers

2.4.1.1. Tris-Saline EDTA (TSE)

50 mM Tris-HCl (Sigma-Aldrich), 150 mM sodium chloride (Univar, Ajax Finechem), 1 mM EDTA (BDH AnalaR®, Merck), 0.1% sodium azide (Sigma-Aldrich), pH 8.0

2.4.1.2. 1% NP40-TSE

1% (v/v) Nonidet P40 (NP40, Fluka Chemie, Sigma-Aldrich, Buchs, Switzerland), 50 mM Tris-HCl, 150 mM sodium chloride, 1 mM EDTA, 0.1% sodium azide, in water, pH 8.0.

2.4.1.3. 0.1% NP40-TSE

0.1% (v/v) Nonidet P40, 50 mM Tris-HCl, 150 mM sodium chloride, 1 mM EDTA, 0.1% sodium azide, in water, pH 8.0.

2.4.1.4. Protease Inhibitor

One Complete Protease Inhibitor Cocktail Tablet (Roche Molecular Biochemicals, Mannheim, Germany) was dissolved in 1 ml water to produce a 50 x stock solution.

2.4.2. Biotinylation of Cell Surface Antigens and Preparation of NP40 Lysates

Biotinylated cell surface lysates were essentially prepared as described previously (Cole et al., 1987). Approximately 1 x 10^8 cells were washed three times in cold PBS, counted, and resuspended in PBS at a concentration of 1 x 10^8 cells per ml. Cell surface antigens were biotinylated with Sulfo-NHS-Biotin (Pierce Biotechnology, Rockford, IL, USA), by addition of 2.2 mg dissolved in 50 µl PBS per 10^8 cells. The mixture was incubated on ice for 30 minutes with occasional gentle mixing. Biotinylated cells were subsequently washed three times in cold PBS, and resuspended at 2 x 10^7 cells/ml in cold PBS. Protease inhibitor was added to the cell solution at a final concentration of 2 x, prior to cell lysis, so

as to prevent endogenous proteases released from lysed cells from degrading the proteins within the lysate. Lysates were prepared by addition of an equal volume (to total cell solution volume) of 1% NP40-TSE and incubated on ice for 30 mins with occasional gentle mixing. The mixture was centrifuged at 1400 rpm for 10 mins at 4°C, and 1 ml aliquots of supernatant were carefully transferred to fresh tubes and used immediately for immunoprecipitation or stored at -20°C. Prior to use lysates were centrifuged at 14000 rpm for 10 mins at 4°C to remove cell nuclei and debris.

2.4.3. Preparation of Unbiotinylated NP40 Lysates for Cell Surface Antigen Analysis.

Approximately 2 x 10^7 cells were washed three times in cold PBS, counted and resuspended at a concentration of 2 x 10^8 cells/ml. Protease inhibitor must be added prior to cell lysis to prevent endogenous proteases released from lysed cells from degrading the proteins within the lysate. Protease inhibitor was added to cell solution to a final concentration of 2 x. An equal volume (to total cell solution volume) of 1% NP40 in TSE was added to cells and incubated on ice for 30 mins with occasional gentle mixing. The mixture was centrifuged at 14000 rpm for 10 mins at 4°C and supernatant was carefully transferred to a fresh tube and stored at -20°C.

2.4.4. Pre Clearing Lysate

In order to remove non specific binding of cell lysates to Dynabeads® (Dynal®, Invitrogen, Oslo, Norway), the lysate was pre-cleared. For each IP, 25 µl uncoated Dynabeads® (appropriate for primary antibody isotype) were washed three times in a solution of 1% NP40 with 0.5 x protease inhibitor. Briefly, solution was added to tube, inverted, and placed on a magnet for at least 30 seconds to separate beads from the wash solution. Supernatant was carefully removed and fresh solution replaced immediately. Following the third wash, cell lysate was added to the washed beads and the mixture placed on a nutator or rotator at 4°C overnight.

2.4.5. Arming of Dynabeads with Monoclonal Antibodies

Primary antibodies of interest for immunoprecipitation were armed with appropriate isotype matched Dynabeads. For each IP, 50 µl of Dynabeads were washed three times in 0.1% BSA in PBS. Either 3 µg of purified monoclonal antibody or 500 µl supernatant

antibody was added to the washed beads. The mixture was placed on a nutator or rotator at 4°C overnight.

2.4.6. Immunoprecipitation from NP40 Lysates

Beads armed with antibody of interest were washed once in 0.1% BSA in PBS, and then washed once in 1% NP40-TSE with 0.5 x protease inhibitor. Concurrently, the lysate incubated with beads for pre clearing was placed on a magnet to separate beads from lysate. The lysate supernatant was removed and retained, and beads (containing non specifically bound protein) were discarded. Thus pre cleared lysate was added to the armed Dynabeads and incubated on a nutator or rotator at 4°C for 2 hours.

Following incubation, the bead/lysate mixture was washed three times in 1% NP40-TSE, twice in 0.1% NP40-TSE and finally once in TSE. During the TSE wash and prior to placement on the magnet, the solution was transferred to a 1.7 ml microcentrifuge tube. After removal of the TSE on the magnet, lysate bound beads were resuspended in 20 µl of 1 x non reducing or reducing buffer. Samples were then boiled for 5 mins to facilitate removal of protein from the beads

2.5. Protein Gel Electrophoresis: Sodium Dodecyl Sulphate Polyacrylamide Gel Electrophoresis (SDS-PAGE)

2.5.1. Buffers and Reagents

2.5.1.1. Reducing Sample Buffer

1 ml 0.5 M Tris-HCl, pH 6.8, 800 µl glycerol (Univar, Ajax Finechem), 1.6 ml 10% SDS (BDH AnalaR®, Merck), 400 µl β-mercaptoethanol (Gibco, Invitrogen), 200 µl 0.05% bromophenol blue (BDH AnalaR®, Merck) and 4 ml Milli-Q water.

2.5.1.2. Non Reducing Sample Buffer

1 ml 0.5 M Tris-HCl, pH 6.8, 800 µl glycerol, 1.6 ml 10% SDS, 200 µl 0.05% bromophenol blue and 4.4 ml Milli-Q water.

2.5.1.3. Electrophoresis Running Buffer

0.3% Tris-HCl, 1.44% Glycine (Unilab, Ajax Finechem), 0.1% SDS, pH 8.3 in water.

2.5.1.4. Semi Dry Transfer Buffer

0.3% Tris-HCl, 1.44% Glycine, 20% Methanol (Univar, Ajax Finechem), pH 8.3 in water.

2.5.2. Polyacrylamide Gel Preparation

To analyse cell surface antigens following immunoprecipitation, protein samples were separated on a 10% acrylamide SDS-PAGE gel. The constituents of a 10% gel are as follows: 6.7 ml 30% Acrylamide Mix (Bio-Rad Laboratories), 5.0 ml 1.5 M Tris pH 8.0, 0.2 ml 10% SDS, and 7.9 ml water. Immediately prior to pouring, 8 µl TEMED (MP Biomedicals, Irvine, CA, USA) and 0.2 ml 10% ammonium persulphate (APS, Sigma-Aldrich) were added to the gel solution. After pouring the gel was immediately overlaid with water. Following polymerisation of the acylamide, a stacking gel was prepared, consisting of: 1.7 ml 30% Acrylamide Mix, 1.25 ml 1.5 M Tris pH 8.0, 0.1 ml 10% SDS, and 6.8 ml water. Similarly, 1 µl TEMED and 0.1 ml 10% ammonium persulphate (APS) were added to the gel solution immediately prior to pouring, and once poured, overlaid with water.

Approximately 25 to 30 µl of each sample was loaded into wells of the acrylamide gel, and a similar volume of sample buffer was loaded into empty lanes to maintain a level running buffer front. The size of the immunoprecipitated protein s were estimated by comparison with the pre-stained protein molecular weight standard, SeeBlue® Plus 2 (Invitrogen). The gel was electrophoresed at 20 mA until the bromophenol blue buffer front entered the separating gel, at which point the voltage was raised to 30 mA until the bromophenol blue buffer front migrated to the end of the gel.

2.5.3. Coomassie Blue Staining

To prepare stain, 0.1% (w/v) Coomassie Blue (Sigma) was added to a solution of 50% (v/v) methanol in water. Prior to use, acetic acid was added to a final concentration of 10% (v/v). Acrylamide protein gels were stained for 2 hours with gentle agitation at RT.

To improve the resolution of Coomassie staining, gels were subsequently destained in a solution of 5% (v/v) methanol in water. Just before use, acetic acid was added to destain solution to a final concentration of 7.5% (v/v). Acrylamide protein gels were destained for

at least 2 hours with gentle agitation at RT. Sponges were placed in solution to aid this process and when required, fresh destain was exchanged.

2.5.4. Silver Staining

The silver staining method for protein detection was initially developed by Switzer et al (1979), and is a more sensitive technique than Coomassie staining for the identification of protein samples (Switzer et al., 1979). All incubations were performed at RT. SDS-PAGE acrylamide gels were prefixed in a solution of 50% (v/v) methanol, 10% (v/v) acetic acid in water for 30 mins. Gels were then gently rocked for a further 30 mins in a solution of 5% (v/v) methanol and 7% (v/v) acetic acid in water. Gels were soaked overnight in a large volume of water, and rinsed in fresh water for 30 mins the following morning. A solution of 5 mg/ml dithiothreitol (DTT) (Sigma-Aldrich) in water was prepared, and gels soaked for 30 mins. Without rinsing the DTT solution was decanted and a solution of 0.1% (w/v) silver nitrate (Rhone Poulenc, France) was added and incubated for 30 mins. The silver solution was decanted, and the gel rinsed briefly once with a splash of water, and then a splash of developer solution (solution will turn silvery brown). Developer solution consisted of 50 µl 37% (v/v) formaldehyde in 100 ml 3% sodium carbonate (BDH AnalaR®, Merck) in water. Following the quick rinse in developer solution, fresh solution was added and gently rocked under close observation until staining was sufficient. The reaction was stopped by the addition of 5% (v/v) acetic acid in water. Following rehydration in water the gel was preserved by vacuum drying at 80°C.

2.5.5. Detection of Cell Surface Antigens by Immunoblotting/Western Blotting

2.5.5.1. Identification of Biotinylated Lysates

Following gel electrophoresis, proteins were transferred onto Hybond PVDF membrane (Amersham Biosciences, Buckinghamshire, UK) overnight at 20 mA using a blotting apparatus (Hoefer Scientific Instruments, San Francisco, CA, USA). Note the membrane was soaked in methanol for 5 mins prior to transfer assembly. Following transfer non specific binding sites were blocked for 1 hour at RT in 5% (w/v) skim milk powder in 1% Tween-20 (Sigma-Aldrich) in PBS (PBST). The membrane was then rinsed briefly three times in PBST, and then washed 3 x 5 mins in PBST. Samples were subsequently rocked for 45 mins at RT in streptavidin-alkaline phosphatase conjugate (2 mg/ml, Molecular

Probes, Invitrogen) diluted 1/4000 in PBST. The membrane was rinsed three times and washed 3 x 5 mins in PBST.

To visualise nitrocellulose staining and thus localisation of biotinylated protein, the membrane was incubated for 2 mins in Vistra ECF substrate (Amersham Biosciences) and scanned using ECF Blue Program Typhoon at 100 μM at 600V.

2.5.5.2. Western Blotting with HSP-90 Antibody

Following gel electrophoresis, proteins were transferred onto Hybond PVDF membrane (Amersham Biosciences, Buckinghamshire, UK) overnight at 20 mA using a blotting apparatus (Hoefer Scientific Instruments, San Francisco, CA, USA). Note the membrane was soaked in methanol for 5 mins prior to transfer assembly. Following transfer non specific binding sites were blocked for 1 hour at RT in 5% (w/v) skim milk powder MANUF in 1% Tween-20 (MANUF) in PBS (PBST). The membrane was then rinsed briefly three times in PBST, and then washed 3 x 5 mins in PBST. Following blocking and PBST washes, the nitrocellulose membrane was incubated in Heat Shock Protein-90 mAb (HSP-90 α/β H-114, 200 μg/ml, Santa Cruz Biotechnology, Santa Cruz, CA, USA) diluted 1/600 in block solution for 1 hour. The membrane was rinsed and washed in PBST as specified earlier, and incubated in sheep anti rabbit IgG alkaline phosphatase (Amersham Life Sciences) diluted 1/2000 in blocking solution for 1 hour at RT. After immunolabelling, the membranes were rinsed three times and washed 3 x 5 mins in PBST, and subsequently reacted with Vistra ECF substrate (Amersham) and scanned using ECF Blue Program Typhoon Fluorimager (Molecular Dynamics) at 100 μM at 600V.

2.6. Xenotransplantation of Ovine Cells

All procedures described below were performed after obtaining approval from the Animal Ethics Committee of the University of Adelaide and the Royal Adelaide Hospital/IMVS, South Australia for the duration of the project. The animals used were six week old SCID or Nude mice and were housed in sterile microisolator cages in the sterile barrier room in the animal facility of the University of Adelaide. All surgical procedures were performed in a non-biohazard laminar flow cabinet using sterile instruments. Prior to operating the mice were anaesthetised by a gas mixture of nitrous oxide (0.4 L/min), oxygen (1.0 L/min)

and 2-3% halothane. Animals were maintained under anaesthesia with reduced air flow with 1-2% halothane.

2.6.1. Ectopic Bone Assay

2.6.1.1. Preparation of Cells and Scaffolds

This technique for ectopic bone formation in vivo is essentially as described by Gronthos et al (Gronthos et al., 2003). Adherent MSC from two separate sheep BM donors were harvested by trypsin digestion, passed through a 70 μm cell strainer to ensure cultures were in single cell suspension and resuspended at 2×10^6 cells/ml in α-MEM-10. To prepare the scaffold, 40 mg of hydroxyapatite/tricalcium phosphate ceramic particles (Zimmer Corporation, Warsaw, IN, USA) were washed in 1 ml α-MEM-10 media for 30 mins at 37°C on a nutator. The particles were then centrifuged at 1000 rpm for 2 mins to collect, and supernatant was aspirated. For each transplant, 2×10^6 cells in 1 ml media was added to the ceramic particles and incubated on a nutator at 37°C for approximately 1 hour to facilitate attachment of the cells to the scaffold. Samples were gently centrifuged at 1000 rpm for 2 mins and the supernatant was aspirated. To the cell/particle aggregate, 20 μl of fibrinogen and 20 μl thrombin were sequentially added and carefully combined, forming a fibrin glue to consolidate the cell scaffold composite.

2.6.1.2. Implantation of Cell Preparations

Six week old SCID mice were anesthetised as described above and shaved on the dorsal side parallel to the shoulders. The site of incision was swabbed with a sterile isopropanol wipe. A 1 cm longitudinal incision was made centrally along the skin using small curved scissors. The skin lateral to the incision was teased away from the underlying tissue using blunt scissors to form a pocket behind the shoulder. This procedure was then repeated on the contralateral side. Following this, one ceramic particle-cell aggregate was inserted into each subcutaneous pocket. The opening in the skin was closed by applying 2 to 3 sterile wound clips. The wound was washed liberally with Betadine and the mice were allowed to recover in clean microisolator cages.

2.6.1.3. Tissue Processing

After 8 weeks, mice were euthanized and transplants were recovered. Excess subcutaneous tissue was trimmed and transplants were cut in half. Samples were fixed overnight in 4% (v/v) formaldehyde in PBS at 4°C. The following morning, transplants were washed three times in PBS and decalcified for 14 days in a solution of buffered 10% EDTA (BDH AnalaR®, Merck) (pH 8.0), which was replaced daily. After decalcification, samples were placed again in 4% (v/v) formaldehyde in PBS at 4°C, prior to embedding in paraffin.

2.6.2. In Vivo Chondrogenesis Assay

2.6.2.1. Preparation of Cells and Scaffolds

Prior to transplantation, cryopreserved ovine MSC and cultured chondrocytes were thawed into flasks containing α-MEM-10. One day prior to surgery, media and scaffolds were prepared. Double strength chondrogenic media consisted of 2 x DMEM (high glucose) supplemented with ITS+ Premix, penicillin (100 i.u./ml)/streptomycin sulphate (100 μg/ml), 4 mM L-glutamine, 200 μM L-ascorbate-2-phosphate, dexamethasone (2×10^{-7} M), 2% BSA in DMEM, 1 mM 2-ME, and growth factor TGF-β1 (20 ng/ml). The solution was filter sterilised prior to use and stored at 4°C.

Using sterile technique under laminar flow hood, Gelfoam sponge was cut to approximately 10 x 8 mm squares. Ethisorb (Vicryl/Polyglactin 910 and Poly-P-Dioxanon, Codman, MA, USA) scaffold was cut into discs of approximately 1 cm in diameter. The required number of scaffolds were transferred to a 50 ml polypropylene tube containing α-MEM (without serum) and gently washed overnight at RT on a nutator.

On the day of surgery the scaffolds and cells were prepared for seeding and subsequent transplantation. Using a cut off tip, sodium hyaluronate (1.4% Healon GV, Pharmacia AB, Sweden) was mixed 1:1 with chondrogenic media. The mixture was vortexed intensively to form an emulsion. Cells were detached by trypsin digestion, washed twice in HHF, a cell count performed, and were resuspended in chondrogenic media at a concentration of 1×10^8 cells/ml.

2.6.2.2. Assembly of Gelfoam Transplant Using Fibrin Glue

To a round bottom cryovial (Greiner Bio-One), 20 µl of fibrinogen (gift from Rick Tocchetti, IMVS, Adelaide, Australia) was added. With forceps, the Gelfoam gelatin sponge (Pharmacia & Upjohn, Kalamazoo, MI, USA) was carefully removed from the wash solution, and placed on sterile gauze to draw excess liquid. Chondrogenic media (20 µl) was blotted onto the sponge by gentle rolling of the scaffold whilst adding media, to ensure liquid was evenly distributed. Thus the same static seeding technique was employed for chondrocyte media containing MSC (therefore 2×10^6 cells). The scaffold with or without cells was then placed at the bottom of the cryovial containing fibrinogen, and 20 µl of thrombin (gift from Rick Tocchetti, IMVS, Adelaide, Australia) was dotted on the scaffold to cross link and retain cells within the sponge. To facilitate mixing of the fibrin glue, the transplant was delicately moved around with a pipette tip, taking care not to damage the scaffold. After 5-10 mins the fibrin glue had congealed and the scaffold was overlaid with 200 µl of chondrogenic media. Samples were kept on ice and transported immediately to theatre.

2.6.2.3. Assembly of Ethisorb Transplant Using Fibrin Glue

To a round bottom cryovial (Greiner Bio-One), 20 µl of fibrinogen was added. With forceps, the Ethisorb discs were carefully removed from the wash solution, and placed on sterile gauze to draw excess liquid. To the fleecy (cream) side of one disc, 10 µl of fibrinogen was added. To another disc, 10 µl of thrombin was added to the fleecy cream face. Next, 10 µl of cells in chondrocyte/hyaluronate media was blotted onto each disc, and the two discs were folded together in a sandwich like arrangement, ensuring the cream fleecy surfaces were facing one another. These discs were then carefully transferred to the cryovial containing fibrinogen, and 20 µl of thrombin was dotted on the scaffold to consolidate. To facilitate mixing of the fibrin glue, the transplant was delicately moved around with a pipette tip, taking care not to dislodge the scaffold components. The same static seeding technique was employed for control samples containing chondrocyte media and hyaluronate only. After 5-10 mins the fibrin glue had congealed and the scaffold was overlayed with 200 µl of chondrogenic media. Samples were kept on ice and transported immediately to theatre.

2.6.2.4. Implantation of Cell Preparations

Six week old SCID mice were anesthetised as described above and shaved on the dorsal side parallel to the shoulders. The site of incision was swabbed with a sterile isopropanol wipe. A 1 cm longitudinal incision was made centrally along the skin using small curved scissors. The skin lateral to the incision was teased away from the underlying tissue using blunt scissors to form a pocket behind the shoulder. This procedure was then repeated on the contralateral side. A second incision was made posteriorly to the initial incision, to allow the transplantation of two additional transplants, using the same procedure outlined above. Following this, one scaffold was inserted into each subcutaneous pocket. The opening in the skin was closed by applying 2 to 3 sterile wound clips. The wound was washed liberally with Betadine and the mice were allowed to recover in clean microisolator cages.

Following transplantation, cell counts using Trypan blue were performed on the media overlaying the scaffold to determine the loss of cells from the transplant into the surrounding supernatant.

2.6.2.5. Tissue Processing

After 6 weeks, mice were euthanized and transplants were recovered. Excess subcutaneous tissue was trimmed and Ethisorb transplants were cut in half. Samples were fixed for 48 hours in 4% (v/v) formaldehyde in PBS at 4°C prior to embedding in paraffin.

2.7. Autologous Transplantation of Ovine MSC

Merino cross sheep 8 to 10 weeks of age were used and were selected to be of similar size and weight. All procedures were sanctioned by the institutional animal ethics committee and performed under sterile conditions.

2.7.1. Isolation of Autologous Bone Marrow Aspirates

Bone marrow was harvested from five lambs at 8 weeks of age, approximately two weeks prior to growth plate surgery. Lambs were masked with Isoflurane and 10-20 ml of bone marrow was collected as described in Section 2.1.3.1. Post-biopsy analgesia, anti-

inflammatory, and antibiotic were administered consisting of Flunixin meglumine (Flunixil, Troy Laboratories, Smithfield, NSW, Australia, 2 mg/kg) and Gentamycin (DBL, 1.6 mg/kg) respectively.

Collection of the MNC population from each marrow was performed following the technique outlined in Section 2.1.3.1, using density gradient centrifugation. Single cell suspensions of MNC were plated at approximately 6.4 to 10.2 x 10^4 MNC/cm^2. MSC were thus isolated according to plastic adhering capability and non adherent cells were removed after three days. Cells were cultured in α-MEM-20 and incubated at 37°C in the presence of 5% CO_2. By 8 days, most flasks were approaching confluence, so cells were passaged at lower density in α-MEM-10. Once confluent again (P1), cells were cryopreserved to minimise passaging of MSC prior to transplantation.

2.7.2. Preparation of Scaffolds for Transplantation

Two days prior to transplantation, cryopreserved lamb MSCs were thawed into flasks containing α-MEM-10. One day prior to surgery, media and scaffold were prepared. Double strength chondrogenic media consisted of 2 x DMEM (high glucose) supplemented with ITS+ Premix, penicillin (100 i.u./ml)/streptomycin sulphate (100 μg/ml), 4 mM L-glutamine, 200 μM L-ascorbate-2-phosphate, dexamethasone (2 x 10^{-7} M), 2% BSA in DMEM, 1 mM 2-ME, and growth factor TGF-β1 (20 ng/ml). The solution was filter sterilised prior to use and stored at 4°C. Using sterile technique under laminar flow hood, Gelfoam sponge was cut to approximately 10 x 8 mm squares. The required number of scaffolds were transferred to a 50 ml polypropylene tube containing α-MEM (without serum) and gently washed overnight at RT on a nutator.

On the day of surgery the scaffolds and cells were prepared for seeding and subsequent transplantation. Using a cut off tip, 500 μl sodium hyaluronate (1.4% Healon GV) was added to 4.5 ml of 2 x chondrogenic media. The mixture was vortexed intensively to form an emulsion. Autologous lamb MSC were detached by trypsin digestion, washed twice in HHF and a cell count performed. MSC were resuspended in double strength chondrogenic media at 6.6 x 10^7 cells/ml, and mixed thoroughly to minimise the potential of cell aggregates.

To a round bottom cryovial (Greiner Bio-One), 30 µl of fibrinogen was added. With forceps, the gelfoam sponge was carefully removed from the wash solution, and placed on sterile gauze to draw excess liquid. Chondrogenic media (60 µl) was blotted onto the sponge by gentle rolling of the scaffold whilst adding media, to ensure liquid was evenly distributed. Thus the same static seeding technique was employed for chondrocyte media containing MSC (therefore 4 x 10^6 cells). The scaffold with or without cells was then placed at the bottom of the cryovial containing fibrinogen, and 30 µl of thrombin was dotted on the scaffold to cross link and retain cells within the sponge. To facilitate mixing of the fibrin glue, the transplant was delicately moved around with a pipette tip, taking care not to damage the scaffold. After 5-10 mins the fibrin glue had congealed and the scaffold was overlaid with 500 µl of chondrogenic media. Samples were kept on ice and transported immediately to theatre.

On the completion of surgery, cell counts were performed on the media overlaying the scaffold to determine the loss of cells from the transplant into the surrounding supernatant.

2.7.3. Creation of Growth Plate Defect

Prior to surgery, animals were measured for post surgery body weight. Lambs were sedated by intravenous administration of thiopentone sodium BP (Pentothal, 25 mg/kg, 500 mg, Abbott Australasia, Botany, NSW. Australia) into the external jugular vein. Following intubation (7.5 mm outside diameter endotracheal tube), general anaesthesia was induced with halothane (1.5% in 2:1 oxygen:air, 12 L/min, NO_2 at 4). The site of surgery was shaved, scrubbed and sterilised with betadine to minimise infection. A longitudinal incision was made on the medial side of the leg, exposing the proximal tibia. The bone periosteum was lifted to expose the growth plate. Using a 2 mm dental burr, a defect of 10 mm deep x 10 mm wide x 5 mm high was created. Bone fragments were removed by constant irrigation with sterile saline, and additionally to minimise heat damage to the growth plate during drilling. The defect site was then immersed in 100 µl of 1 Unit/ml Chondroitinase ABC (Sigma-Aldrich), which was removed by aspiration and blotted dry after 5 mins. Titanium Kirschener wires (K-wires) were inserted perpendicular to the growth plate, proximally and distally to the defect site using a template of 20 mm separation. Caution was taken to avoid the joint cavity and superfluous wire was trimmed flush to the bone surface.

Four groups were included in the experiment. Each lamb was assigned two treatment groups, one for each hind leg, to allow for contralateral comparison within animals. Two weeks prior to surgery, autologous bone marrow was harvested from five lambs, these subjects received 1) scaffold plus MSC to growth plate injury, 2) scaffold without MSC to growth plate injury. Four lambs which did not undergo bone marrow harvest were assigned 3) growth plate defect with no treatment, and 4) growth plate intact (K-wires only), a control to measure the normal growth rate.

Following transplantation of engineered tissue, the periosteum was sutured over the defect, retaining the scaffold within the defect site. Subcutaneous tissue was closed and sutured. At the conclusion of the surgical procedure, the long acting analgesic Bupivacaine hydrochloride monohydrate was administered intramuscularly to each leg at several points around the injury site (Marcain 0.5%, Astra Zeneca, North Ryde, NSW, Australia, 5mg/ml, 5ml per leg,). Each leg also received intramuscular injection of antibiotic Cephalothin sodium (Keflin, DBL, 1g/vial, 40 mg/kg) and analgesic/anti-inflammatory Flunixin meglumine (Flunixil, Troy Laboratories, 2 mg/kg). Once the animal had recovered from the anaesthesia, on the day of surgery X-rays were taken of each operated leg.

2.7.4. Post Operative Care

Lambs were closely monitored post operatively for any signs of pain or distress, and recovered resiliently from the anaesthetic. As a precaution, animals were administered Flunixin meglumine (Flunixil, Troy Laboratories, 2 mg/kg) on day 1 post surgery, and additionally received Gentamycin (DBL, 1.6 mg/kg) and Benzyl penicillin sodium (Benpen, CSL, Parkville, Victoria, Australia, 600 mg, 4.48 mg/kg) for 3 days following surgery.

2.7.5. Euthanasia, Perfusion Fixation, and Tissue Collection

2.7.5.1. 0.2 M Phosphate Buffer

To prepare 0.2 M phosphate buffer, 7.8 g of sodium dihydrogen phosphate ($NaH_2PO_4.H_2O$, Univar, Ajax Finechem) and 21.4 g of disodium hydrogen phosphate (Na_2HPO_4, Univar, Ajax Finechem) were added to 800 ml of MQ water, and once dissolved the solution was topped up to 1 L.

2.7.5.2. 0.1 M Phosphate Buffer with 1% Sodium Nitrite

To prepare this solution, 20 g of sodium nitrite ($NaNO_2$, Sigma-Aldrich) was dissolved in 1 L of 0.2 M phosphate buffer, and mixed with 1 L of MQ water.

On the day prior to euthanasia, a second X-ray was performed for each leg, of the proximal tibia and joint. All animals used in this study were sacrificed five weeks post operatively. In order to perfuse, fix, and collect tissue specimens, animals were sedated and general anaesthesia was induced as described in Section 2.7.3. The femoral artery and vein were exposed and excess tissue and nerve were carefully separated from vessels. The femoral artery was catheterised with a 0.8 mm intravenous catheter. The femoral vein was also catheterised to allow flow through of liquid during perfusion. All tubes were flushed with 100 U/ml heparin in saline (stock 1000 U/ml, DBL, part of Mayne-Pharma, Lake Forest, IL, USA). Heparin was also flushed into the artery, and a smaller volume into the vein. The leg was then perfused with 500ml of 1% sodium nitrite in 0.1 M phosphate buffer. During the sodium nitrite perfusion, the animal was euthanized by an overdose of sodium pentobarbitone (10ml, Lethabarb, Virbac, Milperra, NSW, Australia). Subsequently, each leg was perfused with 500 ml of 10% buffered formalin (courtesy of Department of Histopathology, WCH). The hind leg was removed and the distance between Kirschener wires measured. Soft tissue was stripped, and the injury site was excised using a saw. The excised portion containing the defect was then cut in half (cross section) using an Isomet Low Speed Saw (Buehler Ltd, Lake Bluff, IL, USA) and placed in a solution of 10% buffered formalin for 48 hours. The other half was wrapped in saline gauze and stored at -80°C. Following fixation, the sample was briefly washed in saline before decalcification in Immunocal (United Biosciences, Carindale, Qld, Australia) for at least 72 hours. These samples were then washed for 1 hour in MQ water and transferred to 70% ethanol ready for paraffin embedding.

2.8. Histochemistry

2.8.1. Paraffin Embedding

After decalcification, bone samples to be embedded in paraffin wax were relocated to plastic embedding cassettes, and routinely processed for paraffin embedding.

2.8.2. Sectioning of Tissue

Paraffin sections were cut on a Leitz 1512 microtome. Sections were floated on a 50°C water bath and carefully transferred to SuperFrost™ slides (Menzel-Glaser, Braunschweig, Germany). Slides and sections were allowed to dry overnight at room temperature.

2.8.3. Histological Staining of Paraffin Embedded Tissue

2.8.3.1. Haematoxylin and Eosin

Paraffin sections were heated overnight at 65°C. On the following day, sections were dewaxed in the xylene substitute solvent Solv21C (United Biosciences) and rehydrated through a series of ethanol washes (2 x 100% and 1 x 70%) to water. Sections were then stained with Haematoxylin (Sigma-Aldrich) for 2-5 mins, rinsed thoroughly in water and differentiated in lithium carbonate (Sigma-Aldrich). Following another extensive wash in water, sections were stained in Eosin (Sigma-Aldrich) for 1-2 mins, and rinsed in water. The sections were sequentially dehydrated in 70% ethanol, 100% ethanol to Solv21C and mounted using Fast Dry Mounting Media (United Biosciences) mounting solution.

2.8.3.2. Alcian Blue

To prepare solution, 1% Alcian blue (Sigma-Aldrich) was dissolved in 3% (v/v) glacial acetic acid (Ajax Finechem) in water. Solution was agitated for 2 hours with a magnetic stirrer under gentle heat. Using NaOH, pH was carefully adjusted to pH 2.5, and solution stored at 4°C.

To stain paraffin embedded sections with Alcian Blue, samples were dewaxed and rehydrated through a series of washes (2 x 6 mins Solv21C, 1 x 3 mins 100% ethanol, 2 x 3 mins 70% ethanol) to water. Sections were immersed in Alcian Blue solution for 40 mins at RT, and then rinsed well in water. If required, samples were counterstained with Haematoxylin and Eosin, prior to dehydration and mounting.

2.8.4. Immunohistochemistry

Following heating overnight at 60°C, paraffin embedded sections were dewaxed and rehydrated through a series of decreasing ethanol concentration washes (2 x 100%, and 1 x 70%) to water. Sections were quenched in 1% (v/v) hydrogen peroxide (H_2O_2, Univar, Ajax Finechem) in PBS for 30 mins to inhibit endogenous peroxidase activity, and then washed twice in water for 5 mins each. Antigen retrieval was undertaken using 1 μg/ml Proteinase K (Roche Molecular Biochemicals) in PBS for 15 mins at RT. Two 5 min washes in water, and one wash in PBS ensued. Slides were then soaked in 0.2% glycine (Unilab, Ajax Finechem) in PBS for 30 mins to block the remaining reactive sites of the fixative, and then washed twice in water. Sections were blocked in 1% casein (Roche Diagnostics) in PBS containing 10% pig/rabbit/sheep serum for 90 mins at RT. After blocking, sections were briefly washed in PBS and primary antibody (diluted in block solution) was added. In these studies, the primary antibodies used were Col-2 (Santa Cruz) (diluted 1/600), and deer type 10 Collagen (diluted 1/600, kindly provided by Dr Gary Gibson at the Henry Ford Clinic, Detroit, USA). Incubation time with primary antibody was either 2 hours at RT or overnight at 4°C, both in a humidified chamber. The sections were washed in 0.01% Tween-20 in PBS for 5 mins, followed by two 5 min washes in PBS. Biotin conjugated multi link swine α goat, mouse, rabbit secondary antibody (DAKO, Glostrup, Denmark) was diluted in 1% block and incubated on sections for 1 hour at RT in a humidified chamber, followed by 3 x 5 min washes in PBS. Streptavidin ABC HRP complex (DAKO) was prepared 30 mins prior to use, incubated on slides for 1 hour, and then removed by 3 x 5 min washes in PBS. Liquid DAB + chromagen (DAKO) substrate was added to sections and left at RT until colour developed. Sections were rinsed in water, counterstained in Haematoxylin, differentiated in lithium carbonate, dehydrated through washes in increasing ethanol to Solv21C and xylene (BDH AnalaR®, Merck), and finally coverslipped.

2.9. Growth Plate Injury Measurements and Statistical Analysis

The measurement of different tissue types with lamb growth plate defects was performed using the Olysia BioReport software imaging system (Olympus Corporation, Tokyo, Japan). Measurements were taken within a defined area adjacent to the intact growth plate and calculated as the percentage of the total area measured. The measurements for each group were combined and compared for statistical significance using either a paired t-test

or for non parametric data, the Mann-Whitney test. Statistical significance was confirmed where $p<0.05$.

CHAPTER 3

ISOLATION AND IN VITRO CHARACTERISATION OF THE PROLIFERATIVE AND MULTIPOTENTIAL DIFFERENTIATION CAPACITY OF OVINE BONE MARROW-DERIVED MESENCHYMAL STEM CELLS

3.1 Introduction

The constitutively active process of haematopoiesis (blood formation) within the bone marrow (BM) is dependent upon three cellular constituents, cells of haematopoietic (including the common pluripotent progenitor cell known as the haematopoietic stem cell (HSC)), vascular and stromal cell lineages. Stromal cells can be loosely described as non-haematopoietic connective tissue cells of mesenchymal origin. It is the interaction of HSC, stromal cells and the extracellular matrix of the bone marrow microenvironment that regulates formation of the blood cell constituents (Allen et al., 1990; Dexter et al., 1977; Lichtman, 1981; Weiss, 1976).

The concept that adult haematopoiesis occurs within the stromal microenvironment of bone marrow was first demonstrated by Dexter and colleagues (1982), following establishment of the long term bone marrow culture system, containing a diverse population of adherent stromal like cells which supported maintenance of HSC in vitro (Dexter et al., 1977). Furthermore, the ability of BM to be regenerated and reconstituted following ablation by mechanical disruption set the precedent for the theoretical existence of a bone marrow stromal cell population with the potential to proliferate and differentiate into the multitude of stromal elements located within the BM microenvironment (Knospe et al., 1966; Owen, 1988; Patt and Maloney, 1975; Tavassoli and Crosby, 1968). Not only are these cells responsible for the extensive reconstitution of BM observed following insult, they are also necessary for the general turnover of the stromal tissue during normal steady state conditions (Amsel and Dell, 1971; Knospe et al., 1972; Owen, 1988; Patt and Maloney, 1975; Simmons et al., 1987).

Potential stromal progenitor cells were initially identified in several species, characterised by their ability to form colonies of cells resembling fibroblasts when plated as single cell suspensions of BM explants at appropriate densities. These clonogenic precursor stromal cells which give rise to distinct colonies were termed Colony Forming Unit-Fibroblast (CFU-F) cells, and described as adherent, non-phagocytic clonogenic cells capable of

extended proliferation (Castro-Malaspina et al., 1980; Friedenstein, 1980; Friedenstein et al., 1970). A variety of different techniques have collectively indicated that each colony is derived from an individual cell (Castro-Malaspina et al., 1980; Friedenstein et al., 1970; Perkins and Fleischman, 1990). A proportion of larger colonies exhibited extensive replating potential upon passaging (Friedenstein et al., 1987). In addition, a small proportion of clonally expanded mouse CFU-F could develop into a wide range of stromal cell types when transplanted in vivo (Friedenstein, 1980). These observations suggest that within the bone marrow there exists a small population of self-renewing, pluripotent stromal cells which give rise to a hierarchy of differentiating cells (Owen and Friedenstein, 1988). These progenitor cells are commonly referred to as BM stromal cells, stromal precursor cells, BM stromal stem cells, or mesenchymal stem cells (MSC). Subsequent studies examining the developmental capability of MSC in vitro have confirmed the ability of these cells to differentiate into osteoblasts, adipocytes, chondrocytes, myocytes, fibroblasts, marrow stroma, and cells of neural phenotype (Bianco et al., 2001; Bruder et al., 1994; Bruder et al., 1998a; Gronthos et al., 2003; Johnstone et al., 1998; Pittenger et al., 1999; Prockop, 1997; Woodbury et al., 2000; Xu et al., 2004; Yoo et al., 1998; Zhao et al., 2002).

More recently, several studies have confirmed that the localisation of MSC is not restricted to the bone marrow. It has been found that MSC-like populations reside in a diverse range of adult tissues and possess the ability to generate cell types specific for each tissue. Progenitor cells capable of multi-lineage differentiation have been discovered in adipose (Gronthos et al., 2001a; Zannettino et al., 2008; Zuk et al., 2001), synovium (De Bari et al., 2001b), periosteum (De Bari et al., 2001a; Nakahara et al., 1991), muscle (Bosch et al., 2000), dermis (Young et al., 2001), pericytes (Brighton et al., 1992; Reilly et al., 1998), blood (Kuznetsov et al., 2001; Zvaifler et al., 2000), cord blood (Hou et al., 2003; Korbling et al., 2005), dental tissues (Gronthos et al., 2000; Miura et al., 2003; Seo et al., 2004) and trabecular bone (Noth et al., 2002; Osyczka et al., 2002; Tuli et al., 2003). However, in most studies, it remains to be seen whether the cells isolated from these alternate tissues represent true stem cells or a diverse mixture of lineage specific progenitors.

The observation of heterogeneity within BM MSC populations derived from various animal sources has stimulated interest in the application of MSC for therapeutic benefit in translational animal studies. To date, in addition to humans, MSC have been identified in large and small animals including goat (Fischer et al., 2003; Murphy et al., 2003), rat

(Javazon et al., 2001; Lennon and Caplan, 2006; Yoshimura et al., 2007), rabbit (Awad et al., 1999; Tsutsumi et al., 2001), mouse (Phinney et al., 1999; Tropel et al., 2004), horse (Fortier et al., 1998), cow (Bosnakovski et al., 2005), dog (Kadiyala et al., 1997), cat (Martin et al., 2002), sheep (Jessop et al., 1994; Rhodes et al., 2004; Zhang et al., 2004), pig (Moscoso et al., 2005; Ringe et al., 2002; Vacanti et al., 2005) and non-human primates (Devine et al., 2003). Interestingly, BM derived CFU-F colonies from virtually all species examined are heterogeneous in size, morphology, proliferation and differentiation potential (Friedenstein et al., 1987; Gronthos et al., 2003; Kuznetsov et al., 1997; Owen, 1988). Although more sophisticated isolation techniques exist for human MSC due to the extensive range of human specific markers and antibodies, MSC isolated from the aforementioned species were directly attained from bone marrow aspirates based on their ability to adhere to plastic in monolayer culture.

The use of sheep as a large animal model for orthopaedic research continues to increase in popularity due to similarities with humans in weight, size, joint structure and bone regenerative processes. Since the discovery of adult progenitor cells with the capacity to differentiate into cells of musculoskeletal tissues, significant research has focussed on the application of MSC in bone and cartilage repair (Barry and Murphy, 2004; Bianco et al., 2001; Cancedda et al., 2003; Cancedda et al., 2007; Otto and Rao, 2004; Xian and Foster, 2006b). Although knowledge regarding human MSC properties and characteristics has been comprehensively investigated, very little characterisation of sheep MSC has been undertaken. Thus, any similarities and differences between ovine and human MSC remain unknown, the outcome of which may lead to discrepancies in preclinical studies. In this chapter, the in vitro characteristics of sheep bone marrow MSC were examined, in regard to yield, frequency, proliferative response to growth factors, and their multi-lineage differentiation potential.

3.2 Results

3.2.1 Ovine Bone Marrow Collection and Isolation of MNC Population

Although sheep MSC have previously been described in animal studies (Chen et al., 2005; Frosch et al., 2006; Li et al., 2005b; Rhodes et al., 2004), very little information exists regarding the frequency and yields of ovine MSC from the bone marrow. In the current study, aspirates (yields ranging from 20 to 45 ml) were collected from 10 adult sheep under general anaesthesia under sterile conditions using a children's size bone marrow biopsy needle. Samples were subsequently transferred to a previously heparinised tube to prevent clotting of the marrow (Figure 3.1). Prior to density gradient centrifugation, the quantity of mononuclear cells was assayed and ranged from 2×10^8 to 9.6×10^8 total cells with a mean of $4.4 \pm 0.9 \times 10^8$ SEM. Fractionation of the mononuclear cell (MNC) population via density gradient centrifugation is the well established standard procedure for MNC isolation in human clinical studies. Following centrifugation, a post-processing count of the BM MNC collected at the Percoll interface was performed to determine a viable number and percentage yield of MNC. Post-processing counts spanned 1.3×10^7 to 1.8×10^8 total mononuclear cells (mean $7.3 \pm 1.6 \times 10^7$), and the percentage yield fell between the extremes of 1% and 43% with a mean of 20.9% ± 4.2%.

In order to determine the optimal seeding density for CFU-F evaluation, sheep BM MNC were plated at various cell densities in triplicate, in 6 well plates ($9.6cm^2$). Samples were cultured in αMEM-20% for 11 days, at which point CFU-F colony numbers were assessed. While colonies failed to grow adequately when MNCs were plated below 10,000 cells per well, the number of CFU-F increased in a linear fashion between 100,000 and 1,000,000 MSC plated per well (Figure 3.2). Based on this observation, it was determined that the optimal seeding density for efficient CFU-F formation should fall within these figures.

The incidence of progenitor cells in ovine bone marrow was assessed using the well documented CFU-F assay. Freshly isolated BM MNC suspensions were seeded at 2×10^5 and 5×10^5 cells per well in 6-well plates, in triplicate. MNC suspensions were cultured for 10-14 days in the presence of 20% FCS. The number of colonies per 1×10^5 cells plated was determined and averaged to assess the incidence of CFU-F for each donor sample (Figure 3.3). The frequency of colony forming units was relatively consistent at both cell densities examined. Considerable heterogeneity in colony size and density was

Figure 3.1: Collection of bone marrow aspirates from adult sheep. Using a human child size bone marrow biopsy needle, bone marrow was collected from the iliac crest of adult sheep under general anaesthesia. Specimens were extracted under sterile conditions in pre-heparinised syringes and transferred to heparinised tubes. Prior to bone marrow aspiration, the site of extraction was shaved and antiseptic applied to minimise the risk of microbial contamination.

A

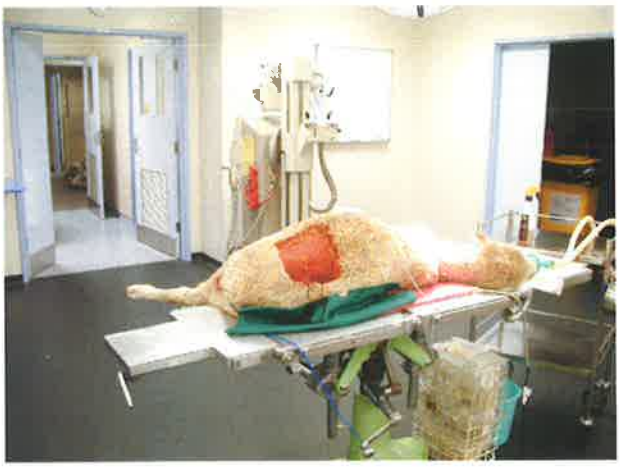

B

Table 3.1. Collection of bone marrow aspirates from 10 adult sheep. The ensuing table provides information regarding the volume, MNC number prior to and following subjection of bone marrow to density gradient centrifugation, and overall yield from each sample.

Sheep Number	Bone Marrow Volume (ml)	MNC Number Pre Processing (per 10^7 cells)	MNC Number Post Processing (per 10^7 cells)	Yield (%)
1	40	52.9	10.0	18.9
2	45	29.9	9.9	33.1
3	40	38.3	4.6	12.0
4	20	21.6	3.9	17.9
5	20	22.3	4.3	19.1
6	25	20.1	7.5	37.3
7	35	93.4	18.3	19.5
8	40	96.4	1.3	1.4
9	20	37.0	2.4	6.4
10	40	26.1	11.3	43.3

Figure 3.2: Determination of optimal seeding density for sheep CFU-F establishment. Bone marrow derived MNC were plated in 6 well plates at increasing cell densities. The data indicates the mean number of CFU-F colonies ± SEM of triplicate cultures. Cells were grown in α-MEM media supplemented with 20% FCS for a period of 11 days. No colonies were observed at low cell densities. A correlation between MNC number and colony number became apparent between 1×10^5 and 1×10^6 MNC plated per well. Thus efficient colony establishment lies within this series.

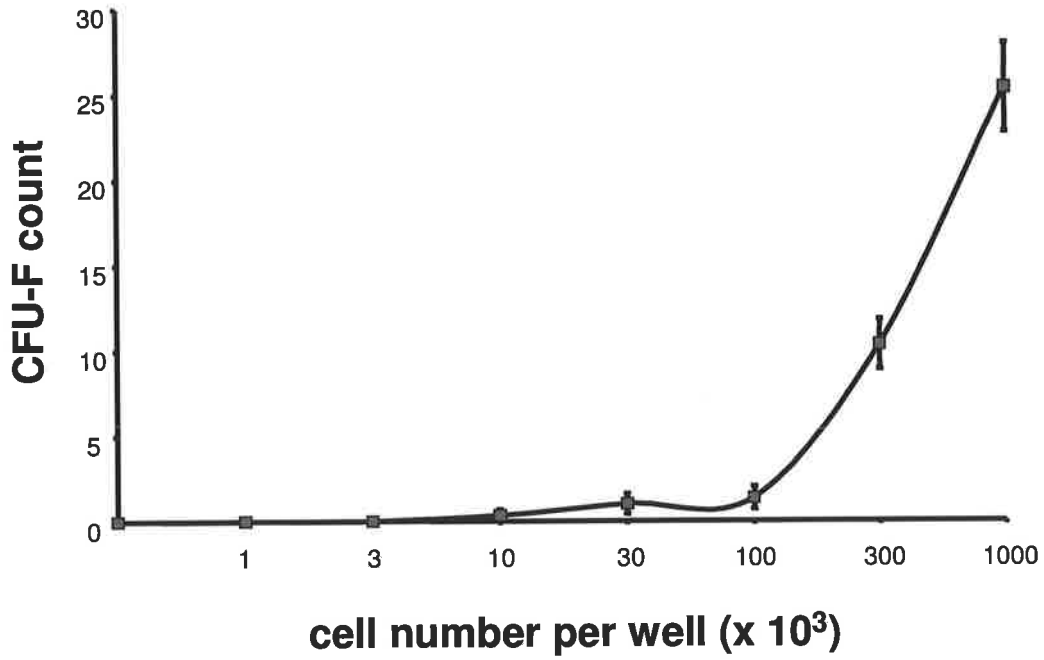
CFU-F count
30
25
20
15
10
5
0
1
3
10
30
100
300
1000
cell number per well (x 10³)

Figure 3.3: CFU-F yield from 10 sheep bone marrow aspirates. Single cell suspensions of bone marrow MNC were plated at two densities in 6 well plates in triplicate. Following 10 to 14 days incubation in α-MEM + 20% FCS, cells were stained and colonies scored. Data is presented as the mean colony number across both cell densities ± SEM. The number of colony forming cells from each bone marrow sample was variable, ranging from 1.0 to 9.2 MSC per 1 x 10^5 MNC plated, with a mean of 4.6 ± 0.7 SEM.

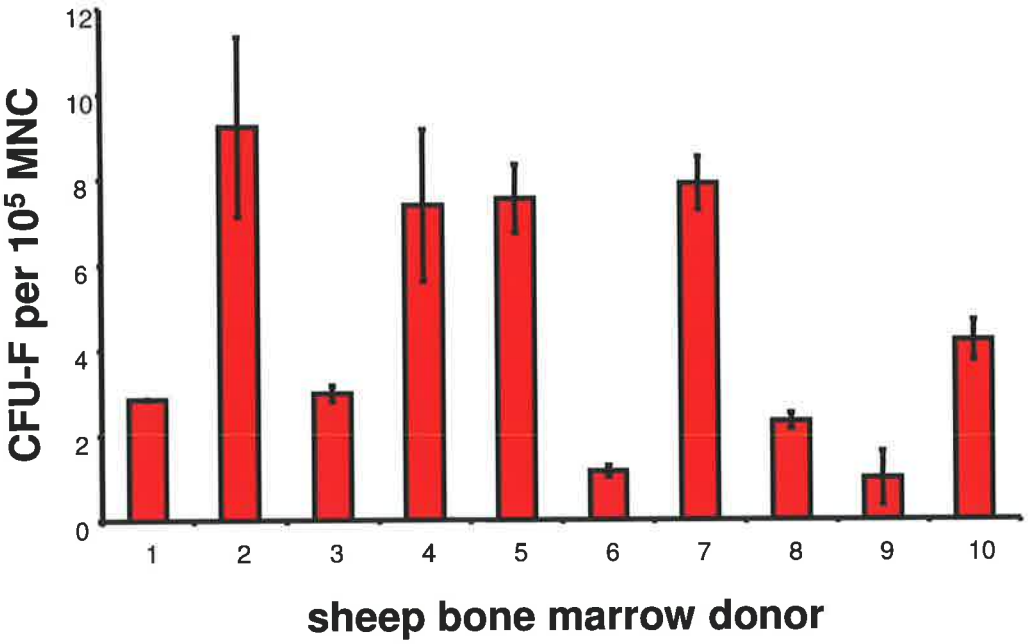
CFU-F per 10^5 MNC
12
10
8
6
4
2
0
1
2
3
4
5
6
7
8
9
10
sheep bone marrow donor

observed between and within donors (Figure 3.4A and B). Overall, the mean frequency of CFU-F across the 10 sheep bone marrow aspirates assessed was 4.6 ± 0.7 per 1 x 10^5 MNCs, with individual variation ranging from 1.0 to 9.2 colonies per 1 x 10^5 MNCs seeded (Figure 3.3). Thus the incidence of CFU-F forming MSC within the BM MNC population is approximately 0.001% to 0.010%.

Morphologically, sheep MSC are large adherent cells resembling fibroblasts (Figure 3.4). There appeared to be a wide variation and heterogeneity within MSC derived from a single animal. These cells were polygonal, stellate, and spindle shaped with long processes. At low density sheep MSC appeared more polygonal (Figure 3.4C) and upon reaching confluence become more spindle shaped (Figure 3.4B). Compared to human MSC, sheep MSC appear to proliferate at a more rapid rate. When plated at a similar density of 6000 cells/cm^2, sheep MSC achieve confluence within 2 days, whereas human cells reach confluence by 3 days (data not shown).

3.2.2. Proliferative Response of Ovine MSC to Growth Factors

Whilst there exists an extensive array of human, mouse and rat recombinant growth factors for cell culture studies for MSC expansion ex vivo, there are very few growth factors available developed specifically for sheep cells. Nonetheless, growth factors across mammalian species generally exhibit a high level of structural and functional conservation. On this premise, sheep MSC were exposed to a variety of human recombinant growth factors that have previously shown to stimulate human MSC proliferation or to be important in the regulation of chondrocytes and chondrogenesis. The proliferative response of sheep MSC with growth factor incubation was monitored using the colorimetric WST-1 assay, which is a non radioactive alternative to thymidine incorporation assays and quantifies both cell proliferation and cell viability.

Under serum free conditions, ovine BM derived MSC were exposed to 7 different growth factors individually at 5 concentrations ranging from 0.1 to 100 ng/ml. PDGF and EGF, which have demonstrated mitogenic properties on human MSC, were assessed at 10 ng/ml, which is the concentration previously defined to be optimal for proliferation of human MSC (Gronthos , 1995). In addition to a serum free control, 2 positive control groups were supplemented with 10% and 20% FCS respectively, as a comparison to the amount of growth in response to standard proliferative culture media. Compared to the serum free

Figure 3.4: Morphological phenotype of ovine bone marrow derived MSC. A representative example of a CFU-F colony stained with Toluidine blue at day 14 (10x) (A). Example of a low density CFU-F colony under higher magnification (20x) (B). On closer examination (20x), the morphology of ovine MSC following ex vivo expansion is typical of fibroblastic like cells (C). At low density, MSC appear polygonal and stellate (black arrow), and at higher density resemble more spindle shaped cells (open arrow).

A

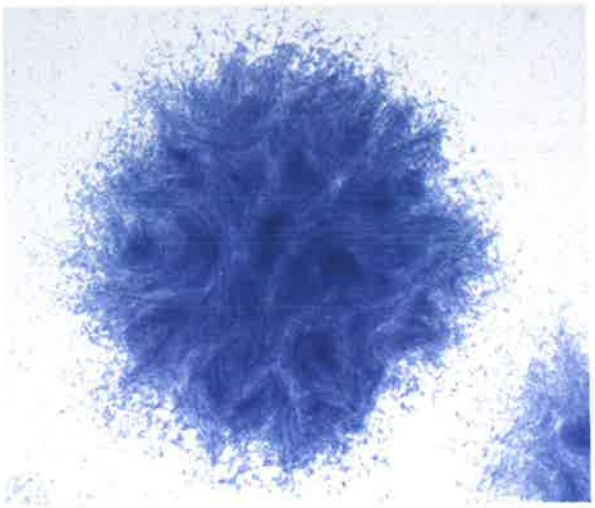

B

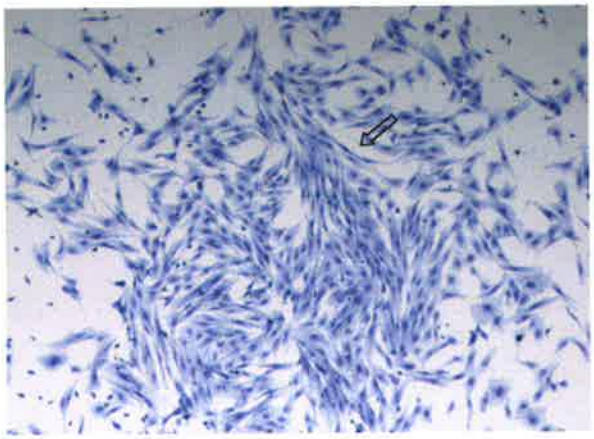

C

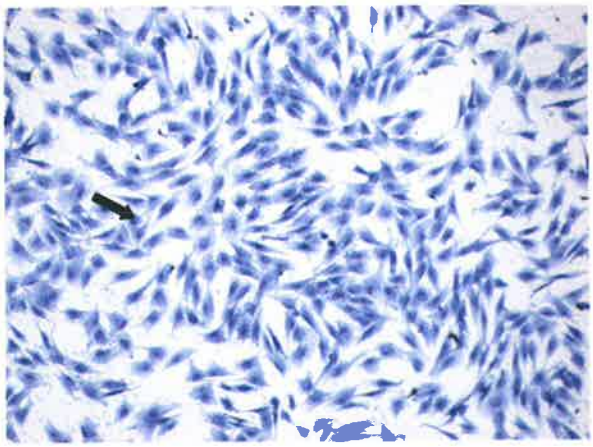

conditions, the addition of FCS stimulated growth significantly ($p<0.05$, Paired *t*-test) and was proportional to the amount of serum added, with growth being highest in the presence of 20% serum. PDGF and EGF exhibited significant mitogenic effects ($p<0.05$, Paired *t*-test) compared to the serum free sample, and also exceeded growth levels observed with 10% FCS (Figure 3.5A).

Sheep MSC cultured in the presence of BMP-2 exhibited little stimulatory activity at the majority of concentrations assessed, with the exemption of a significant spike in proliferation at 100 ng/ml ($p<0.05$, Paired *t*-test) (Figure 3.5B). Similarly, in response to BMP-7, an increase in proliferation was only notable and significant ($p<0.05$, Paired *t*-test) at the highest concentration assessed of 100 ng/ml (Figure 3.5C). Interestingly, the presence of BMP-7 at 30 ng/ml induced a significant reduction in cell number. Overall, in both the BMP-2 and BMP-7 samples assayed, MSC were unresponsive to concentrations of BMP growth factor below 100 ng/ml, with cell numbers equivalent to the serum deprived conditions. Thus, it appears that stimulation of cell growth by BMP-2 or BMP-7 is dependent on a high concentration of growth factor.

Some disagreement currently exists in the literature as to whether FGF-2 has a mitogenic effect on MSC (Baddoo et al., 2003; Bianchi et al., 2003; Gronthos and Simmons, 1995; Locklin et al., 1995; Solchaga et al., 2005; Sotiropoulou et al., 2006). In this study, incubation with FGF-2 within the range of 1 to 30 ng/ml induced a significant ($p<0.05$, Paired *t*-test) mitogenic response in MSC (Figure 3.5D), comparable to the addition of 10% FCS. However, the presence of FGF-2 at 100 ng/ml sharply decreased proliferation equivalent to the serum free control, suggesting that excessive amounts of FGF-2 have cytostatic or inhibitory effects.

A dose dependent increase in cell number was observed in response to increasing concentrations of IGF-1 (Figure 3.5E). The entire spectrum of IGF-1 concentrations assayed induced a significant ($p<0.05$, Paired *t*-test) upregulation of cell proliferation analogous to that observed between 10% and 20% FCS supplementation.

A significant ($p<0.05$, Paired *t*-test) and potent mitogenic effect was observed in response to the addition of TGFα at all concentrations assayed (Figure 3.5F). The TGFα protein exhibits 33% homology to the EGF molecule and binds to the membrane bound EGF receptor, initiating tyrosine phosphorylation of the EGF receptor indistinguishable from

Figure 3.5: Proliferative response of sheep BM derived MSC to various growth factors. MSC derived from bone marrow were seeded in triplicate in 96 well plates at a cell density of 2,000 cells per well. The cells were permitted to attach overnight, following which, cells were cultured in the presence of growth factor at concentrations ranging from 0.1 to 100 ng/ml. Cell number was assayed and quantitated at day 5 using WST-1, as described in methods (refer to section 2.1.7.2). The results displayed represent the mean growth observed from triplicate cultures as a percentage of growth achieved under serum deprived conditions ± SEM for each concentration. Significant proliferation was apparent in response to incubation with PDGF and EGF at 10 ng/ml (A). Supplementation with BMP-2 exhibited a proliferative effect on cell number at the highest concentration of 100 ng/ml (B). Similarly, MSC were only stimulated to proliferate in response to BMP-7 at 100 ng/ml (C). In contrast, FGF-2 increased cell number most effectively between the concentration range of 1 to 30 ng/ml, but was not mitogenic at 100 ng/ml (D). Cellular proliferation correlated with IGF-1 supplementation dose dependently (E). Incubation with TGF-α considerably and most effectively enhanced cell number across the spectrum of factor concentrations (F). The addition of TGF-β1 to MSC appeared to have a significantly inhibitory effect on cell proliferation (G). TGF-β3 stimulated cell growth at all the concentrations assessed. The presence of an * indicates statistical significance according to Paired *t*-test where $p<0.05$.

A

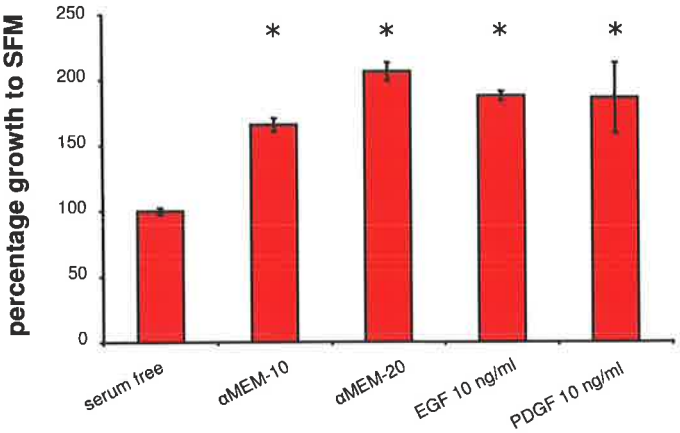

BMP-2

B

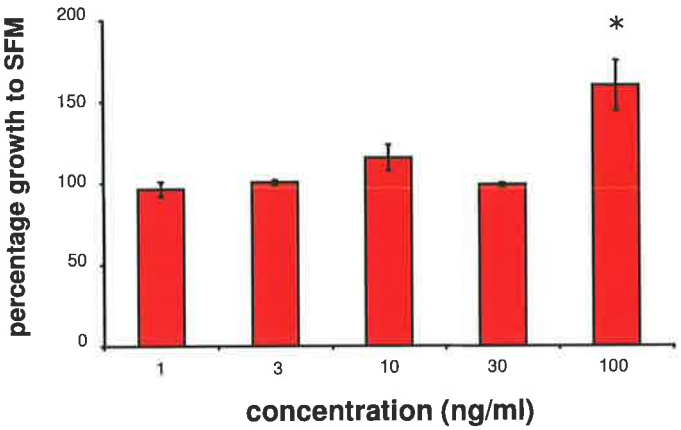

BMP-7

C

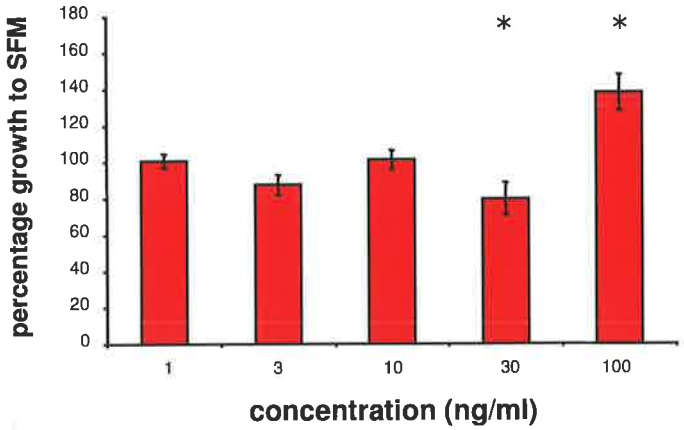

D

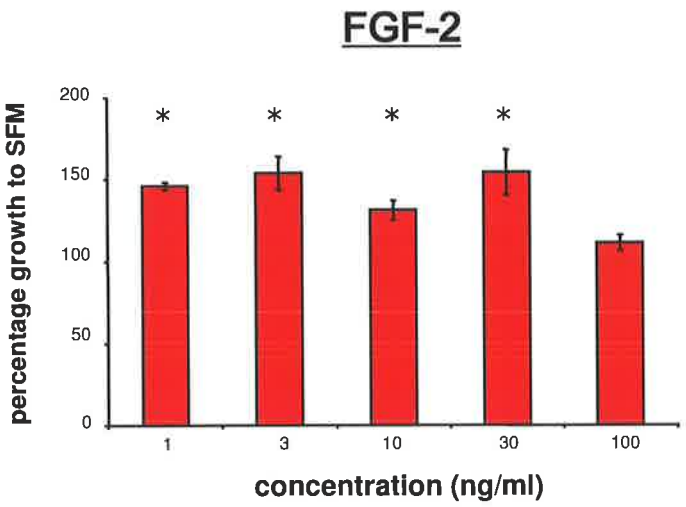
FGF-2
percentage growth to SFM
200
150
100
50
0
*
*
*
*
1
3
10
30
100
concentration (ng/ml)

E

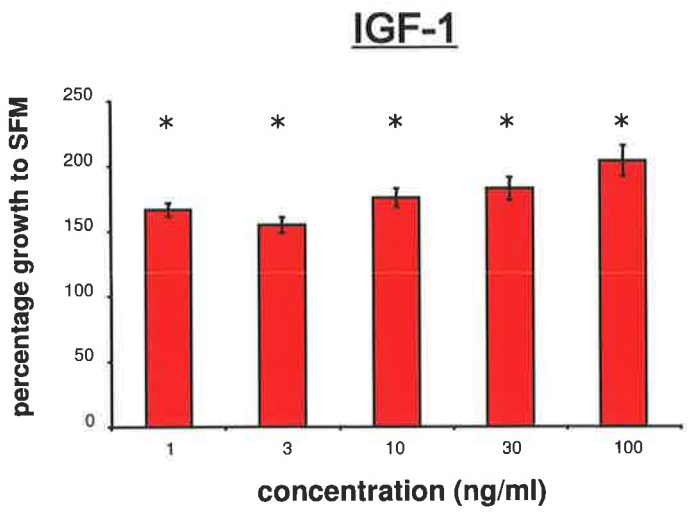
IGF-1
percentage growth to SFM
250
200
150
100
50
0
*
*
*
*
*
1
3
10
30
100
concentration (ng/ml)

F

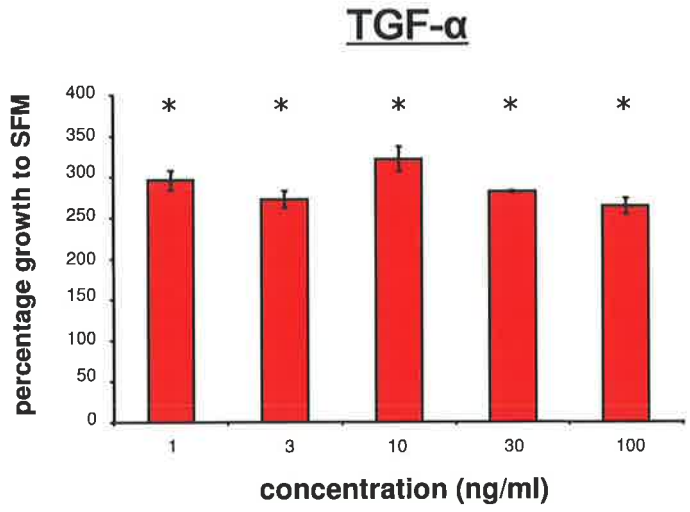
TGF-α
percentage growth to SFM
400
350
300
250
200
150
100
50
0
*
*
*
*
*
1
3
10
30
100
concentration (ng/ml)

G

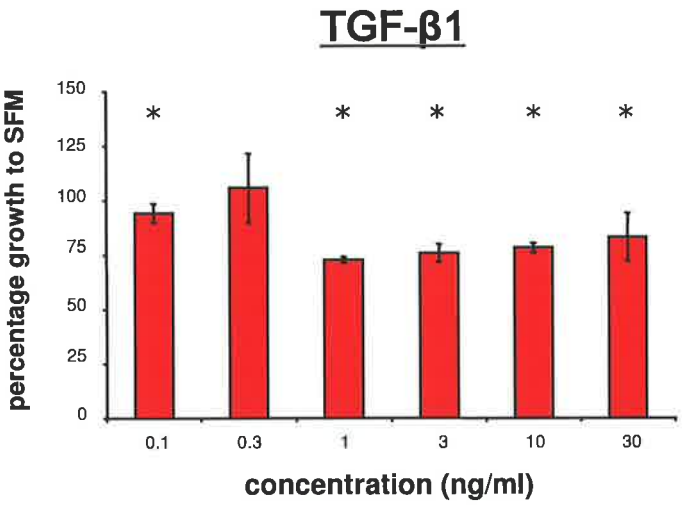
TGF-β1
percentage growth to SFM
150
125
100
75
50
25
0
*
*
*
*
*
0.1
0.3
1
3
10
30
concentration (ng/ml)

H

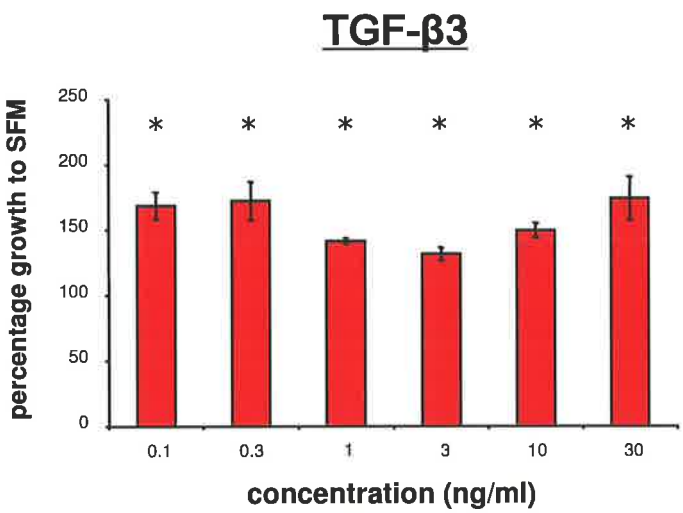
TGF-β3
percentage growth to SFM
250
200
150
100
50
0
*
*
*
*
*
*
0.1
0.3
1
3
10
30
concentration (ng/ml)

EGF (Lee, 1985). Although optimal growth was observed at 10 ng/ml; in comparison, even the lowest concentration (1ng/ml) assessed surpassed proliferation of MSC by 20% FCS. At 10 ng/ml, cell numbers were 3 fold greater than the serum deprived control, twice that observed with 10% FCS, and approximately 30% greater than 20% FCS stimulation. The findings here indicate TGFα to be an effective stimulator of cell proliferation in sheep MSC.

Significant inhibition ($p<0.05$, Paired *t*-test) of MSC viability and cell activity was evident in a dose dependent response to cultivation with TGF-β1 (Figure 3.5G). Theoretically, if sheep MSC were unresponsive to this factor, the addition of human recombinant TGFβ1 would present readings comparable to the absence of serum. Lowest readings were inversely associated with higher amounts of TGF-β1 present in the media, and in one instance was 40% less than the level observed with the serum free media control (SFM). Thus, TGFβ1 is clearly not a stimulatory mitogen and may instead have a role of TGFβ1 in differentiation or lineage fate determination of sheep MSC.

In contrast to the findings reported for TGF-β1, the presence of TGF-β3 induced a significant ($p<0.05$, Paired *t*-test) upregulation of cell number at all concentrations assessed (Figure 3.5H). Proliferation with TGF-β3 was optimal at the low and high concentration extremities in a double peak distribution, approximately to the levels achieved with 10% FCS supplementation.

3.2.3. Multilineage Differentiation Potential of Ovine BM MSC

It has been well reported that MSC derived from human and animal sources possess the potential to differentiate down multiple lineages. In this study, we assessed whether sheep bone marrow MSC are also multipotential in vitro, and performed experiments to determine if sheep MSC could be induced to differentiate into cells of osteogenic, adipogenic and chondrogenic lineage.

3.2.3.1 Osteogenic Differentiation

The technique for in vitro osteogenesis has been widely applied and further optimised for human bone marrow cells by Gronthos et al (1994) (Gronthos et al., 1994). Sheep MSC were isolated by plastic adhering capacity and cultured in the presence of osteoinductive

medium containing 10% FCS, ascorbate-2-phosphate (Asc-2P), dexamethasone (Dex) and inorganic phosphate (PO_{4i}). After 2 weeks in osteogenic growth conditions, rapid mineralisation of the extracellular matrix had occurred as indicated by calcium deposits stained with Alizarin Red (Figure 3.6A). By 4 weeks, the adherent cell layer had mineralised further and the staining of calcium was intense and extensive. Total RNA was collected at days 17, 26 and 35, and expression of bone related genes was assessed by semi quantitative RT-PCR (Figure 3.6B), with the data expressed as the ratio of GAPDH expression (Figure 3.6C). Core binding factor alpha 1 (Cbfa-1) is an essential transcriptional activator of osteoblast differentiation. Expression of Cbfa-1 was upregulated by day 17 and continued to increase along the course of the experiment (Figure 3.6C). Collagen type-1 (Col-1) is the most abundant bone extracellular matrix protein expressed by osteoblasts. Under osteoinductive conditions, Col-1 expression increased at day 17, declined slightly at day 26 and increased again at day 35 (Figure 3.6C). Interestingly, expression of Cbfa-1 and Col-1 were detected in samples cultured under normal conditions, but to a lesser extent than following induction, consistent with human studies (Gronthos 2003). By D17, the expression levels of Cbfa-1 and Col-1 had increased by over 50% of that observed in uninduced conditions. Cbfa-1 expression levels increased by almost three quarters and was doubled by D26 and D35 respectively. Compared to basal expression level at D0, following induction, expression of the Col-1 gene increased by over one quarter, and three quarters by D26 and D35 respectively.

3.2.3.2 Adipogenic Differentiation

Adipogenesis in human and rat BM MSC cultures can be induced in the presence of methylisobutylmexanthine, hydrocortisone, and indomethacin as described previously (Gimble, 1998). Following this established protocol for differentiation of MSC into fat forming cells, sheep MSC were cultured for up to four weeks in media containing the aforementioned combination. Photomicrographs of cultures stained with the fat soluble marker Oil Red O at 4 weeks revealed substantial clusters of positively staining lipid-laden adipocytes (Figure 3.7A). Total RNA harvested at days 12, 18, and 30 were used for semi quantitative RT-PCR analysis of gene expression for markers of adipogenesis, including leptin (which is produced by adipose tissue and regulates appetite and metabolism) lipoprotein lipase (LPL) (an enzyme responsible for lipid hydrolysis of lipoproteins), and peroxisome proliferator activated receptor-gamma (PPARγ) (an early adipogenic transcription factor) (Gimble, 1998) (Figure 3.7B). Alteration in levels of gene expression

Figure 3.6: Bone marrow derived sheep MSC are capable of osteogenic differentiation *in vitro*. Sheep MSC were seeded in T25 flasks at a cell density of 200,000 cells per flask, and allowed to attach overnight. On the following day, cells were cultured in osteoinductive media as described in the methods. Fresh media was replaced twice per week, for a period of up to 5 weeks. Representative micrographs of histochemical analysis of *in vitro* mineralisation stained with Alizarin Red (A). By two weeks, extensive calcium rich deposits were evident, as indicated by the presence of Alizarin Red stain. At approximately four weeks, further deposition of mineralised matrix was observed as denoted by intensified Alizarin red stain (10x). Total RNA was isolated from samples at approximately 2, 4 and 5 weeks, and gene expression was examined by semi-quantitative RT-PCR. Transcripts analysed in this study were Cbfa-1 (an essential transcription factor for osteoblast differentiation), and Col-1 (major bone extracellular matrix molecule) (B). Product bands from RT-PCR were semi-quantitated and plotted as a histogram representing the ratio of gene expression relative to the expression of the house keeping gene GAPDH (C). Relative gene expression of Cbfa-1 increased linearly over the course of the experiment. Even though MSC express Col-1 under normal culture conditions, expression was increased in response to osteoinductive medium, when compared to non induced controls.

A

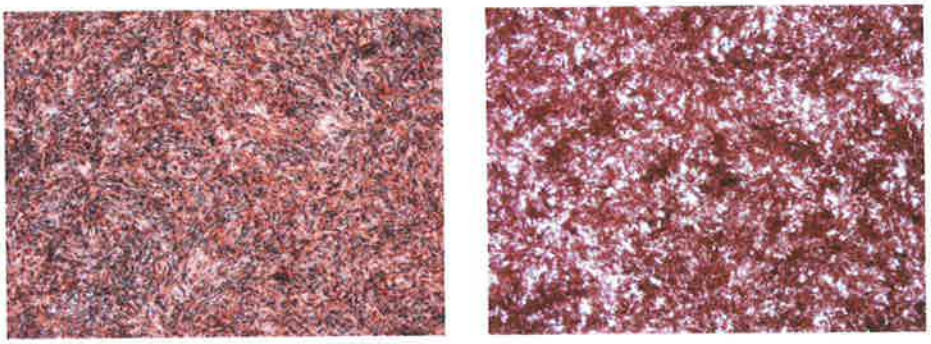

2 weeks

4 weeks

B

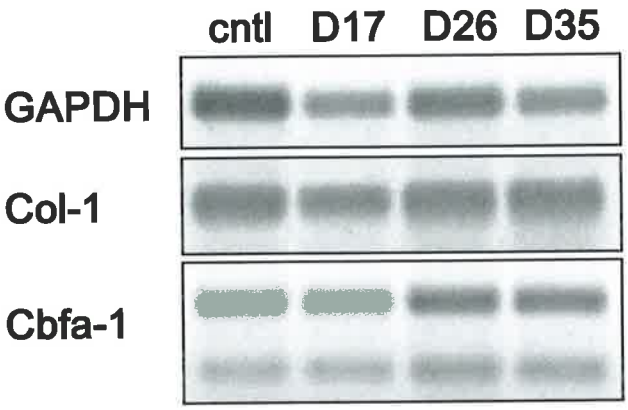

C

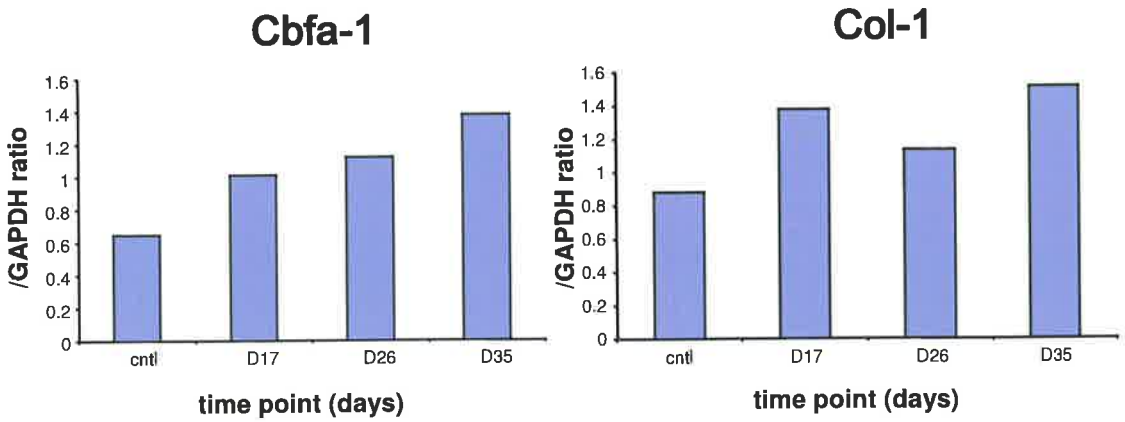

Figure 3.7: Bone marrow derived sheep MSC exhibit adipogenic potential *in vitro*. Sheep MSC were seeded in T25 flasks at a cell density of 200,000 cells per flask, and allowed to attach overnight. On the following day, cells were cultured in adipogenic media as described in the methods. Fresh media was replaced twice per week, for a period of up to 4 weeks. Representative micrographs of histochemical analysis of *in vitro* adipogenesis stained with the fat soluble dye Oil Red O (A). Cultures were counter stained with Haematoxylin. At 4 weeks, the formation of large clusters of Oil Red O positive adipocytes was observed (10x) (B). The left hand panel represents a magnified view of fat laden adipocyte droplets. Total RNA was isolated from samples at approximately 2, 3 and 4 weeks, and gene expression was examined by semi-quantitative RT-PCR. Transcripts analysed in this study were leptin, lipoprotein lipase (LPL) and transcription factor peroxisome proliferator activated receptor (PPARγ) (B). Product bands from RT-PCR were semi-quantitated and plotted as a histogram representing the ratio of gene expression relative to the expression of the house keeping gene GAPDH (C). Leptin expression continuously increased in a linear fashion from 2 weeks until 4 weeks, in comparison to control. LPL was markedly upregulated at two weeks, following which expression was gradually down regulated over time. Comparable to LPL, expression of the early adipogenic transcription factor PPARγ was significantly upregulated at two weeks, and decreased progressively at 3 and 4 weeks.

A

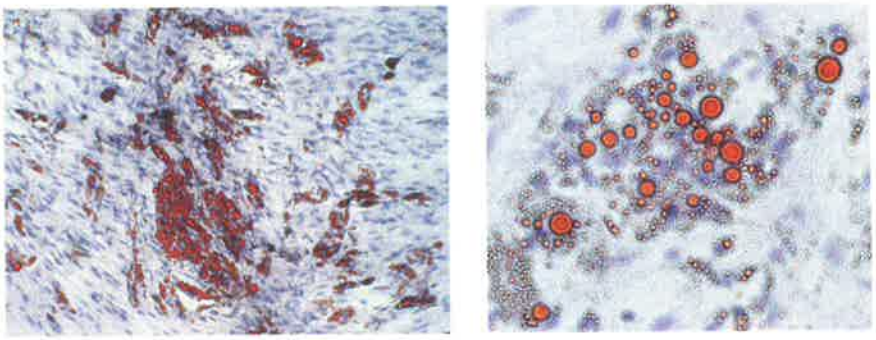

B

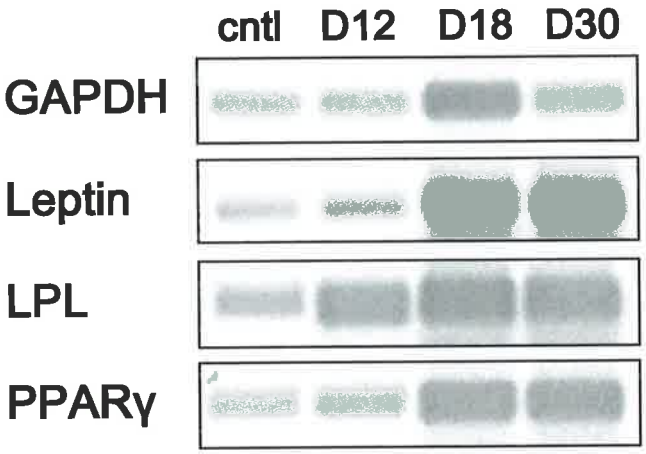
cntl
D12
D18
D30
GAPDH
Leptin
LPL
PPARγ

C

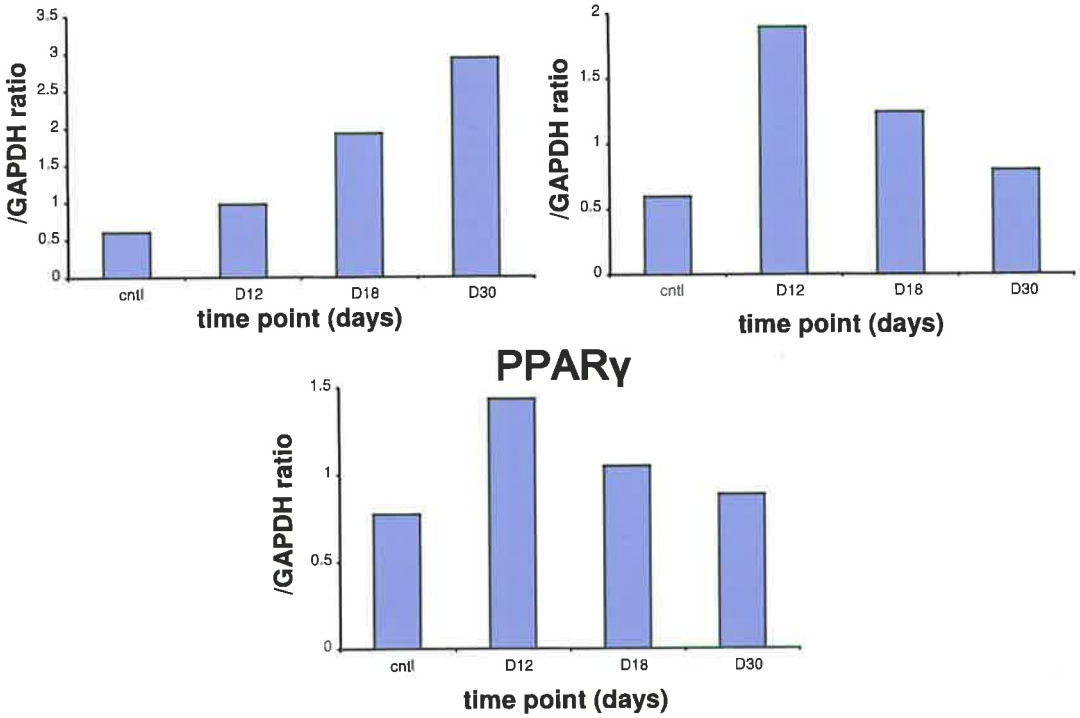
Leptin
/GAPDH ratio
3.5
3
2.5
2
1.5
1
0.5
0
cntl
D12
D18
D30
time point (days)
LPL
/GAPDH ratio
2
1.5
1
0.5
0
cntl
D12
D18
D30
time point (days)
PPARγ
/GAPDH ratio
1.5
1
0.5
0
cntl
D12
D18
D30
time point (days)

was assessed by presenting data as a ratio of GAPDH expression (Figure 3.7C). Expression of leptin was induced by day 12, and increased in a time-dependent fashion over the course of the experiment. Compared to the uninduced control, leptin levels increased by over half at D12, and were 3 fold and 5 fold greater at D18 and D30 respectively. In contrast, LPL expression was drastically upregulated by 3 fold at the first time point assessed, followed by a linear decline to day 30 (two fold increase) with the levels only one quarter greater at D30, similar to the undifferentiated sample. As an early essential transcription factor for adipogenesis, PPARγ accordingly was stimulated most markedly in expression in the initial stages of the assay, at day 12 (86% increase compared to D0), which diminished by D18 and D30 to 35% and 10% upregulation compared to the control sample. Although all three genes were constitutively expressed by control samples, the levels at D0 were markedly lower than those observed following adipogenic induction.

3.2.3.3 Chondrogenic Differentiation

For the aim of this study, it was important to determine whether sheep MSC could be induced to differentiate down a chondrogenic lineage. It is well known that chondrocytes require a three dimensional arrangement in order to maintain their chondrocytic phenotype (Benya, 1988; Benya and Shaffer, 1982). Likewise, the transition of MSC to chondrocyte-like cells also necessitates a concentrated cell and matrix environment. The use of aggregate culture for chondrocyte differentiation of human MSC was developed by Johnstone et al (1998), and is now widely used as an indicator of chondrogenic potential in vitro(Johnstone et al., 1998). Employing this technique, sheep MSCs were aggregated into a three dimensional pellet by low centrifugation. The cell pellet was subsequently cultured for 21 days in the presence of various growth factors. The growth factors assessed were those previously demonstrated to induce chondrogenesis of human MSC in vitro, or have been identified as important regulators of growth plate chondrocytes (Freed et al., 1999; van der Eerden et al., 2003; Xian and Foster, 2006a; Xian and Foster, 2006b)including BMP-2 (50ng/ml), BMP-7 (100ng/ml), FGF-2 (10 ng/ml), TGF-β1 (10 ng/ml), TGF-β3 (10 ng/ml), and combinatorial factors BMP-2/TGF-β3 (50 and 10 ng/ml respectively) and BMP-7/TGF-β1 (100 and 10 ng/ml respectively).

Following three weeks of culture, MSC pellets exhibited widely differing morphologies (Figure 3.8A-D). For example, cells incubated in TGF-β3 appeared small, round, and densely arranged (Figure 3.8A). Interestingly, cultures supplemented with BMP-7/ TGF-

Figure 3.8: Histological evaluation of *in vitro* chondrogenic differentiation of bone marrow derived MSC. Using the previously described pellet culture technique for chondrogenesis, 250,000 sheep MSC were transferred to a 13 ml pointy nose polypropylene tube and spun at 1400 rpm for 10 mins to aggregate cells into a three dimensional pellet. Cells were then cultured in single or combinatorial growth factors. In this assay, the various growth factors assessed were: BMP-2 (50 ng/ml), BMP-7 (100 ng/ml), FGF-2 (10 ng/ml), TGF-β1 (10 ng/ml), TGF-β3 (10 ng/ml) and the BMP/TGF-β combinations of BMP-2/TGF-β3 (50 ng/ml and 10 ng/ml respectively) and BMP-7/TGF-β1 (100 ng/ml and 10 ng/ml respectively). Media was replaced 3 times per week for 21 days. Pellets were subsequently paraffin embedded and transverse sections cut. Representative photomicrographs of histological staining of pellets following *in vitro* chondrogenesis. Panels A-D were stained with Haematoxylin and Eosin. Panels E-F were assayed using the glycosaminoglycan indicator Alcian Blue. The size of chondrocyte pellet was significantly larger when cultured in the presence of BMP-7/TGF-β1 compared to control and single factor pellets. Additionally the BMP-7/TGF-β1 pellet was characterised with three distinct zones with differential morphology. Alcian blue staining was most intense in the periphery of BMP-2/TGF-β3 and BMP-7/TGF-β1 samples.

A. TGF-β3 (10x)

B. BMP-7/TGF-β1 (10x)

C. BMP-2/TGF-β3 (20x)

D. BMP-7/TGF-β1 (20x)

E. TGF-β3 (10x)

F. BMP-7/TGF-β1 (10x)

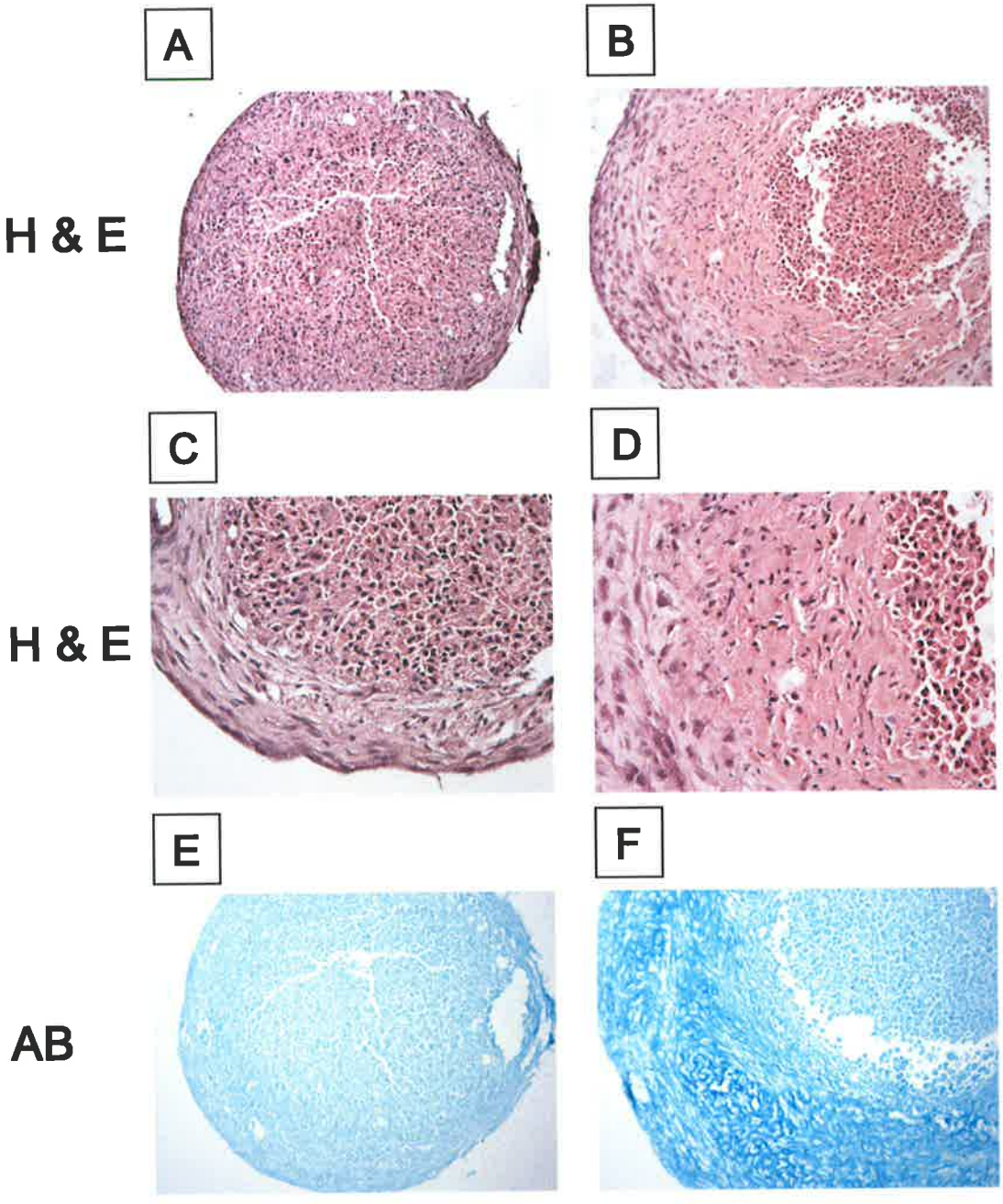
A
B
H & E
C
D
H & E
E
F
AB

β1 exhibit three distinct morphological zones within the pellet (Figure 3.8B and D). The inner zone appeared to contain a high population of small densely associated round cells. Cells of the intermediate zone exhibited condensed nuclei and were more sparsely positioned within a more extensive and well developed extracellular matrix. In contrast, the outer zone encapsulating the pellet appeared to be a more fibrous tissue, composed of elongated cells with large nuclei. A similar, yet different phenotype was observed in response to supplementation with BMP-2/ TGF-β3 (Figure 3.8C). Two zones were apparent, namely an outer fibrous sheath and a proliferative core, which had a comparable morphology to the BMP-7/ TGF-β1 pellet. However, this sample did not include the intermediate zone as observed in the BMP-7/ TGF-β1 sample.

Alcian blue is a histological cationic dye used to distinguish the presence of cartilage glycosaminoglycans. Alcian blue positive staining was moderately detected in all samples examined, including the one cultured with TGF-β3 alone (Figure 3.8E) and was strongly detected in the outer regions of the BMP-7/ TGF-β1-cultured pellet (Figure 3.8F).

Immunohistochemical analysis of MSC chondrogenesis assay samples revealed an absence of collagen type 2 (Col-2) protein expression in all MSC aggregates assayed (Figure 3.9A), except for the BMP-7/ TGF-β1-culured sample, where Col-2 was detected within the more fibrous periphery of cell pellet (Figure 3.9B). Expression of collagen type 10 (Col-10), which is collagen protein expressed by hypertrophic matured chondrocytes, was only observed in the BMP-7/ TGF-β1-cultured sample (but not others), localising to the intermediate zone of the tri-zonal pellet (Figure 3.9C).

Examination of gene expression of pellet cultures was undertaken by RT-PCR from isolated cellular RNA, for genes essential for chondrocyte differentiation (Sox-9), or extracellular matrix molecules identified in cartilage tissue (aggrecan, Col-2, and Col-10). The house keeping gene GAPDH was included as an internal loading control for each sample (Figure 3.10A), with levels of expression of each gene semi quantitated and presented as a ratio of GAPDH (Figure 3.10B). Aggrecan levels were unaltered following incubation in SFM, BMP-2, BMP-7 and FGF-2. However, expression was markedly increased in response to TGF β3 and TGF-β1. Low levels of aggrecan expression were detected in the BMP-2/TGF β3 sample. Expression of Col-2 is the primary marker of chondrogenesis, as Col-2 is specific to cartilage secreted into the extracellular matrix by chondrocytes, contributing to 90% of the collagen component. Gene expression of Col-2

Figure 3.9: Immunohistochemical evaluation of *in vitro* chondrogenic differentiation of bone marrow derived MSC. Paraffin sections were incubated overnight with monoclonal anti Collagen-2 (Col-2) antibody or polyclonal anti Collagen-10 (Col-10) antibody. The antigen was detected using the DAB substrate. At day 21, minimal Col-2 protein expression was observed following culture of MSC with TGF-β3 (10x) (A). In contrast, Col-2 expression was detected in the extracellular matrix of cells located within the periphery of the pellet exposed to BMP-7/TGF-β1 (10x) (B). Col-2 protein expression was the greatest in this sample. The presence of Col-10 staining was only identified in one instance (C). Pelleted cells subjected to BMP-7/TGF-β1 (10x) produced collagen, which localised to the outer region of the pellet core, but within the Col-2 synthesising periphery.

A

Col-2

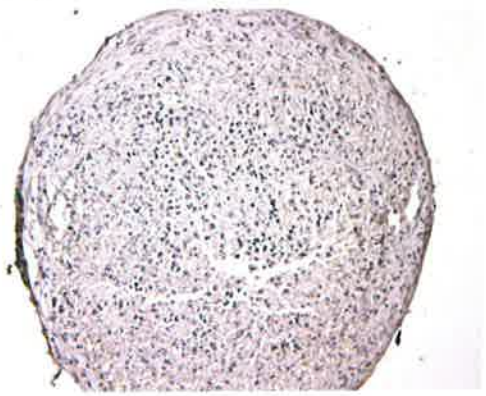

B

Col-2

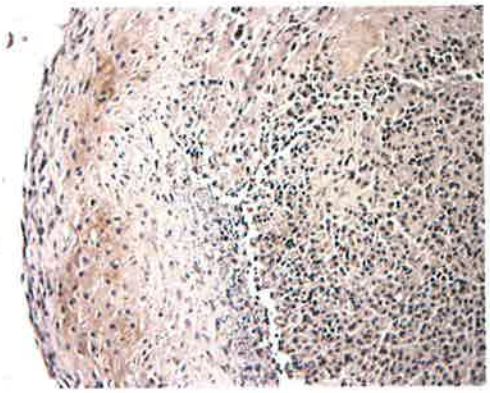

C

Col-10

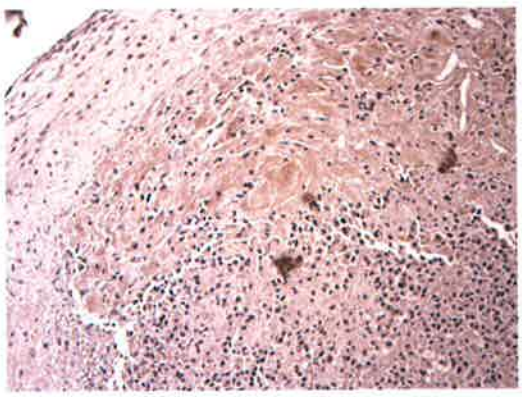

Figure 3.10: Gene expression analysis following *in vitro* chondrogenic differentiation of bone marrow derived MSC. Total RNA was isolated from samples at 21 days, and gene expression was examined by semi-quantitative RT-PCR. Transcripts analysed in this study were cartilage extracellular matrix molecules aggrecan, collagen-2, and collagen-10, and the crucial early transcription factor for chondrocyte differentiation Sox-9 (A). Product bands from RT-PCR were semi-quantitated and plotted as a histogram representing the ratio of gene expression relative to the expression of the house keeping gene GAPDH (B). Aggrecan expression was markedly upregulated following exposure to TGF-β1 and TGF-β3. Levels of the matrix molecule unique to cartilage, Col-2, was most significantly increased in TGF-β1 and BMP-7/TGF-β1 pellets. Samples supplemented with no growth factor, TGF-β1, TGF-β3, and most considerably BMP-7/TGF-β1 displayed upregulation of Col-10. At day 21, induction of Sox-9 gene expression was most apparent in pellets cultured with TGF-β1 and TGF-β3.

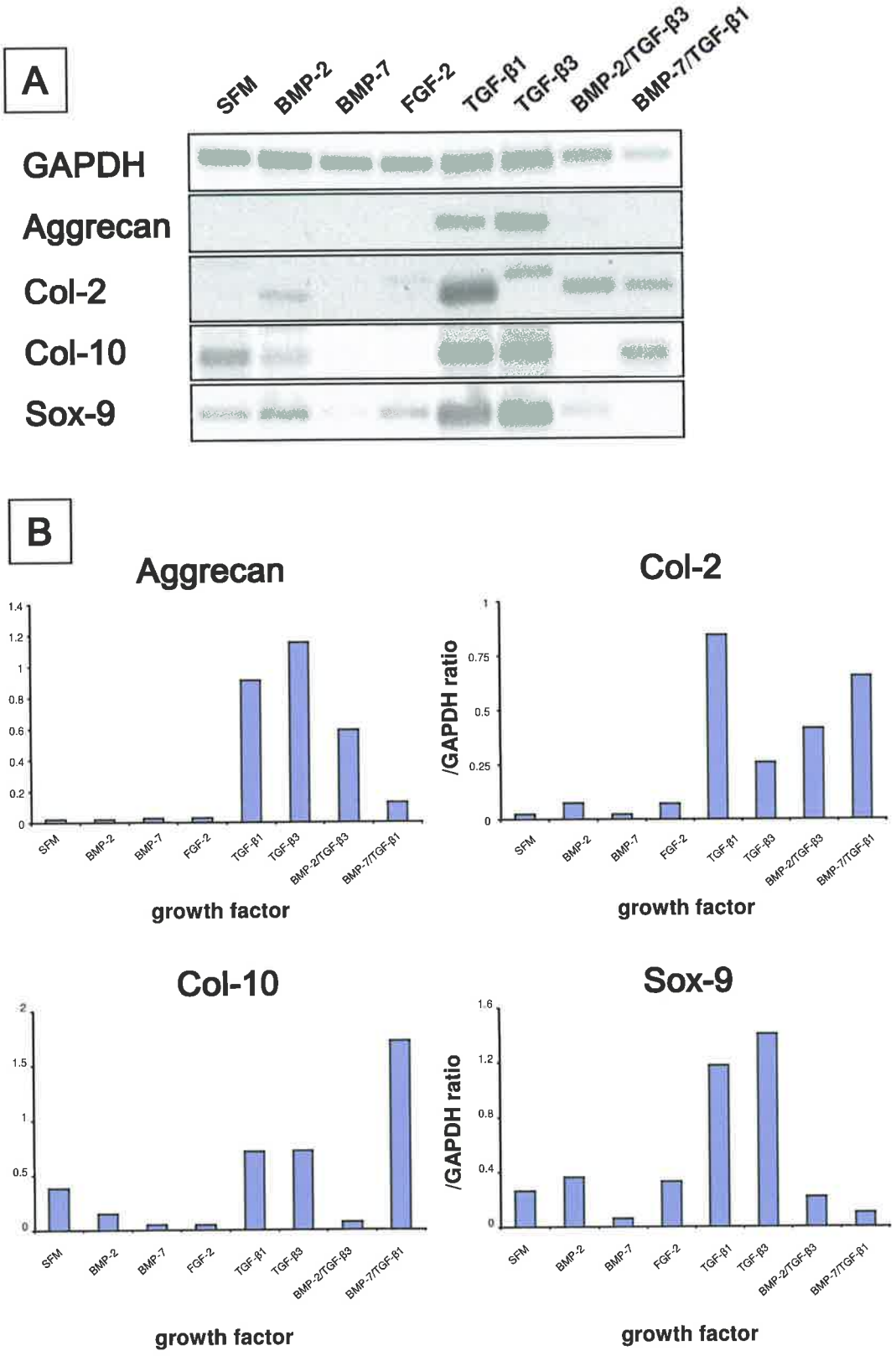
A
SFM
BMP-2
BMP-7
FGF-2
TGF-β1
TGF-β3
BMP-2/TGF-β3
BMP-7/TGF-β1
GAPDH
Aggrecan
Col-2
Col-10
Sox-9
B
Aggrecan
/GAPDH ratio
growth factor
Col-2
/GAPDH ratio
growth factor
Col-10
/GAPDH ratio
growth factor
Sox-9
/GAPDH ratio
growth factor

was negligible in control cultures, but was markedly upregulated in the presence of TGF-β1 alone, or in combination with BMP-7. Levels were increased by individual exposure to TGF-β3, or combined with BMP-2, but not to the same magnitude as induced by TGF-β1. In addition, Col-10 is widely associated as a marker of maturing and mineralising cartilage, at the growth plate, and at the calcified cartilage interface of articular cartilage and the subchondral bone. Expression of Col-10 was moderately upregulated as a consequence of exposure to SFM, TGF-β1, and TGF-β3, although the most sizeable increase observed was in reaction to BMP-7/TGF-β1. Lastly, Sox-9 is a transcription factor that plays a key role in chondrogenic cell fate determination, by interaction with the Col-2 gene enhancer. Samples exposed to TGF-β3 or TGF-β1 alone demonstrated considerable upregulation of Sox-9 expression.

3.2.4. Redifferentiation of Cultured Chondrocytes

Changes to gene expression and loss of chondrocyte specific morphology occurs as a consequence of culturing chondrocytes in monolayer (Benya et al., 1978; Grundmann et al., 1980; Haudenschild et al., 2001; Schnabel et al., 2002). Expression of Col-2 is down regulated and cells exhibit a fibrous morphology, due to the transition from a three dimensional to two dimensional spatial arrangement. In this study, using the in vitro aggregate technique as described above, we wished to analyse the potential of dedifferentiated chondrocytes to be redifferentiated into chondrocytes using an array of culture conditions. Some insight into the optimal growth factors for chondrogenic stimulation may be gained using these dedifferentiated 'prechondrocytic' cells. Moreover, even though cultured chondrocytes may have regressed to a more primitive state, these cells still retain some level of commitment, thus redirection of these cells to a chondrogenic phenotype should be somewhat easier, and may aid as a positive control for the chondrogenesis of MSC. The ability to expand chondrocytes in culture with ease and potential to redifferentiate creates an additional alternative for cartilage regeneration.

Chondrocytes were liberated from healthy sheep cartilage by enzymatic digestion and cultured in monolayer in the presence of 10% FCS. Morphologically, chondrocytes are smaller and rounder than sheep MSCs, and rapidly adhere to plastic in vitro. Upon reaching confluence in monolayer, cells were reseeded at a lower density and subsequently used for the experiment. Aggregated dedifferentiated chondrocytes were cultured for 21

days in the presence of various growth factors with media changes three times per week, and subsequently assessed for chondrogenesis as described in section 2.1.10.

Histological analysis of dedifferentiated chondrocyte aggregates revealed considerable disparity in cell morphology. In the absence of any growth factor or serum supplement, the pellets remained small, with a necrotic appearance, containing cells of inconsistent nuclear size (Figure 3.11A). In contrast, supplementation with BMP-7/TGF-β1 in combination resulted in a large pellet, homogeneously comprising of cells with enlarged nuclei and large lacunae, closely resembling hyaline cartilage (Figure 3.11B). Furthermore, no surrounding fibrous sheath was observed. In parallel studies, cell aggregates were surrounded by a thin fibrous layer and contained cells with enlarged nuclei and ample cytoplasm throughout the pellet after exposure to TGF-β1 alone (Figure 3.11C). Although bearing similarity to fibrocartilage, cell organisation appeared less uniform, more dense, and with less interstitial matrix than conventional fibrocartilage (Figure 3.11C). Cell pellets cultured with BMP-2/TGF-β3 exhibited densely arranged cells with inconsistent and condensed nuclei, encapsulated by a thin ring of fibrous tissue (Figure 3.11D).

Alcian blue staining of matrix proteoglycan was uniformly distributed throughout the TGF-β1-cultured pellet (Figure 3.11E). Although positive staining was wide spread in the BMP-7/TGF-β1-cultured sample, levels were more intense in the more fibrous periphery, suggesting a denser sulfated proteoglycan matrix (Figure 3.11F).

Examination of Col-2 and Col-10 protein distribution within the dedifferentiated cell pellets was undertaken using immunohistochemical analysis. Small pockets of Col-2 staining were apparent in dedifferentiated chondrocyte aggregate cultures without exposure to growth factors (Figure 3.12A). Extensive immuno-localisation of Col-2 was noted in samples supplemented with BMP-7/TGF-β1 (Figure 3.12B), with Col-2 staining being uniform and intense, with the exception of the cell lacuna and a pocket of densely populated cells. Similar patterns of staining were observed in TGF-β1-cultured (Figure 3.12C) and BMP-2/ TGF-β3-cultured (Figure 3.12D) aggregates, although the Col-2 staining was less intense compared to BMP-7/TGF-β1-treated samples (Figure 3.12B). As a marker for hypertrophic and mineralising cartilage, Col-10 was only detected in cell pellets treated with BMP-7/TGF-β1, with staining localised to nuclei and weakly in the surrounding interstitial cellular matrix (Figure 3.12E).

Figure 3.11: Histological evaluation of *in vitro* chondrogenic redifferentiation of cultured chondrocytes. Sheep chondrocytes were liberated by enzymatic digestion from cartilage samples. These chondrocytes were then cultured in monolayer resulting in dedifferentiation of chondrocyte phenotype to a more fibroblast like cell type. Using the previously described pellet culture technique for chondrogenesis, 250,000 dedifferentiated chondrocytes spun to aggregate cells into a three dimensional pellet. Cells were then cultured in single or combinatorial growth factors. In accordance with the previous chondrogenic assay of sheep MSC, the various growth factors assessed were: BMP-2 (50 ng/ml), BMP-7 (100 ng/ml), FGF-2 (10 ng/ml), TGF-β1 (10 ng/ml), TGF-β3 (10 ng/ml) and the BMP/TGF-β combinations of BMP-2/TGF-β3 (50 ng/ml and 10 ng/ml respectively) and BMP-7/TGF-β1 (100 ng/ml and 10 ng/ml respectively). Media was replaced 3 times per week for 21 days. Pellets were subsequently paraffin embedded and transverse sections cut. Representative photomicrographs of histological staining of pellets following *in vitro* chondrogenesis. Panels A-D were stained with Haematoxylin and Eosin. Panels E-F were assayed using the glycosaminoglycan indicator Alcian Blue. Pellets cultured in BMP-7/TGF-β1 appeared much larger in size than the majority of samples assayed. Morphologically, cells within the BMP-7/TGF-β1 pellet resembled native chondrocytes, rounded cells with large cytoplasm. Cells exposed to TGF-β1 alone appeared to be healthier and larger but more fibrous in morphology. Staining with alcian blue was consistent throughout the entire TGF-β1 pellet, and most intense in the periphery of cells supplemented with BMP-7/TGF-β1.

A. SFM (10x)

B. BMP-7/TGF-β1 (10x)

C. TGF-β1 (10x)

D. BMP-2/TGF-β3 (20x)

E. TGF-β1 (10x)

F. BMP-7/TGF-β1 (10x)

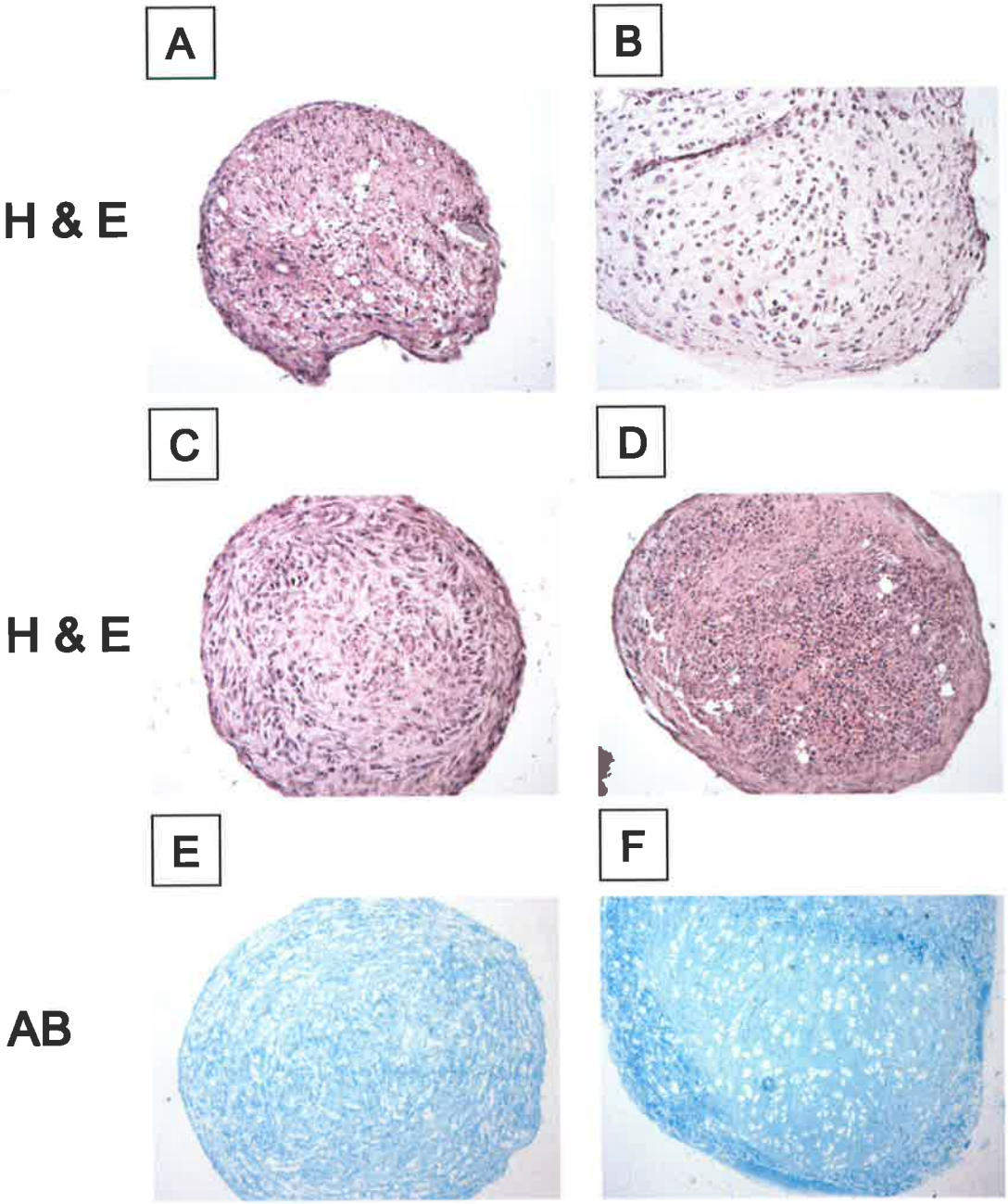
A
B
H & E
C
D
H & E
E
F
AB

Figure 3.12: Immunohistochemical evaluation of *in vitro* chondrogenic redifferentiation of culture chondrocytes. Paraffin sections were incubated overnight with monoclonal anti Collagen-2 antibody or polyclonal anti Collagen-10 antibody. The antigen was detected using the DAB substrate. At three weeks, small isolated pockets of Col-2 expression were observed in cells cultured without the presence of serum or growth factor (A). In contrast dedifferentiated chondrocytes cultured in BMP-7/TGF-β1 displayed extensive and intense Col-2 staining throughout most of the cell pellet (B). Incubation in TGF-β1 alone also was sufficient to induce Col-2 protein secretion within the extracellular matrix (C). In a similar distribution pattern to TGF-β1, pellets exposed to BMP-2/TGF-β3 exhibited Col-2 expression in the pellet periphery (D). Localisation of Col-10 was restricted to cells cultured in the presence of BMP-7/TGF-β1 (E).

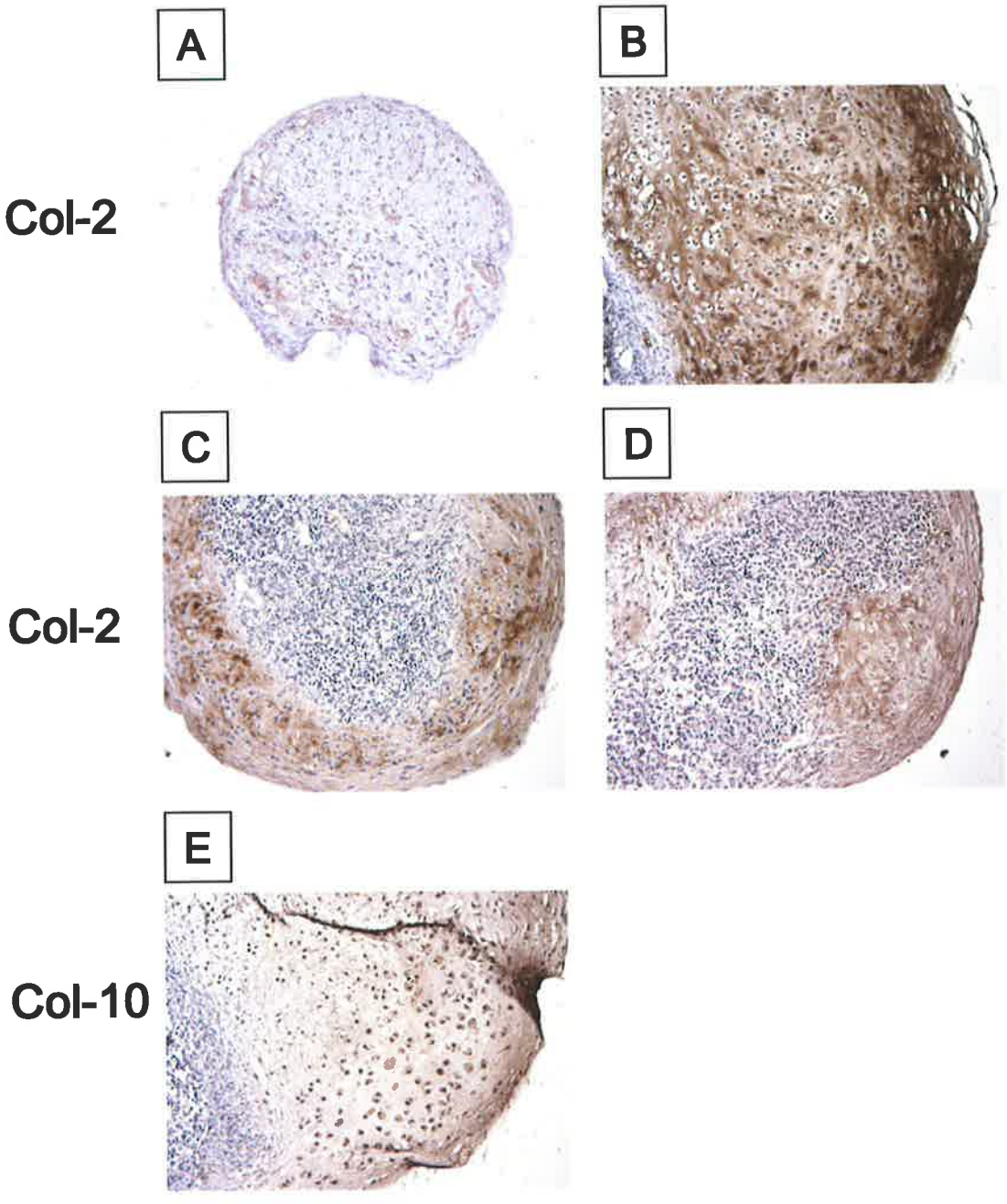
A
B
Col-2
C
D
Col-2
E
Col-10

Similarly, RT-PCR analysis was conducted to examine changes in expression levels of genes (aggrecan, Col-2, Col-10, and Sox-9) in dedifferentiated chondrocyte cell pellets (Figure 3.13). Upregulation of aggrecan occurred in all samples except for SFM, BMP-2, and FGF-2-treated samples. Increased levels were greatest in the TGF-β3 pellet, followed by TGF-β1. Collagen-2 was most notably induced by supplementation with (in decreasing order) TGF-β1, TGF-β3, BMP-7/TGF-β1, BMP-7, and BMP-2/TGF-β3. Interestingly, although detected in most samples, Col-10 was most notably increased following exposure to BMP-7/TGF-β1. Expression of transcription factor Sox-9 was identified in all aggregate samples including the SFM control, with levels being highest after TGF-β3 exposure, followed by TGF-β1 and FGF-2 supplementation.

Figure 3.13: Gene expression analysis following *in vitro* chondrogenic redifferentiation of cultured chondrocytes. Total RNA was isolated from samples at 21 days, and gene expression was examined by semi-quantitative RT-PCR. Transcripts analysed in this study were cartilage extracellular matrix molecules aggrecan, collagen-2 (Col-2), and collagen-10, and the crucial early transcription factor for chondrocyte differentiation Sox-9 (A). Product bands from RT-PCR were semi-quantitated and plotted as a histogram representing the ratio of gene expression relative to the expression of the house keeping gene GAPDH (B). Aggrecan expression was upregulated most significantly in pellets exposed to BMP-7, TGF-β1 and TGF-β3. The level of Col-2 expression compared to control was greatest in TGF-β1 and TGF-β3 pellet samples, and was similarly upregulated by growth factors BMP-7 alone, BMP-2/TGF-β3, and BMP-7/TGF-β1. Interestingly, Col-10 gene expression was only considerably increased following incubation in BMP-7/TGF-β1 combined. Finally, expression of the essential chondrocyte transcription factor Sox-9 was greatest in TGF-β3 cultured pellets, followed by TGF-β1 and FGF-2.

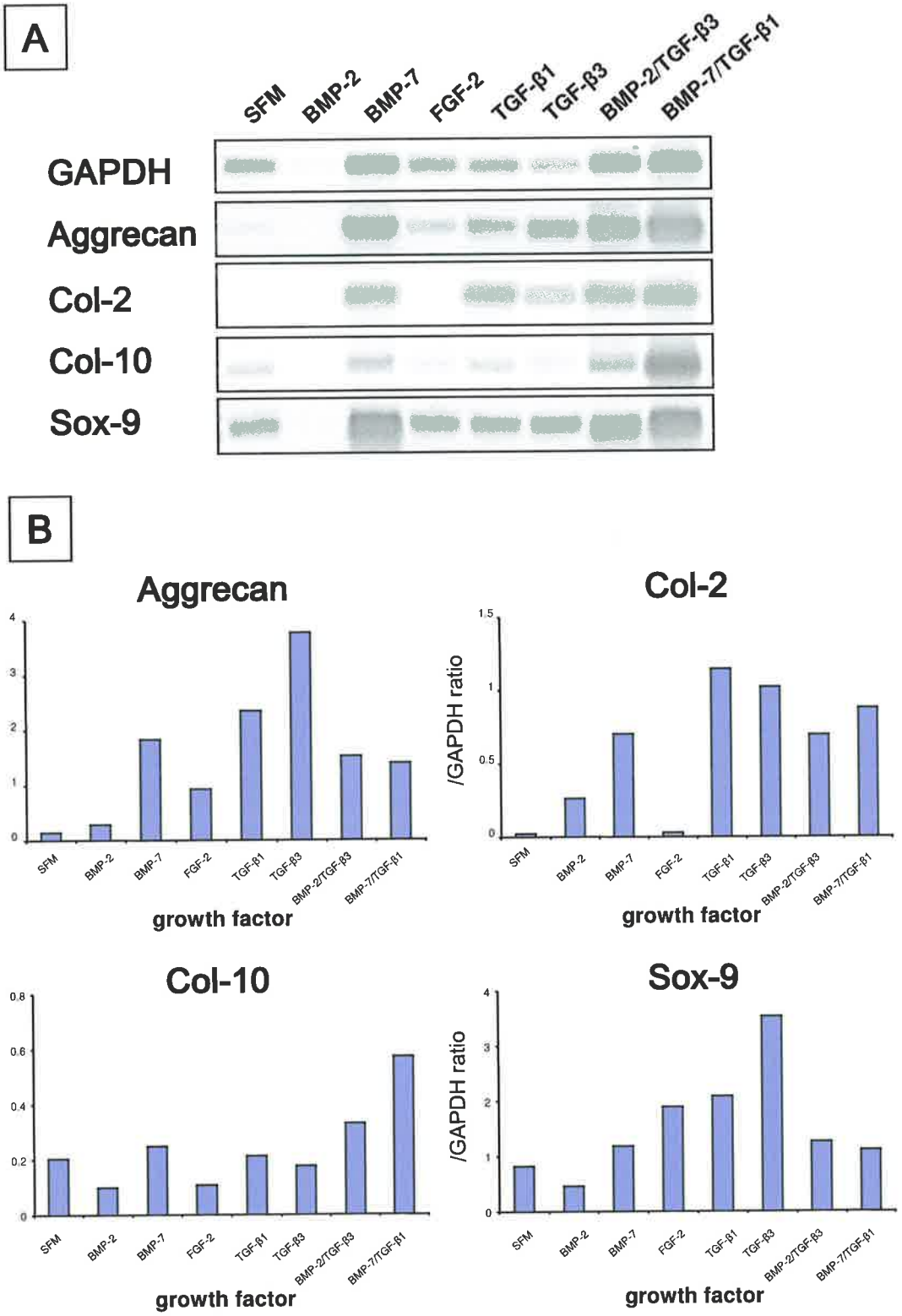
A
SFM
BMP-2
BMP-7
FGF-2
TGF-β1
TGF-β3
BMP-2/TGF-β3
BMP-7/TGF-β1
GAPDH
Aggrecan
Col-2
Col-10
Sox-9
B
Aggrecan
Col-2
Col-10
Sox-9
/GAPDH ratio
growth factor
SFM
BMP-2
BMP-7
FGF-2
TGF-β1
TGF-β3
BMP-2/TGF-β3
BMP-7/TGF-β1

3.3. Discussion

Since the discovery of adult stromal progenitor cells with high proliferative and multipotential capacity, considerable interest has been generated for the application of bone marrow MSCs for musculoskeletal tissue repair and regeneration. Currently, it is considered that bone marrow is the most accessible and enriched source of MSC. Clinically, the harvest of bone marrow is a relatively straightforward well established technique, which is readily accessible, requires only a local anaesthetic, and yields a large number of mononuclear cells. In addition, the bone marrow stroma contains a common pool of multipotential progenitor cells that access various tissues through the circulation. These cells may then adopt characteristics unique for the maintenance and repair of specific tissue types. Previous studies have confirmed that clonally expanded human BM MSC can give rise to a variety of connective tissues in vitro and multiple cell types upon transplantation in vivo (Bianco et al., 2001; Friedenstein, 1980; Gronthos et al., 2003; Haynesworth et al., 1992b; Pittenger et al., 1999). To date, MSC have been discovered from many animal species including mouse, rat, rabbit, dog, cat, goat sheep, cow, and horse. Orthopaedic research frequently necessitates the utilisation of large animal models (such as sheep, goat, pig, dog and horse), due to similarities to humans in size, architecture, and healing mechanisms. Examples of orthopaedic research using large animal models include spinal fusion (Drespe et al., 2005; Gupta et al., 2007), large non-union segmental bone defects (Cancedda et al., 2007; Kon et al., 2000; Quarto et al., 2001), craniofacial repair (De Kok et al., 2003; Krebsbach et al., 1998), and cartilage regeneration (Foster et al., 1990; Johnstone et al., 2002; Murphy et al., 2003; Thomas et al., 2005). As MSC can be harvested from adult tissues, and rapidly expanded in culture, potential therapies for human musculoskeletal diseases are commonly attempted using animal models. In spite of this, the similarities and disparities in MSCs between human and large animals have generally been inadequately investigated. Through isolation and phenotypical analysis in vitro, the present study demonstrated the existence of MSC-like cells in sheep bone marrow.

In order to determine the optimal plating density for efficient CFU-F formation, BM MNC were plated at increasing density to define the point at which MNC number plated correlated with the number of colonies established. Results from the current study suggest that colony formation rate of BM ovine MSCs in vitro appears to be dependent on plating at an optimal cell density, as growth is not linear at high or low seeding densities as

previously described for human BM MSC (Gronthos and Simmons, 1995). This may be due in part to the low frequency of MSC in the bone marrow population, and limitation of serum based culture systems. It has been previous suggested that unfractionated bone marrow cultured at high density introduces accessory cells including macrophages, T-cells, and megakaryocytes, which are capable of producing cytokines that can affect growth or inhibit CFU-F, and additionally may modify exogenously added factors (Gronthos and Simmons, 1995). Immunoselection with STRO-1 was found to exclude these contaminating cell populations. Furthermore, culturing of cells at low density minimises the effects of autocrine inhibitory and stimulatory signals, and subsequent passaging reduces the prevalence of contaminating cell types. Using plastic adherence to isolate MSC, after the first cell passage primary cultures are typically depleted of the nonadherent haematopoietic cell fraction, but contain a proportion of adherent macrophage, which can be minimised by subsequent passaging. In the current study, a linear CFU-F incidence occurred within the seeding densities between 100,000 and 1,000,000 sheep bone marrow MNC per well. It has been observed that the optimal seeding density for CFU-F formation is 1×10^6 cells/60 cm^2 dish (equates to 1.6×10^5 cells per 9.6 cm^2 6 well plate) for cells derived from rat bone marrow (Yoshimura et al., 2007), and between 10^3 and 10^4 cells per cm^2 (approx 1×10^4 to 1×10^5 cells per 9.6 cm^2 well) (Sakaguchi et al., 2005) or 10^4 and 10^5 cells per cm^2 (Friedenstein et al., 1970) for cells from human bone marrow. Our observation therefore is consistent with the plating densities described for rat BM CFU-F assays and the standard technique employed for human CFU-F assays within this laboratory.

Recent evidence suggests that the expansion capacity and overall yield of multipotential progenitors is inversely proportional to plating density and length of passage time. Previous studies described that human cells proliferate most rapidly and retain multipotentiality longer when plated at low density (Colter et al., 2000; Colter et al., 2001). Although cell doubling per day is initially greatest at low density (10-50 cells/cm^2), the final yield of cells was ultimately lower. Somewhat contradictory, Sakaguchi and colleagues (2005) found MSC replated at a low density 50 cells/ cm^2 versus 5000 cells/ cm^2 resulted in a greater cumulative number of cells(Sakaguchi et al., 2005). Supporting evidence confirms the observation that initial culture at low density improves proliferative potential at later passage, and enhances differentiation in vitro (Sekiya et al., 2002). Rat BM derived MSC have been reported to expand more rapidly and extensively than human MSC in response to seeding at low density (Javazon et al., 2001). On the other hand,

feline MSC fail to proliferate adequately when plated at low cell densities (below 100 MSC per cm^2) (Martin et al., 2002).

Our observations across 10 adult Merino sheep found that the frequency of CFU-F capable cells was highly variable, but fell within the range of 1.0 and 9.2 CFU-F per 1 x 10^5 cells with a mean of 4.6 ± 0.7 SEM. A cluster of four donors showed a relatively high CFU-F potential exceeding 7 MSC per 1 x 10^5 MNC plated. Another five samples displayed less CFU-F ability, below 4 CFU-F per 100,000 MNC. Although comparisons are hardly unequivocal due to the small sample size, the two observed extremes of CFU-F potential are curious. The incidence of sheep CFU-F reported in this study surpass that of most other animal BM CFU-F assays, but lie within the normal frequency range reported for human bone marrow CFU-F. Interestingly, Rhodes et al (2004) have previously characterised the incidence and expansion of sheep BM derived MSC(Rhodes et al., 2004). Unlike the present study study, MNCs were not collected by density gradient separation. Instead whole marrow was cultured in vitro, producing an incidence of MSC at 1 to 1000 cells per 1 x 10^5 MNC, almost one hundred times more prevalent than detected in this current study (Rhodes et al., 2004). However, these calculations were estimated by extrapolation of the growth curve back to 0 days, and as such were not true measurements at the time of harvest. In combination with the similar figures observed in humans and other animals, it seems more plausible that the incidence of sheep CFU-F is as observed in the current study.

The incidence of CFU-F in bone marrow suspension between and within species is inconsistent. In human bone marrow aspirates, the yield of CFU-F colonies per 1 x 10^5 plated mononuclear cells ranges from 1 to 20 (Castro-Malaspina et al., 1980; Simmons and Torok-Storb, 1991b). The variability observed between species may arise from different in vitro culture conditions and the differential requirements between species for expansion. For instance, rat bone marrow CFU-F requires the presence of irradiated feeder cells for optimal colony establishment (Kuznetsov and Gehron Robey, 1996), whereas human CFU-F are feeder-cell independent. Furthermore, variation within species has been demonstrated by Phinney et al (1999), who observed considerable discrepancies in CFU-F yield, growth kinetics and differentiation between three inbred mouse strains (Phinney et al., 1999). CFU-F assays with bone marrow from rats, dogs, cats, mice, rabbits and guinea pigs generally yield 0.1 to 5 MSC per 1 x 10^5 mononuclear cells (Friedenstein, 1980;

Kadiyala et al., 1997; Martin et al., 2002; Owen, 1988; Simmons et al., 1991; Yoshimura et al., 2007).

In vivo, BM MSC are predominantly quiescent, with approximately 90% of cells in a non-cycling state (Castro-Malaspina et al., 1981; Gronthos et al., 2003; Kaneko et al., 1982; Van Vlasselaer et al., 1994). Once cultured in vitro, these cells quickly enter a proliferative phase in the presence of serum. Thus, formation of clonogenic CFU-F clusters from bone marrow is dependent on the presence of 10-20% foetal calf serum (FCS) in the media (Castro-Malaspina et al., 1980; Friedenstein et al., 1970). Until the last 10 years the majority of reported studies used FCS and as such, the physiological signals required for efficient attachment and expansion of CFU-F have been limited. It has been observed that the growth of MSC from different BM samples is often variable when grown in the presence of FCS. Both colony number and proliferation (colony size) of the same BM sample can be variably affected by different serum batches. It is widely accepted that serum and plasma contain undefined and varying amounts of growth factors, cytokines, inhibitors, and hormones. Moreover, the presence of FCS within media can inhibit or enhance the effect of exogenously added growth factors, which has lead to conflicting evidence in respect to defining the role of any one mitogen in CFU-F establishment. In a clinical setting, the culture of cells in the presence of FCS should be minimised. Potential hazards of FCS contact that should not be neglected include biosafety issues such as the transmission of viral and prion diseases, and the potential initiation of a xenogenic immune response within the host. Therefore, the lack of understanding of FCS constitution, inherent disadvantages of FCS supplementation, and resultant interactions limiting the study of individual mitogens prompted the investigation of defined molecules necessary for efficient colony formation under serum deprived conditions, and development of a stringent and consistent serum free culture system was essential for the further study investigating growth factors that regulate MSC proliferation and differentiation.

Serum free conditions for the propagation of BM MSC cultures were conclusively established by Gronthos & Simmons (1995). Under serum deprived media, the growth of MSC was entirely dependent on the presence of exogenously added factors and a source of extracellular matrix such as fibronectin (Gronthos and Simmons, 1995). Using STRO-1 immuno-selected cells devoid of haematopoietic cell contaminants, it was demonstrated that basal serum free medium required supplementation with L-ascorbate and the glucocorticoid dexamethasone to facilitate CFU-F colony formation, as the absence of

either factor resulted in a lack of colony development. In addition, clonogenic growth of human BM CFU-F exclusively required the addition of either 10ng/ml EGF and PDGF. Individually, each mitogen stimulated an equal number of colonies however, when added in combination; the average colony diameter was significantly increased when compared to each mitogen alone. These findings correlate with previous observations that megakaryocytes, which secrete high levels of PDGF and EGF via platelet α-granules, can stimulate MSC in vitro (Ben-Ezra et al., 1990; Castro-Malaspina et al., 1981; Kimura et al., 1988), and that the mitogenic activity of serum is contributed by EGF and PDGF (Walthall and Ham, 1981). The clonogenic growth of human bone marrow CFU-F in serum-free media was found to be comparable to, or exceeding that of 20% FCS supplementation. On the other hand, proliferation and colony size were not stimulated by any of the interleukin molecules assayed, by colony stimulating factor LIF, inflammatory mediator TNF-α, growth factor BMP-2, TGF-β, IGF-1 or FGF-2 (Gronthos and Simmons, 1995). Inhibition of CFU-F establishment was observed dose dependently in response to IFNa and IL-4. Characterisation of the conditions required for the culturing of progenitor cells from mouse and rat bone marrow found that murine cells required leukaemia inhibitory factor (LIF) for expansion, whereas rat cells were dependent on supplementation with EGF and PDGF, in addition to LIF (Jiang et al., 2002). However, this study did not exclude FCS from the expansion media, although FCS was present at a lower concentration of 2%.

Using the colourimetric WST-1 proliferation assay, sheep MSC were analysed for their response to a range of growth factors. The rationale behind this assay was to determine if sheep cells responded to human growth factors (due to the paucity of sheep growth factors available commercially). The number of sheep MSC increased proportionally to the concentration of FCS, tested here at 10% and 20% compared to the serum free control. Supplementation with EGF and PDGF individually exhibited mitogenic activity above that of 10% FCS supplementation, analogous to studies of MSC in humans and rats, where both EGF and PDGF are highly mitogenic (Gronthos and Simmons, 1995; Jiang et al., 2002).

Human MSC have been demonstrated to express the PDGF receptor (Gronthos and Simmons, 1995). Inhibition of the PDGF receptor in long term bone marrow cultures resulted in a dose dependent interference in the proliferation and function of stromal fibroblasts and endothelial cells (Duhrsen et al., 2001). Genetic manipulation of the PDGF genes and receptors has shown the dependence of mesenchymal progenitors on PDGF signalling for growth and tissue development during embryogenesis (Betsholtz, 2003).

Overexpression of PDGF has been implicated in many types of malignant transformation, and may function in autocrine stimulation of tumour cells and angiogenesis (Alvarez et al., 2006). More recently, the angiogenic factor VEGF was found to be able to stimulate and signal via the PDGF receptor of human MSCs to regulate proliferation and migration (Ball et al., 2007). Overall, PDGF appears to be important in the regulation of proliferation of MSC.

In addition to aforementioned mitogenic effects of EGF on MSC, supplementation with heparin binding EGF has been demonstrated to reversibly preclude the differentiation of MSC along the osteogenic, adipogenic and chondrogenic lineage under culture conditions which facilitate these changes in vitro (Krampera et al., 2005). Furthermore, culture of MSC in EGF does not alter the differential potential of these cells, or spontaneously induce differentiation of MSC toward a particular lineage (Krampera et al., 2005; Tamama et al., 2006), making EGF an appealing candidate for ex vivo expansion of MSC under serum free conditions. EGF has also been reported to negatively regulate chondrogenesis of the chick limb bud by inhibition of the mesenchymal progenitors from forming precartilage condensations (Yoon et al., 2000). Similarly, EGF has been shown to stimulate proliferation of osteoblasts (Fang et al., 1992; Ng et al., 1983) but inhibit osteoblastic differentiation (Hata et al., 1984; Kumegawa et al., 1983). Taken together, data suggests that EGF may function in MSC to maintain self renewal and proliferation, and prevent differentiation of these cells toward a committed lineage.

The most significant ($p<0.05$, Paired *t*-test) induction of proliferation of sheep MSCs was observed in response to TGFα, a peptide structurally related to EGF and member of the EGF family of growth factors (Xian, 2007). The TGFα ligand binds to the EGF receptor, mediating tyrosine phosphorylation of the EGF receptor in a manner identical to that observed with EGF (Lee et al., 1985). Human STRO-1^+ immunoselected bone marrow CFU-F have been shown to constitutively express the EGF receptor (Gronthos and Simmons, 1995). Even at the lowest dose of 1 ng/ml, cell numbers were elevated three times that of the serum free control, and nearly twice that observed with 10% FCS. Not unlike EGF in functionality, treatment with TGFα has been found to inhibit cartilage nodule formation by mesenchymal progenitors derived from rat mandibles and embryonic limb bud, to prevent chondrogenesis (Huang et al., 1996). In vitro, the EGF receptor on osteogenic cell lines is necessary for osteoblast proliferation and inhibition of osteogenic maturation (Chien, 2000), an observation confirmed by in vivo genetic studies (Sibilia et

al., 2003). Therefore, comparable to EGF, it appears that TGFα may also function to maintain MSC in an undifferentiated proliferative state and negatively regulate commitment of progenitor cells. As to why TGFα supplementation resulted in a larger response than EGF in this study remains to be investigated in further studies, but may be due to differential ligand receptor affinity.

In this current study, FGF-2 supplementation overall, stimulated the proliferation of sheep MSC. Proliferation was comparable to 10% FCS, and virtually equivalent within the concentration range of 1 ng/ml to 30 ng/ml. Interestingly, at the highest concentration (100 ng/ml), cell numbers reverted to levels equivalent to the serum free control, indicative of an inhibitory effect of FGF-2 at extreme dosages. This finding correlates with observations in chondrocytes where in low doses FGF-2 is mitogenic, but continual activation of the FGF receptor inhibits proliferation and drives terminal chondrocyte differentiation (Coffin et al., 1995; Makower et al., 1989; Mancilla et al., 1998; Nagai et al., 1995). In vitro analysis of chondrocytes suggests a mitogenic role of FGF-2 (Trippel et al., 1993), in contrast to in vivo studies where FGF-2 is involved in the regulation of terminal differentiation (Kronenberg, 2003). Contradictory evidence regarding the mitogenic influence of FGF-2 on MSC proliferation has been reported in multiple species including human, mouse and rat (Baddoo et al., 2003; Bianchi et al., 2003; Locklin et al., 1995). FGF-2 supplementation was found to prolong population doubling (life span) of BM MSC whilst maintaining differentiation potential, and thus may function as a mitogen and self maintenance factor (Bianchi et al., 2003). Solchaga (2005) demonstrated FGF-2 not only increases MSC proliferation but enhances chondrogenic differentiation(Solchaga et al., 2005), whereas Gronthos (2005) did not observe CFU-F proliferation in response to FGF-2 supplementation(Gronthos and Simmons, 1995). Analysis of optimal culture conditions for large clinical scale production of MSC for therapeutic application found that FGF-2 increased MSC proliferation and immunosuppressive potential (Sotiropoulou et al., 2006). The majority of evidence from in vitro studies suggests the role for FGF-2 in MSC proliferation. However, the complex and contradictory evidence provided by in vivo examinations (namely of the growth plate) suggests numerous and complicated biological functions for FGF-2.

Since their discovery (Urist, 1965), it has been established that BMPs are also essential for the proliferation and differentiation of MSC and chondrocytes during endochondral ossification, and regulation of osteoblast differentiation (Balemans and Van Hul, 2002).

The BMPs exhibit a broad range of biological activities including roles in proliferation, differentiation, and migration during fracture repair, endochondral ossification, and embryogenesis. At the growth plate BMP-2 is expressed by prehypertrophic and hypertrophic chondrocytes, and BMP-7 in proliferative chondrocytes (Haaijman et al., 2000) suggesting a role in differentiation and proliferation respectively. In vitro studies of the effect of BMPs (2, 4 and 6) on growth plate chondrocytes found these morphogens to be negative regulators of chondrocyte proliferation (Olney et al., 2004). However, the culture of foetal metatarsal explants in BMP-2 resulted in stimulation of chondrocyte proliferation and maturation (De Luca et al., 2001). Analysis of human BM MSC found BMP-2 supplementation was unable to stimulate growth (Gronthos, 1995), and furthermore, at high concentrations was inhibitory (Fromigue et al., 1998).

In the current study, the effect of BMP-2 and BMP-7 on the proliferation of sheep BM derived MSC somewhat contradicts the response observed in human MSC. Ovine MSC were unresponsive to supplementation with BMP-2 with the exception of the highest concentration tested (100 ng/ml), which stimulated a significant proliferative response ($p<0.05$, Paired *t*-test). This observation lies in direct opposition to the study by Fromigue (1998) where 100ng/ml BMP-2 inhibited cell number(Fromigue et al., 1998), but is in accordance with the in vivo explant study where BMP-2 was mitogenic (De Luca et al., 2001). However the Fromigue study did not exclude the presence of serum in the culture medium (present at a low concentration). Analysis of the outcome of BMP-7 addition similarly did not follow the trends of previous observations. At the concentration range of 1 ng/ml to 10 ng/ml, sheep MSC were unresponsive to BMP-7, and cell numbers were equivalent to the serum free control. At 30 ng/ml, BMP-7 resulted in a significant reduction of cell number, beneath that of the serum lacking control. Nonetheless, and analogous to the dose response of BMP-2 reported in this study, significant ($p<0.05$, Paired *t*-test) proliferation was only achieved at the largest BMP-7 concentration of 100 ng/ml, but did not exceed that of 10% FCS stimulation. Previously, proliferation of the stromal cell line BMS2 was found induced by the addition of BMP-7 (Chen et al., 2001). Discrepancies in the literature may arise from differences in culture conditions, medium composition, cell origin, and cellular arrangement.

Previously, IGF-1 has not been found to exert a mitogenic effect on human MSC (Gronthos and Simmons, 1995), a finding confirmed by the inability of IGF-1 in vitro to induce proliferation or early osteogenic differentiation of MSC (Walsh et al., 2003). Our

observations contradict these observations for ovine MSC. The proliferation of ovine MSC increased dose dependently in parallel with increasing concentration of IGF-1, corresponding to the observations reported with chondrocytes (Olney et al., 2004; Trippel et al., 1992). Although perplexing, overall, it is possible that the MSC analysed in this study and others may represent a heterogeneous population of cells, perhaps exhibiting differential populations of progenitor, pre-committed, and committed cell types, which might explain the discrepancies observed here, between and within the literature. Null mutations of IGF-1 and the type 1 receptor have demonstrated their critical function during bone growth and chondrogenesis, as indicated by the severe growth failure observed in these animals (Baker et al., 1993). Upregulation of IGF-1 gene expression was reported in osteoarthritic lesions of human arthritis patients, suggesting a role in the recruitment of MSC and chondrocytes to the injured site for wound repair (Middleton and Tyler, 1992; Olney et al., 1996). Furthermore, in vitro soluble IGF-1 is a potent inducer of MSC migration, suggesting IGF-1 may function to mobilise and home MSC to sites of injured tissues (Ponte et al., 2007). Moreover, cell migration was further enhanced by pre-incubation in the inflammatory cytokine TNFα.

Members of the TGF-β superfamily have essential functions in skeletal development, growth, maintenance and fracture repair. TGF-β can either stimulate or inhibit cell proliferation depending on the stage of cell maturation (Carrington and Reddi, 1990; Ingram et al., 1994; Lomri and Marie, 1990; Olney et al., 2004; Robey et al., 1987; Rosier et al., 1989; Schwartz et al., 1993). For example, TGF-β family members promote early chondrogenesis and osteogenesis of MSCs, but inhibit myogenesis, adipogenesis and late stage osteogenic differentiation (Roelen and Dijke, 2003). In the current study, it was observed that TGF-β1 had a significant ($p<0.05$, Paired *t*-test) inhibitory effect on cell proliferation. Similarly, under the serum free growth factor assay established by Gronthos (1995), human BM MSCs were not induced to proliferate by the addition of TGF-β (Gronthos and Simmons, 1995). In vitro, TGF-β1 is one of the predominant factors identified for chondrogenesis of MSC (Johnstone et al., 1998; Mastrogiacomo et al., 2001). Overall, the role of TGF-β1 in MSC regulation suggests an association with directing cell fate decisions and less with proliferation. In contrast, supplementation with TGF-β3 consistently and significantly ($p<0.05$, Paired *t*-test) stimulated proliferation to levels observed by the addition of 10% serum, notably in a double peak distribution at high and low doses. Thus there appears to be some conflicting data on the proliferative effects of

TGF-β on different cell types in vitro, which may be dependent on environment, cell type and maturity.

Taken together, previous studies have demonstrated that the serum free media conditions for MSC expansion in vitro (for the clinical need of generating large numbers of MSCs in minimal time without the use of FCS supplementation), is dependent on the exogenous source of appropriate growth factors. In this study, due to the shortage of commercially available sheep growth factors it was necessary to determine whether sheep MSCs responded to human growth factors, and if so how and to what extent. Furthermore, in a clinical setting, the identification of a suitable mitogen for rapid cell expansion, so as to circumvent the requirement of FCS supplementation is important. Selection of a potential mitogen for translational studies should fulfil certain criteria, namely consistency between species, and reliability between subjects within a species. Under these principles this study demonstrated that PDGF, EGF and TGFα show the most promise as appropriate expansion modulators for sheep MSCs. It is well accepted that PDGF and EGF are the key mitogens present in FCS. Although IGF-1 strongly stimulated MSC proliferation at the entire concentration range assessed, variability within the literature suggests more comprehensive studies are required. Supplementation with FGF-2 was mitogenic at lower concentrations, and evidence suggests this mitogen to be cytostatic at higher concentrations. However, reports on the effect of FGF-2 on MSC are similarly contradictory. Both BMP-2 and BMP-7 were exclusively mitogenic at higher doses, and the addition of TGF-β1 to cell cultures appeared to have an inhibitory influence on cell proliferation. Finally, it should not be assumed that no change in cell number indicates unresponsiveness to a particular growth factor, as factors unable to stimulate proliferation of MSC may be acting to promote differentiation towards specific cell lineages.

Numerous studies of human and animal MSC have ascertained that these progenitor cells are capable of differentiation down several mesodermal lineages. Although in this thesis our interest is mainly the investigation of the potential of MSC to regenerate growth plate cartilage, we had determined whether sheep MSC resemble their species counterparts and are multipotential by performing previously established assays for the differentiation of MSC towards the osteogenic, adipogenic and chondrogenic lineages. Following two weeks culture in osteoinductive media, confluent MSC had begun to deposit calcium crystals within the extracellular matrix, which by four weeks were extensive and intense throughout the entire culture. Consistently, there was a time-dependent upregulation of the

essential early transcription factor for osteogenesis, Cbfa-1, and Col-1, which is the predominant collagen extracellular matrix molecule of bone, was concomitantly elevated following osteoinduction. Low levels of expression of both Cbfa-1 and Col-1 were detected in uninduced samples, correlating with the gene expression profiles of human immunoselected MSCs described by Gronthos et al (1995).

Adipogenesis of sheep MSC occurred within four weeks of culture as indicated by the presence of multiple clusters of lipid-laden fat cells. Examination of genes with expression restricted to adipocytes revealed that LPL and the early adipocytic transcription factor PPARγ were initially markedly upregulated after which slowly declined over the course of the experiment. Conversely, the expression of Leptin mRNA increased in a time-dependent fashion. Unexpectedly, transcripts for all three adipocyte related genes were detected in control samples. In contrast, cultured human MSCs have been reported to constitutively express LPL only (Gronthos et al., 2003). This observed divergence from the human data raises the possibility that sheep MSC may exist in a pre-committed state, or that upon reaching confluence in monolayer culture, intimate cell to cell contact in combination with the presence of serum may be sufficient to drive early adipogenesis.

Analysis of chondrogenic potential was assessed using the established pellet micromass culture technique as differentiation of MSC and maintenance of chondrogenic phenotype is dependent on a close cell and matrix interrelationship. Initial attempts of MSC chondrogenesis assays used the spot micromass technique, where a small volume of cells suspended at high density were positioned in the centre of a 12 well polypropylene plate, and were permitted to attach prior to the overlay of chondrogenic media. Frustratingly, the cluster of cells would either detach from the well within 24 hours, or upon well confluence, the highly populous central aggregate would lift leaving a monolayer of cells. Effort to vary cell density, total cell number, micromass volume and attachment conditions were futile. It is possible that this technique was unsuccessful due to the rapid rate at which sheep MSCs proliferate. Thus, the pellet micromass culture technique established by Johnstone (1998) was employed (Johnstone et al., 1998). As the most effective growth factors for sheep MSC chondrogenesis have not been defined, several different factors were assessed in this current study.

Following 21 days in culture with chondroinductive media, the largest MSC pellet observed was that incubated with BMP-7 and TGF-β1 in combination. The pellet cultured

with BMP-2/TGF-β3 combination was also considerably larger in size than all other pellets analysed. This observation is analogous to a study by Shirasawa et al (2006) who reported that the combination of BMP-2 and TGF-β3 dramatically increased pellet size and matrix synthesis, in comparison to TGF-β3 alone (Shirasawa et al., 2006). Other studies have also reported augmentation of chondrogenesis with combined use of BMP and TGF-β (Sekiya et al., 2001; Sekiya et al., 2005). Evidence suggests the enlargement in pellet size is due to an increase in extracellular matrix production but not the cell number. Histologically, of interest is the tri-zonal morphology of the BMP-7/TGF-β1 aggregate. Interestingly, the central zone of highly populated cells with little extracellular matrix resembles the morphology of dedifferentiated chondrocytes undergoing redifferentiation in monolayer (Imabayashi et al., 2003). The intermediate zone consists of round sparsely populated cells surrounded by a matrix which is positive for Col-10 protein expression, suggesting presence of hypertrophic chondrocytes. Finally, the outer zone is constituted by cells with enlarged nuclei in a fibrous matrix which displays Col-2 immunoreactivity. Taken together, the differences in cell morphology and protein expression within each zone appears to somewhat recapitulate some characteristics of the growth plate or the articular cartilage, with an inner proliferative zone and zones of progressive maturation.

Consistent with the chondrogenic differentiation of the cultured sheep MSCs, analysis of mRNA transcripts within the cell pellets revealed an upregulation of several cartilage genes proceeding culture of MSC in chondrogenic media. Extracellular matrix molecule aggrecan was most notably upregulated in samples cultured with TGF-β. Col-2, which is unique to cartilage tissue, was most significantly elevated in TGF-β1 and BMP-7/ TGF-β1 aggregates. At the protein level Col-2 was only detected in the BMP-7/ TGF-β1 sample. Splice variants of Col-2 were noted for samples cultured in FGF-2 and TGF-β3 and have previously been described (Sandell et al., 1991; Sandell et al., 1994). Sox-9, the essential early transcription factor for condensation and initiation of chondrogenesis, was most markedly elevated in samples receiving TGF-β. Interestingly, although Sox-9 is known to directly regulate Col-2 expression, Col-2 protein was not detected in the TGF-β3 pellet. However, as expression of Sox-9 was most notable in TGF-β samples at 21 days, perhaps these cells are at an earlier stage of chondrogenic differentiation, where gene expression of Sox-9 and thus Col-2 have been induced but is not yet discernible as detectable Col-2 matrix protein expression. Transcripts for Col-10, a marker of maturing cartilage, were identified in several samples, particularly the BMP-7/ TGF-β3 aggregate, analogous to immunohistochemical observations. Interestingly, both Col-10 and Sox-9 mRNA were

detected in aggregates cultured in serum free media, verified by the observation that both uncultured and cultured human STRO-1-selected MSCs constitutively express Col-10 (Gronthos et al., 2003). Thus Sox-9 expression may be induced purely by the three dimensional arrangement of cells at high density. In contrast to the results reported here and human studies, Mwale et al (2006), reported aggrecan, but not Col-10, to be constitutively expressed by human MSC (Mwale et al., 2006). These discrepancies may reflect differences in isolation strategies and culture conditions between different research laboratories.

To date, the potential use of autologous chondrocyte transplantation for cartilage regeneration has been limited by the obstacle of expanding large yields of chondrocytes whilst maintaining phenotype. It is well accepted that once chondrocytes are removed from their native spatial arrangement within the cartilage tissue matrix and cultured in monolayer, they dedifferentiate, lose their round phenotype, become fibroblastic, regain the ability to proliferate, and switch expression of collagen matrix proteins (Benya et al., 1978; Grundmann et al., 1980; Haudenschild et al., 2001; Schnabel et al., 2002). However, these cells do retain some chondrocyte characteristics and as such can be redifferentiated in vitro (Benya and Shaffer, 1982; Schulze-Tanzil et al., 2002; Solursh, 1991; Thorogood and Hinchliffe, 1975). In fact, a comparison of human BM MSC and cultured chondrocytes has demonstrated that both cell types exhibit similar morphology, cell surface expression profile, and furthermore that cultured chondrocytes are multipotential (Barbero et al., 2003; de la Fuente et al., 2004; Tallheden et al., 2003). Therefore, as the optimal growth factors and culture conditions for chondrogenesis of sheep MSC have not been described or defined, the use of cells with a predetermined potential or inclination to form chondrocytes will be most beneficial. Furthermore, the ability to generate large numbers of precommitted cells which can be readily redifferentiated into chondrocytes presents an additional alternative for cartilage regeneration. Under conditions and using growth factors equivalent to those ascertained for MSC, cultured sheep chondrocytes were redifferentiated using pellet culture micromass. Several different morphologies were observed from samples with different treatments, including those resembling hyaline and fibrous cartilage, often exhibiting a core of small densely populated cells. The morphological arrangement of TGF-β3 pellet shares some similarity with the outer zone of the BMP-7/TGF-β1 MSC pellet. Interestingly, the pattern of gene expression show a greater similarity to that observed for MSC, with aggrecan expression being greatest in the TGF-β3-treated sample, Col-2 most elevated in TGF-β1-treated pellet, and Col-10

markedly upregulated following culture with BMP-7/ TGF-β1. As for sheep MSC cultured in SFM, dedifferentiated chondrocytes constitutively express Col-10 and Sox-9, and to a lesser extent express aggrecan. Immunohistochemical analysis of Col-2 and Col-10 expression correlated with the upregulation of mRNA transcripts. This may be in part due to rearrangement of cells in close cell-matrix proximity. In addition, pockets of Col-2 protein staining can be observed in the SFM-cultured pellet, which may attributed to reestablishment of a three dimensional arrangement and not due to exogenously added factors. Overall, in comparison to the chondrogenesis of sheep MSC, redifferentiated cultured chondrocytes more closely resembled native cartilage in histological structure and in cartilage protein expression. Taken together, our observations suggests the optimal growth factor for sheep MSC chondrogenesis is either TGF-β1 alone or BMP-7 in combination with TGF-β1. However, although in this analysis the combinatorial use of TGF-β and BMP upregulated Col-10, a marker of maturing and hypertrophic cartilage, some evidence suggests Col-10 is often expressed as an early event in chondro-induction, often prior to Col-2, and thus is not necessarily a good indicator of cartilage hypertrophy (Mwale et al., 2006).

In summary, cells exhibiting the characteristics of human MSC can be isolated from the bone marrow of adult sheep. The frequency of MSC was variable between subjects and ranged from 1 to 9.2 CFU-F per 1 x 10^5 mononuclear cells. Under serum deprived conditions, sheep MSC were induced to proliferate by the addition of PDGF, EGF, FGF-2 IGF-1 and most notably TGFα, achieving levels equal to or surpassing that observed by 10-20% FCS supplementation. The effect of mitogenic stimulation (under serum depleted conditions) on the multipotential differentiation capacity of MSC remains to be determined, and may influence the commitment of MSC along a particular lineage. Nonetheless, in vitro, ovine MSC cells are capable of induction along the osteogenic, adipogenic and chondrogenic lineage as determined morphologically and molecularly. The optimal growth factor(s) for chondrogenesis of MSC and cultured chondrocytes was found to be either TGF-β1 alone or TGF-β1 in combination with BMP-7. Furthermore, sheep chondrocytes expanded in monolayer are capable of redifferentiation to a chondrocytic phenotype in vitro using the similar growth factors. In conclusion, it appears sheep bone marrow possesses MSC with similarities and few differences to those reported in humans and other mammals.

CHAPTER 4

CHARACTERISATION OF THE CELL SURFACE PROTEIN EXPRESSION PATTERN OF SHEEP MSC

4.1. Introduction

In contrast to the haematopoietic stem cell, the immunophenotype of CFU-F forming MSC and their progeny has not been well described. The identification of a heterogeneous population of MSC has been limited by the low incidence of MSC in BM aspirates, and compounded by the paucity of specific antibodies which are used to identify, isolate, enrich and functionally characterise MSC. To date the majority of phenotypic characterisation has been performed on cultured cells, and for the reasons provided above, relatively little is known of the primary clonogenic precursors responsible for producing MSC. However, considerable effort has been expended to characterise the cell surface expression profile of MSC, and to generate antibodies for the selection and enrichment of these progenitor cells.

Early efforts to identify MSC progenitors based upon cell surface expression characteristics suggested a common precursor between the haematopoietic and mesenchymal lineages. Based upon flow cytometric sorting of foetal BM, the common precursor cells were characterised by a $CD34^+$, $CD38^-$, HLA DR^- phenotype (Huang and Terstappen, 1992). However, this finding was later modified upon the discovery that the haematopoietic and mesenchymal progenitors could be fractionated within the $CD34^+$ population based upon differential expression of the CD50 surface marker (Waller et al., 1995). Cells of haematopoietic lineage positively expressed CD50, whereas mesenchymal lineage cells were CD50 negative. Antibodies to CD34 have been found to bind to CFU-F in adult BM, although at considerably lower levels than reported in foetal tissue (Simmons and Torok-Storb, 1991a). Furthermore, immunoselection with CD34 is insufficient and does not recover all CFU-F (Simmons and Torok-Storb, 1991a). Interestingly, expression of the CD34 antigen is absent from in vitro culture expanded MSC (Pittenger et al., 1999), suggesting that CD34 is expressed by primary MSC isolated directly from bone marrow, but is lost upon expansion.

One of the first antibodies shown to enrich CFU-F in fresh bone marrow aspirates was STRO-1 (Simmons and Torok-Storb, 1991b). STRO-1 has been identified as an antibody

that is cross-reactive with human bone marrow MSC but not haematopoietic precursor cells. Identifying a minor subpopulation of adult human bone marrow, positive STRO-1 expression correlated with all detectable clonogenic CFU-Fs in human bone marrow, and immunoselection of bone marrow aspirates with STRO-1 enriched for MSC relative to the unseparated BM fraction (Simmons and Torok-Storb, 1991b). However, enrichment of CFU-F progenitors with STRO-1 selection alone is insufficient to obtain a pure population of MSC progenitors. This is due to the presence of contaminating populations of glycophorin-A^+ nucleated red blood cells and a small subset of $CD19^+$ B lymphocytes, with CFU-F activity restricted to the glycophorin negative cells (Simmons and Torok-Storb, 1991b). The isolation of a discrete highly enriched subpopulation of BM MSC devoid of contaminating cells types can be resolved by selection with STRO-1 in combination with vascular cell adhesion molecule (VCAM, CD106) (Gronthos et al., 2003). Positive expression of STRO-1 by active CFU-F corresponded with undetectable levels of haematopoietic markers CD3, CD33, CD34, CD38 and CD45 (Simmons and Torok-Storb, 1991b; Simmons et al., 1994).

Several other antibodies have been associated with MSC progenitor cells. The SB-10 antibody has been shown to be reactive with an antigen present on undifferentiated MSC, which is down-regulated upon differentiation along the osteogenic lineage (Bruder et al., 1997). Shortly thereafter, the SB-10 antigen was identified as activated leucocyte cell adhesion molecule (ALCAM, CD166) (Bruder et al., 1998b). Generated specifically against human MSC, the SH2 antibody has been demonstrated to react with an epitope present on the TGFβ receptor endoglin (CD105) (Haynesworth et al., 1992a). Endoglin is predominantly associated with endothelial cells, but also expressed on erythroblasts, monocytes and connective tissue stromal cells (Cheifetz et al., 1992). Two antibodies, SH3 and SH4 have been reported to recognise separate epitopes found on the membrane-bound ecto-5' nucleotidase molecule CD73, which plays a role in B cell activation (Barry et al., 2001a; Haynesworth et al., 1992a). The SH2, SH3 and SH4 antibodies are reported to be non reactive with haematopoietic cells or osteocytes (Haynesworth et al., 1992a). However, expression of these antibodies is not restricted to or specific for MSC, since a variety of other cell types also share expression of these antigens (Cheifetz et al., 1992). Thus, these antibodies are not sufficient alone to isolate or enrich MSC.

MUC-18 or CD146 is a member of the immunoglobulin superfamily and has been identified to be expressed by human bone marrow MSC (Filshie et al., 1998). MUC-18

has previously been located on metastatic melanoma cells, endothelial cells, and smooth muscle cells (Sers et al., 1994; Shih et al., 1994), and subsequent generation of monoclonal antibodies against human MSC has confirmed the expression of this marker on human BM MSC (Filshie et al., 1998). Furthermore, highly enriched populations of MSC can be obtained from human bone marrow aspirates by immunoselection based on CD146 and STRO-1 expression (Shi and Gronthos, 2003). Other Ig superfamily molecules known to be expressed by endothelial cells are ICAM-1 (CD54), PECAM-1 (CD31), VCAM-1 (CD106), Thy-1 (CD90), and ALCAM (CD166) (Carlos and Harlan, 1994; Gougos and Letarte, 1990; Ishizu et al., 1995; Mason et al., 1996; Ohneda et al., 2001; Osborn et al., 1989; Simmons et al., 1990; Wetzel et al., 2004; Zannettino et al., 2007), which are similarly found to be expressed by MSC.

The HOP-26 antibody has been demonstrated to be strongly reactive with early stage BM MSC cultures. This antibody is non reactive with blood cells and can be used to select for CFU-F progenitors in bone marrow aspirates. Immunostaining of foetal tissue has shown cells immunoreactive with this antibody lie in close proximity to the developing bone (Joyner et al., 1997). More recently, HOP-26 has been identified as recognising an antigen of tetraspanin family cluster differentiation marker CD63 (Zannettino et al., 2003), which is known to be potentially involved in cell adhesion mechanisms.

Flow cytometric analysis of surface proteins has indicated MSC express a large spectrum of cell adhesion molecules known as integrins (Gronthos et al., 2001b; Majumdar et al., 2003). It is believed that these membrane molecules are important in the interactions necessary for homing to sites of injury, binding to extracellular matrix molecules, and cell-cell interactions. The integrin receptors identified on MSC correspond to ligands present on mature haematopoietic cells, correlating with the interactions between MSC and haematopoietic cells and their subsequent roles during haematopoiesis (Majumdar et al., 2003). The β1 integrin family has been established as an essential adhesion receptor subfamily for the mediation of MSC adherence and proliferation, via matrix molecules found within the BM microenvironment and bone surfaces (Gronthos, 2001). Functional blocking of the β1 integrin (CD29) subunit on MSC significantly diminished the ability of these progenitor cells to undergo osteogenesis, by impairing the initiation of matrix mineralisation (Gronthos et al., 2001b). Moreover, immunoselection of bone marrow cells with an anti-CD49a (α1β1 subunit) antibody resolved a population of MSC with unaltered differentiation potential (Deschaseaux et al., 2003).

CD44 is the receptor for hyaluronic acid and is uniformly expressed by MSC (Gronthos et al., 2001b; Pittenger et al., 1999). The importance of CD44 in MSC/HSC interactions during haematopoiesis has been confirmed by blocking studies conducted by Miyake et al (1990). In addition to the aforementioned cell surface markers, MSC have also been described as positively expressing endopeptidases CD10 and CD13, CD71, adhesion molecules CD90 (Thy-1) and CD49a, receptors for PDGF, EGF, IGF-1 and NGF, among many other surface proteins (Deans and Moseley, 2000; Gronthos and Simmons, 1995; Pittenger et al., 1999; Simmons et al., 1994).

The cocktail of cell surface markers identified on MSC provides some insight in the mechanism and roles of these progenitor cells in fundamental processes such as the regulation of haematopoiesis, homing mechanisms and injury repair, lineage specific differentiation, proliferation, and interactions with the extracellular matrix. In addition, characterisation of the MSC immunophenotype will augment the selection, enrichment, and characterisation of 'true' self renewing multiprogenitor cells. To date, the majority of studies have examined the expression profile of human MSC, with some research in rodents. However, there is very little information available on the cell surface characteristics of ovine MSC, and antibodies that can be used to immunoselect for these cells. This is compounded by the scarcity of antibodies specific for sheep, and relevance for use in ovine orthopaedic studies. This chapter will assess the cell expression profile of ovine MSC and chondrocytes using antibodies specifically generated for reactivity with human cells. Furthermore, a series of novel antibodies generated against sheep MSC by Dr. A. Zannettino (Myeloma & Mesenchymal Research Laboratory, Institute of Medical & Veterinary Science, Adelaide, Australia) will be examined. Antibodies potentially applicable for immunoselection of CFU-F progenitors will be investigated for the ability to select for and enrich ovine MSC.

4.2. Results

4.2.1. Characterisation of the Cell Surface Expression Profile of Sheep Bone Marrow Derived MSC.

Single cell suspensions of sheep bone marrow MNC were cultured in vitro in monolayer to generate a heterogeneous population of MSC according to plastic adherence. Contaminating non adherent cell types were removed by media replacement following two days in culture. Upon confluence, the adherent cells were recultured at a lower density and on reaching confluence once again were harvested for analysis. The cell surface expression profile of MSCs derived from three different sheep donors were investigated using single colour immunofluorescence analysis as described in the methods (Chapter 2.3.1). The antibodies selected for examination were those previously demonstrated to show immunoreactivity with human MSC, commercially available antibodies specifically raised against sheep cell types, and a series of uncharacterised monoclonal antibodies specifically targeted against sheep adherent MSC which were generated by Dr. A. Zannettino (Myeloma & Mesenchymal Research Laboratory, Institute of Medical & Veterinary Science, Adelaide, Australia). Positive fluorescence was defined as the level of fluorescence greater than 99% of the isotype matched control.

When separated according to size and granularity (forward and side scatter respectively) by flow cytometry, cultured MSC represented a heterogeneous population of cells (Figure 4.1A). This observation was consistent between all donors examined. Ovine MSC (n=3) uniformly displayed a high level of expression of the hyaluronate receptor CD44 (H9H11, mean 99.3% ± 0.3 SEM), and of the uncharacterised hybridomas B (mean 99.5% ± 0.4 SEM), H (mean 99.3% ± 0.3 SEM) and I (mean 97.7% ± 1.1 SEM). Representative histograms of the immunofluorescence intensity of each antibody assessed can be observed in Figure 4.1B. Cultured MSC were similarly strongly immunoreactive with an antibody recognising CD166, also known as activated leucocyte cell adhesion molecule (mean 89.0% ± 7.5 SEM). Cells exhibited intermediate fluorescence to the macrophage/monocyte marker CD14 (mean 28.5% ± 13.8 SEM), and to a more variable extent than the aforementioned antibodies. Expression of Hybridoma E was restricted to a minor subset population of MSC (mean 16.0% ± 1.4 SEM), which was surprisingly consistent between subjects. However, the majority of antibodies assessed did not exhibit any reactivity with sheep derived MSC. Included within this category were STRO-1,

Figure 4.1: Cell surface expression profile of adult sheep bone marrow derived MSC. Primary MSC cultures were generated from BM MNC preparations according to plastic adherence and expanded in vitro. Upon confluence, cells were harvested by trypsin digestion and assessed for cell surface antigen expression by immunofluorescence flow cytometric analysis. (A) Representative dot plot of the BM MSC population based upon forward scatter (cell size) and side scatter (granularity). (B) All subsequent studies using flow cytometric analysis were conducted on 1×10^4 cells residing within the R1 quadrant and collected as listmode data. Representative frequency histograms of the immunoreactivity of sheep BM MSC to a variety of monoclonal antibodies coupled to FITC. The data is presented as the relative cell count (y-axis) versus the fluorescence intensity (log scale). Positive fluorescence was classed as levels of fluorescence greater than 99% of the appropriate isotype matched control.

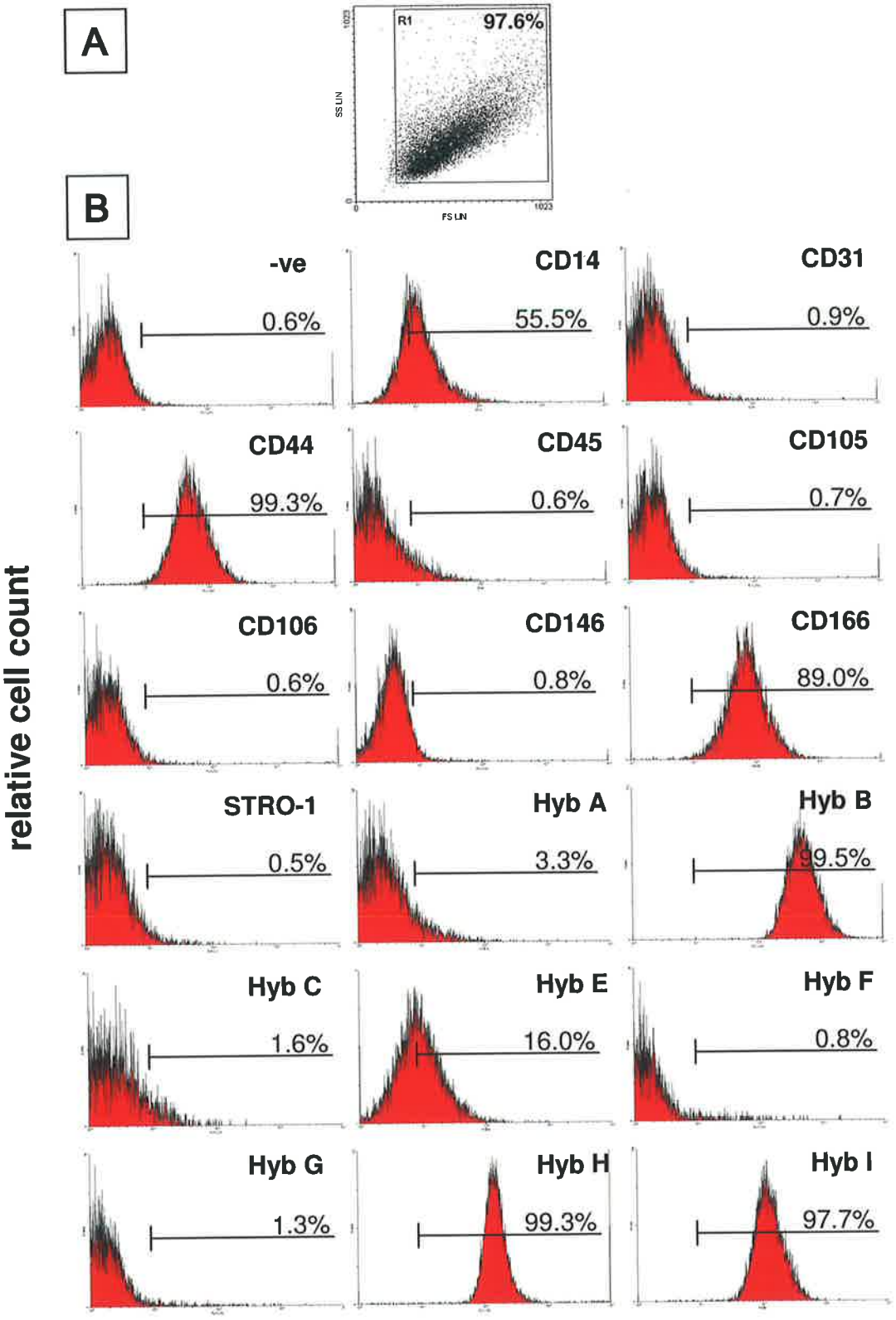
A
R1
97.6%
SS LIN
FS LIN
1023
0
B
-ve
0.6%
CD14
55.5%
CD31
0.9%
CD44
99.3%
CD45
0.6%
CD105
0.7%
CD106
0.6%
CD146
0.8%
CD166
89.0%
STRO-1
0.5%
Hyb A
3.3%
Hyb B
99.5%
Hyb C
1.6%
Hyb E
16.0%
Hyb F
0.8%
Hyb G
1.3%
Hyb H
99.3%
Hyb I
97.7%
relative cell count
fluorescence intensity

MUC-18, CD31, CD90, and CD105, all previously developed as markers of human MSC. Ovine MSC did not express the haematopoietic cell surface marker CD45. Combined data of the mean incidence of fluorescence from 3 donors is presented in Table 4.1.

4.2.2. Characterisation of the Immunophenotype of Freshly Isolated Ovine Chondrocytes.

In order to determine differences in the expression of cell surface markers between sheep MSC and sheep chondrocytes, articular cartilage scrapings were collected from three adult sheep. The chondrocytes were liberated from the cartilage extracellular matrix by overnight enzymatic digestion in a collagenase/dispase solution. These cells were immediately assessed by immunofluorescence flow cytometry using the panel of antibodies examined for sheep MSC, in order to define the cell surface expression of chondrocytes directly from their native extracellular and spacial environment, circumventing changes that may occur following in vitro culture. According to the scatter profile dot plot, uncultured articular chondrocytes exhibit a more homogenous cell population than sheep MSC (Figure 4.2A). Representative histograms of fluorescence intensity can be observed in Figure 4.2B. Interestingly, the immunophenotype of articular chondrocytes is considerably different to the profile observed in sheep MSC (Table 4.2). Consistent with MSC, the majority of sheep chondrocytes expressed hybridoma B (mean 89.8% ± 3.4 SEM), and hybridoma I (mean 84.1% ± 8.1 SEM), although intensity was slightly lower and less uniform in distribution. In contrast to sheep MSC where positive fluorescence exceeded 90%, chondrocytes lacked expression of adhesion molecules CD166 and CD44, and Hybridoma E. Additionally, Hybridoma H, which exhibited almost 100% expression by BM MSC cultures, displayed only 2.6% ± 0.4 reactivity in chondrocytes. Expression of the CD14 marker, which is specifically expressed by monocytes/macrophages, was also observed to be diminished in chondrocyte preparations, in comparison to cultured sheep MSC. Interestingly, a minor population of sheep chondrocytes displayed positive fluorescence for CD31 and CD45.

4.2.3. Characterisation of the Immunophenotype of Cultured Ovine Chondrocytes.

It is widely accepted that significant changes in morphology and gene expression occur once chondrocytes are permitted to adhere in vitro and cultured in monolayer. Chondrocytes dedifferentiate to a fibroblast-like morphology which is concomitantly associated with an alteration in extracellular matrix synthesis and cell surface marker

Table 4.1. Immunophenotype of ovine bone marrow derived MSC. Primary MSC cultures were generated according to plastic adherence and expanded in vitro (P3-P4). Cells were harvested by trypsin digestion and assessed for cell surface antigen expression by immunofluorescence flow cytometric analysis. Positive fluorescence was classed as levels of fluorescence greater than 99% of the appropriate isotype matched control. Analysis was conducted on 1×10^4 cells and all results are expressed as mean percentage positive fluorescence ± SEM (n=3 different BM aspirates).

Cell Surface Molecule	Antibody Name	Mean % Fluorescence (± SEM)
IgG_1 negative control	1B5	0.6 ± 0.1
IgG_2 negative control	1D4.5	0.6 ± 0.2
IgM negative control	1A6.12	0.7 ± 0.1
Alkaline Phosphatase	B478	0.6 ± 0.1
CD14 (Sheep)		28.5 ± 13.8
CD31 (Sheep)		0.9 ± 0.2
CD44	H9H11	99.3 ± 0.3
CD45 (Sheep)		0.6 ± 0.1
CD45 (Sheep)	SBU-LCA	0.5 ± 0.0
CD90		0.4 ± 0.2
CD105	AB11	0.7 ± 0.2
CD105	XB1	1.0 ± 0.3
CD106/VCAM-1 (Sheep)	QE4G9	0.6 ± 0.1
CD146	CC9	0.8 ± 0.3
CD146	EB4	0.5 ± 0.1
CD166		89.0 ± 7.5
STRO-1		0.5 ± 0.0
	Hyb A (Sheep)	3.3 ± 1.2
	Hyb B (Sheep)	99.5 ± 0.4
	Hyb C (Sheep)	1.6 ± 0.2
	Hyb E (Sheep)	16.0 ± 1.4
	Hyb F (Sheep)	0.8 ± 0.2
	Hyb G (Sheep)	1.3 ± 0.1
	Hyb H (Sheep)	99.3 ± 0.3
	Hyb I (Sheep)	97.7 ± 1.1

Figure 4.2: Cell surface expression profile of adult sheep articular chondrocytes. Chondrocytes were liberated from scrapings of articular cartilage by overnight enzymatic digestion in a collagenase/dispase solution. Single cell suspensions were then assessed for cell surface antigen expression by immunofluorescence flow cytometric analysis. (A) Representative dot plot of the chondrocyte population based upon forward scatter (cell size) and side scatter (granularity). (B) All subsequent studies using flow cytometric analysis were conducted on 1×10^4 cells residing within the R1 quadrant and collected as listmode data. Representative frequency histograms of the immunoreactivity of sheep chondrocytes to a variety of monoclonal antibodies coupled to FITC. The data is presented as the relative cell count (y-axis) versus the fluorescence intensity (log scale). Positive fluorescence was classed as levels of fluorescence greater than 99% of the appropriate isotype matched control.

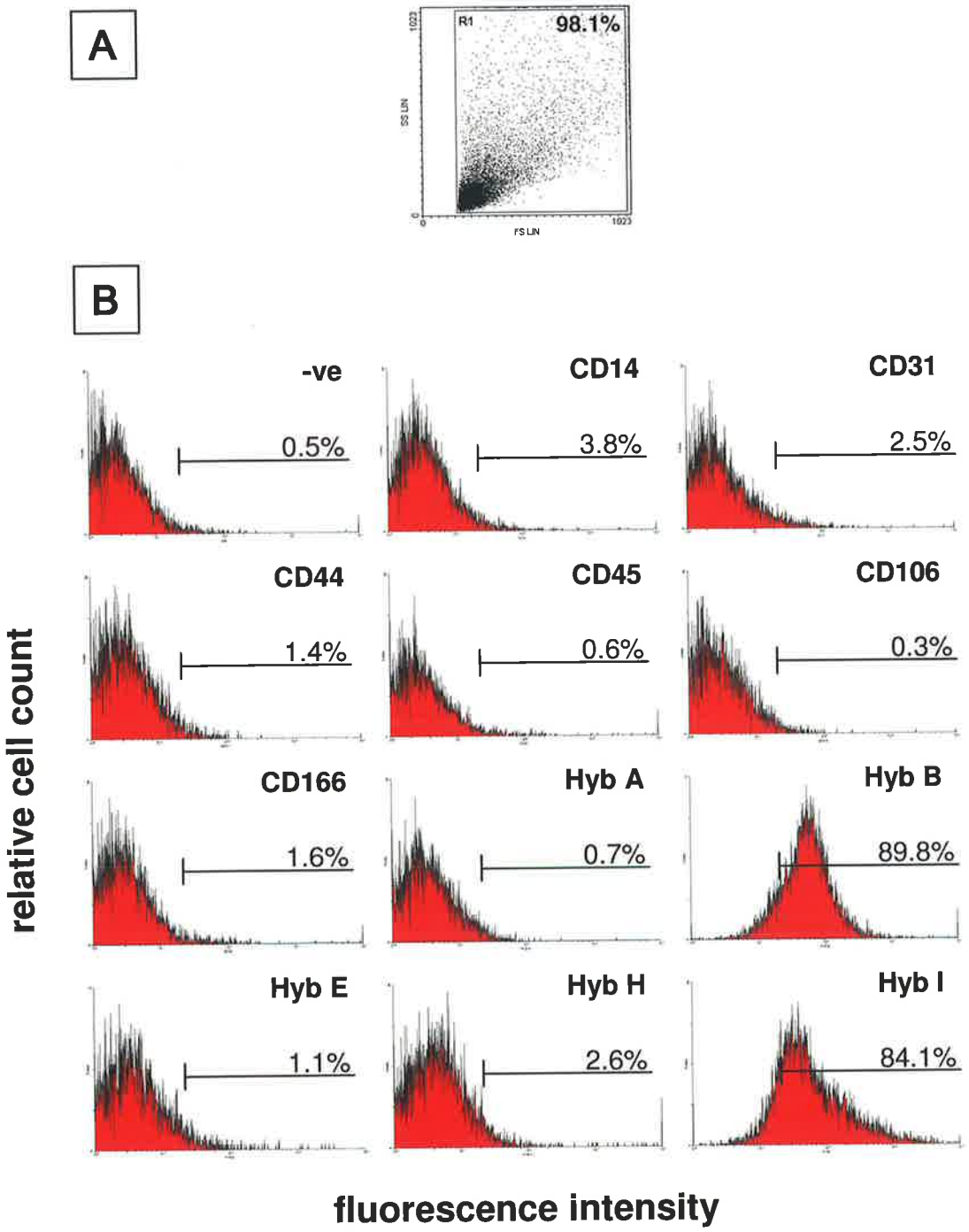
A
R1
98.1%
SS LIN
FS LIN
1023
0
B
-ve
0.5%
CD14
3.8%
CD31
2.5%
CD44
1.4%
CD45
0.6%
CD106
0.3%
CD166
1.6%
Hyb A
0.7%
Hyb B
89.8%
Hyb E
1.1%
Hyb H
2.6%
Hyb I
84.1%
relative cell count
fluorescence intensity

Table 4.2. Immunophenotype of uncultured ovine articular chondrocytes. Following enzymatic release from the cartilage extracellular matrix, chondrocyte cell surface antigen expression was assessed using immunofluorescence flow cytometric analysis. Positive fluorescence was classed as levels of fluorescence greater than 99% of the appropriate isotype matched control. Analysis was conducted on 1 x 10^4 cells and all results are expressed as mean percentage positive fluorescence ± SEM (n=3 different cartilage donors).

Cell Surface Molecule	Antibody Name	Mean % Fluorescence (± SEM)
IgG_1 negative control	1B5	0.7 ± 0.2
IgG_2 negative control	1D4.5	0.4 ± 0.1
IgM negative control	1A6.12	0.5 ± 0.2
Alkaline Phosphatase	B478	0.5 ± 0.1
CD14 (Sheep)		3.8 ± 0.8
CD31 (Sheep)		2.5 ± 1.5
CD44	H9H11	1.4 ± 0.3
CD45 (Sheep)		2.4 ± 0.6
CD45 (Sheep)	SBU-LCA	0.6 ± 0.3
CD90		0.5 ± 0.3
CD105	AB11	0.4 ± 0.0
CD105	XB1	0.6 ± 0.2
CD106/VCAM-1 (Sheep)	QE4G9	0.3 ± 0.1
CD146	CC9	0.7 ± 0.1
CD146	EB4	0.3 ± 0.1
CD166		1.6 ± 1.3
	Hyb A (Sheep)	0.7 ± 0.2
	Hyb B (Sheep)	89.8 ± 3.4
	Hyb E (Sheep)	1.1 ± 0.3
	Hyb H (Sheep)	2.6 ± 0.4
	Hyb I (Sheep)	84.1 ± 8.1

expression (Benya and Shaffer, 1982). So as to assess the changes that occur in the cell surface marker profile of chondrocytes following culture and dedifferentiation, articular chondrocytes corresponding to the donors used above (n=3) were expanded in monolayer. At passage 1, the dedifferentiated chondrocytes were harvested by trypsin detachment and subjected to single colour immunofluorescence flow cytometric analysis as described in the methods (Chapter 2.3.1). The panel of antibodies assessed were identical to those used for freshly isolated articular chondrocytes. Representative histograms displaying the observed fluorescence intensity and distribution of selected antibodies of interest highlighted multiple changes in cell surface expression profile (Figure 4.3B). Positive fluorescence from the three donors analysed was combined to provide the mean fluorescence of each antibody (Table 4.3). Several markers were moderately upregulated following culture in monolayer, including CD14 (mean 12.3% ± 8.4), CD166 (mean 5.7% ± 0.4) and Hybridoma E (mean 13.9% ± 6.7) antibodies, whose expression in uncultured chondrocytes ranged between 1 and 3%. Although expressed by a majority of uncultured chondrocytes (around 85%), the incidence of positive fluorescence with Hybridoma B (mean 99.5% ± 0.2) and Hybridoma I (mean 98.6% ± 0.7) was similarly increased to greater than 98% of cells analysed. Of particular interest, the culture of chondrocytes in monolayer instigated a significant upregulation in the surface expression of CD44 (mean 98.5% ± 0.9) and Hybridoma H (mean 99.6% ± 0.3), from negligible levels in uncultured chondrocytes to positive expression by almost the entirety of cells assessed. Conversely, the incidence of CD31 and CD45 expression was down regulated to virtually undetectable levels. Overall, cultured chondrocytes exhibit a similar immunophenotype to that observed for sheep BM MSC.

4.2.4. Characterisation of the Immunophenotype of Human BM Derived MSC and Osteoblasts with Hybridoma Supernatants Reactive Against Cultured Sheep MSC.

Although the cell surface expression profile of human MSC has been extensively characterised, the cross reactivity of human MSC with the series of monoclonal antibodies generated against sheep MSC was undetermined. Thus, single cell suspensions of human BM derived MSC from three individuals were analysed by single colour flow cytometric analysis. Established markers of human MSC were included as positive controls. Representative histograms demonstrating the fluorescence intensity and distribution patterns of cells analysed are presented in Figure 4.4. The data from three donors was combined to provide mean fluorescence for each antibody examined (Table 4.4). As

Figure 4.3: Cell surface expression profile of adult sheep dedifferentiated chondrocytes. Chondrocytes isolated from articular cartilage were cultured in vitro in monolayer to facilitate dedifferentiation of chondrocyte phenotype. Once confluent, cells were detached by trypsin digestion and recultured. Upon reaching confluence again, adherent cells were detached and assessed for cell surface antigen expression by immunofluorescence flow cytometric analysis. (A) Representative dot plot of the cultured chondrocyte population based upon forward scatter (cell size) and side scatter (granularity). (B) All subsequent studies using flow cytometric analysis were conducted on 1×10^4 cells residing within the R1 quadrant and collected as listmode data. Representative frequency histograms of the immunoreactivity of sheep cultured chondrocytes to a variety of monoclonal antibodies coupled to FITC (B). The data is presented as the relative cell count (y-axis) versus the fluorescence intensity (log scale). Positive fluorescence was classed as levels of fluorescence greater than 99% of the appropriate isotype matched control.

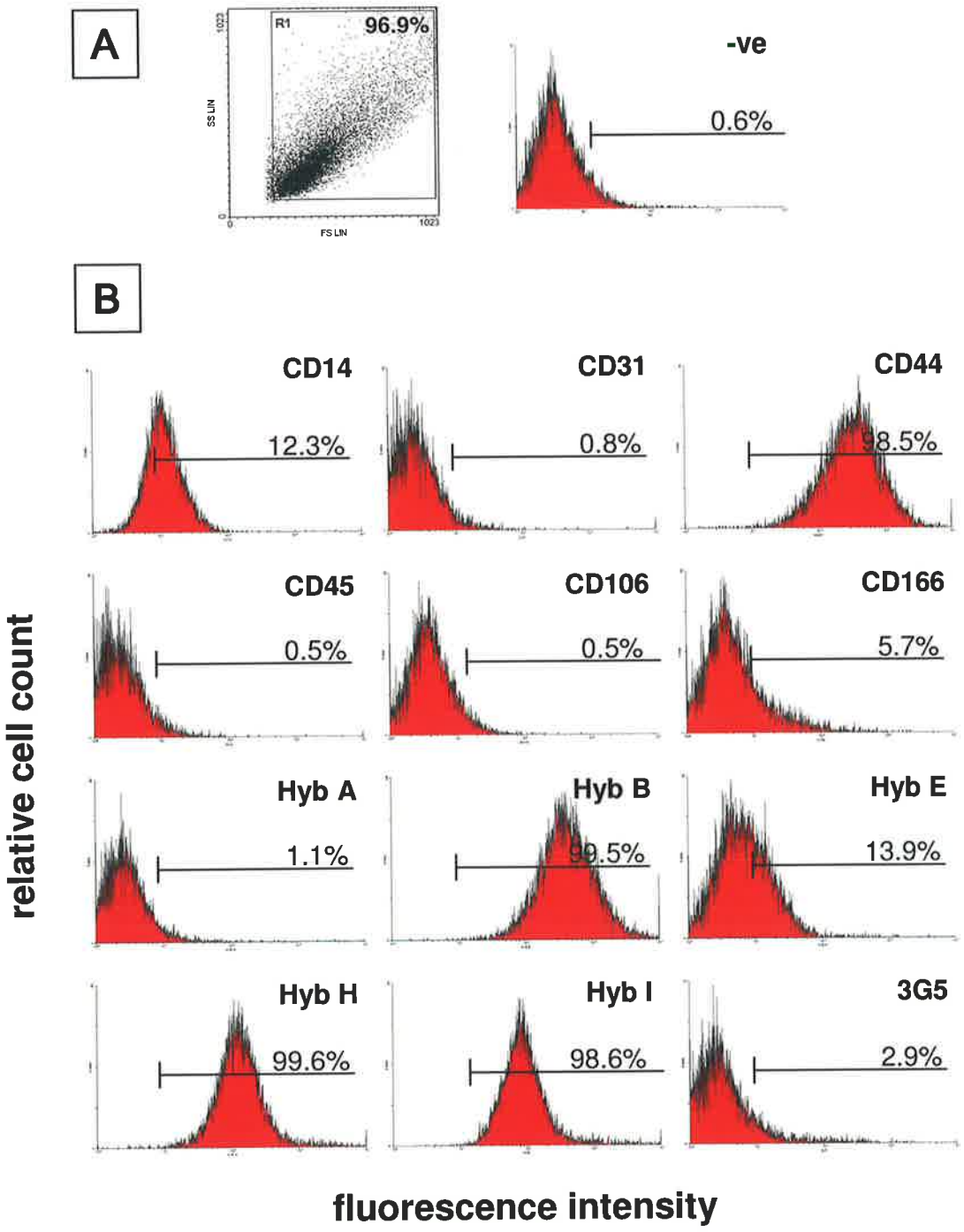
A
R1
96.9%
SS LIN
FS LIN
-ve
0.6%
B
CD14
12.3%
CD31
0.8%
CD44
98.5%
CD45
0.5%
CD106
0.5%
CD166
5.7%
Hyb A
1.1%
Hyb B
99.5%
Hyb E
13.9%
Hyb H
99.6%
Hyb I
98.6%
3G5
2.9%
relative cell count
fluorescence intensity

Table 4.3. Immunophenotype of dedifferentiated ovine articular chondrocytes. Cells isolated from cartilage tissue were cultured in vitro in monolayer to initiate dedifferentiation phenotype. Upon confluence (P1-P2), primary cultures were harvested by trypsin digestion and assessed for cell surface antigen expression by immunofluorescence flow cytometric analysis. Positive fluorescence was classed as levels of fluorescence greater than 99% of the appropriate isotype matched control. Analysis was conducted on 1 x 10^4 cells and all results are expressed as mean percentage positive fluorescence ± SEM (n=3 different cartilage donors, with chondrocyte samples matching those of the same donors used in Table 4.2).

Cell Surface Molecule	Antibody Name	Mean % Fluorescence (± SEM)
IgG_1 negative control	1B5	0.5 ± 0.2
IgG_2 negative control	1D4.5	0.7 ± 0.4
IgM negative control	1A6.12	0.4 ± 0.1
Alkaline Phosphatase	B478	0.3 ± 0.1
CD14 (Sheep)		12.3 ± 8.4
CD31 (Sheep)		0.8 ± 0.0
CD44	H9H11	98.5 ± 0.9
CD45 (Sheep)		0.7 ± 0.0
CD45 (Sheep)	SBU-LCA	0.5 ± 0.2
CD90		0.3 ± 0.2
CD105	AB11	0.4 ± 0.1
CD105	XB1	0.4 ± 0.1
CD106/VCAM-1 (Sheep)	QE4G9	0.5 ± 0.3
CD146	CC9	0.5 ± 0.2
CD146	EB4	0.2 ± 0.1
CD166		5.7 ± 0.4
	3G5	2.9 ± 1.4
	Hyb A (Sheep)	1.1 ± 0.8
	Hyb B (Sheep)	99.5 ± 0.2
	Hyb E (Sheep)	13.9 ± 6.7
	Hyb H (Sheep)	99.6 ± 0.3
	Hyb I (Sheep)	98.6 ± 0.7

Figure 4.4: Cell surface expression profile of adult human bone marrow derived MSC. Primary MSC cultures were generated from BM MNC preparations according to plastic adherence and expanded in vitro. Upon confluence, cells were harvested by trypsin digestion and assessed for cell surface antigen expression by immunofluorescence flow cytometric analysis. Specifically, human MSC were assessed for immunoreactivity to monoclonal antibodies recognising sheep MSC. (A) Representative dot plot of the BM MSC population based upon forward scatter (cell size) and side scatter (granularity). (B) All subsequent studies using flow cytometric analysis were conducted on 1×10^4 cells residing within the R1 quadrant and collected as listmode data. Representative frequency histograms of the immunoreactivity of human BM MSC to a variety of monoclonal antibodies coupled to FITC. The data is presented as the relative cell count (y-axis) versus the fluorescence intensity (log scale). Positive fluorescence was classed as levels of fluorescence greater than 99% of the appropriate isotype matched control.

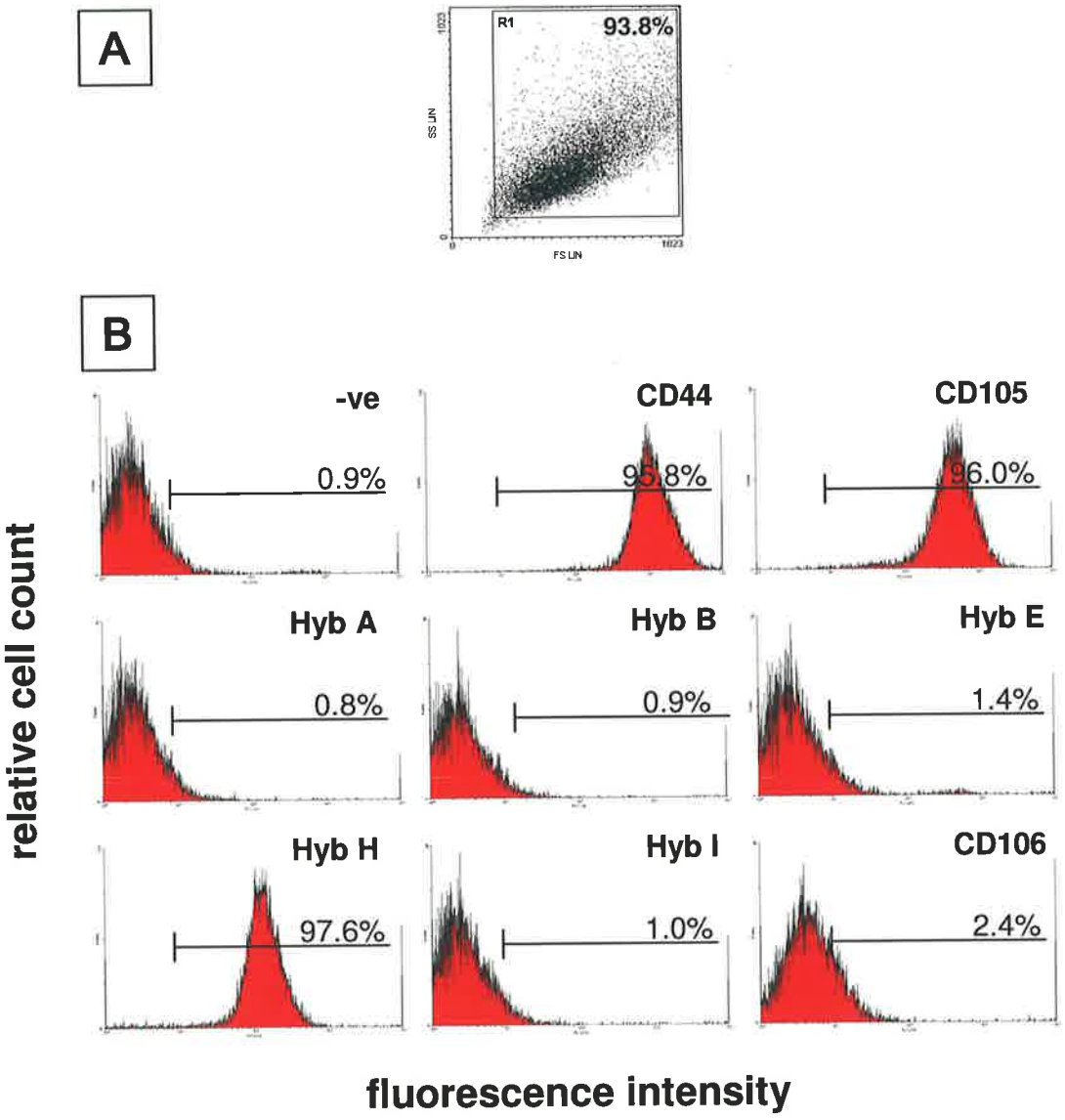
A
R1
93.8%
SS LIN
FS LIN
B
-ve
0.9%
CD44
95.8%
CD105
96.0%
Hyb A
0.8%
Hyb B
0.9%
Hyb E
1.4%
Hyb H
97.6%
Hyb I
1.0%
CD106
2.4%
relative cell count
fluorescence intensity

Table 4.4. Cell surface markers expressed by human bone marrow derived MSC. Primary MSC cultures were generated according to plastic adherence and expanded in vitro (P3-P4). Cells were harvested by trypsin digestion and assessed for cell surface antigen expression by immunofluorescence flow cytometric analysis. Positive fluorescence was classed as levels of fluorescence greater than 99% of the appropriate isotype matched control. Analysis was conducted on 1 x 10^4 cells and all results are expressed as mean percentage positive fluorescence ± SEM (n=3 different BM aspirates).

Cell Surface Molecule	Antibody Name	Mean % Fluorescence (± SEM)
IgG_1 negative control	1B5	0.9 ± 0.2
IgG_2 negative control	1D4.5	0.9 ± 0.3
IgM negative control	1A6.12	0.6 ± 0.4
Alkaline Phosphatase	B478	23.4 ± 12.9
CD44	H9H11	95.8 ± 2.1
CD105	AB11	96.0 ± 1.8
CD105	XB1	95.6 ± 2.1
CD106/VCAM-1 (Sheep)	QE4G9	2.4 ± 2.2
CD146	CC9	28.3 ± 8.3
CD146	EB4	15.0 ± 7.1
	Hyb A (Sheep)	0.8 ± 0.4
	Hyb B (Sheep)	0.9 ± 0.2
	Hyb E (Sheep)	1.4 ± 0.6
	Hyb H (Sheep)	97.6 ± 0.8
	Hyb I (Sheep)	1.0 ± 0.3

expected, human MSC exhibited uniformly positive expression of CD44 and CD105, and intermediate expression of alkaline phosphatase and CD146 (MUC-18). Of the uncharacterised hybridomas generated against sheep MSC, levels of immunoreactivity were virtually undetectable for all antibodies assessed, except for Hybridoma H (mean 97.6% ± 0.8 SEM), which exhibited a strong immunofluorescence in the majority of human BM MSC examined.

Human osteoblasts were correspondingly investigated for cross reactivity with the sheep specific hybridoma panel. Cultured osteoblasts from 3 healthy adult human osteoblast donors (OD) were analysed by flow cytometric analysis and representative histograms of relative fluorescence intensity and distribution are presented in Figure 4.5. Positive fluorescence from the three donors analysed was combined to provide the mean fluorescence of each antibody (Table 4.5). Consistent with human MSC, human osteoblasts were immunoreactive with CD44, CD105 and CD146, and displayed cross reactivity only with monoclonal anti-sheep MSC Hybridoma H (99.3% ± 0.2). The remaining hybridomas failed to recognise osteoblast cells of human origin.

4.2.5. Spatial Localisation and Resolution of Sheep CFU-F Progenitor Cells within MNC Preparations by Flow Cytometric Analysis.

Across all species, the relative incidence of CFU-F within bone marrow aspirates is consistently low. This study aimed to more accurately discriminate the region in which MSC reside according to cell size and granularity, so as to more precisely target cells for FACS immunoselection. Furthermore, specifying the region known to harbour CFU-F progenitors diminishes the likelihood of contaminating non specific Fc binding. Two separate sheep bone marrow aspirates were subjected to FACS which characterised each cell by size (forward light scatter) and granularity (side light scatter). Examination of the resulting dot plot histograms revealed three distinct cell sub populations (Figure 4.6A). These MNC sub populations are loosely categorised as the lymphocyte (R1), monocyte (R2), and granulocyte (R3) fractions. Lymphocytes comprise the majority of MNC, followed by monocytes and granulocytes (Figure 4.6B).

In order to determine which fraction the CFU-F progenitors reside in, each subpopulation was gated horizontally, and cells within each region were collected. The cells from each gated region were subsequently cultured under standard CFU-F assay conditions. After

Figure 4.5: Cell surface expression profile of adult human osteoblasts. Primary osteoblast cultures were generated from normal osteoblast donors and cultured in vitro. Upon confluence, cells were detached by collagenase/dispase digestion and assessed for cell surface antigen expression by immunofluorescence flow cytometric analysis. Specifically, human osteoblasts were assessed for immunoreactivity to monoclonal antibodies recognising sheep MSC. (A) Representative dot plot of the human osteoblast population based upon forward scatter (cell size) and side scatter (granularity). (B) All subsequent studies using flow cytometric analysis were conducted on 1×10^4 cells residing within the R1 quadrant and collected as listmode data. Representative frequency histograms of the immunoreactivity of human osteoblasts to a variety of monoclonal antibodies coupled to FITC. The data is presented as the relative cell count (y-axis) versus the fluorescence intensity (log scale). Positive fluorescence was classed as levels of fluorescence greater than 99% of the appropriate isotype matched control.

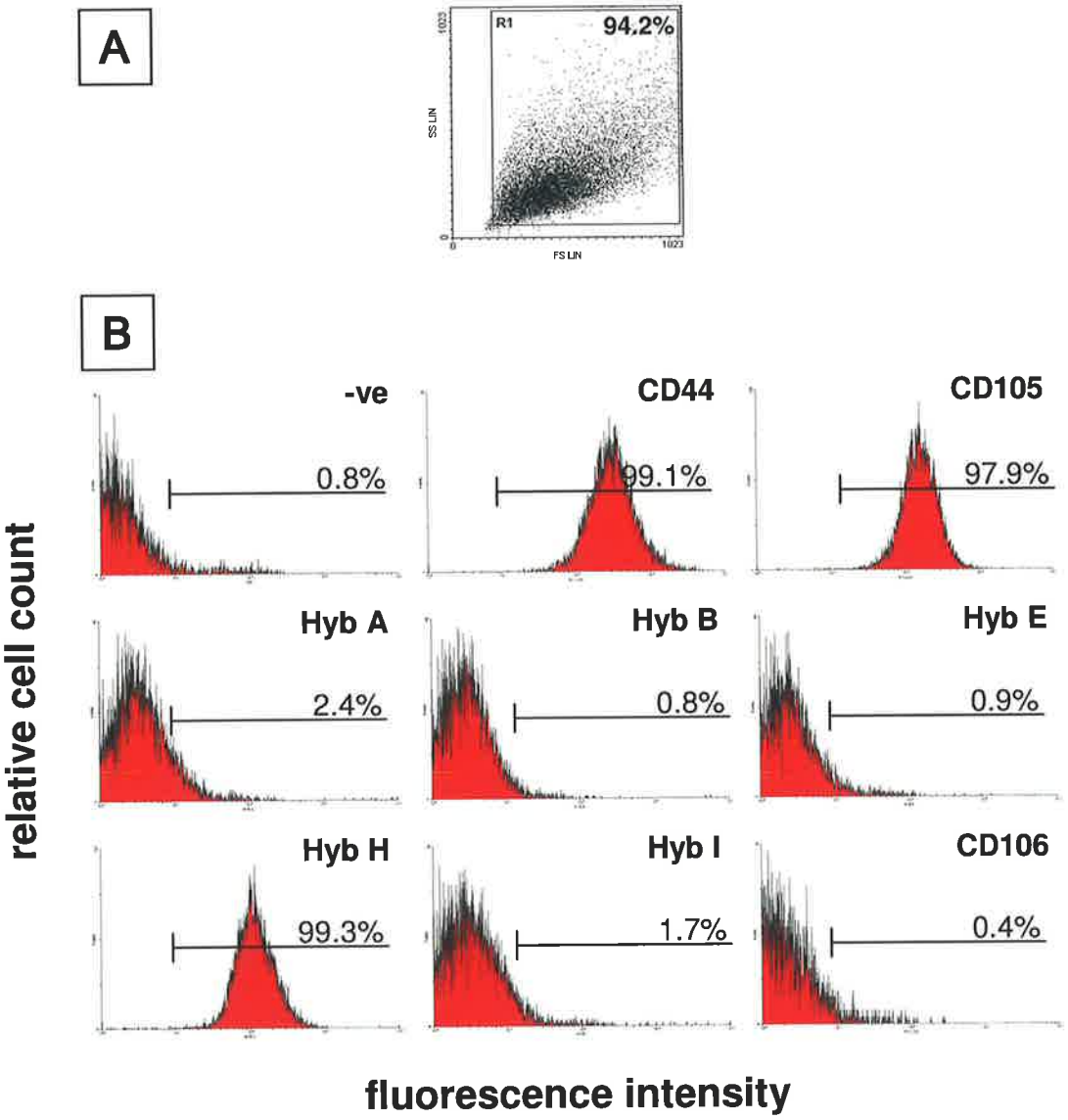
A
R1
94.2%
SS LIN
FS LIN
1023
0
B
-ve
0.8%
CD44
99.1%
CD105
97.9%
Hyb A
2.4%
Hyb B
0.8%
Hyb E
0.9%
Hyb H
99.3%
Hyb I
1.7%
CD106
0.4%
relative cell count
fluorescence intensity

Table 4.5. Cell surface markers expressed by human normal osteoblasts. Primary cultures were collected by collagenase/dispase digestion of bone trephine chips and assessed for cell surface antigen expression by immunofluorescence flow cytometric analysis. Positive fluorescence was classed as levels of fluorescence greater than 99% of the appropriate isotype matched control. Analysis was conducted on 1 x 10^4 cells and all results are expressed as mean percentage positive fluorescence ± SEM (n=3 different OB donors).

Cell Surface Molecule	Antibody Name	Mean % Fluorescence (± SEM)
IgG_1 negative control	1B5	0.8 ± 0.4
IgG_2 negative control	1A6.12	0.9 ± 0.1
IgM negative control	1D4.5	0.5 ± 0.2
Alkaline Phosphatase	B478	2.4 ± 1.2
CD44	H9H11	99.1 ± 0.4
CD105	AB11	97.9 ± 1.1
CD105	XB1	89.4 ± 1.9
CD106/VCAM-1 (Sheep)	QE4G9	0.4 ± 0.2
CD146	CC9	41.9 ± 7.8
CD146	EB4	1.0 ± 0.6
	Hyb A (Sheep)	2.4 ± 1.0
	Hyb B (Sheep)	0.8 ± 0.2
	Hyb E (Sheep)	0.9 ± 0.3
	Hyb H (Sheep)	99.3 ± 0.2
	Hyb I (Sheep)	1.7 ± 0.9

Figure 4.6: Spatial localisation of CFU-F progenitor cells within ovine BM MNC preparations. Using a flow cytometer, BM MNCs from two sheep donors were distributed according to physical characteristics by forward scatter (size) and side scatter (granularity) following density gradient centrifugation. In each instance, three discrete subpopulations of the bone marrow fraction were collected using horizontal gates representing the lymphocyte (R1), monocyte (R2) and granulocyte (R3) fractions. (A) Representative dot plot of the bone marrow MNC scatter profile observed with corresponding gates. (B) The average percentage of each sub-fraction ± SEM within the total cell pool was assessed, with lymphocytes contributing to the majority of cells collected. (C) Each sub-fraction was cultured in triplicate according to CFU-F assay technique. The number of colony forming units derived from each population was ascertained following 10-14 days in culture. The 'pre' sample represents a complete, ungated MNC fraction. The greatest proportion of CFU-F capable progenitors was derived from the granulocyte (R3) fraction, exceeding the pre sort control, monocyte (R2) population, and the lymphocyte (R1) fraction.

A

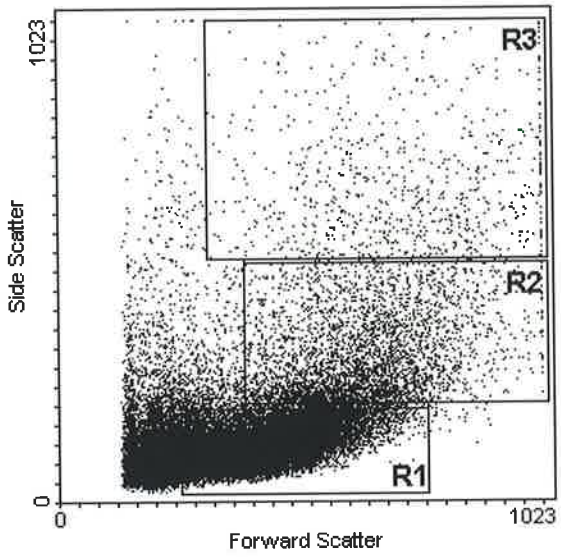

B

Region	% Total Cells (n=4)
R1	42.3± 3.7
R2	14.2 ± 2.5
R3	2.3 ± 0.5

C

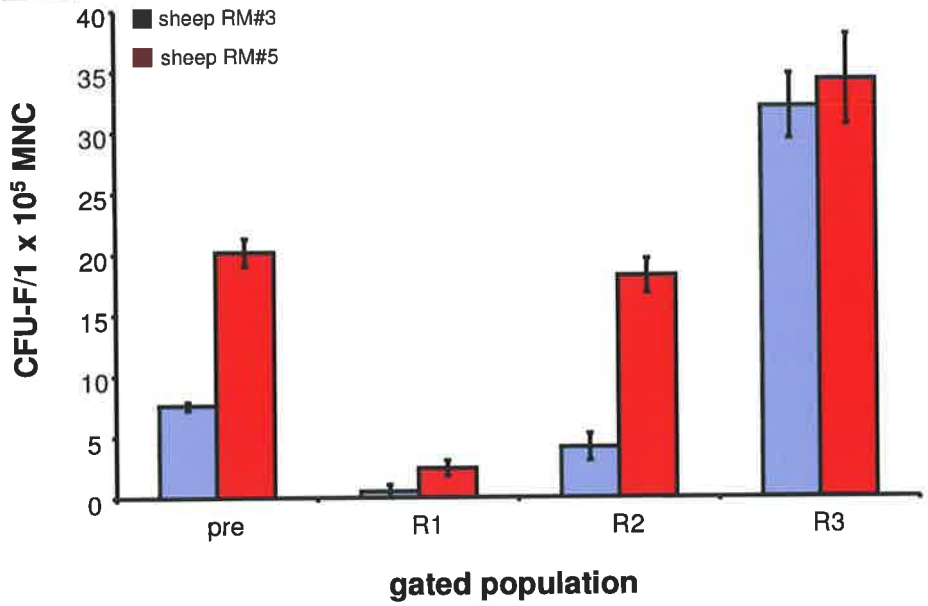

10-14 days, the number of colonies formed from the three fractions was assessed and is presented as the incidence of CFU-F per 1 x 10^5 MNC plated for each subject (Figure 4.6C). Results for the two donors were combined to provide the mean CFU-F for each fraction, and fold enrichment compared to the unfractionated MNC population (Table 4.6). CFU-F progenitors were clearly absent from the lymphocyte fraction (R1, mean 1.5 ± 1.0 CFU-F per 1 x 10^5 MNC). The incidence of CFU-F within the monocyte population (R2, mean 11.2 ± 7.0 CFU-F per 1 x 10^5 MNC) was comparable to the unfractionated MNC control (mean 13.9 ± 6.3 CFU-F per 1 x 10^5 MNC). Cells within the granulocyte region (R3, mean 33.2 ± 1.1 CFU-F per 1 x 10^5 MNC) contained the highest frequency of CFU-F, with enrichment almost three times that of unfractionated cells. Whilst the majority of CFU-F exist within the granulocyte fraction, progenitor cells can also be recovered from the monocyte fraction. Therefore the assignment of gates requires re-evaluation so as to include all CFU-F progenitors.

As separation of MNC subpopulations based upon horizontal gates failed to resolve a fraction of cells containing the entire subset of CFU-F, two vertical gates were assigned to the MNC preparation (excluding the lymphocyte population) (Figure 4.7A). BM aspirates from two subjects were analysed, and cells within each region were collected and cultured under standard CFU-F assay procedure as described in the methods. Cells of the R1 and R2 regions comprised approximately 3.5% and 1% of the total MNC population respectively (Figure 4.7B). The yield of CFU-F per 1 x 10^5 MNC within each region for each subject is presented in Figure 4.7C. Although consistent between gated groups, the two subjects display a large variation in CFU-F potential. Data from each subject were combined and are presented as mean number of CFU-F per 1 x 10^5 MNC plated, and fold enrichment in comparison to the unfractionated control was tabulated (Table 4.7). Collection of cells within the R1 region significantly decreased enrichment of CFU-F, and contained virtually no CFU-F (mean 1.0 ± 0.5 CFU-F per 1 x 10^5 MNC). Conversely, the R2 region appeared to contain the entire CFU-F population (mean 31.2 ± 20.6 CFU-F per 1 x 10^5 MNC), resulting in a two fold enrichment of progenitor cells compared to the unfractionated MNC sample (18.6 ± 13.2 CFU-F per 1 x 10^5 MNC). Collectively, results suggest that the entire ovine MSC population resides within the horizontal region R2. The subsequent immunoselection of cells within the designated region by FACS may augment the characterisation of cells with CFU-F potential from BM aspirates.

Table 4.6. Spatial localisation/identity of CFU-F progenitor cells within ovine BM MNC preparations. MNC were separated by a flow cytometer based upon forward scatter (size) and side scatter (granularity). Cells were horizontally gated into subpopulations according to scatter profile, and cultured for 10-14 days according to CFU-F technique. The data presented below represent mean CFU-F ± SEM per 1 x 10^5 MNC, and mean fold ± SEM enrichment compared to unseparated control (n=2 different BM donors).

Gated Population	CFU-F ± SEM per 1 x 10^5 MNC	Fold Enrichment (± SEM)
Unfractionated BM MNC	13.9 ± 6.3	1.0 ± 0.0
R1	1.5 ± 1.0	0.1 ± 0.0
R2	11.2 ± 7.0	0.7 ± 0.2
R3	33.2 ± 1.1	3.0 ± 1.3

Figure 4.7: Fractionation of CFU-F progenitor cells within ovine BM MNC preparations according spatial distribution. Using a flow cytometer, BM MNCs from two sheep donors were fractionated according to physical characteristics by forward scatter (size) and side scatter (granularity) following density gradient centrifugation. In each instance, two discrete subpopulations of the bone marrow fraction were collected using vertical gating to avoid cells of the lymphocyte fraction. (A) Representative dot plot of the bone marrow MNC scatter profile with corresponding gates. (B) The average percentage (± SEM) of each sub-fraction within the total cell pool, with the R1 fraction contributing to approximately 8% of cells collected, and R2 population consisting of less than 1% of the total MNC population. (C) Each sub-fraction was cultured in triplicate for 10-14 days according to CFU-F assay technique and the number of colony forming units derived from each population was ascertained. The 'pre' sample represents a complete, ungated MNC fraction. The complete CFU-F fraction was contained within cells of the R2 region, with CFU-F virtually undetectable in the R1 subpopulation.

A

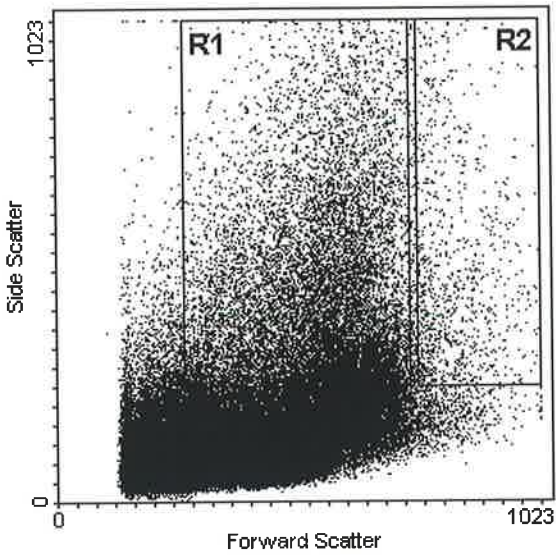

B

Region	% Total Cells (n=2)
R1	8.4 ± 5.9
R2	0.9 ± 0.3

C

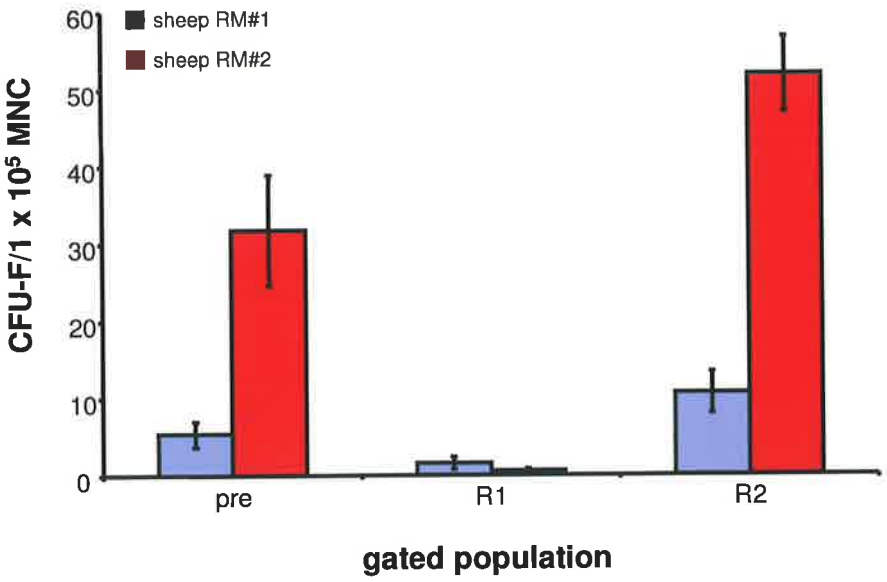

Table 4.7. Spatial localisation/identity of CFU-F progenitor cells within ovine BM MNC preparations. MNC were separated by a flow cytometer based upon forward scatter (size) and side scatter (granularity). Cells were vertically gated into subpopulations according to scatter profile, and cultured for 10-14 days according to CFU-F technique. The data presented below represent mean CFU-F ± SEM per 1 x 10^5 MNC plated, and mean fold ± SEM enrichment compared to unseparated control (n=2 different BM donors).

Gated Population	CFU-F ± SEM per 1 x 10^5 MNC	Fold Enrichment (± SEM)
Unfractionated BM MNC	18.6 ± 13.2	1.0 ± 0.0
R1	1.0 ± 0.5	0.2 ± 0.1
R2	31.2 ± 20.6	1.8 ± 0.2

4.2.6. Immunoselection and Enrichment of CFU-F Progenitors from Ovine BM MNC Preparations by Fluorescence Activated Cell Sorting (FACS).

Following analysis of the cell surface expression profile of ovine MSC, an assortment of uncharacterised hybridomas reactive with cultured sheep MSC were chosen for examination of their potential to directly select for and enrich the yield of MSC. Preparations of BM MNC were immunostained with each hybridoma of interest and fluorescence intensity was measured by FACS. As the spatial location of CFU-F within the MNC population has been defined, cells were selected within the region previously confirmed to contain these progenitor cells. Cells positive and negative for the expression of each antibody, compared to the isotype matched control, were collected and subjected to a standard CFU-F assay procedure. To determine enrichment due to selection with the particular monoclonal antibody the relative yield of CFU-F per 1 x 10^5 MNC was calculated and compared to CFU-F yield from an unfractionated control.

When BM MNC were immunoselected within the gated region R1, by monoclonal antibody Hybridoma A coupled to FITC, the dot plot histogram of the MNC distribution pattern depicted a heterogeneous population of cells (Figure 4.8A). A frequency histogram representing the immunoreactivity of R1 gated BM MNC with Hybridoma A is presented in Figure 4.8B. Cells expressing Hybridoma A to a level greater than 99% of the isotype matched control were classed as positively expressing cells and were collected (M1). The horizontal bar denoting M2 region represents the R1 gated cells negative for expression of the Hybridoma A antibody, which were also collected for analysis. MNC within the R1 region represented 0.6% of the total cell population. Immunoreactivity with Hybridoma A was detected in 16.4% of cells within the R1 region, representing 0.1% of the total number of cells analysed. In vitro culture of Hybridoma A^+ cells under CFU-F assay conditions resulted in the formation of 94.4 ± 18.9 CFU-F per 1 x 10^5 MNC. In contrast, Hybridoma A^- cells failed to form any detectable CFU-F colonies. Compared to the unfractionated control this selection process with the Hybridoma A antibody yielded a 33.7 fold enrichment of CFU-F content (Table 4.8).

Immunoreactivity with the monoclonal Hybridoma B antibody was almost ubiquitous within the MNC population. Similarly, within the R1 region (comprising 0.55% of the total MNC population), 97.4% cells displayed positive immunoreactivity with Hybridoma B (Figure 4.9B). The region M1 represents positive fluorescence greater than 99% of the

Figure 4.8: Immunoselection of adult sheep BM MNC with the monoclonal antibody Hybridoma A. (A) Representative dot plot demonstrating the heterogenous nature of the BM MNC population based upon forward scatter (cell size) and side scatter (granularity). (B) Frequency histogram representing the immunoreactivity of R1 gated BM MNC with the FITC coupled Hybridoma A, with data presented as the relative cell count (y-axis) versus the fluorescence intensity (log scale). The horizontal bar (region M1) represents the level of fluorescence greater than 99% of the FITC coupled isotype matched control (1A6.12), and horizontal bar (M2 region) represents the R1 gated cells negative for Hybridoma A.

A

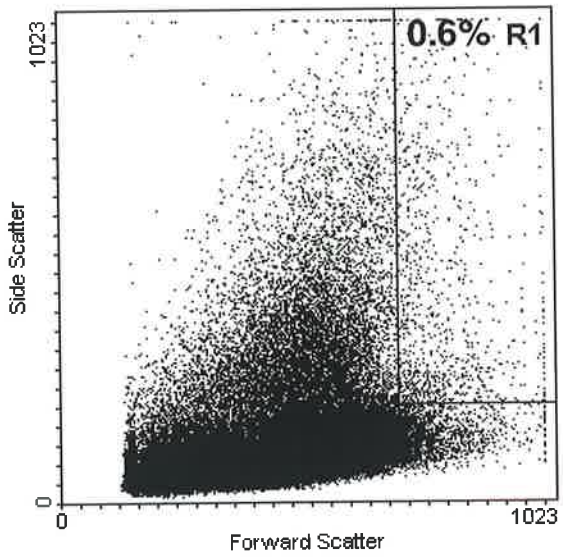

B

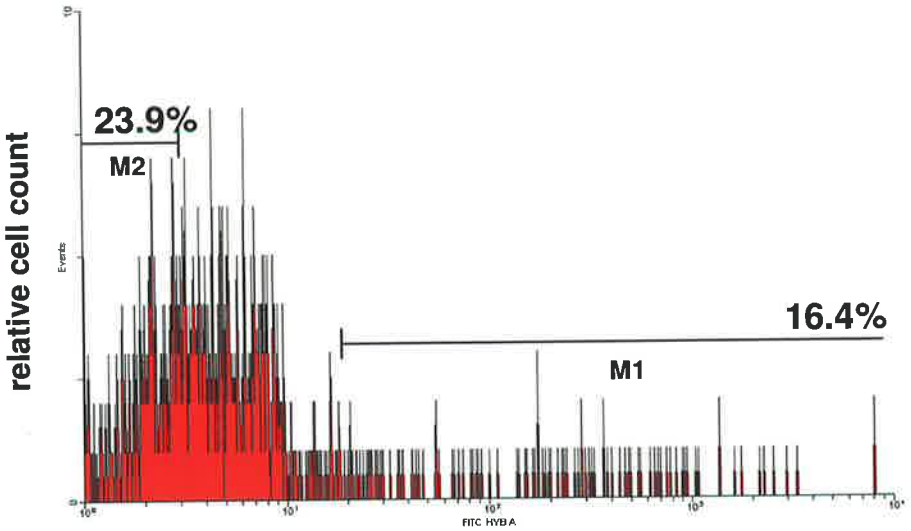

Hybridoma A-FITC

Figure 4.9: Immunoselection of adult sheep BM MNC with the monoclonal antibody Hybridoma B. (A) Representative dot plot demonstrating the heterogenous nature of the BM MNC population based upon forward scatter (cell size) and side scatter (granularity). (B) Frequency histogram representing the immunoreactivity of R1 gated BM MNC with the FITC coupled Hybridoma B, with data presented as the relative cell count (y-axis) versus the fluorescence intensity (log scale). The horizontal bar (region M1) represents the level of fluorescence greater than 99% of the FITC coupled isotype matched control (1B5). The horizontal bar denoting M2 region represents the R1 gated cells negative for Hybridoma B. The horizontal bar (region M3) indicates a subpopulation of cells which express the Hybridoma B antigen more intensely than the rest of the positive BM MNC population.

A

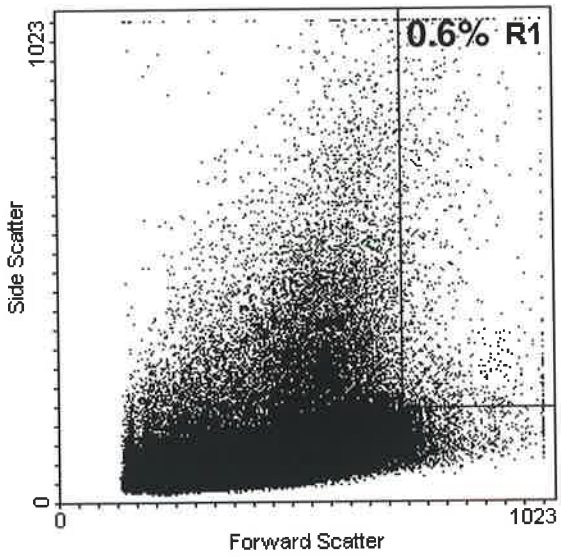

B

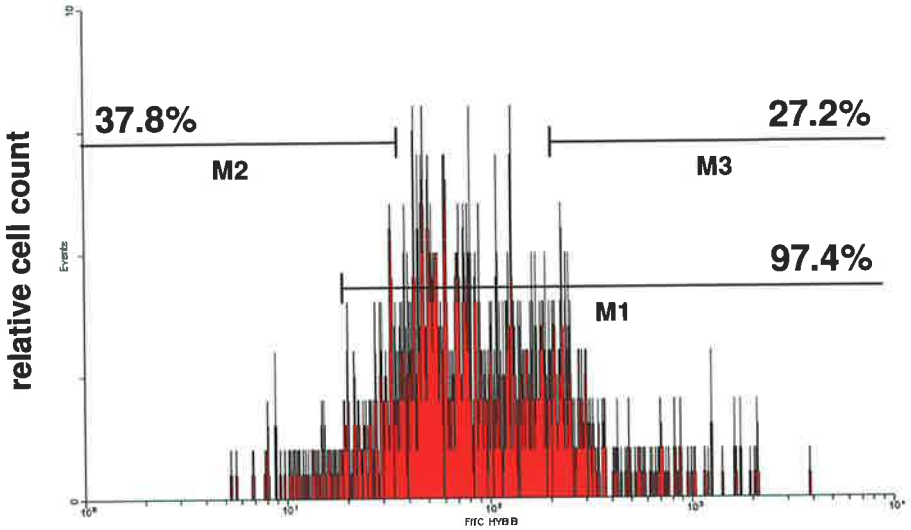

Hybridoma B-FITC

isotype matched control. As virtually the entire population displays reactivity with Hybridoma B, cells demonstrating elevated levels of the antigen were collected as Hybridoma B^+ fraction, as indicated by the horizontal bar M3. This Hybridoma B bright subfraction constituted 27.2% of cells within the R1 region, and 0.2% of the total. Cells classed as negative for expression of Hybridoma B are indicated by the M2 horizontal bar, representing 37.8% of R1 gated cells, and 0.2% of the entire population. In vitro culture of immunoselected MNC revealed that whilst Hybridoma B^- cells were unable to produce any CFU-F, Hybridoma B^+ cells produced 62.1 ± 20.7 CFU-F per 1 x 10^5 MNC (Table 4.8). This immunoselection process with Hybridoma B produced a 22.2 fold enrichment of CFU-F content compared to the unselected preparations.

Hybridoma E immunoreactivity within the overall mononuclear cell population was nominal. Cells within the R1 region constitute 3.0% of the total cell number (Figure 4.10A), and within this subset, 13.6% of cells exhibit positive immunoreactivity with Hybridoma E (Figure 4.10B). Hybridoma E^+ (region M1) and Hybridoma E^- (region M2) cells were collected and cultured. Hybridoma E^+ MNC gave rise to 103.9 ± 26.0 CFU-F per 1 x 10^5 MNC (Table 4.8), whereas in contrast, Hybridoma E^- cells failed to produce any detectable CFU-F. Evaluation of the enrichment as a result of positive immunoselection with Hybridoma E compared to the unfractionated control revealed an 11.9 fold increase in CFU-F content.

Of the heterogeneous MNC population assessed for immunoreactivity against Hybridoma H, cells of the R1 region comprised only 2.7% of the total cell number (Figure 4.11A). Within this fraction, 12% of cells were positive for Hybridoma H (Figure 4.11B), as defined by the horizontal region M1. Cells considered to be Hybridoma H^- are indicated by the marker M2, and were collected in conjunction Hybridoma H^+ cells. Similar to the other hybridoma supernatants assessed Hybridoma H^- cells did not give rise to any CFU-F (Table 4.8). On the contrary, 153.9 ± 31.9 CFU-F per 1 x 10^5 MNC resulted from immunoselection with Hybridoma H^+, equivalent to a 44.1 fold enrichment of CFU-F content from the unselected MNC preparations.

Following immunostaining with Hybridoma I, within the R1 gated region (3.7% of the total cell pool) (Figure 4.12A), 54.6% of the gated cells exhibited positive fluorescence, designated by the horizontal bar M1 (Figure 4.12B). Interestingly, the fluorescence distribution pattern of Hybridoma I was similar to that observed for Hybridoma B, despite

Figure 4.10: Immunoselection of adult sheep BM MNC with the monoclonal antibody Hybridoma E. (A) Representative dot plot demonstrating the heterogenous nature of the BM MNC population based upon forward scatter (cell size) and side scatter (granularity). (B) Frequency histogram representing the immunoreactivity of R1 gated BM MNC with the FITC coupled Hybridoma E, with data presented as the relative cell count (y-axis) versus the fluorescence intensity (log scale). The horizontal bar (region M1) represents the level of fluorescence greater than 99% of the FITC coupled isotype matched control (1A6.12). The horizontal bar denoting M2 region represents the R1 gated cells negative for Hybridoma E.

A

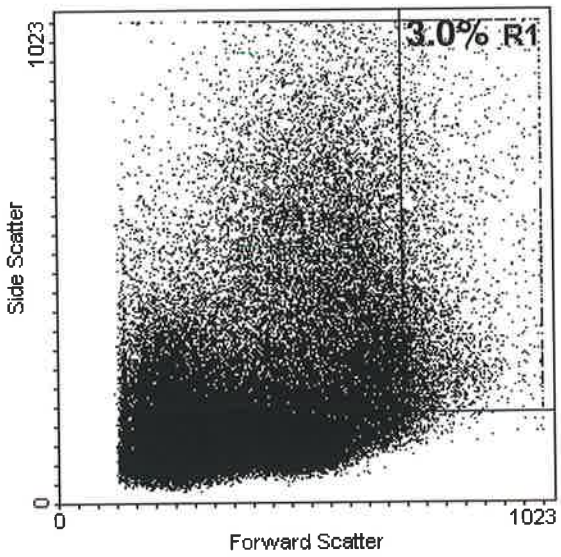
3.0% R1
1023
Side Scatter
0
0
1023
Forward Scatter

B

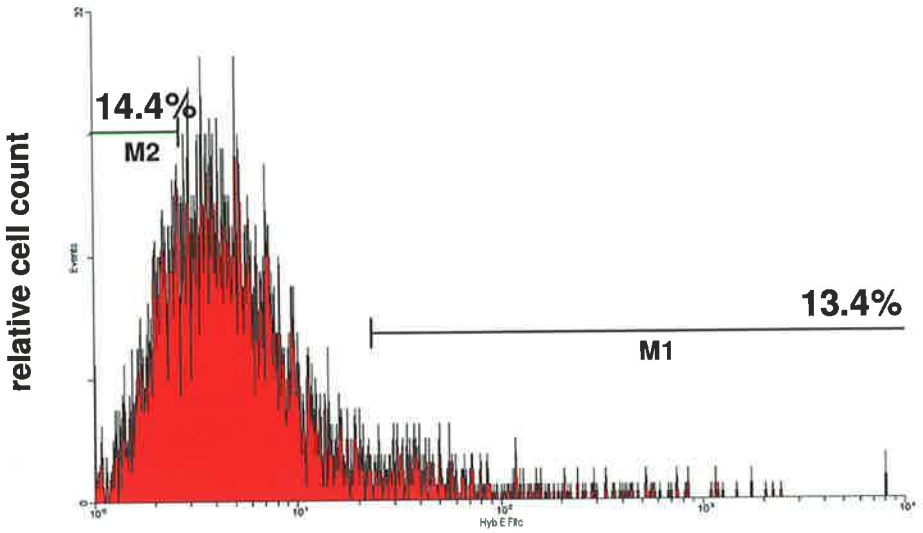
14.4%
M2
13.4%
M1
relative cell count
Hybridoma E-FITC

Figure 4.11: Immunoselection of adult sheep BM MNC with the monoclonal antibody Hybridoma H. (A) Representative dot plot demonstrating the heterogenous nature of the BM MNC population based upon forward scatter (cell size) and side scatter (granularity). (B) Frequency histogram representing the immunoreactivity of R1 gated BM MNC with the FITC coupled Hybridoma H, with data presented as the relative cell count (y-axis) versus the fluorescence intensity (log scale). The horizontal bar (region M1) represents the level of fluorescence greater than 99% of the FITC coupled isotype matched control (1B5). The horizontal bar denoting M2 region represents the R1 gated cells negative for Hybridoma H.

A

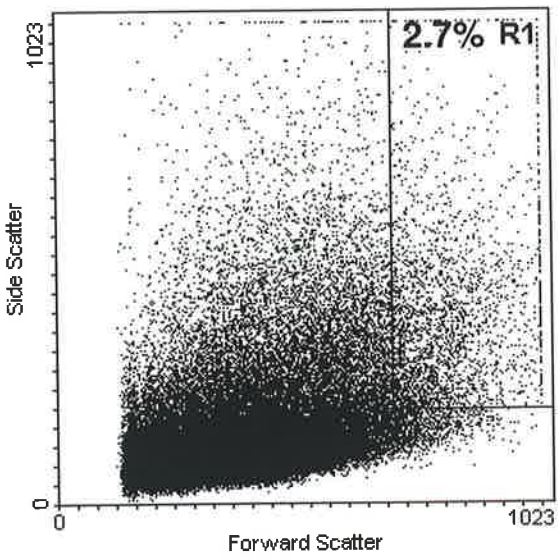
2.7% R1
1023
Side Scatter
0
0
1023
Forward Scatter

B

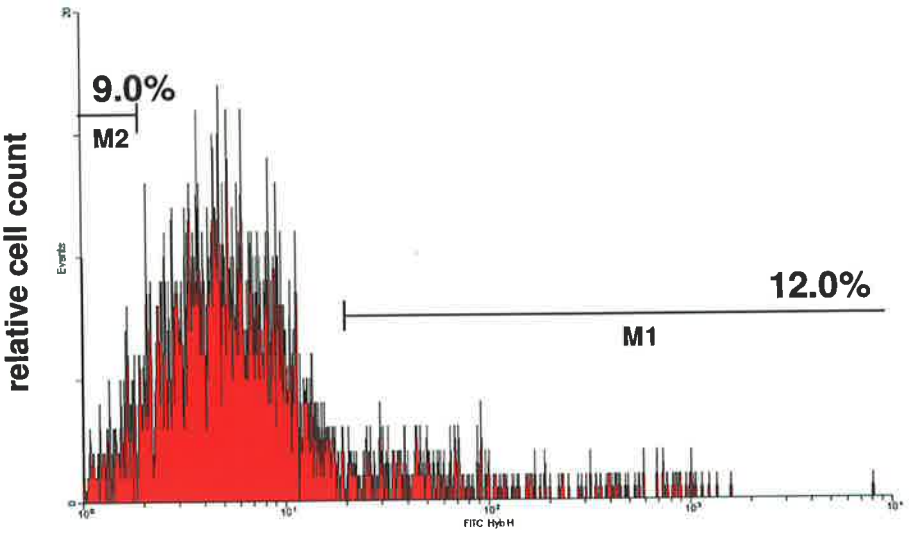
9.0%
M2
12.0%
M1
relative cell count
Hybridoma H-FITC

Figure 4.12: Immunoselection of adult sheep BM MNC with the monoclonal antibody Hybridoma I. (A) Representative dot plot demonstrating the heterogenous nature of the BM MNC population based upon forward scatter (cell size) and side scatter (granularity). (B) Frequency histogram representing the immunoreactivity of R1 gated BM MNC with the FITC coupled Hybridoma I, with data presented as the relative cell count (y-axis) versus the fluorescence intensity (log scale). The horizontal bar (region M1) represents the level of fluorescence greater than 99% of the FITC coupled isotype matched control (1A6.12). The horizontal bar denoting M2 region represents the R1 gated cells negative for Hybridoma I. The horizontal bar (region M3) indicates a subpopulation of cells which express the Hybridoma I antigen more intensely than the rest of the positive BM MNC population.

A

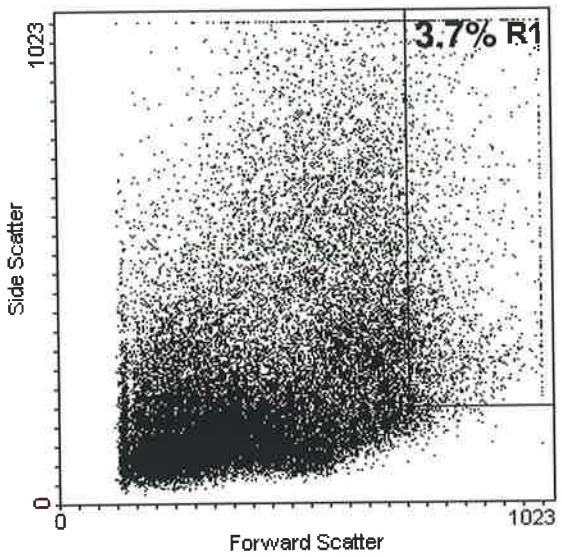
3.7% R1
1023
Side Scatter
0
0
1023
Forward Scatter

B

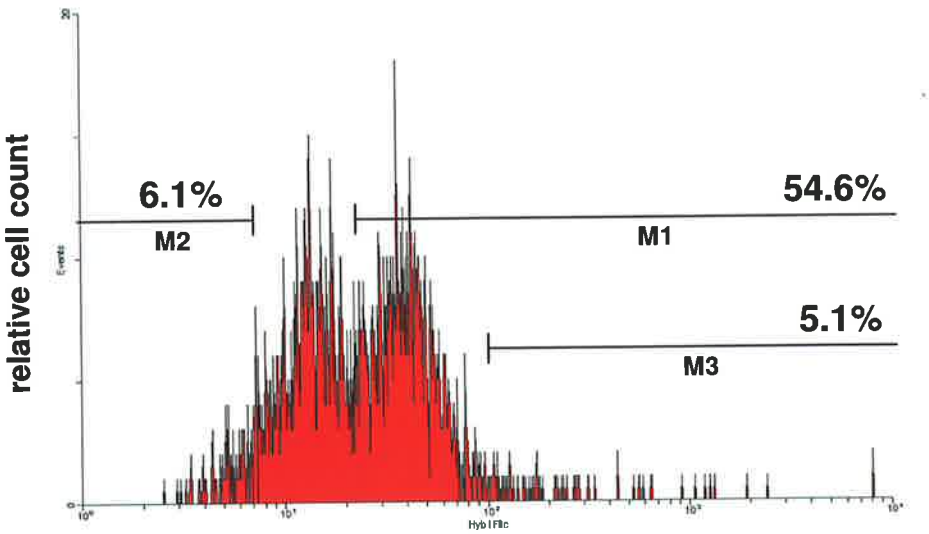
relative cell count
6.1%
M2
54.6%
M1
5.1%
M3
Hybridoma I-FITC

a decreased intensity in fluorescence. Due to the widespread expression of this antigen, cells brightly positive for Hybridoma I were collected as the Hybridoma I^+ population, indicated by the horizontal bar M3, and constituting 5.1% of cells within the R1 region (Figure 4.12B). Cells collected within the M2 bar were considered to be negative for Hybridoma I and made up 6.1% of the cells residing in the R1 region. Under standard CFU-F culture conditions, the Hybridoma I^+ fraction exhibited 294.7 ± 22.7 CFU-F per 1 x 10^5 MNC, yielding a 33.7 fold enrichment of, compared to the unfractionated control sample (Table 4.8). No visible CFU-F were detected by cells derived from the Hybridoma I^- fraction.

Examination of the QE4G9 antibody specifically raised against the sheep VCAM-1 antigen (Dr R. Krishnan, Queen Elizabeth Hospital, Adelaide, Australia) revealed 10.0% positive immunoreactivity in cells found within the R1 region (3.2% of the total cell population) (Figure 4.13A). Cells positive (M1 bar) and negative (M2 bar) for QE4G9 expression were collected and cultured (Figure 4.13B). Whereas $QE4G9^-$ cells did not yield any demonstrable CFU-F, the $QE4G9^+$ subset formed 294.7 ± 22.7 CFU-F per 1 x 10^5 MNC, corresponding to a 28.0 fold enrichment compared to the pre sort population (Table 4.8).

4.2.7. Characterisation of the Hybridoma B and Hybridoma H Antigens.

Since sheep MSC exhibited strong immunoreactivity with some of the uncharacterised hybridomas raised against sheep MSC, it was of particular interest to further studies to elucidate the antigen specifically targeted by these antibodies. The molecular weight of the putative polypeptide recognised by the Hybridoma B monoclonal antibody was determined using protein extracts of cell membranes isolated from single cell suspensions of ovine MSC. Initially, biotinylated preparations of cell membrane proteins were immunoprecipitated using Hybridoma B antibody. Immunoprecipitated samples were subsequently processed by SDS-PAGE gel electrophoresis, transferred onto nitrocellulose, and immunoselected biotin-labelled proteins were detected by western blot using streptavidin-alkaline phosphatase. The Hybridoma B antibody was consistently immunoreactive with a protein exhibiting a molecular weight of approximately 100 kDa (Figure 4.14A). Although occasionally this protein was visualised as two bands, and more commonly one band, the molecular weight of the protein recognised by Hybridoma B was consistent under reduced and non reduced conditions. Moreover, the molecular weight of the immunoreactive protein identified by Hybridoma B was identical between different

Figure 4.13: Immunoselection of adult sheep BM MNC with the monoclonal antibody QE4G9. (A) Representative dot plot demonstrating the heterogenous nature of the BM MNC population based upon forward scatter (cell size) and side scatter (granularity). (B) Frequency histogram representing the immunoreactivity of R1 gated BM MNC with the FITC coupled monoclonal antibody QE4G9, with data presented as the relative cell count (y-axis) versus the fluorescence intensity (log scale). The horizontal bar (region M1) represents the level of fluorescence greater than 99% of the FITC coupled isotype matched control (1B5). The horizontal bar denoting M2 region represents the R1 gated cells negative for QE4G9.

A

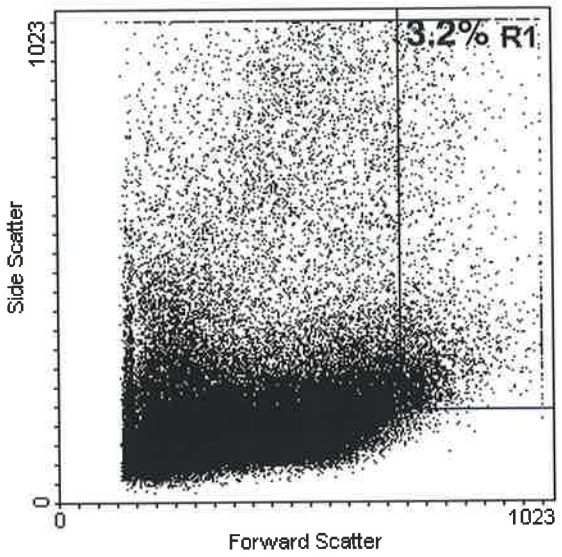
3.2% R1
1023
Side Scatter
0
0
1023
Forward Scatter

B

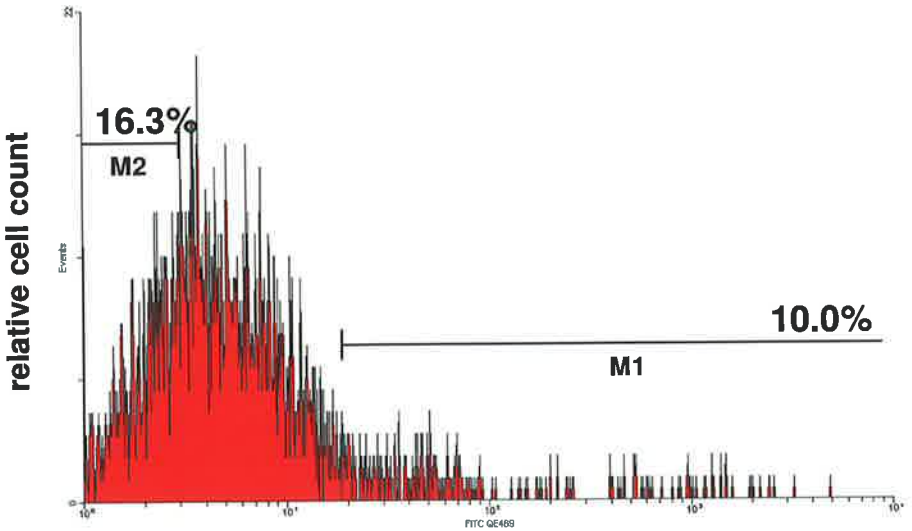
relative cell count
16.3%
M2
10.0%
M1
QE4G9-FITC

Table 4.8. Enrichment of sheep CFU-F by immunoselection with antibodies specifically raised against sheep BM MSC. BM MNC preparations were selected by FACS. Cells positive and negative for each antibody (compared to isotype matched control) were collected and subjected to CFU-F technique for 10-14 days. The data represents the mean number of CFU-F colonies per 10^5 MNC plated ± SEM (n=triplicate cultures), and mean fold enrichment compared to unfractionated control.

Antibody	CFU-F ± SEM per 1 x 10^5 MNC	Fold Enrichment
Unfractionated BM MNC[#]	3.5 ± 1.1	1.0
Hybridoma A^+	94.4 ± 18.9	33.7
Hybridoma A^-	0	0
Hybridoma B^+	62.1 ± 20.7	22.2
Hybridoma B^-	0	0
Hybridoma E^+	103.9 ± 26.0	11.9
Hybridoma E^-	0	0
Hybridoma H^+	153.9 ± 31.8	44.1
Hybridoma H^-	0	0
Hybridoma I^+	294.7 ± 22.7	33.7
Hybridoma I^-	0	0
QE4G9 (ShVCAM-1)$^+$	58.9 ± 11.4	28.0
QE4G9 (ShVCAM-1)$^-$	0	0

[#] n=6 different BM aspirates

Figure 4.14: Immunoprecipitation of cell surface antigens identified by the monoclonal antibodies Hybridoma B and Hybridoma H. (A) Biotinylated cell surface membrane preparations of ovine MSC were immunoprecipitated with magnetic beads using either monoclonal antibody Hybridoma B or Hybridoma H, or an isotype matched control (1B5). Preparations were then separated on duplicate gels by 10% SDS polyacrylamide gel electrophoresis under reduced conditions. One gel was transferred onto a nitrocellulose membrane and detected by incubation with streptavidin-alkaline phosphatase conjugate and ECF substrate solution, followed by visualisation using a Fluorimager. (B) Biotinylated proteins reactive with each monoclonal antibody were alternatively detected using silver stain. (C) Unbiotinylated membrane preparations of ovine MSC were similarly immunoprecipitated, separated by SDS-PAGE electrophoresis and detected by silver staining. The Hybridoma B antibody identified an antigen with a molecular mass of approximately 100 kDa (lane 2 in each gel). The Hybridoma H antibody demonstrated immunoreactivity with an antigen of approximately 90 kDa (lane 3 in each gel). The only bands observed within the isotype matched control correlated with light and heavy chain immunoglobulin.

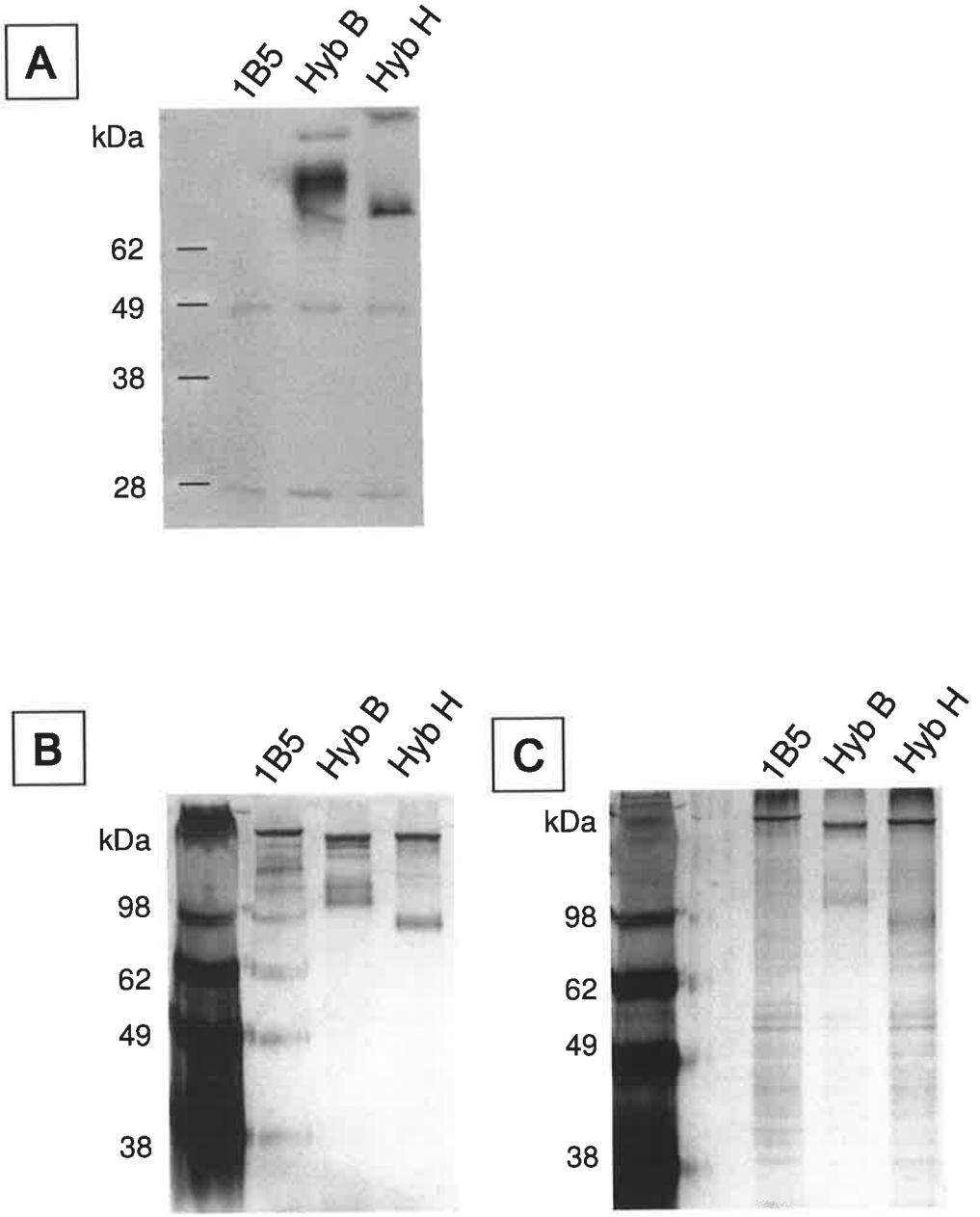
A
1B5
Hyb B
Hyb H
kDa
62
49
38
28
B
1B5
Hyb B
Hyb H
kDa
98
62
49
38
C
1B5
Hyb B
Hyb H
kDa
98
62
49
38

ovine tissues, for example, MSC, cultured chondrocytes, dental pulp stem cells, and cells isolated from the periodontal ligament (in collaboration with Mr K. Mrozik, IMVS, Adelaide, Australia). In order to confirm the identity of the immunoreactive protein, unbiotinylated lysates were prepared and separated by SDS-PAGE gel electrophoresis. A small aliquot of the sample was stained with silver stain to confirm the presence of the desired protein (Figure 4.14B). The majority of the sample was stained with coomassie stain, carefully excised and submitted for analysis by Data Direct Analysis technique mass spectrometry microsequencing (Hanson Institute Protein Core Facility, Adelaide, Australia). The data was analysed with ProteinLynx and the resulting sequence tags were used to probe the SwissProt database. The database search displayed a strong match to integrin beta 1 fibronectin receptor (accession number 1708573) among a number of species, most strongly that of bovine. The bovine protein sequence was used to undertake a BLAST search for ovine homologues and displayed high homology to a fragment of ovine integrin beta 1 (AAK52482). A whole length ovine sequence was not represented in the database. Thus it appears that the Hybridoma B monoclonal antibody recognises an epitope of ovine integrin beta 1, also known as CD29.

Similarly, the relative molecular weight of the putative polypeptide recognised by the Hybridoma H monoclonal antibody was determined. The protein consistently precipitated by the Hybridoma H antibody possessed a molecular weight of approximately 95 kDa (Figure 4.14A). The molecular weight of the putative protein was also consistent under reduced and non reduced conditions, and appeared identical in samples derived from different ovine tissues. Similar procedures were undertaken to confirm the identity of the immunoreactive protein (Figure 4.14B), however repeated attempts to identify the protein recognised by Hybridoma H by microsequencing were unsuccessful.

Unlike most of the hybridomas assessed, Hybridoma H displayed cross reactivity with both human MSC and human osteoblasts. The inability to characterise the epitope recognised by Hybridoma H may in part be due to the scarcity of ovine sequences within most common protein databases. Analysis of the immunoreactive protein derived from human cells may facilitate identification of the protein of interest. Two human cells lines were screened for cross reactivity with the hybridoma panel (Figure 4.15). The osteosarcoma cell lines MG63 and SAOS-2 were assessed by single colour immunofluorescence flow cytometry, and exhibited positive fluorescence to Hybridoma H. Unbiotinylated lysates prepared from MG63 cells were immunoprecipitated with Hybridoma H and similarly

Figure 4.15: Immunoreactivity of sheep specific monoclonal antibodies on MG63 and SAOS-2 stromal cell lines, as assessed by immunofluorescence flow cytometric analysis. (A) Representative dot plot of the cell population distribution based upon forward scatter (cell size) and side scatter (granularity). All subsequent studies using flow cytometric analysis were conducted on 1×10^4 cells residing within the R1 quadrant and collected as listmode data. (B) Representative frequency histograms of the immunoreactivity of MG63 and SAOS-2 cells to monoclonal antibodies Hybridoma A, B, E. H and I, all coupled to FITC. The data is presented as the relative cell count (y-axis) versus the fluorescence intensity (log scale).

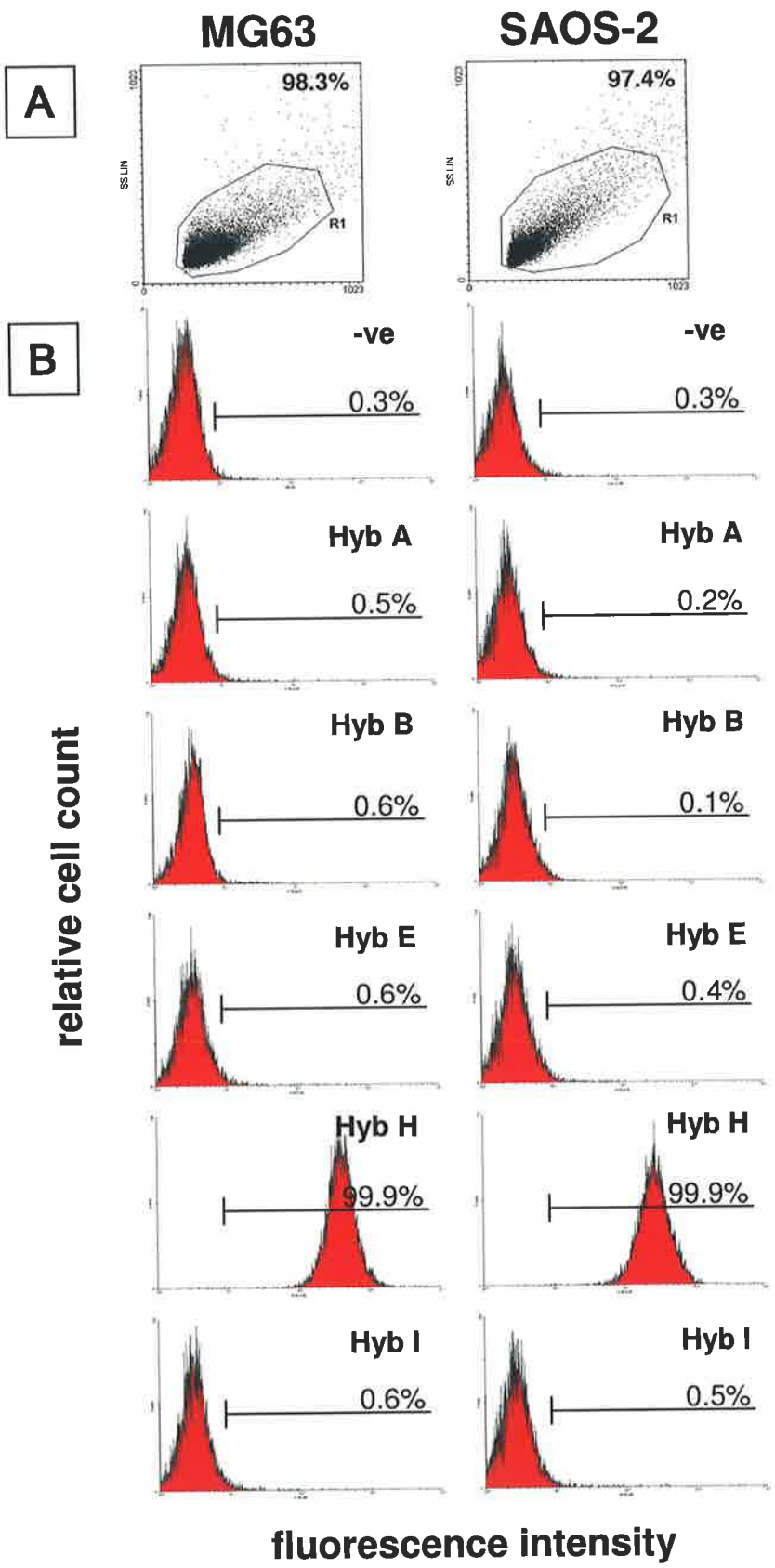
MG63
SAOS-2
A
98.3%
97.4%
SS LIN
R1
B
-ve
0.3%
Hyb A
0.5%
0.2%
Hyb B
0.6%
0.1%
Hyb E
0.6%
0.4%
Hyb H
99.9%
Hyb I
0.6%
0.5%
relative cell count
fluorescence intensity

analysed by MALDI-TOF mass spectrometry (Australian Proteome Analysis Facility Ltd, Sydney, Australia). The resulting sequence was exported to the database search program Mascot (Matrix Science, London UK) and exhibited a high homology with the human heat shock protein 90 beta (HSP-90β). To confirm the epitope identified by Hybridoma H as belonging to HSP-90β, unbiotinylated membrane preparations and whole lysates of MG63 cells were immunoprecipitated with Hybridoma H, separated by SDS-PAGE gel electrophoresis, transferred on to nitrocellulose, and western blotted with an antibody recognising HSP-90 (Figure 4.16). The HSP-90 antibody positively reacted with a single band corresponding to the size of the protein immunoprecipitated by Hybridoma H, with an approximate molecular mass of 95 kDa. Taken together, evidence generated by mass spectrometry and western analysis strongly suggests the Hybridoma H monoclonal antibody recognises an epitope of the HSP-90β cell surface protein.

Figure 4.16: Determination of the cell surface antigen identified by monoclonal antibody Hybridoma H using western blot analysis. Unbiotinylated cell surface membrane preparations of the human MG63 cell line were subjected to immunoprecipitation with Hybridoma H magnetic bead complex. Samples were then separated by 10% SDS polyacrylamide gel electrophoresis and transferred onto a nitrocellulose membrane. Whole MG63 lysate (WL) was included as a positive control. Membranes were subsequently probed with a Heat Shock Protein-90 monoclonal antibody, a secondary IgG antibody conjugated to alkaline phosphatase, visualised by exposure to Vistra ECF substrate and analysed by fluorescence using a Fluorimager. The result demonstrated that the Hybridoma H monoclonal antibody recognises an antigen corresponding to the HSP-90 cell surface protein.

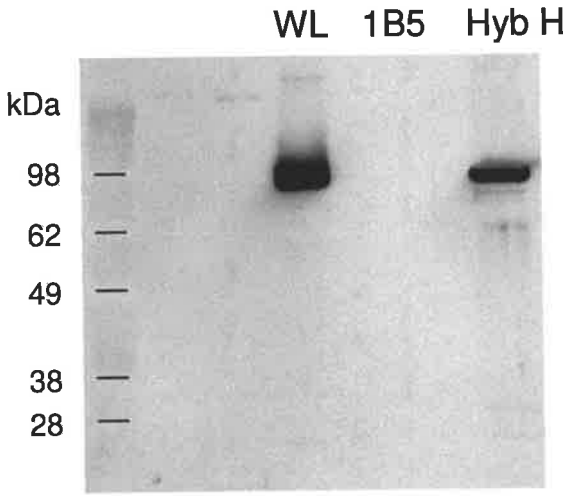
WL
1B5
Hyb H
kDa
98
62
49
38
28

4.3. Discussion

This chapter aimed to identify and characterise the cell surface marker expression of sheep MSC for two major reasons. Firstly, the immunophenotype of ovine bone marrow derived MSC has not been ascertained, and thus similarities and differences between ovine and human MSC has not been defined. Secondly, the identification of cell surface marker characteristic of ovine MSC may augment the immunoselection and enrichment of these progenitor cells from MNC preparations, and present a standardised method of MSC isolation.

The antigenic phenotype of ovine chondrocytes and dedifferentiated chondrocytes has not been reported. Characterisation of the cell surface expression profile of chondrocytes prior to, and following expansion in monolayer, may provide valuable information on modifications that occur during the dedifferentiation process. Furthermore, the similarities and differences between these cells and MSCs, may indicate potential markers of chondrocyte commitment, differentiation, and maturation.

Cultured plastic adherent bone marrow stromal cells constituted a heterogeneous population of fibroblast like cells that were termed MSC. Immunofluorescence analysis using antibodies previously described to identify MSC, and uncharacterised hybridomas raised against sheep MSC, revealed that ovine MSC moderately expressed the monocyte/macrophage associated LPS receptor CD14, and the Hybridoma E antigen. A small subset of cells displayed positive fluorescence to Hybridoma A. The sheep MSC used in this study were generated by plastic adherence and assessed at an early passage, hence the existence of a minor population of $CD14^+$ cells may be attributed to a residual population of contaminating/accessory adherent monocytes/macrophages.

In contrast, sheep MSC exhibited strong positive fluorescence for the adhesion molecules CD44 and CD166, and Hybridoma B, H, and I. Immunoanalysis of human MSC have correspondingly reported positive expression of CD44 and CD166, but interestingly not CD14 (Azizi et al., 1998; Bruder et al., 1998b; Gronthos et al., 2001b; Pittenger et al., 1999). However, the absence of a $CD14^+$ population in these studies may be dependent on the cell passage used for MSC generated by plastic adherent technique, or be attributed to immunoselection upfront to eliminate CD14 positive cells. Although characteristically expressed by human MSC, antibodies against the CD105, CD146, CD90 and STRO-1

(Filshie et al., 1998; Gronthos et al., 2002; Simmons and Torok-Storb, 1991b) molecules did not positively react with sheep MSC. This is most likely to be due to limitations in the cross reactivity of these antibodies between species, and does not exclude the possibility of expression of these molecules by sheep MSC. Moreover, recognition of the epitope by these antibodies may be altered by the glycosylation pattern of the peptide, which may differ between species.

Expression of alkaline phosphatase is inconsistent within human MSC donors and was not detected in sheep MSC. Consistent between human and ovine MSC was the absence of expression of the endothelial associated adhesion marker CD31, and haematopoietic LCA marker CD45 (Gronthos et al., 1994) as confirmed by antibodies that are specific for the equivalent ovine antigens.

The immunophenotype of sheep articular chondrocytes was assessed to define the similarities and differences between the expression of molecules found on chondrocytes and MSC, and to determine any changes to cell surface markers as a result of chondrocyte expansion in vitro. To date, there have been very few studies characterising the expression profile of freshly isolated chondrocytes. Flow cytometric analysis of human articular chondrocytes has reported positive expression CD14, CD68, CD90, CD11a and CD18 antigens (Summers et al., 1995). Immunohistological analysis of integrin expression by human chondrocytes in vivo detected strong levels of the integrin subunits CD39 and CD49e, together forming the fibronectin receptor VLA-5, and low levels of CD49a and CD49c (Salter et al., 1992). Integrin subunits CD18 and CD61 in addition to others analysed were absent.

The current study demonstrated many divergences between the immuno profile of ovine chondrocytes and MSC. Consistent with MSC, articular chondrocytes exhibited ubiquitously positive expression of Hybridoma B and I antigens, but did not react to any extent with antibodies targeting CD105, alkaline phosphatase, CD146, and CD90. As stated earlier this may be attributed to a lack of antigen cross reactivity between species. Sheep chondrocytes were negative for CD45 and Hybridoma A molecules. Interestingly, several antibodies stained a minor subset of cells (1-4%) within the population, including antibodies recognising CD14, CD31, CD166, CD44, Hybridoma E, and Hybridoma H antigens. This is in stark contrast to ovine MSC, which exhibited intermediate expression

of CD14 and Hybridoma E antigen, and extremely high levels of CD166, CD44, Hybridoma H antigen.

Whereas the immunophenotype of articular chondrocytes has been practically uncharacterised, a handful of studies have assayed the cell surface profile of cultured articular chondrocytes. The monolayer culture of chondrocytes is a basic approach for cell expansion, but has been associated with a loss of chondrocyte phenotype and changes in gene expression (Benya and Shaffer, 1982). In this study, the expansion of chondrocytes in monolayer corresponded with moderate increase in the expression of CD14, CD166 and Hybridoma E molecules, and a significant upregulation of CD44, and Hybridoma H, compared to uncultured chondrocytes. Expression of Hybridoma B and I antigens was positive in both cultured and uncultured chondrocytes, however in vitro culture increased the proportion of positively expressing cells by approximately 10%, equivalent to levels observed in MSC cultures. Cultured ovine chondrocytes did not appear to cross react with antibodies identifying human CD105, CD146, alkaline phosphatase antigens, and were negative for expression of CD31, CD45 and Hybridoma A, closely resembling the observations reported for ovine uncultured chondrocytes and ovine MSC.

Comprehensive analysis of the human articular chondrocyte immunoprofile following monolayer culture has demonstrated that these cells positively express integrins CD44, CD106, CD166, and receptor molecules CD105, CD14, and CD90, but lack expression of CD31 and CD45 (de la Fuente et al., 2004; Diaz-Romero et al., 2005), largely consistent with the findings reported here. Elevated expression levels of CD44, CD49 and CD151 are indicative of cells possessing greater chondrogenic capacity, and immunoselection of cultured chondrocytes according to bright levels of CD44 and CD151 markers appears to identify more chondrogenic clones (Grogan et al., 2007). Overall, the cell surface molecule expression profile of cultured ovine chondrocytes bears a particularly close resemblance to cultured ovine MSC, analogous to observations previously reported (de la Fuente et al., 2004). Interestingly, human dedifferentiated chondrocytes were found to exhibit phenotypical similarities to MSC and endothelial cells, and possessed the potential for multilineage differentiation.

Due to the paucity of antibodies specifically reactive with ovine MSC, and the low content of multipotential cells within the bone marrow mononuclear cell population, attempts were made to define the spatial locality of MSC according to their light scatter distribution

pattern. Delineation of MSC within the BM fraction will augment the enrichment and isolation of MSC by immunoselection, and minimise non specific Fc antibody binding. BM MNC preparations were subjected to flow cytometric cell sorting and separated according to size and granularity. The BM MNCs displayed a light scatter distribution pattern that can be loosely classed into three cell subpopulations, the lymphocyte, monocyte and granulocyte fractions. Initially, cells were gated according to each subcategory and collected for analysis. Although the granulocyte fraction constituted the smallest proportion of total cell number, the majority of colony forming cells were found within this group, and enriched for CFU-F three fold compared to the control. Conversely, cells classed as lymphocytes comprised most of the cells within the MNC population but were a poor source of CFU-F. The monocyte population produced a similar number of CFU-F per 1 x 10^5 MNC as the unfractionated control. Therefore, separation of cells according to cell subcategory was not sufficient to exclusively demarcate the CFU-F progenitor cells, as CFU-F were observed in both the granulocyte and monocyte fractions. This may reflect the heterogeneous nature of the total MSC population in vivo, which is thought to represent a continuum of immature through to more committed stromal progenitor cells with slightly different properties and characteristics (Owen, 1988).

In an effort to circumvent this problem, two vertical gates were established to include granulocytes and monocytes of similar size but differing granularity, to the exclusion of lymphocytes. The cells within the R1 and R2 regions constituted a small proportion of the total MNC fraction. Analysis of cells contained within the R1 fraction revealed the presence of CFU-F to be virtually non existent. On the contrary, cells isolated according to the R2 gate consistently produced almost twice the number of colonies than the control. Taken together, these experiments indicate that nearly the entire population of MSC can be exclusively located within the vertical region termed R2, according to phenotypic characteristics. This work is supported by murine (Van Vlasselaer et al., 1994) and human (Shi et al., 2002) studies that demonstrate that MSC have high side and forward light scatter properties relative to haematopoietic stem cells that reside in the lymphocyte/blast window.

To date, there are only a small number of antibodies to specifically target human MSC, and the availability of antibodies for sheep MSC isolation is non existent. A panel of antibodies specifically targeting antigens present on sheep MSC was generated by Dr. A. Zannettino, and screened for immunoreactivity with cultured sheep MSC.

As the spatial locality of CFU-F progenitors within the MNC scatter profile has been established, this knowledge was implemented for the immunoselection of MSC from BM preparations using fluorescence activated cell sorting with members of the anti-sheep MSC hybridoma panel. Analysis with the Hybridoma A antibody revealed this uncharacterised IgM stained 16.4% of MNC within the gated region, corresponding to approximately 0.1% of the total MNC population, and immunoselection of MNC by Hybridoma A resulted in a 33 fold enrichment of CFU-F. No CFU-F colonies were observed by Hybridoma A^- MNC, suggesting MSC indeed express the Hybridoma A antigen. However, culture expanded MSC exhibited around 3% positive fluorescence. Thus it may be possible that the Hybridoma A antigen is expressed by CFU-F producing MNC in vivo, but its expression is diminished upon culture in vitro. Reactivity with Hybridoma A was negligible in chondrocytes and remained unchanged in cultured chondrocytes. Human MSC and osteoblasts were found to be non reactive with Hybridoma A.

The Hybridoma B antibody was almost ubiquitously expressed by 97.4% of MNC within the R1 gated region. As the distribution of Hybridoma B was relatively uniform, cells were discriminated by bright expression of the Hybridoma B antigen, which constituted slightly more than 25% of cells within R1. Immunoselection of Hybridoma B bright MSC led to a 22 fold enrichment of CFU-F progenitors. Hybridoma B dull cells were also collected and failed to form any CFU-F colonies. Analogous to MNC, Hybridoma B antigen was expressed by greater than 90% of expanded MSC, chondrocytes and dedifferentiated chondrocytes, but was not cross reactive with human MSC and osteoblasts. The universal expression of Hybridoma B restricts the application of this antibody for immunoselection of MSC progenitors, but may be a useful antibody in combination with other more exclusively expressed markers.

Immunoselection of MNC preparations with the Hybridoma E antibody revealed expression of the antigen by approximately 13% of the R1 gated population, comprising 0.4% of the total cell pool, with immunoselection resulting in an enrichment of CFU-F colonies by 12 fold. The intermediate level of immunoreactivity in the MNC was recapitulated in culture expanded MSC. Whilst Hybridoma E did not stain freshly isolated chondrocytes, positive antigen expression was observed in culture expanded chondrocytes, to levels comparable to MSC. Cross reactivity was not observed with human derived adherent cell types. Thus the expression pattern of Hybridoma E suggests this antibody

may potentially be of use as a marker to differentiate between MSC and primary or culture induced chondrocytes.

Characterisation of the expression patterns of the IgG Hybridoma H proved this to be both highly useful and interesting. Sheep BM MNC preparations exhibited approximately 12% reactivity by cells located within the R1 gated region, representing 0.3% of the total cell pool. Selection by this marker alone resulted in an enrichment of CFU-F by 44 fold in comparison to the unfractionated MNC population. Interestingly, the antigen on sheep MSC recognised by Hybridoma H was significantly and consistently upregulated upon culture in monolayer to approximately 99% positive fluorescence. Similarly, the immunoreactivity of Hybridoma H on freshly isolated chondrocytes was low, but was rapidly upregulated upon monolayer culture in vitro, to levels comparable to cultured MSC. Moreover, unlike the remainder of hybridomas assessed in this chapter, the Hybridoma H antibody was cross reactive across species, demonstrating high immunoreactivity to the antigen expressed by human MSC and osteoblasts, which corresponds to observations in sheep MSC and cultured chondrocytes. Therefore, it appears that the antigen recognised by Hybridoma H is expressed at low level by cells in vivo, and induced upon monolayer expansion. Furthermore this antibody may be potentially useful for immunoselection of progenitor cells for therapeutic application not only because it can identify a narrow subpopulation of cells within the BM, but possesses cross reactivity between species, which may be a useful tool in translational large animal pre-clinical studies that utilise sheep for different orthopaedic applications.

Selection of ovine BM MNC with the IgM Hybridoma I revealed positive fluorescence by approximately 55% of cells within the R1 gated region. Due to the widespread presence of this antigen, cells immunoselected for analysis were the brightest 5% and constituted only 0.1% of the total cell pool, with immunoselection resulting in an enrichment of CFU-F by 33 fold. Expression of Hybridoma I by cultured MSC exceeded 97%. Over 80% of primary chondrocytes exhibited positive presence of the Hybridoma I antigen, which was upregulated in dedifferentiated chondrocytes to levels observed in expanded MSC. No species cross reactivity was observed between Hybridoma I and human adherent cell types.

The uncharacterised antibodies described here may be potentially useful reagents for the immunoselection of ovine MSC, and may also be beneficial as negative markers of chondrogenic differentiation. The antigenic identity of two of these monoclonal

antibodies, the IgG isotype hybridoma B and H were investigated. Preliminary cell staining data suggested these antibodies identify distinct proteins, based upon differential expression by ovine BM MNC, MSC, and chondrocytes. Immunoprecipitation experiments ascertained that the Hybridoma B antibody identified a protein of approximately 100 kDa under reduced and non reduced conditions, which was consistent between ovine MSC, cultured chondrocytes and dental pulp stem cells. Occasionally, this protein was observed as two bands of similar molecular size, which may be attributed to differences in glycosylation. Mass spectrometry and microsequencing of the band of interest revealed this protein exhibited a high homology to bovine integrin beta 1 fibronectin subunit, also termed CD29. A sheep CD29 homologue was not represented on the protein sequence database. Thus it appears that Hybridoma B recognises an epitope of the ovine cell adhesion molecule CD29. CD29 is a beta subunit member of the integrin family of molecules, which function in various heterodimer pairs as receptors to mediate extracellular matrix and cell-cell adhesion interactions. Integrins and their ligands contribute to cellular processes including proliferation, differentiation, cell survival, motility, and apoptosis (Boudreau and Jones, 1999; Hynes, 1992). The identification of the Hybridoma B antigen as CD29 is consistent with our observations where this antibody detects nearly the entire population of ovine BM MNC, MSC, chondrocytes and cultured chondrocytes. Moreover, human studies have correspondingly detected high levels of CD29 expression by primary and cultured BM MSC (Gronthos et al., 2001b; Majumdar et al., 2003) articular chondrocytes (Loeser et al., 2000; Salter et al., 1992), and dedifferentiated chondrocytes (Goessler et al., 2006).

Immunoprecipitation with the Hybridoma H revealed a protein with a relative molecular weight of approximately 95 kDa. Repeated attempts to microsequence the protein using sheep lysates were unsuccessful, possibly due to the paucity of sheep protein sequences in the majority of protein databases. Interestingly, this antibody was also found to be cross reactive with human MSC and osteoblasts, as well as human osteosarcoma cell lines MG63 and SAOS-2. Furthermore, immunoprecipitation studies followed by mass spectrometry and microsequencing analysis with MG63 cell surface lysates revealed a reactive protein with a high similarity to the human HSP-90β molecule. The identification of Hybridoma H to recognise an epitope of HSP-90β was confirmed by western blot analysis of immunoprecipitated lysates with a commercially available HSP-90 antibody.

HSP-90β is a ubiquitously expressed molecular chaperone isotype of the HSP-90 family, essential for cell viability under all growth conditions not only during times of stress. The most common, versatile and abundant of the heat related proteins, HSP-90 is highly conserved and is involved in the chaperoning of numerous client proteins. Not only important in protein folding, transport and activation, HSP-90 also plays a role in signalling and tumour repression (Schmitt et al., 2007). Furthermore, HSP-90 is important in the stabilisation of integrin linked kinase to facilitate cell adhesion (Aoyagi et al., 2005). HSP-90β is involved in the maturation of protein associated in the growth response to extracellular factors and cancer transformation (Schilb et al., 2004). More recently, evidence has indicated HSP-90 to be important not only intracellularly, but to possess important extracellular functions. Whilst intracellular HSP-90 is indispensable in a cryoprotective function, the extracellular location of transmembrane HSP-90 appears to mediate immunological responses (Eustace and Jay, 2004). The inducible alpha isotype of HSP-90 has been identified on the surface of fibrosarcoma cells and shown to assist the activation of metalloprotease MMP-2, to mediate vascular invasion (Eustace et al., 2004). However in that study, HSP-90β was not detected intracellularly. The presence of extracellular HSP-90β has not been reported in the literature, and detection on the surface of ovine MSC, human MSC and ovine dedifferentiated chondrocytes in the current study represents a unique and interesting discovery. While the function and role of extracellular HSP-90β remains to be established, potential functions may include the mediation of vascularisation during osteogenesis, or cell adhesion.

In summary, the present study has partially characterised the cell surface antigen expression of ovine BM derived MSC. Although the availability of antibodies reactive with sheep MSC is poor, these cells share a similar immunophenotype to human MSC. The comparison between ovine MSC and articular chondrocytes has elucidated some significant and expected differences between the surface marker expression of these cell types. Very little data exists on the antigenic profile of human uncultured articular chondrocytes, probably due to the impediments in isolating large quantities of cells. The current study has not only characterised the profile of freshly isolated chondrocytes from sheep but concurrently assessed changes to cell surface expression following dedifferentiation of chondrocytes following ex vivo expansion. Furthermore, the immunophenotype of cultured chondrocytes mirrors that observed in MSC, an observation previously reported by others. In addition, a panel of uncharacterised monoclonal antibodies were investigated for the potential to enrich CFU-F progenitors by

immunoselection directly from MNC preparations. All five hybridomas analysed exhibited differential immunoreactivity patterns across several cell types, and enriched progenitor cells to varying extents. Moreover, it may be interesting to determine if immunoselection with a particular antibody or antibody combination specifically selects for cells of a predetermined lineage. Lastly, Hybridoma B and H were characterised by immunoprecipitation and peptide microsequencing analysis which were identified as epitopes associated with CD29 and HSP-90β molecules respectively. Of particular interest is the HSP-90β antibody, due to the novel identification of this molecule on the plasma membrane surface, and for its cross reactivity with both human and sheep cells. Overall, the description of cell surface molecules expressed by ovine MSC, chondrocytes, and expanded chondrocytes described here may augment the enrichment and selection of cells specifically required for therapeutic applications.

CHAPTER 5

DEVELOPMENTAL POTENTIAL OF OVINE BONE MARROW MSC IN MICE AND TREATMENT EFFECTS IN THE AUTOLOGOUS REPAIR OF GROWTH PLATE CARTILAGE.

5.1. Introduction

The identification of multipotential progenitor cells with self renewable capacity has stimulated significant interest and promise for the utilisation of these cells in regenerative medicine and tissue engineering. Since the discovery of putative MSC with the ability to form adherent clonogenic clusters (CFU-F) from bone marrow suspensions (Friedenstein et al., 1970), MSC have now been isolated from numerous connective tissues (Xian and Foster, 2006b). In vitro studies have confirmed that MSC from all reported tissues can be directed to differentiate along several defined pathways, including the osteogenic, adipogenic and chondrogenic lineages upon exposure to appropriate stimuli. MSC isolated from some tissues, for example bone marrow, can differentiate into cells beyond those of bone, fat, and cartilage, thus developmental potential may reflect the local environment of the harvest tissue. Furthermore, MSC appear to share similar characteristics across species, which has facilitated the application of MSC in translational studies using animal models. To date, the therapeutic application of bone marrow derived MSC in animal models have included cardiovascular repair (Orlic et al., 2001a; Stamm et al., 2003), spinal fusion (Muschler et al., 2005), segmental bone defects (Petite et al., 2000; Quarto et al., 2001), craniotomy defects (De Kok et al., 2003; Krebsbach et al., 1998), articular cartilage defects (Murphy et al., 2003; Ponticiello et al., 2000; Solchaga et al., 2002; Wakitani et al., 1994), and growth plate injury repair (Chen et al., 2003a; Hui et al., 2005; Li et al., 2004).

The success of regeneration in tissue engineering is often dependent on the selection of an appropriate supporting scaffold or matrix. Delivery of a cellular population requires some sort of vehicle to which the cells and factors can attach, and to provide a structural template to fill the damaged tissue. Ideally the scaffold should be non immunogenic, non toxic, biocompatible and biodegradable, and may be synthetic or naturally derived (Cancedda et al., 2003). Some of the scaffolds currently utilized for bone and cartilage studies are hydroxyapatite, tricalcium phosphate, collagen, hyaluronic acid matrices, polylactic/polyglycolic acid derivatives, and hydrogels (Luyten et al., 2001; Xian and Foster, 2006b).

The fundamental principle of stem cell therapy proposes that undifferentiated stem cells can be delivered to a site of injury, and under the influence of local signals be directed to cells of the appropriate lineage. These cells will subsequently contribute to repair of the damaged tissue. However, in the circumstance of growth plate injury, evidence demonstrates that it is an inappropriate repair response at the site of injury that leads to the undesirable formation of a bone bridge instead of repaired cartilage, which can impair structure and function and lead to growth abnormalities.

Several growth factors have been identified which mediate chondrogenesis of MSC in vitro and facilitate cartilage formation and regeneration in vivo. Although many growth factors and hormones have been implicated in the regulation of chondrogenesis, growth factors that have been assessed for chondro-inductive ability in chondrogenesis assays and cartilage repair models include TGF-β, BMPs, FGF-2, and IGF-1 (Cook et al., 2003; Fortier et al., 2002a; Fortier et al., 2002b; Fujimoto et al., 1999; Indrawattana et al., 2004; Johnstone et al., 1998; Majumdar et al., 2001; Pittenger et al., 1999; Solchaga et al., 2005). The inclusion of these growth factors for cartilage tissue engineering may augment the cartilage formation process and direct undifferentiated cells to commit to the desired lineage.

Investigation of growth plate injury has employed numerous animal models including rats (Phieffer et al., 2000; Xian et al., 2004), mice (Cundy et al., 1991), rabbits (Chen et al., 2003a; Hui et al., 2005; Li et al., 2004; Osterman, 1972) and sheep (de Pablos et al., 1986; Foster, 1989b; Foster et al., 1990; Johnstone et al., 2002; Peltonen et al., 1984a; Thomas et al., 2005; Wirth et al., 1994). Whilst the use of small animal models for characterisation of the mechanisms of growth plate injury repair has many merits, there are several advantages in the use of sheep (or other large animal models) to investigate potential therapies for the repair of growth plate cartilage. Sheep have a longer period of immaturity (before growth plate closure), a large skeleton that grows sufficiently post injury (to permit observation of deformity), and comparable morphology and histology to humans (de Pablos et al., 1986; Peltonen et al., 1984b). Surgical procedures are more easily and accurately performed in large animal models. Previous studies using small animal models have occasionally failed due to secondary bone fracture following surgery (Sledge and Noble, 1978). Moreover, in the instance of tissue engineering, the size of transplants required is not only more convenient to prepare and transplant, but may resemble the dimensions necessary for human studies.

Our laboratory has undertaken numerous studies employing a sheep model to investigate mechanisms of growth plate injury repair, techniques for the prevention of bone bridge formation, and reversal of skeletal deformity (Foster, 1989a; Foster, 1989b; Foster et al., 1990; Hansen et al., 1990; Johnstone et al., 2002; Thomas et al., 2005; Wirth et al., 1994). Several interpositional materials have been assessed for their potential to impede or prevent bone formation and regenerate the damaged cartilage. These include fat (Foster, 1989a), cultured chondrocytes (Foster et al., 1990; Hansen et al., 1990), cartilage (Wirth et al., 1994), periosteum (Wirth et al., 1994), and a type 1 collagen paste (Johnstone et al., 2002). Briefly, the interposition of fat, chondrocytes and cartilage tissue prevented formation of the bone bridge, but did not stimulate regeneration of the growth plate. Interposition of periosteum and a collagen-1 paste (in conjunction with BMP-7), failed to regenerate the growth plate cartilage, and the defect sites were replaced with bone.

In this study, the in vivo developmental potential of ovine bone marrow MSC has been investigated. More specifically, MSC have been subjected to conditions suitable for the development of ectopic bone in an immunocompromised mouse model. Similarly, but using alternative scaffolds, MSC and cultured chondrocytes were compared and assessed for their capabilities in forming cartilage in vivo. Finally, MSC were harvested from the bone marrow of lambs, and autologous transplantation of these cells into a growth plate injury defect was performed, to examine the potential of these cells to regenerate growth plate cartilage.

5.2. Results

5.2.1. Osteogenic Potential of Ovine BM MSC In Vivo

The technique for determining the osteogenic potential of BM MSC in vivo by subcutaneous transplantation into immunocompromised mice has been described previously (Gronthos et al., 2000; Gronthos et al., 2003; Kuznetsov et al., 1997). Sheep MSC were isolated from bone marrow aspirates by plastic adherence and allowed to grow to confluence. Cells from two donors were subcultured for three to four passages in αMEM-10 media. Single cell suspensions of 2×10^6 undifferentiated cells were harvested and transferred in duplicate to hydroxyapatite/tricalcium phosphate (HA/TCP) ceramic particles, which act as the delivery vehicle for this assay. Implants were subsequently transplanted subcutaneously to the dorsal surface of immunocompromised NOD/SCID mice as described in section 2.6.1, recovered after 8 weeks and subjected to fixation, processing and paraffin embedding. Upon examination, the samples were consistent in that all had formed considerable ectopic bone within the implants (Figure 5.1A). Residual HA/TCP scaffold was also observed within all transplants assessed. Moreover, within one of the transplants, there was an infiltration of cells closely arranged within fat-like tissue, closely resembling bone marrow (Figure 5.1B). Under higher magnification, several cell or tissue types were formed within these transplants, including bone, fat, and fibrous tissue (Figure 5.1C), however the predominant tissue type in all samples was bone. Osteocytes trapped within lacuna of the bone extracellular matrix were also visible (Figure 5.1C).

5.2.2. Chondrogenic Potential of Ovine BM MSC In Vivo

In order to determine the chondrogenic potential of ovine BM MSC in vivo, a pilot study was undertaken to define the appropriate scaffold for chondrogenesis using the subcutaneous xenotransplantation technique. As the range of delivery vehicles previously applied for the chondrogenesis of MSC and chondrocytes in vivo is vast and considerably divergent, two scaffolds were selected for their ability to support chondrogenesis of MSC and chondrocytes based upon previously studies.

Synthetically manufactured from VICRYL (Polyglactin 910) and PDS (Poly-P-Dioxanon), Ethisorb is an absorbable implant used in medical surgery to minimise leaking of cerebrospinal fluid (Figure 5.2A). Polyglactin is a copolymer of polyglycolic and

Figure 5.1: Transplantation of ovine MSC in vivo using hydroxyapatite tricalcium phosphate (HA/TCP) ceramic particles. Bone marrow derived MSC were isolated by plastic adherence and expanded in vitro. In order to determine the osteogenic potential of ovine BM MSC in vivo, cells from 2 donors were subsequently implanted into subcutaneous pockets of 2 different immunocomprimised NOD/SCID mice, using a HA/TCP carrier. Implants were harvested 8 weeks after surgery. Representative micrographs display paraffin embedded cross sections stained with Haematoxylin and Eosin. Ectopic osteogenesis was observed within all implants assessed. (A) Representative example of new bone formation (4x). (B) Another example of the establishment of ectopic bone in vivo (4x). Inside the implant, the accumulation of cells, resembling haematopoiesis within bone marrow, is indicated by a closed arrow. (C) A magnified view of the different tissue types observed within the implants, including bone (B), fibrous tissue (Fi), and fat (F) (10x). Residual HA/TCP scaffold was also present (HA/TCP). Ectopic bone contained osteocytes (open arrow) trapped within the newly deposited bone.

A

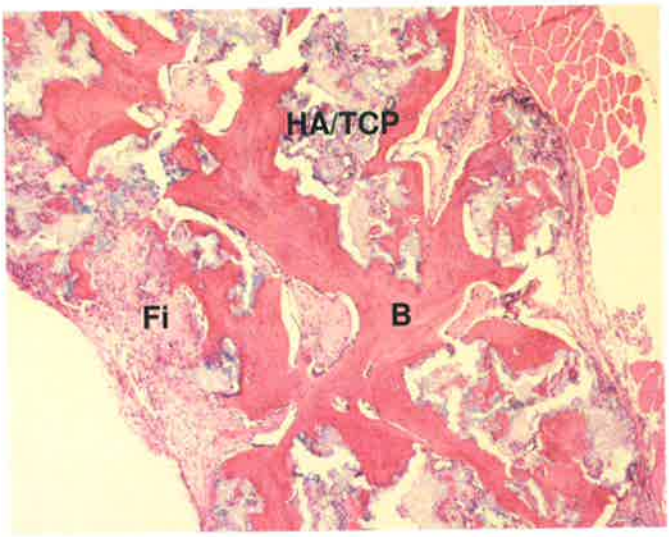

B

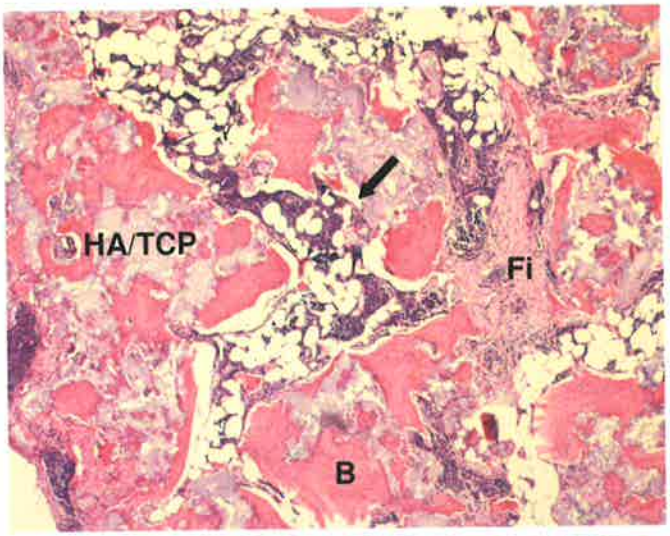

C

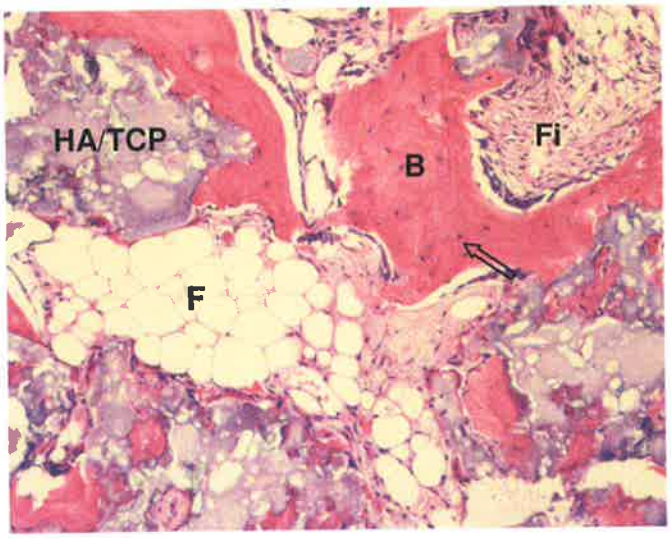

Figure 5.2: Examples of Ethisorb and Gelfoam scaffolds. These two scaffold types were selected for application in determining the chondrogenic potential of ovine BM MSC in vivo. Ethisorb is an inexpensive, flexible, biodegradable implant medically applied as a hemostatic agent in oral and maxillofacial surgery (A). Synthetic in origin, Ethisorb is composed of Vicryl (Polyglactin 910) and undyed PDS (Poly-P-Dioxanon). Ethisorb is relatively flat in comparison to Gelfoam, and under magnification has a fleece like characteristics (B & C). Gelfoam is an inexpensive, absorbent, water soluble, porous, and pliable scaffold derived from purified porcine gelatin, and is traditionally used in medical circumstances as a hemostatic agent (D). On closer examination, the appearance of Gelfoam resembles a sponge (E & F).

A ethisorb

B

C

D gelfoam

E

F

polylactic acids. Under magnification, the morphology of Ethisorb is not unlike a fleece and is relatively flat (Figure 5.2B-C). The VICRYL fleece permits cell or tissue growth, and the scaffold is porous, pliable, non-toxic, biocompatible and absorbed by the body.

Gelfoam is a medical device used clinically due to its haemostatic properties (Figure 5.2D). Prepared from purified porcine skin gelatin, Gelfoam is water insoluble, non elastic, non toxic, porous, pliable, biocompatible and biodegradable. In addition, it can absorb and hold within its interstices many times its weight in fluid. On closer examination, Gelfoam has a randomly organised sponge like appearance (Figure 5.2E-F), and is approximately 7 mm deep when dry.

Bone marrow derived MSC were expanded in monolayer in αMEM-10 media. Upon confluence, cells were harvested and combined with serum free chondrogenic media containing TGF-β1 (10 ng/ml) and sodium hyaluronate (1:1), and 2×10^6 cells were statically seeded in duplicate onto either the Ethisorb or Gelfoam transplantation vehicles. Consolidation of the cells within the scaffold was achieved using fibrin glue. Each cell/scaffold combination was subsequently implanted subcutaneously on the dorsal surface of immunocompromised NOD/SCID mice, and transplants were harvested 6 weeks following surgery. Details of these techniques can be found in section 2.6.1.2.

In order to determine the chondrogenic potential of ovine BM MSC in vivo, chondrogenesis of the MSC was evaluated in subcutaneous pockets of immunocompromised mice with Ethisorb or Gelfoam as scaffold. Upon recovery of transplants at 6 weeks, samples were processed and qualitatively scored for the presence of residual scaffold, cell density, and density of the tissue within the transplant (Table 5.1).

MSCs seeded into the Ethisorb scaffold displayed two predominant morphologies (Figure 5.3A), consisting of elongated fibrous cells and small and large cells with a rounder appearance. The surrounding matrix comprised of dense fibrous tissue. Staining with Alcian Blue revealed the presence of a concentrated proteoglycan matrix (Figure 5.3B). Areas of fibrous tissue displayed positive staining with the cartilage marker Col-2 as detected by immunohistochemistry (Figure 5.3C), with the majority of the transplant strongly expressing the marker of maturing cartilage, Col-10 (Figure 5.3D). Unresorbed scaffold could not be ascertained by visual detection but would most likely still be present, as manufacturer information indicates resorption my take up to 90 days.

Table 5.1. Qualitative description of transplants analysed for in vivo chondrogenic potential. Cells and scaffolds were transplanted into subcutaneous pockets of immunocomprimised mice and harvested after 5 weeks. Transplants were assessed histologically and scored for the presence of residual scaffold, relative population of cells within the transplant, and density of fibrous tissue formed. Each category was graded on a scale from absent (0) to a maximum (+++).

Cell Type	Scaffold	Residual Scaffold	Cell Number	Tissue Density
MSC	Gelfoam	++	+/++	++
MSC	Gelfoam	++	++	++
MSC	Ethisorb	0	++	++/+++
MSC	Ethisorb	0	+++	+++
Cultured Chondrocytes	Gelfoam	+++	+/++	++
Cultured Chondrocytes	Gelfoam	+++	+	+
Cultured Chondrocytes	Ethisorb	0	++	++
Cultured Chondrocytes	Ethisorb	0	++/+++	++/+++

Figure 5.3: Transplantation of ovine MSC in Gelfoam and Ethisorb scaffolds. Ovine BM MSC were generated according to plastic adherence and expanded in vitro. In order to determine the chondrogenic potential of MSC in vivo, cells were transplanted on each scaffold into subcutaneous pockets of immunocomprimised NOD/SCID mice. Implants were harvested 6 weeks post surgery. Representative micrographs show paraffin embedded cross sections stained with Haematoxylin and Eosin (A & E), Alcian blue (B & F), immunohistochemistry with Col-2 antibody (C & G), and Col-10 antibody (D & H). (A) MSC seeded onto Ethisorb transplants displayed heterogenous morphology of rounded cells and elongated cells within fibrous tissue (20x). (B) MSC deposited an extracellular matrix rich in proteoglycan as indicated by positive Alcian Blue staining (40x). (C) Immunohistochemical analysis revealed areas of positive expression of the cartilage specific matrix molecule Col-2 (20x) and (D) very strong expression of the Col-10 molecule (20x), the latter of which is indicative of maturing cartilage. (E) MSC seeded onto the Gelfoam sponge exhibited a relatively consistent morphology of cells with round and slightly spindle appearance and dense deposits of fibrous tissue within the scaffold (40x). (F) Alcian Blue staining revealed distinct regions of proteoglycan deposition within the extracellular matrix fibres (40x). Residual scaffold did not stain with Alcian Blue and is indicated by an arrow. (G) Immunohistochemistry of Gelfoam/MSC constructs with cartilage matrix markers revealed extensive and dynamic positive expression of Col-2 (20x). (H) In contrast to the Ethisorb implant, Col-10 was not detected in the extracellular matrix of MSC/Gelfoam transplant, but was faintly expressed in the nuclei of these cells only (20x).

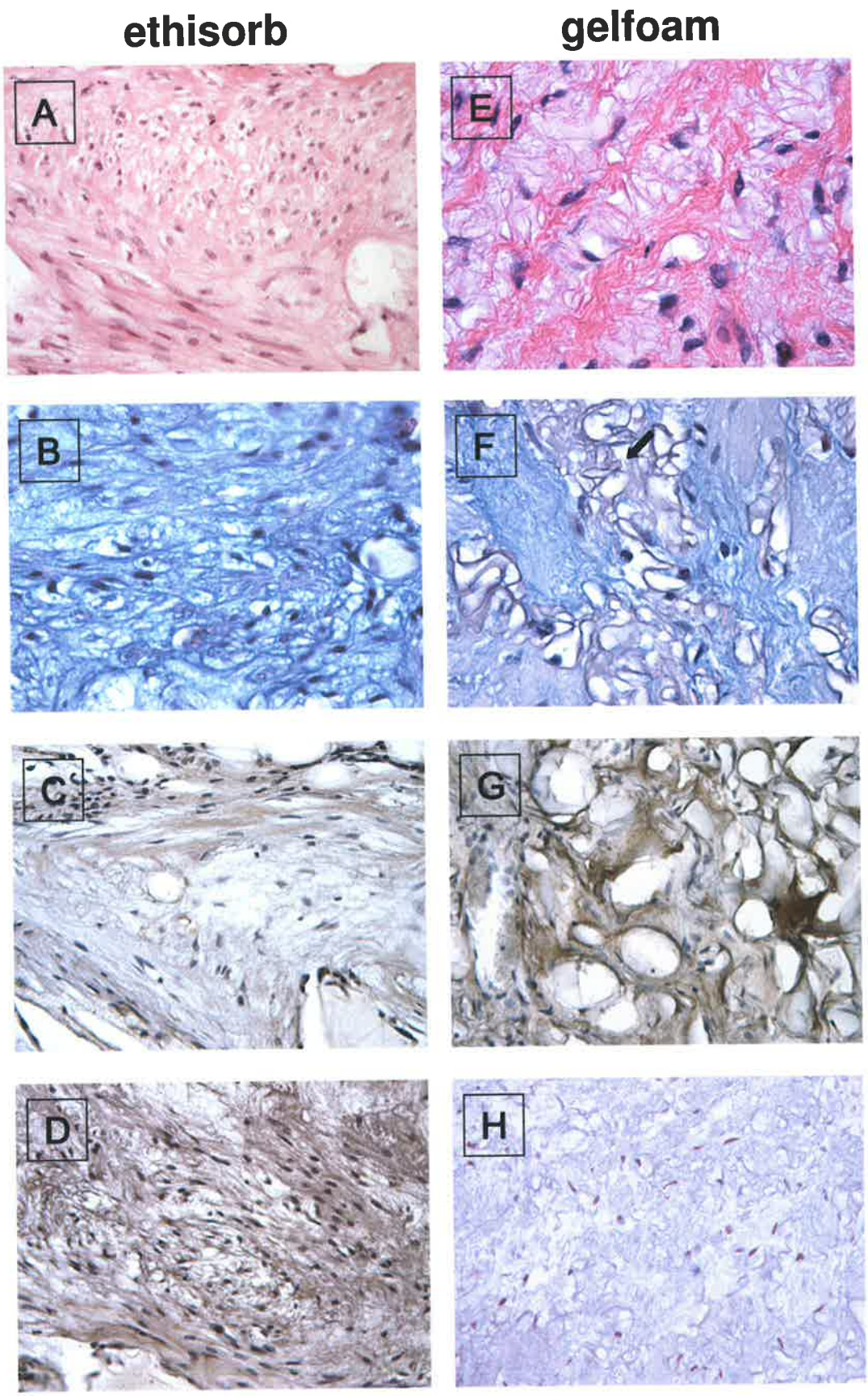
ethisorb
gelfoam
A
E
B
F
C
G
D
H

Examination of Gelfoam transplants seeded with MSC revealed some differences. Cells within the transplants were evenly distributed throughout the scaffold and were uniform in appearance, exhibiting a polygonal morphology (Figure 5.3E). Regions within the implants were rich in proteoglycan as indicated by positive Alcian Blue staining (Figure 5.3F). Residual scaffold was observed in all Gelfoam implants. Immunohistochemical analysis using cartilage matrix molecules Col-2 revealed strong expression throughout the entire implants in a dynamic pattern (Figure 5.3G). In contrast, Col-10 immunoreactivity was only observed faintly in the nuclei of cells, with no detectable staining within the extracellular matrix (Figure 5.3H).

5.2.3. Redifferentiation Potential of Ovine Cultured Chondrocytes In Vivo

Sheep chondrocytes were isolated from scrapings of articular cartilage and liberated from the extracellular matrix by enzymatic digestion. Single cell suspensions were subsequently cultured in monolayer to initiate dedifferentiation of chondrocytic phenotype as described in section 2.1.3.4. Cultured chondrocytes can be redifferentiated with relative ease, but is dependent on arrangement in a three dimensional structure. In this assay of in vivo chondrogenesis, cultured (or dedifferentiated) chondrocytes were included as a control as even dedifferentiated, these cells can be considered to be pre-committed chondrocytes. Thus it was assumed that these cells are more conducive to chondrogenesis than uncommitted MSC.

Concurrently with, and similar to the technique described for transplantation of BM MSC, cultured chondrocytes were harvested and combined with serum free chondrogenic media containing TGF-β1 (10 ng/ml) and sodium hyaluronate (1:1). Cells at 2×10^6 cells per transplant were statically seeded in duplicate onto either the Ethisorb or Gelfoam transplantation scaffold and consolidated using fibrin glue. Transplants were implanted subcutaneously on the dorsal surface of immunocompromised NOD/SCID mice and harvested 6 weeks following surgery as previously described.

In this in vivo chondrogenesis assay using immunocompromised mice, cultured (or dedifferentiated) chondrocytes were included as a control, and it was assumed that these cells constitute pre-determined chondrocytes, which are more conducive to chondrogenesis than uncommitted MSC. Similarly, the resultant samples were processed and qualitatively

scored for the presence of residual scaffold, cell density, and density of the tissue within the transplant (Table 5.1). Cultured chondrocytes seeded onto the Ethisorb scaffold exhibited a fibrous morphology with patches of cells displaying a rounded nucleus within a large cytoplasm, reminiscent of hyaline cartilage (Figure 5.4A). Moreover, as indicated by Alcian Blue, the extracellular matrix contained a high proteoglycan content (Figure 5.4B). Expression of Col-2 was not ubiquitous, with intense staining restricted to regions with distinct chondrocyte-like histology (Figure 5.4C). Immunohistochemical analysis of Col-10 revealed that although many cells were positively stained for this marker, expression was not uniform and was not detected in the extracellular matrix of these transplants (Figure 5.4D).

The cells observed within Gelfoam transplants seeded with cultured chondrocytes were evenly distributed throughout the transplants and exhibited a polygonal morphology (Figure 5.4E). The appearance of cultured chondrocytes in the Gelfoam scaffold is similar to the phenotype of MSC in the same scaffold, suggesting the choice of delivery vehicles may play a role in determining cellular morphology. Dense regions of proteoglycan synthesis were identified, as assessed by Alcian Blue staining (Figure 5.4F). Residual scaffold can be observed and is not reactive with Alcian Blue. Distinct and intense patches of Col-2 deposits were observed throughout the implants, as demonstrated by immunohistochemical staining of Col-2 (Figure 5.4G). Expression of Col-10 was moderately detected in extracellular areas of the implants, but did not stain the cells themselves (Figure 5.4H).

Once each implant was prepared, chondrogenic media was overlayed so as to maximise cell survival and prevent dehydration of the matrix, as described in the methods. Following transplantation, a cell count was performed on the supernatants to determine the loss of cells from the scaffold into the surrounding media. In each case the loss of cells into the supernatant was negligible, ranging from 0 to 3% of the total cell number (data not shown).

5.2.4. Isolation of BM MSC from Lambs for Autologous Transplantation

Bone marrow aspirates were harvested from five 6-8 week old Merino cross lambs by anaesthesia under sterile conditions using a children's size bone marrow biopsy needle. The yield of bone marrow collected from each lamb varied from 11 to 20 ml (Table 5.2).

Figure 5.4: Transplantation of ovine cultured chondrocytes in Ethisorb and Gelfoam scaffolds. Ovine chondrocytes were isolated from articular cartilage by enzymatic digestion, cultured in monolayer and expanded in vitro, leading to dedifferentiation of chondrocyte phenotype. In order to determine the potential of cultured chondrocytes to be redifferentiated in vivo, cells were transplanted on each scaffold into subcutaneous pockets of immunocomprimised NOD/SCID mice. Implants were harvested 6 weeks post surgery. Representative micrographs show paraffin embedded cross sections stained with Haematoxylin and Eosin (A & E), Alcian blue (B & F), immunohistochemistry with Col-2 antibody (C & G), and Col-10 antibody (D & H). (A) Cultured chondrocytes seeded onto Ethisorb transplants displayed a morphology of rounded cells with large cytoplasm, similar to hyaline cartilage (40x). (B) Cultured chondrocytes deposited an extracellular matrix rich in proteoglycan as indicated by positive Alcian Blue staining (40x). (C) Immunohistochemical analysis of the cartilage specific matrix molecule Col-2 revealed temporal patches of strong expression which were closely associated with regions closely resembling cartilage morphology (20x). (D) Col-10 protein was not uniformly expressed by all cells within the transplant, and positive staining was detected only in the nucleus and not the extracellular matrix (20x). The absence of Col-10 staining in this sample is indicated by an open arrow. (E) Cultured chondrocytes seeded onto the Gelfoam sponge exhibited a consistent appearance of cells with round and slightly spindle appearance (40x). (F) Alcian Blue staining revealed dense extracellular matrix deposition rich in proteoglycans (40x). Residual scaffold did not stain with Alcian Blue and is indicated by an arrow. (G) Immunohistochemistry of Gelfoam/cultured chondrocyte constructs with the Col-2 cartilage matrix marker revealed regions of strong expression of Col-2 (20x), and (H) light areas of Col-10 positive expression in the extracellular matrix and not cell nuclei (20x).

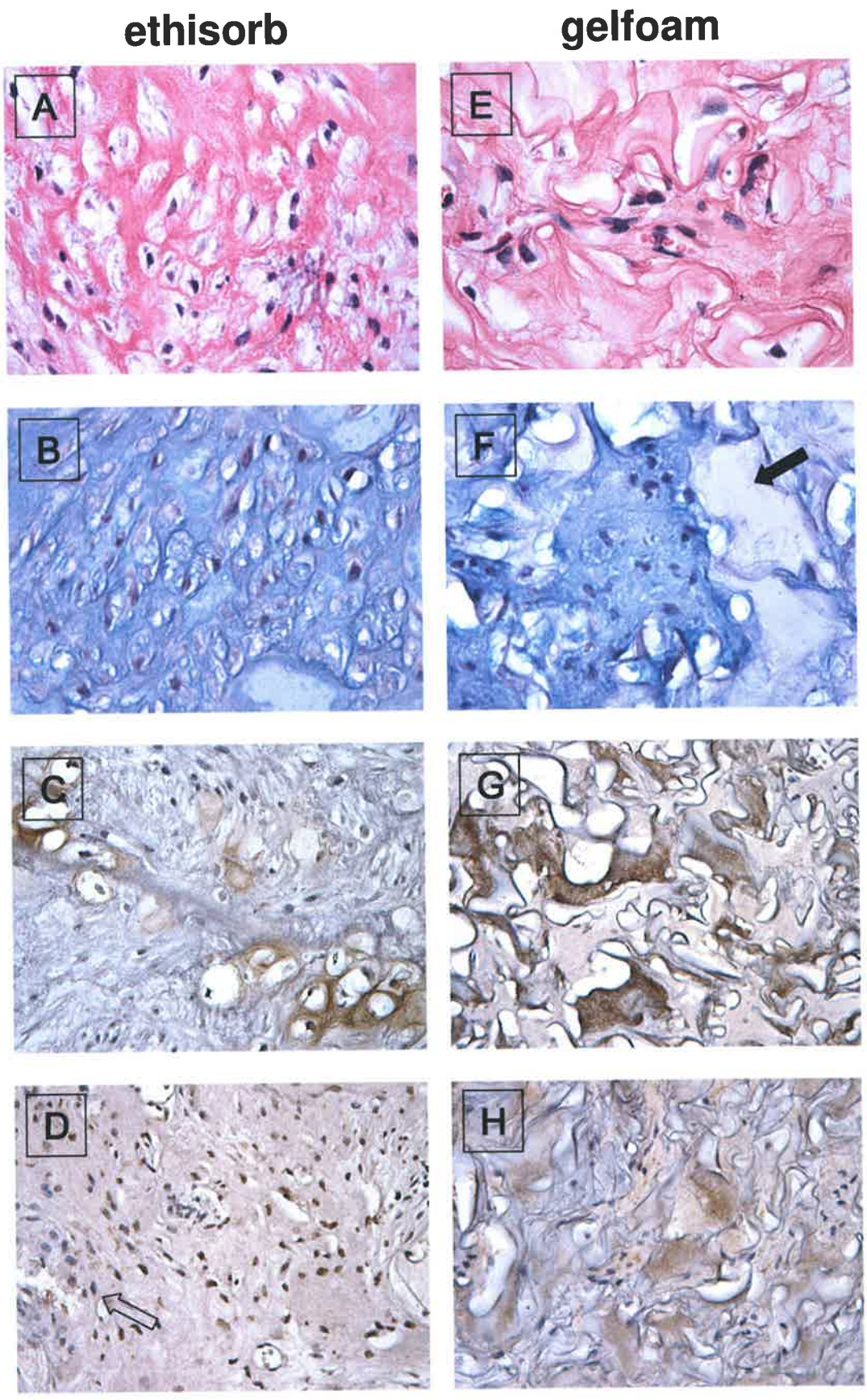
ethisorb
gelfoam
A
E
B
F
C
G
D
H

Table 5.2. Collection and isolation of MNCs from the bone marrow aspirates of 5 lambs. The ensuing table provides information pertaining to the volume, MNC number prior to and following density gradient centrifugation, and overall yield from bone marrow aspirates.

Lamb Number	Bone Marrow Volume (ml)	MNC Number Pre Processing (per 10^7 cells)	MNC Number Post Processing (per 10^7 cells)	Yield (%)
1	18	6.52	1.05	16.1
2	15	8.94	1.53	17.1
3	11	7.92	9.63	12.2
4	15	4.94	1.01	20.4
5	20	4.81	1.04	21.6

Samples were transferred to a previously heparinised tube to prevent clotting of the marrow. Prior to density gradient centrifugation, the number of mononuclear cells was assessed and ranged from 4.8×10^7 to 8.9×10^7 total cells with a mean of $6.6 \pm 0.8 \times 10^7$ SEM. Following centrifugation over the density gradient, a post-processing count of the BM MNC collected at the Percoll interface was performed to determine the viable cell number and percentage yield of MNC. Post-processing counts spanned 1.0×10^7 to 1.5×10^7 total mononuclear cells (mean $1.1 \pm 0.1 \times 10^7$), and the percentage yield fell between 12% and 22% with a mean of 17.5% ± 1.7%.

Lamb MSCs were generated from the BM MNC population by rapid adherence to plastic. Single cell suspensions of BM MNC were plated and cultured in monolayer at approximately $6\text{-}7 \times 10^4$ cells per cm^2 in αMEM-20 media. Following three days, the non adherent cell population was removed, and the adherent cells were rinsed once in HHF and replaced with media. Within one week, some of the cultures were almost confluent. Once confluent, MSC were re-cultured, and upon nearing confluence again, were cryogenically preserved. This was for three reasons, the proliferation of lamb MSC was so rapid, cells would have undergone many passages before being required, secondly as a safeguard should anything happen to these cells (ie contamination), and finally to enable cells to be used in each animal at identical expansion time points.

5.2.5. Creation of a Growth Plate Defect in Lamb Injury Model

The surgical procedure for the ablation of peripheral growth plate in a sheep model was developed by Foster (1989), based upon the original method of growth arrest reported by Phemister (1933) (Foster, 1989a; Phemister, 1933). The tibia on the hind leg of sheep is represented by a single bone and does not possess a fibula (Sissons, 1953). Thus growth occurs from a single bone, and it not complicated by the presence of an adjacent bone (Sisson, 1975). In addition, the foreleg was also not selected for surgery for mobility reasons, due to reliance of the forelimbs in lying down and standing up. Merino cross lambs (8 to 10 weeks old) were placed under general anaesthetic, and a sterile drape of each limb was performed. A medial longitudinal incision of the soft tissues was made and subcutaneous tissue separated to expose the periosteum. The periosteum was peeled back to expose the cortical bone surface and proximal growth plate (Figure 5.5A). Using a high speed dental drill and small dental burr (2 mm), a single partial peripheral growth plate defect was created of approximately 1 cm^2 (Figure 5.5B). During the drilling, the growth

Figure 5.5: Surgical creation of a growth plate defect and transplantation of Gelfoam scaffold. Surgery was performed on each hind leg of 8 week old lambs. (A) A medial longitudinal incision was made over the proximal tibia. The soft tissues and periosteum were divided to expose the growth plate as indicated by an arrow. The growth plate can be visualised as the thin white line running along the bottom of the defect. (B) An approximately 1 cm^2 excision was made to the growth plate (arrow) using a small dental burr. (C) Transplanted Gelfoam scaffold within the growth plate defect (arrow). As the scaffold is absorbent and pliable, it can easily be placed within, and completely fill the injury site. Following implantation, K-wires were placed 20mm apart in the epiphysis and diaphysis, and the periosteum and soft tissues were closed.

A

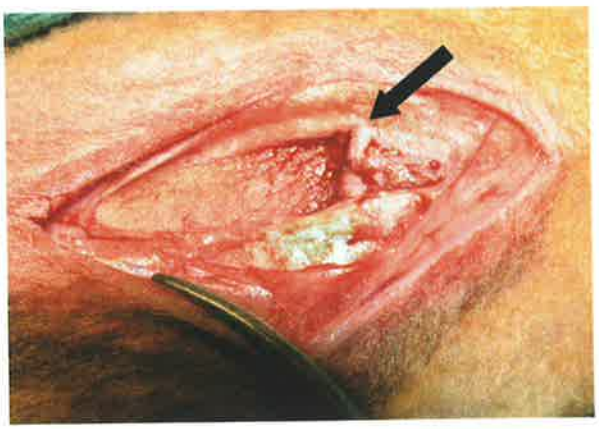

B

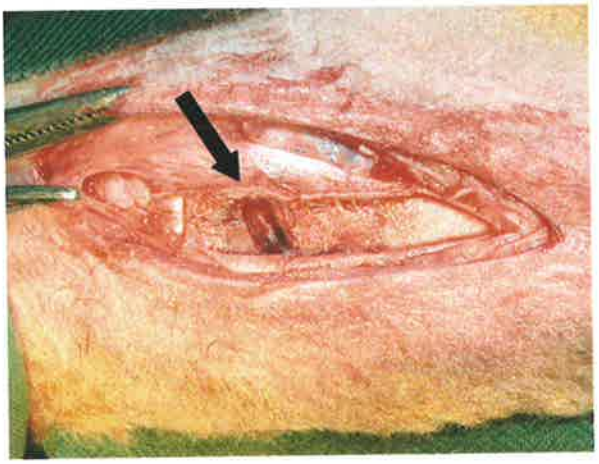

C

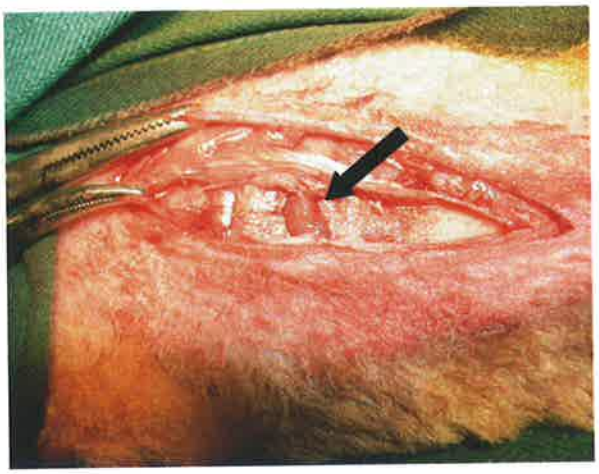

plate was continually irrigated to flush bone fragments and to prevent heat damage to the injury and surrounding areas. In all cases, no other areas of the exposed growth plate of the operative field were removed. In the instance of transplantation with scaffold or scaffold plus autologous MSC, the Gelfoam implant was easily placed and fitted into the defect site, and due to the absorbent and spongy characteristic of the scaffold, was highly compatible with the topography of the defect (Figure 5.5C).

In order to accurately measure the rate of longitudinal bone growth following surgery, Kirschner wires (K-wires) were inserted in the epiphysis and diaphysis adjacent to the growth plate defect at a distance of 20 mm (Figure 5.6A). To ensure parallel and equidistant placement of the K-wires, an F-shaped template was utilised (Figure 5.6B). After insertion of the K-wires, the periosteum was closed, followed by the soft tissues and skin. On recovery from the anaesthesia, lambs were immediately mobile, fully weight bearing, with no visual disturbance to movement or gait. X-rays for each animal were taken following surgery and prior to euthanasia.

Nine lambs were divided into two groups. One group (n=5) received a growth plate defect on both hind legs, with one defect on one limb being filled with Gelfoam scaffold in chondrogenic media containing no cells, and with the other defect on the contralateral limb being delivered with Gelfoam scaffold and 4×10^6 autologous MSC. Following transplantation, a cell count of the media overlaying the implant was performed to determine the loss of cells from the scaffold. In each case, the cells loss was negligible, ranging from 0 to 2% of the total cell number (data not shown). In the second group, while the growth plate defect on one limb was left untreated, the growth plate of the contralateral limb was kept undisturbed although the K-wires were inserted as usual as a measure for monitoring normal bone growth in this growth plate-uninjured limb. Five weeks post surgery, specimens were collected, fixed, decalcified, paraffin embedded, and sections cut from the cental portion of the defect as described in the methods (Section 2.8.1).

5.2.6. Treatment Effects of Autologous BM MSC and Matrix Scaffold Transplantation in Growth Plate Injury Repair Using an Ovine Model

Lambs were weighed immediately before surgery, and prior to euthanasia. The average weight of lambs prior to surgery was 23.9 ± 1.0 kg. At euthanasia, the average weight was 26.7 ± 1.2 kg, thus the average weight gain for all lambs over the 5 week period was 2.8 ±

Figure 5.6: Kirschner wire (K-wire) marker placement as an indicator of bone growth post operatively. (A) Antero-posterial X-ray of a lamb tibia indicating K-wire marker placement. The white arrow indicates the location of the growth plate. Epiphyseal and diaphyseal pins were placed 20 mm apart on the day of surgery using an F shaped template. Upon autopsy, the distance between the pins was measured using callipers to determine the amount of limb growth. (B) Method of pin placement using the F-template, to ensure parallel and equidistant insertion of the K-wires (taken from Foster (1989)).

A

B

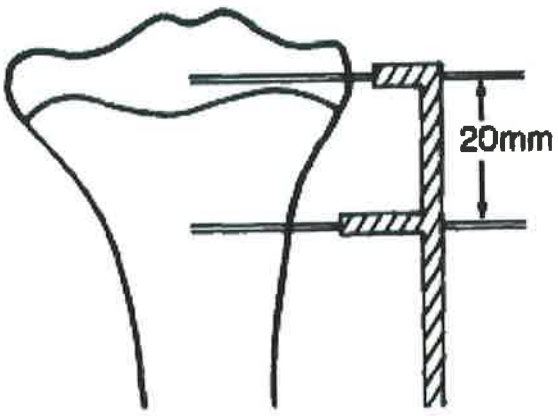

"F" template

0.5 kg (data not shown). To determine if there was any difference in the weight gain between treatment groups, which may influence the rate of bone growth, the average increase in weight over the 5 week period was compared. Group 1 (n=5) exhibited an average weight gain of 3.1 ± 0.8 kg over the course of the experiment, with group 2 (n=4) slightly less at 2.7 ± 0.6 kg (Figure 5.7A). Comparison between the two groups revealed no statistically significant difference ($p>0.05$).

Placement of K-wires either side of the growth plate following surgery facilitated the precise measurement of limb growth following partial growth plate disturbance. Analysis of the growth rate for each group was undertaken to establish whether the small peripheral defect caused arrest or impairment of limb growth, and if any difference in growth rates between the treatment groups was apparent. Limb growth was observed throughout the experiment in all the treatment groups (Figure 5.7B). The mean longitudinal growth of limbs that had an undisturbed growth plate (n=4) was 24.8 ± 0.4 mm by 5 weeks post surgery. A similar growth was observed in the group that received an untreated growth plate defect (24.8 ± 0.5 mm) (n=4). Application of Gelfoam scaffold only to the growth plate defect (n=5) resulted in average limb growth of 24.4 ± 0.5 mm over the course of the experiment. Finally, measurement of limb growth in the group receiving Gelfoam scaffold seeded with autologous MSC revealed mean growth of 24.5 ± 0.3 mm. Therefore, comparison between the different treatment groups at 5 weeks post surgery showed there was no statistically significant difference in the rate of limb growth.

Injured proximal tibia growth plate samples were examined histologically to assess the extent of bone bridge formation and the type of repair tissue formed at the defect site. Examination of the untreated defect revealed contrasting responses following growth plate ablation. Extensive bone formation was observed, both adjacent to the growth plate and throughout the defect site in two of the samples assessed (Figure 5.8A-B). In another sample, the defect area was predominantly comprised of a fat-like tissue, with a medial bony spur adjacent to the growth plate, and regions of trabecular bone originating from the metaphysis and bone plate. The last sample composed of highly cellular fatty tissue resembling bone marrow with the complete absence of a medial bone spur (Figure 5.8H). Samples derived from the limbs with a treated growth plate defect were more consistent. Interposition of Gelfoam scaffold alone to the defect site resulted in repair tissue comprised of dense fibrous tissue, fibrous tissue and fat (Figure 5.8C-D). A medial bone spur was observed in nearly all samples examined, with some trabecular bone deposits

Figure 5.7: Comparison of average weight gain and limb growth between lamb treatment groups. Lambs (n=9) were divided into two groups, each receiving two treatments. One group (n=5) had a growth plate defect created and interpositional scaffold and treated on one limb, whilst the contralateral limb received a growth plate defect and scaffold with MSC. The other group (n=4) received an untreated defect on one limb and the contralateral limb was uninjured. Lamb weight was recorded at the time of surgery and immediately prior to autopsy. (A) Weight gain (kg) is presented at mean weight gain ± SEM at 5 weeks post surgery, showing some variation in weight gain between individuals but no statistical significance between groups. (B) K-wires were inserted proximal and distal to the growth plate at a distance of 20 mm at the time of surgery, and upon autopsy at 5 weeks, the distance between the K-wires was measured using callipers. Total limb growth (mm) is presented as mean limb growth ± SEM, showing no statistically significant differences in the rate of limb growth between groups.

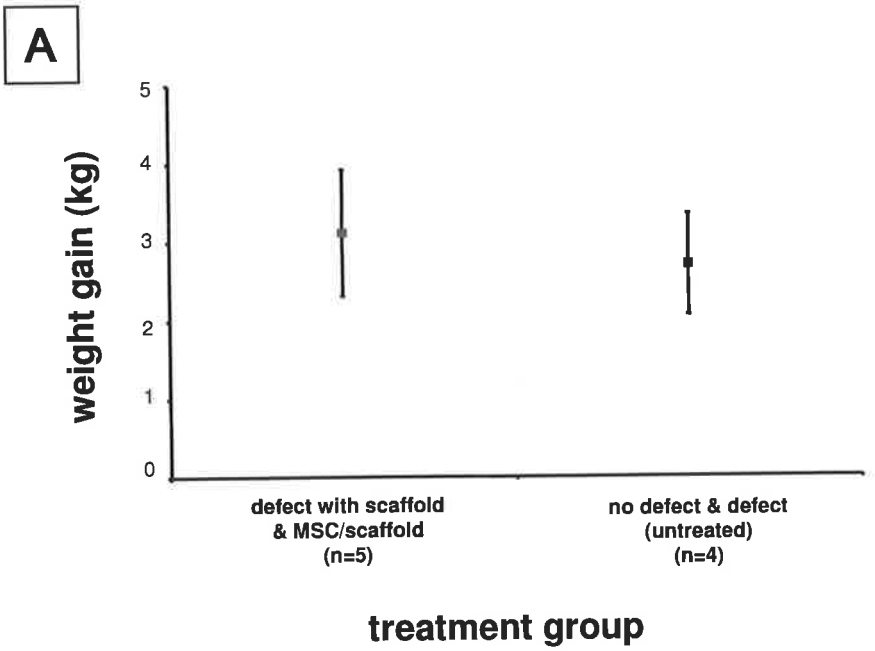
A
weight gain (kg)
5
4
3
2
1
0
defect with scaffold & MSC/scaffold (n=5)
no defect & defect (untreated) (n=4)
treatment group

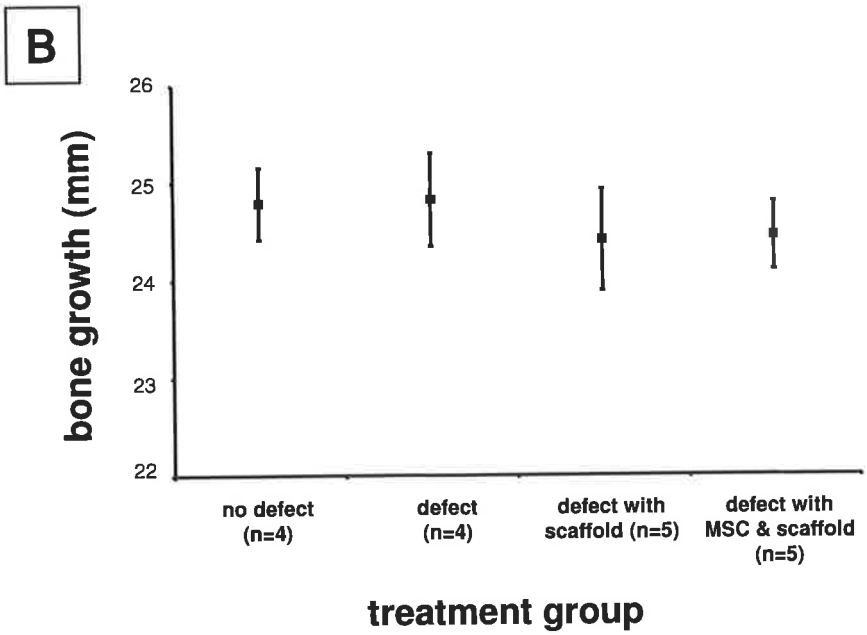
B
bone growth (mm)
26
25
24
23
22
no defect (n=4)
defect (n=4)
defect with scaffold (n=5)
defect with MSC & scaffold (n=5)
treatment group

Figure 5.8: Histological analysis of tissue repair following partial growth plate ablation and treatment with interpositional Gelfoam scaffold or scaffold plus autologous MSC 5 weeks after surgery. Representative photomicrographs of paraffin embedded cross sections stained with Haematoxylin, Eosin, and Alcian Blue (A, C, D, E, G) or Haematoxylin and Eosin (B, F). The location of the growth plate is indicated by *. (A-B) Examples of extensive bone bridge formation in two separate animals within the untreated defect group (2x). Trabecular bone spans the entire defect adjacent to the growth plate - from the bone plate to the metaphysis. (C) A representative example of growth plate defect treated with Gelfoam scaffold only (2x). A medial spur was observed adjacent to the growth plate, with the majority of tissue within the defect site consisting of fibrous tissue and fat. (D) Second example of growth plate defect treated with Gelfoam scaffold only (4x), also showing a medial spur and a small bony island developing from the bony plate and metaphysis, with the central portion of the defect site consisting of fibrous tissue. (E) Representative example of defect treated with Gelfoam scaffold and autologous MSC (2x). Whilst a medial bone spur is apparent, the majority of the defect site consists of dense fibrous tissue and pockets of fat towards the bony plate. (F) A second example of the transplantation of MSC plus Gelfoam into a growth plate defect (4x). Similarly, a medial bone spur is present adjacent to the growth plate, but the ablated growth plate site is comprised of dense fibrous tissue. Residual Gelfoam scaffold is indicated by an arrow. (G) Higher magnification of Gelfoam scaffold that has not been completely resorbed, indicated by an open arrow (10x). (H) Infiltration of blood cells, resembling bone marrow, observed in two samples within the untreated defect group (2x).

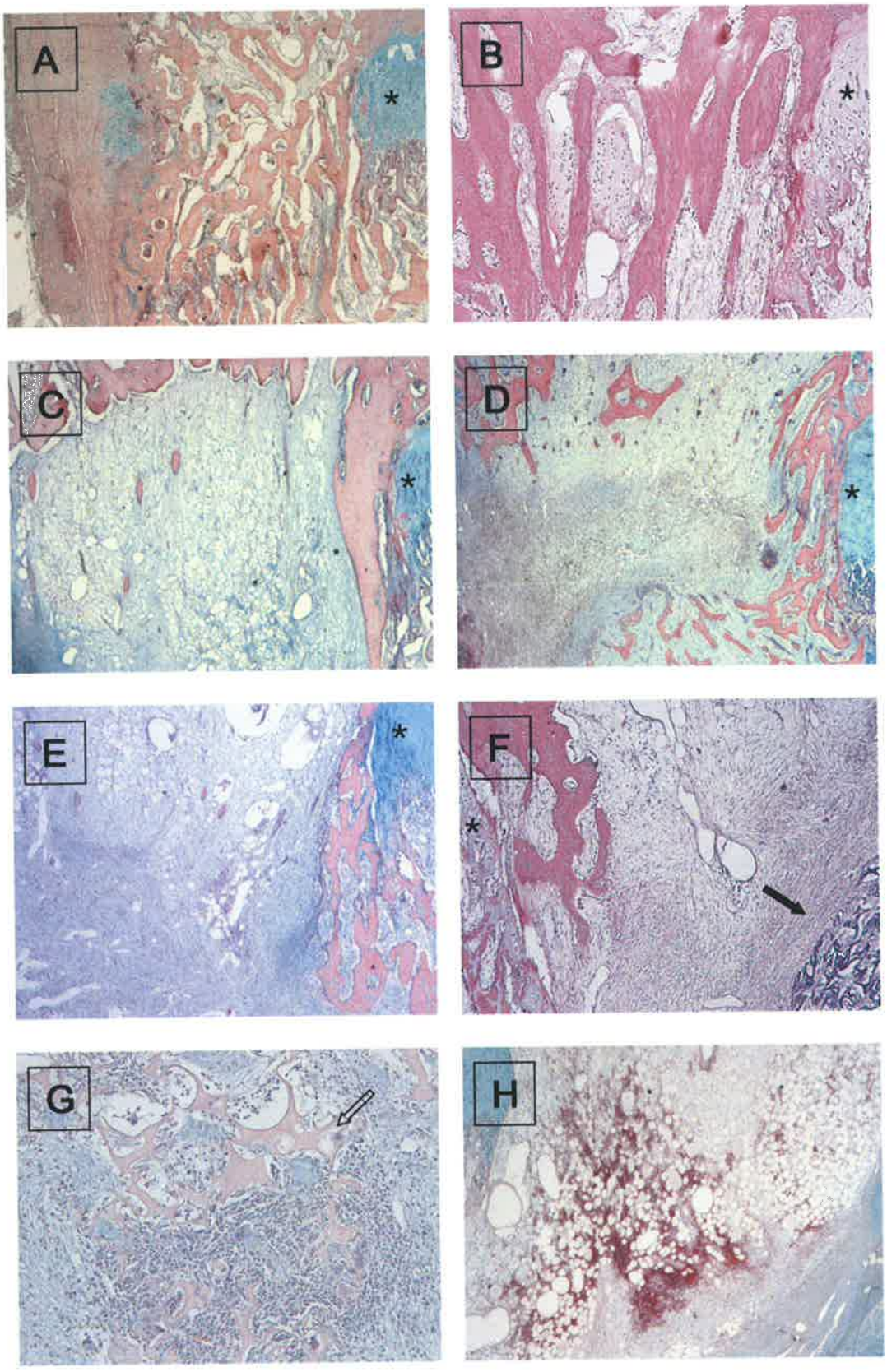
A
B
C
D
E
F
G
H

originating from the metaphysis and bone plate. Nonetheless, the presence of bony deposits within the central portion of defect site was minimal. Histological analysis of the tissue formed within the defect site following transplantation of Gelfoam scaffold loaded with autologous MSC revealed tissue deposits comparable to those in defects treated with scaffold alone (Figure 5.8E-F). Although fibrous tissue, fat, and some bone were also observed, overall the repair tissue was more cellular and extracellular tissue was denser. Almost all samples treated with autologous MSC exhibited a medial bone spur adjacent to the growth plate. Although some bony deposits were identified originating from the periphery (mainly metaphyseal region) of the defect, virtually no bone was detected centrally. Overall, in a small proportion of samples, residual scaffold was detected, surrounded by a large population of cells (Figure 5.8F-G).

So as to more definitively ascertain any differences in the composition of repair tissue following differential treatment of growth plate injury, sections from each sample were analysed using an image analysis software program (Image-Pro PLUS). Tissues within the injury site were categorised into groups according to morphological structure and included bone, dense fibrous tissue, fibrous tissue and fat. An example of the classification of each tissue type is shown in Figure 5.9A. Measurements from each sample were grouped according to tissue type (Figure 5.9B), and are expressed as mean percentage of the total injury area ± SEM.

Quantitative histological analysis show that the predominant tissue observed within the defect site of the untreated group was fat-like tissue (49.4 ± 20.0 % of the total injury area), closely followed by bone (30.0 ± 13.8%). A minor proportion of total defect area comprised of fibrous (18.6 ± 7.0%) and dense fibrous tissue (2.0 ± 2.0%). In contrast, the tissue composition of defects treated with Gelfoam scaffold without cells was, in order, fat (43.1 ± 13.2% of total injury area), dense fibrous tissue (29.0 ± 6.3%), fibrous tissue (20.0 ± 9.2%) and bone (8.3 ± 1.1%). Therefore compared with the untreated control, there was approximately 72% reduction in amount of bone formation when the interpositional Gelfoam scaffold was applied. Moreover, a 14 fold increase in dense fibrous tissue was observed. The quantity of fibrous tissue remained consistent, with fat content decreasing slightly by approximately one tenth. Analysis of growth plate defects treated with Gelfoam scaffold and autologous MSC revealed tissue composition consisting of dense fibrous (38.2 ± 6.1% of the total injury area), fibrous (29.6 ± 10.0%), fat (24.2 ± 6.6%) and bone (7.9 ± 1.8%). In comparison to the untreated control, the proportion of bone

Figure 5.9: Effects of the type of treatment on the repair tissues formed at growth plate injury sites 5 weeks post surgery. (A) Representative micrograph of a paraffin embedded cross section stained with Haematoxylin and Eosin, revealing different tissues observed within defect (4x). In this example the different tissues observed include bone (B), fat (F), fibrous tissue (Fi), and dense fibrous tissue (DF). Using Image Analysis software, the proportions of each tissue type within the defect site was determined for each sample, and is presented at the mean percentage area ± SEM of the total injury area for each treatment group. (B) Measurements grouped by tissue type for comparison between treatments. Statistical significance between the untreated defect and treatment groups is indicated by a * (Mann-Whitney, $p<0.05$).

A

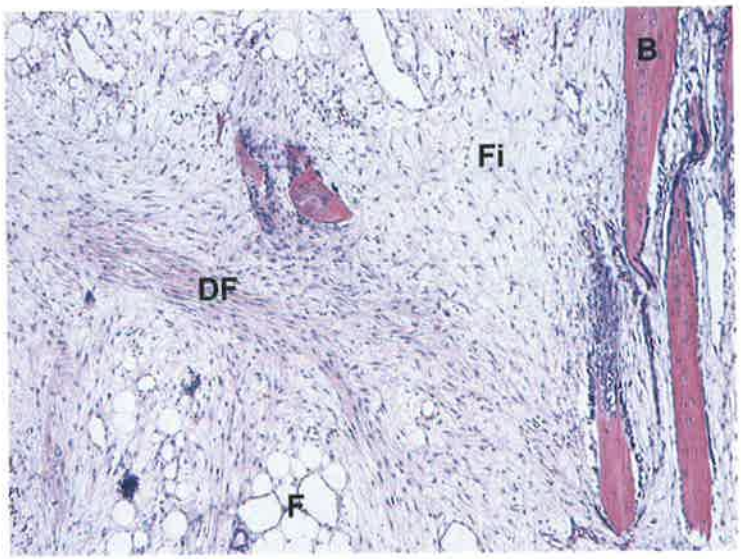
B
Fi
DF
F

B

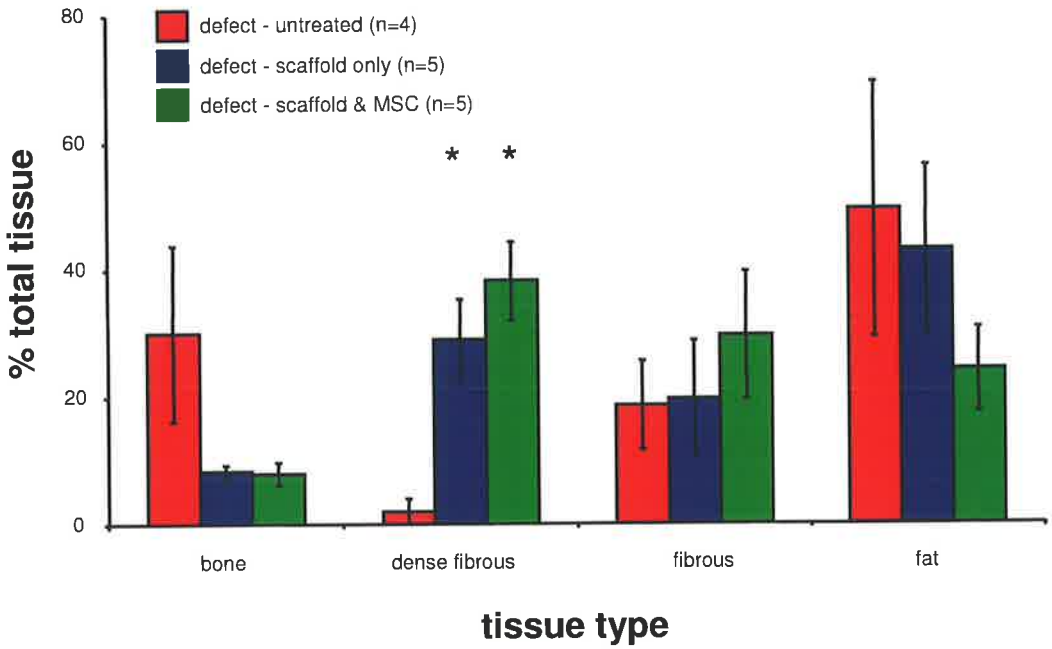
80
60
40
20
0
% total tissue
defect - untreated (n=4)
defect - scaffold only (n=5)
defect - scaffold & MSC (n=5)
*
*
bone
dense fibrous
fibrous
fat
tissue type

formation decreased by approximately three quarters following transplantation of autologous MSC seeded on the Gelfoam scaffold. In addition, a 19 fold increase in dense fibrous tissue was observed. The proportion of fibrous tissue was over one and a half times that of the control group, while conversely, the proportion of fat was halved.

Several differences were observed between treatment with the scaffold alone (interpositional) and the scaffold seeded with autologous BM MSC. Whilst the proportion of bone was equivalent between the two groups, in the group treated with scaffolds seeded with MSC, fibrous tissue was one and a half times greater, and fat content was half that of the scaffold only group. Lastly, the amount of dense fibrous tissue in the scaffold only treatment was three quarters that of scaffold and MSC.

Immunohistochemical analysis of the Col-2 and Col-10 cartilage markers revealed the absence of expression of these molecules within the defect site in all samples assessed (data not shown), suggesting lack of cartilage formation at the injury site 5 weeks after injury.

5.3. Discussion

In the present study, the developmental potential of ovine bone marrow derived MSC in vivo was assessed using a xenotransplant mouse model, and the therapeutic potential of autologous MSC in growth plate cartilage repair was examined in a lamb growth plate injury model.

The appropriate conditions for the differentiation of human MSC towards an osteogenic lineage and formation of ectopic bone in vivo, have been established previously (Gronthos et al., 2000; Gronthos et al., 2003; Kuznetsov et al., 1997). Employing the same technique, ovine MSC were assessed for their potential to form ectopic bone following subcutaneous xenotransplantation into immunocompromised mice using a HA/TCP delivery vehicle. On recovery of the implants at 8 weeks, all transplants had consistently formed extensive deposits of lamellar bone. Although fibrous tissue and fat were also discerned within the implants, the predominant tissue formed was bone. In one sample, the infiltration of haematopoietic cells in close association with adipose elements bore considerable resemblance to bone marrow, suggesting the conditions within the transplant mimicked the bone marrow microenvironment, leading to haematopoiesis. Histological analysis failed to detect any cartilage like tissue in any of the transplants. The observation of ectopic bone, fibrous tissue, haematopoiesis, and absence of cartilage is analogous with studies using HA/TCP seeded with human BM MSC (Gronthos et al., 2000). In this study, the origin of each tissue type is unknown, as ovine MSC were not labelled. However some insights can be gained into the derivation of tissues from analysis using labelled human BM MSC (Gronthos et al., 2000; Gronthos et al., 2003). In these earlier studies, in situ hybridisation using the human *alu* repetitive sequence identified interstitial tissue, osteocytes, and bone lining cells of ectopic bone transplants as human in origin. Conversely, the haematopoietic cells and fat and bone surrounding the transplant were found to be derived from the murine host. Therefore it may be assumed that ovine MSC have the potential to, and contribute to, the formation of ectopic bone following transplantation in vivo.

The inability of ovine BM MSC to form cartilage in vivo using HA/TCP particles as a delivery scaffold is not surprising based upon previous reports coupled with the osteo-conductive nature of HA/TCP. However it does substantiate the notion that selection of a scaffold suitable for and conducive to chondrogenesis is essential for successful cartilage formation in vivo. In this study, two scaffolds were selected to analyse the chondrogenic

developmental potential of ovine BM MSC in vivo, based upon their use in previous chondrogenesis studies. Ethisorb is a synthetic polymer comprised of VICRYL (Polyglactin 910) and PDS (Poly-P-Dioxanon). Polyglactin is a copolymer of polyglycolic acid (PGA) and polylactic acid (PLA) also known as PLGA which has been extensively investigated in cartilage tissue engineering using chondrocytes (Kaps et al., 2006; Park et al., 2004; Rotter et al., 1999; Rudert et al., 2005), cultured chondrocytes (Marijnissen et al., 2002), and MSC (Fan et al., 2006; Uematsu et al., 2005). Ethisorb is inexpensive, pliable, biodegradable and non-toxic, and structurally resembles a non woven fleece. Gelfoam is a haemostatic medial device, naturally derived from purified pork skin gelatin. With a sponge like appearance, Gelfoam has many characteristics advantageous for tissue engineering, such as being porous, pliable, biodegradable, non-toxic, and inexpensive. Moreover, the interstices of Gelfoam are capable of absorbing and holding fluid many times its weight. Gelfoam of gelatin sponges have been applied in studies examining chondrogenesis in vivo and cartilage repair, using both chondrocytes (Chiang et al., 2005; Hoshikawa et al., 2006) and MSC (Ahn et al., 2004; Angele et al., 1999; Ponticiello et al., 2000; Quintavalla et al., 2002).

To assess the chondrogenic potential of ovine MSC in vivo, BM derived MSC were collected and expanded according to plastic adherence. Cells were suspended in serum free chondrogenic media containing chondrogenic growth factor TGF-β1 (10 ng/ml) and sodium hyaluronate, and transplanted subcutaneously into the dorsal surface of immunocompromised NOD/SCID mice using the Ethisorb or Gelfoam scaffold as a carrier. The subcutaneous transplantation technique for ectopic cartilage formation has been applied previously for both scaffolds described (Angele et al., 1999; Kaps et al., 2006; Marijnissen et al., 2002; Park et al., 2004; Rotter et al., 1999). In addition, cultured chondrocytes were also assessed as a partially positive control, representing a population of cells pre-committed along the chondrogenic lineage.

Following retrieval 6 weeks after transplantation, ovine MSC statically seeded onto the Ethisorb scaffold exhibited a fibrous morphology, with deposition of proteoglycans in the extracellular matrix. Immunohistochemical analysis of Col-2 protein expression revealed localisation in regions of the transplants. Interestingly, Col-10 was also detected uniformly throughout the extracellular matrix of the transplants. Although Col-10 is traditionally an indicator of hypertrophic or maturing cartilage, gene expression of Col-10 has been detected in undifferentiated culture expanded MSC (Gronthos et al., 2003). Furthermore,

in a separate study, Col-10 expression has been identified as an early event during chondrogenesis of MSC in vitro (Mwale et al., 2006). Therefore, this observation may indicate maturation of cartilage like tissue akin to endochondral ossification, or may suggest the cells within the implants represent a population of relatively uncommitted fibrous cells. Residual scaffold was not visible in any of the transplants examined, but may not be discernable from the extracellular matrix. Manufacturer information states resorption of Ethisorb is complete within 90 days, however Ethisorb has been reported to degrade within 3 weeks in vitro (Rotter et al., 1998).

Implants with sheep MSC statically seeded onto the Gelfoam scaffold and recovered 6 weeks post transplantation were uniform in appearance, with the cells exhibiting a polygonal morphology. Proteoglycan deposits were apparent within the interstices of the scaffold as indicated by positive staining with Alcian Blue. Immunohistochemical analysis detected extensive deposits of Col-2 protein expression throughout the extracellular matrix in a dynamic pattern. In contrast to the Ethisorb transplants, expression of Col-10 was virtually undetectable. The presence and absence of Col-2 and Col-10 expression respectively, coupled with the deposition of a proteoglycan rich extracellular matrix signifies that MSC seeded onto the Gelfoam scaffold may have undergone chondrogenic differentiation in vivo. However, the morphology of cells within the scaffold does not resemble that of chondrocytes. Previously, comparison of alginate, agarose and gelatin sponge in the in vitro chondrogenesis of adipose derived MSC has revealed that although cells in the gelatin sponge exhibited a polygonal morphology (as observed in this study), there was no hindrance to chondrogenic differentiation (Awad et al., 2004). Significantly, neither bone nor fat was detected in any of the Gelfoam or Ethisorb transplants seeded with ovine BM MSC.

Histological analysis of implants consisting of cultured chondrocytes seeded on the Ethisorb delivery vehicle revealed morphology highly similar to hyaline cartilage. Cells were rounded with large cytoplasm and surrounded by a proteoglycan matrix. Expression of Col-2 was not ubiquitous but localised to extracellular regions of the transplants demonstrating cartilage like morphology. Conversely, immunolocalisation of Col-10 was restricted intracellularly and was not detected in the extracellular matrix. Moreover, Col-10 expression was not detected in all cells within the implants. As only one time point was assessed in this pilot study, it is not possible to gauge whether these cells are upregulating or downregulating Col-10 expression although the cells may be maturing or differentiating

from a less differentiated state. Thus preliminary evidence obtained in this study suggests dedifferentiated chondrocytes can be redifferentiated in vivo upon association with the Ethisorb scaffold, an observation substantiated by the work of Marijnissen (2000), who similarly induced cartilage formation in vivo using passaged chondrocytes seeded on PLGA in a subcutaneous murine transplantation model (Marijnissen et al., 2000). Residual scaffold was not obvious, for reasons aforementioned.

Cultured chondrocytes statically seeded on the Gelfoam scaffold displayed morphology similar to that observed in the MSC/Gelfoam composite. Cells were uniformly polygonal, and had deposited a proteoglycan-rich extracellular matrix. Intense areas of Col-2 staining were observed within extracellular regions of the implants, as indicated by immunohistochemistry with an antibody specific for the Col-2 protein. Col-10 was similarly detected within the implants, however staining was less intense and restricted to the extracellular matrix, with no intracellular expression. As for the transplants seeded with MSC, bone and fat tissues were not observed in Ethisorb and Gelfoam scaffolds loaded with cultured chondrocytes.

Overall, cultured chondrocytes seeded on Ethisorb exhibited a cellular morphology most similar to hyaline chondrocytes. However, the extent of proteoglycan deposition and Col-2 staining was relatively equivalent between both scaffolds and cell types. Examination of implants containing MSC seeded on Ethisorb concurrently revealed strong expression of Col-10, which is considered a marker of maturing cartilage or endochondral ossification. In contrast, expression of Col-10 was virtually undetectable in implants containing MSC seeded on Gelfoam. Although these cells expressed a polygonal morphology that did not resemble native chondrocytes, taken together, the expression of cartilage specific markers was optimal in the combination of MSC and Gelfoam.

There have been very few successful reports of chondrogenesis in vivo using subcutaneous transplantation in immunocompromised mice. Both De Bari (2004) and Pelttari (2006) have confirmed the inability of MSC to form cartilage in vivo using this technique (De Bari et al., 2004; Pelttari et al., 2006). However, these studies transplanted micromass cultures and did not employ a delivery scaffold, which may have contributed to the unsuccessful outcomes. To date, several groups have demonstrated successful in vivo chondrogenesis using this method of transplantation with MSC (Angele et al., 1999; Hwang et al., 2007), and more commonly with chondrocytes (Kaps, 2006; Rotter, 1999;

Park, 2004; Marijnissen, 2002; Jiang, 2003) (Jiang et al., 2003a; Kaps et al., 2006; Marijnissen et al., 2002; Park et al., 2004; Rotter et al., 1999).

Injury or damage to the growth plate of long bones in children can result in limb length discrepancies and angular deformities if left untreated. Current treatments of growth arrest predominantly involve surgical correction of the deformity, and fail to prevent formation of the initial bone bridge. Moreover, surgical intervention does not address regeneration of the growth plate, to impart normal function of this tissue. Since the discovery of multipotential bone marrow progenitor cells potential to differentiate into chondrocytes, considerable interest has been generated in the application of these cells for cartilage tissue engineering. In this study, autologous bone marrow derived MSC were examined for potential repair of growth plate cartilage following injury in a lamb model.

In this study, autologous MSC were isolated from bone marrow using the plastic adherence technique, expanded in culture, and suspended in chondrogenic media supplemented with TGF-β1 (10 ng/ml) and sodium hyaluronate to facilitate differentiation of these cells towards a chondrogenic lineage. Two weeks after isolation 4×10^6 MSC were delivered using a Gelfoam sponge into the site of a growth plate defect in a sheep model. The Gelfoam scaffold was selected for application in the regeneration of growth plate tissue following injury for three distinct reasons. Firstly, transplantation of MSC seeded on Gelfoam sponge in immunocompromised mice exhibited more favourable characteristics akin to cartilage tissue, compared to the Ethisorb scaffold. Secondly, the topography of the Gelfoam sponge renders the scaffold ideal for the dimensions of the growth plate defect to be created. Thirdly, as the Gelfoam scaffold exhibits haemostatic properties, the presence of this scaffold within the defect may impede the infiltration of inflammatory cells early in the fracture repair response, thereby inhibiting the cellular events that facilitate ossification.

In this study, specimens were collected at 5 weeks post surgery since resorption of the Gelfoam scaffold will be nearly complete within 5 weeks, and this is a time period sufficient for establishment of a bone bridge. Examination of growth plate injury in animal models have reported complete bone bridge formation in rats (Garces et al., 1994; Xian et al., 2004), mice (Lee et al., 2000), rabbits (Jaramillo et al., 1990), and dogs (Stadelmaier et al., 1995) 2 to 3 weeks following the surgical procedure. Previous sheep studies have determined an infiltration of inflammatory cells 4 days post surgery, and ossification of the

defect site within 14 days (Johnstone et al., 2002; Thomas et al., 2005; Wirth et al., 1994), comparable to that observed in rats (Xian et al., 2004).

Five weeks following surgery with or without treatment, the limbs of all animals that received a growth plate injury grew to the same extent, regardless of the treatment provided. Furthermore, limb growth was equivalent to the control group where the growth plate remained undisturbed, indicating that the extent of injury created in this model was not sufficient to inhibit longitudinal bone growth within 5 weeks. This observation is not unexpected as the ablated region constitutes a minor proportion of the total growth plate area. It is widely accepted that the size and location of the growth plate injury and subsequent bone bridge formation are directly proportional to extent of growth disturbance (Foster, 1989a; Osterman, 1972), and that small bone bridges cause minimal growth disturbance.

Histological examination of the growth plate defect site five weeks post surgery revealed notable differences between the treatment groups. In the majority of cases, a thin spicule of bone originating from the bony physeal plate was observed at the interface of the defect and the intact growth plate. These thin bone bridges adjacent to the growth plate have been reported previously (Foster, 1989a; Thomas, 2004; Wirth et al., 1994) and do not appear to affect longitudinal bone growth. Some variation was observed in animals receiving the untreated defect. In two samples, complete bone bridge formation was observed, comprising the entire defect site from the physeal bone plate to the metaphysis. The remaining two samples exhibited fat like tissue with some infiltration of bone marrow-like cells from the metaphysis. Interestingly, a peripheral bone spicule was observed in one instance, whereas in the other sample no bone bridge formation adjacent to the growth plate was detected. Inconsistencies in the repair response following ablation of a small region of the growth plate have been documented elsewhere (Foster, 1989a).

The application of Gelfoam scaffold to the growth plate injury served as a mechanism of determining the influence of the scaffold alone as an interpositional material. Analysis of the tissues within the treated defect site revealed a more consistent phenotype than observed for the untreated control. Repair tissue comprised of fibrous and dense fibrous tissue, fat, and bone. The proportion of bone was considerably reduced in samples receiving the scaffold, compared to the untreated defect. Although sizable, the difference was not statistically significant, due to the variation reported in the untreated samples. In

addition, dense fibrous tissue was significantly increased in defects receiving scaffold. The proportion of fat and fibrous tissue was analogous to the untreated group. Interestingly, the delivery of Gelfoam scaffold seeded with autologous MSC presented with tissue repair outcome similar to that with the Gelfoam scaffold treatment only. Five weeks after treatment with Gelfoam and MSC, the proportion of bone within the defect site was markedly reduced, approximately one quarter that of the untreated defect group. Fat like tissue was reduced, concomitant with an increase in fibrous tissue, and a statistically significant increase in dense fibrous tissue. Residual Gelfoam scaffold was observed in some samples, indicating resorption of the delivery vehicle was near completion. The absence of bone marrow-like cells within defects treated with Gelfoam also indicates the scaffold may be functioning as a haemostatic agent, preventing infiltration of non mesenchymal cells.

Preliminary evidence from this study indicates that the delivery of Gelfoam scaffold is sufficient to inhibit bone formation at the growth plate injury site. Moreover, the application of autologous MSC increases the cellular and extracellular density of fibrous tissue within the injury site, and decreases the proportion of fat-like tissue. Most importantly, in this study the application of scaffold with or without MSC did not facilitate or augment bone formation. In contrast, interposition of type I collagen to the site of an excised bone bridge resulted in growth arrest and establishment of a bone bridge within 14 days (Johnstone et al., 2002). Similarly, the interposition of periosteum facilitated the ossification process (Wirth et al., 1994). Unfortunately in this study, tissue reminiscent of hyaline or growth plate cartilage failed to be detected in any defect site. Nonetheless, the reduction of bone content and development of dense fibrous tissue suggest that modification of the chondrogenic stimuli or commitment of MSC in vitro prior to transplantation may improve the likelihood of cartilage tissue formation. In this study it was not possible to gauge the origin of cells within the repair tissue, that is whether the cells constituting the defect site are endogenous or were introduced on the scaffold. It is obvious from the scaffold only group that endogenous cells can migrate and populate the defect site, and that introduction of expanded MSC increases the cellular density of the repair tissue. Thus, labelling of MSC during in vitro expansion may provide supplementary information on the survival and establishment of cells following transplantation. Additionally, it is unknown whether interposition of Gelfoam scaffold with or without cells temporarily delays or permanently prevents establishment of an osseous bridge. Further studies are also required to characterise the tissue constitution of

the injury repair response over a longer time course. Cultured chondrocytes offer another therapeutic option for growth plate restoration, but are limited by the invasive nature of initial autologous chondrocyte harvest.

Successful regeneration of the growth plate cartilage following injury is not widespread, but has been reported following transplantation of chondrocytes (Jin et al., 2006; Lee et al., 1998) and MSC (Chen et al., 2003a; Hui et al., 2005; Li et al., 2004) in a rabbit model of physeal injury. However, the rabbit appears to have a unique predisposition to regenerate cartilage. Whilst prevention of bone bridge formation can be achieved by the insertion of interpositional grafts such as fat (Foster et al., 1990; Foster et al., 2000; Langenskiold, 1975; Langenskiold, 1981), attempts to regenerate growth plate cartilage in other animals has been unsuccessful.

To summarise, in this study, the developmental potential of ovine bone marrow-derived MSC was ascertained using a variety of preliminary studies in vivo. Culture expanded MSC were demonstrated to exhibit osteogenic capability when delivered into immunocompromised mice using a HA/TCP scaffold. Employing a similar transplantation method, ovine MSC were transplanted into mice with an Ethisorb or Gelfoam delivery vehicle to determine the ability of these cells to form ectopic cartilage. Although proteoglycan deposition and Col-2 protein expression were detected in implants using both scaffolds, MSC seeded on the Gelfoam sponge appeared less fibrous and did not express the hypertrophic cartilage marker Col-10. Neither fat nor bone was observed in any of the Ethisorb or Gelfoam transplants. Combined with this observation, the topography of the Gelfoam sponge was ideal for application in a growth plate defect, and so was selected for use in a lamb model of growth plate injury repair. Autologous lamb MSC seeded on the Gelfoam scaffold in the presence of TGF-β1 markedly reduced the presence of bone within the defect site and was accompanied by an increase in dense fibrous tissue. Transplantation of scaffold alone with TGF-β1 also diminished the presence of bony deposits. Significantly, bone formation was not enhanced by the delivery of these treatments. Therefore in conclusion, whilst further studies are crucial, autologous MSC show some promise in the regeneration of growth plate cartilage.

CHAPTER 6
CONCLUSIONS AND FUTURE CONSIDERATIONS

This thesis presents several novel observations of the characteristics and developmental capabilities of ovine bone marrow derived MSC, and their potential application in growth plate cartilage regeneration.

The growth plate is a cartilaginous tissue located at the proximal and distal ends of long bones, which contributes to longitudinal growth until skeletal maturation via the process of endochondral ossification. The incidence of growth plate injury in childhood fractures is reported to range between 15% (Foster, 1989a; Mizuta et al., 1987; Worlock et al., 1986) to 30% (Mann and Rajmaira, 1990). Due to the limited ability of growth plate cartilage to regenerate and repair following trauma, ossification occurs at the site of injury. Depending on the size and location of the fracture and subsequent bone bridge formation, injuries to the growth plate can result in limb length discrepancies and angular deformities. Current therapies for the treatment of growth plate arrest predominately involve surgical correction of the deformity once the outcome of the bone bridge has manifested. In recent years, the discovery of self renewable multipotential progenitor cells with the capacity to differentiate along the chondrogenic lineage has offered an alternative option for cartilage tissue engineering. Using a sheep model, bone marrow derived MSC were isolated and characterised both in vitro and in vivo for eventual application in an attempt to repair growth plate cartilage.

Bone marrow aspirates were collected from adult sheep and found to contain a proportion of CFU-F forming cells with an incidence and morphology highly similar to human MSC (Castro-Malaspina et al., 1980; Friedenstein, 1980; Gronthos et al., 2003; Owen, 1988; Pittenger et al., 1999). Due to the lack of mitogens commercially available specific for sheep cells, a range of human growth factors were assessed for the potential to enhance proliferation of sheep MSC in vitro without the requirement of serum. The expansion of cells in media free of FCS is of importance clinically, due to the risk of transmission of animal borne pathogens. Under serum deprived conditions, supplementation of media with human PDGF, EGF, IGF-1, FGF-2 and particularly TGFα, caused an increase in proliferation of ovine MSC surpassing that achieved by standard culture in 10-20% FCS. The absence of a proliferative response to some other factors such as BMP-7 and TGF-β1 may indicate a potential role of these growth factors in cellular differentiation.

Ovine MSC were induced to differentiate toward an osteogenic, adipogenic, or chondrogenic fate using conditions previously described to differentiate human MSC in vitro (Gimble, 1998; Gronthos et al., 2003; Johnstone et al., 1998). A series of growth factors known to stimulate chondrogenesis of MSC in vitro were assessed. In addition, cultured chondrocytes were included as a control, representing a population of cells with a precommitment to cartilage phenotype, so as to assist determination of the optimal growth factor for chondrogenesis of ovine MSC. Histological and gene expression analysis determined that TGF-β1 alone or in combination with BMP-7 was the most favourable growth factor of MSC chondrogenesis. Ovine cultured chondrocytes were capable of redifferentiation under similar conditions. The demonstrated multipotential capability of ovine MSC may assist translational studies of connective tissue regeneration using sheep models.

Several observations made in this study may warrant further consideration. It is unknown whether mitogenic stimulation of MSC under serum depleted conditions with a specific growth factor affects the multipotential differentiation capacity of MSC. Moreover, the growth factor applied may inherently influence the commitment of MSC along a distinct lineage. This may be beneficial for cartilage tissue engineering studies, where the guidance of undifferentiated MSC to form the desired tissue in vivo is problematic. Thus prior commitment of cells during expansion may be advantageous. Conversely, particular mitogens may enhance osteogenesis and therefore should be avoided. The technique for chondrogenic differentiation of ovine MSC also requires optimisation. This study employed the technique of micromass culture of MSC to induce chondrogenesis as previously described (Gronthos et al., 2003; Johnstone et al., 1998). More recently, it has been reported that the optimal micromass and chondrogenesis is achieved using four times the number of cells compared to the conventional micromass culture (Shirasawa et al., 2006), which may minimise necrosis and histological processing difficulties associated with smaller pellets.

There exists a relative paucity of antibodies by which immunoselection of human MSC from BM is possible, a problem exacerbated in the characterisation of sheep MSC. Nevertheless the cell surface expression profile of ovine BM MNC, MSC, chondrocytes and cultured chondrocytes was analysed. A panel of antibodies specifically generated (by Dr. A Zannettino) against sheep MSC was investigated in conjunction with antibodies reactive with human MSC. High and uniform levels of CD44, CD166, Hyb B, Hyb H and

Hyb I expression were detected on the surface of ovine MSC. Articular chondrocytes uniformly expressed Hyb B and Hyb I, but not CD44 or Hyb H. Interestingly, cultured chondrocytes exhibited a phenotype almost identical to expanded MSC, analogous to previous reports (de la Fuente et al., 2004). Changes in cell surface expression profile of these cells may assist the understanding of cellular mechanisms and changes that occur during monolayer expansion of both MSCs and chondrocytes. The hybridoma H antibody was found to cross react with human MSC and osteoblasts, which is extremely advantageous in therapeutic studies using sheep for eventual application in humans. Immunoselection of MSC directly from processed ovine BM aspirates resulted in enrichment of CFU-F in all instances. To determine the antigenic specificity of two of the uncharacterised antibodies, immunoprecipitation was undertaken. Analysis of the peptide recognised by Hyb B revealed high homology to the integrin beta 1 subunit, CD29. The Hyb H antibody was found to recognise an epitope of HSP-90β molecule. Interestingly, according to the literature, HSP-90β has not been localised to the cell surface previously (Schmitt et al., 2007).

The characteristics and in vitro properties of BM MSC following individual or combinatorial immunoselection with the novel antibodies reactive to sheep MSC, has not been carried out in this study, and would be of particular interest. Investigation of the developmental potential of cells, and comparison between antibodies and unselected cells may prove to be useful in studies where cells of a particular connective tissue lineage are desired. For example, selection with one antibody may result in a population of truly multipotential cells, whereas selection with another antibody may give rise to osteoprogenitor or chondroprogenitor cells. Differences between these cells may not only prove useful in regenerative therapies, but may provide valuable insight on the differences between stem cells and precommitted progenitors.

Preliminary analysis of the in vivo developmental potential of ovine BM MSC was undertaken using the technique of subcutaneous transplantation into immunocompromised mice. MSC demonstrated osteogenic potential upon transplantation with HA/TCP ceramic particles, as indicated by the presence of extensive deposits of bone. In order to investigate the chondrogenic capability of these cells, two scaffolds, synthetic Ethisorb and naturally derived Gelfoam sponge were selected based upon previous studies of in vivo chondrogenesis with MSC and chondrocytes. Ovine MSC seeded on the Gelfoam scaffold displayed phenotypic characteristics of hyaline cartilage as suggested by extracellular

matrix deposits, however the morphology of cells did not resemble chondrocytes. Interestingly, cultured chondrocytes seeded on the same scaffold exhibited a comparable morphology. Therefore the morphology observed may be a consequence of the Gelfoam scaffold applied, and thus the properties of Gelfoam for tissue engineering applications should be investigated further. Of particular note, bone and fat were not observed in either scaffold type when seeded with MSC or cultured chondrocytes. The absence of cartilage in the osteogenesis assay, and bone in the chondrogenesis assay signifies the importance of suitable scaffold selection in the tissue engineering of discrete tissue types. The property of Gelfoam to withhold a high fluid content within its matrices may recapitulate cartilage tissue where the water content can extend to 80% of the wet weight.

Although these results are preliminary, it would be valuable to conduct these experiments on a larger scale at more time points with a range of chondrogenic growth factors, to establish the true potential of Gelfoam, and the subcutaneous method of in vivo chondrogenesis. This may be especially beneficial for application in screening trials demanding a high throughput. The longevity of Gelfoam in vivo may be improved or optimised in combination with matrices or factors that exhibit an extended degradation time such as polyglycolic/polylactic acid copolymers or chitin.

In addition to the favourable characteristics displayed by MSC when seeded on Gelfoam in vivo, Gelfoam scaffold was selected for application in a model of growth plate injury for two reasons. Used clinically as a haemostatic agent, the intrinsic properties of Gelfoam may be beneficial in inhibiting the early inflammatory response that occurs following mechanical disruption of the growth plate, by physically impeding the infiltration of inflammatory cells. Secondly, the topography of Gelfoam renders it ideal for implantation in the defect created here using a lamb model. Using a lamb model, a peripheral defect of the proximal tibial growth plate was created and either left untreated, delivered with Gelfoam scaffold, or delivered with autologous MSC seeded on the Gelfoam scaffold. The extent of disruption to the growth plate was minimal and did not affect longitudinal growth over the course of the experiment. Examination of the tissue repair response following surgery revealed several key differences. Compared to the untreated defect, the interposition of the Gelfoam scaffold markedly reduced the proportion of bone within the defect site, simultaneous with an increase in dense fibrous tissue. The delivery of autologous MSC seeded on Gelfoam similarly diminished the proportion of bone. Taken together these observations suggest Gelfoam is acting as a suitable interpositional graft,

and moreover does not accelerate osteogenesis. The tissue observed following autologous MSC transplantation differed to the scaffold only group in that the repair tissue comprised of more fibrous tissue with increased cellularity and extracellular matrix content. Concurrently, the percentage of fat-like tissue was decreased. Thus it appears the transplantation of MSC does not stimulate bone formation, but increases the proportion and density of fibrous tissue within the repair site. Supplementary experiments following this pilot study may wish to address several key questions that arise. This experiment focussed on an early stage of the repair process, it would be interesting to analyse the tissue composition of the defect site at a later time point(s). Furthermore, it is unknown whether delivery of the Gelfoam scaffold inhibits bone bridge formation within the entire defect temporarily or permanently. Finally the origin of the repair tissue also must be addressed, for example whether the cellular repair constituents are endogenous or were delivered during the transplantation process.

Successful cartilage tissue engineering is dependent on three main objectives, selection of cells with chondrogenic potential that can be expanded in vitro, identification of growth factors to augment the repair process and facilitate chondrogenic differentiation, and finally application of a delivery vehicle conducive to cartilage tissue and well tolerated by the patient (Xian and Foster, 2006b). It would seem there are an unlimited number of potential combinations by which to attempt regeneration of cartilage tissue. Whilst MSC are the most obvious and logical choice, the direction of these cells towards chondrogenesis and formation of stable cartilage in vivo requires investigation. In this study, similarities between MSC and cultured chondrocytes have been established, thus cultured chondrocytes should not be ignored as a potential therapeutic alternative, especially as these cells still maintain commitment to the chondrogenic lineage even when dedifferentiated in monolayer culture. However, there still remains the difficulty and inherent disadvantage of harvesting a cartilage biopsy from an otherwise healthy cartilage source.

The detailed characterisation of sheep MSC is beneficial in translational studies using MSC for eventual therapeutic benefit. In conclusion, ovine MSC have been effectively harvested from bone marrow aspirates and exhibit morphological and multipotential characteristics similar to those observed in human MSC, in vitro and in vivo. The application of MSC to the site of growth plate injury did not result in chondrogenic differentiation or regeneration of the damage cartilage, but formation of dense fibrous

tissue. Nonetheless, bone formation was not accelerated, suggesting that with modification and further investigation, MSC may be a viable therapeutic option for the biological regeneration of the growth plate following injury.

APPENDICIES

Appendix A: Aggrecan Multiple Sequence Alignment

Cow (U76615): 7447 bp
Sheep (AF019758): 393 bp
Human (NM_001135): 4200 bp
Rat (J03485): 6939 bp

The alignment presented here represents a specific region of high homology between several species. The sequence in bold indicates the primers designed for RT-PCR use.

```
                1081       1091       1101       1111       1121       1131
Cow             TTCCCGGCGTGAGAACCTACGGCATCCGGGACACCAACGAAACCTATGACGTGTACTGCT
Sheep           ------------------------------------------------------------
Human           TTCCTGGTGTGAGGACGTATGGCATCCGAGACACCAACGAGACCTATGATGTGTACTGCT
Rat             TCCCTGGAGTGAGGACCTATGGAATCCGAGACACCAACGAGACCTATGATGTGTACTGCT

                1141       1151       1161       1171       1181       1191
Cow             TCGCGGAGGAGATGGAGGGCGAGGTCTTCTATGCAACATCCCCGGAGAAGTTCACCTTCC
Sheep           ------------------------------------------------------------
Human           TCGCCGAGGAGATGGAGGGTGAGGTCTTTTATGCAACATCTCCAGAGAAGTTCACCTTCC
Rat             TCGCTGAAGAGATGGAGGGTGAGGTCTTTTATGCCACATCCCCGGAGAAATTCACCTTCC

                1201       1211       1221       1231       1241       1251
Cow             AAGAGGCAGCCAACGAGTGCCGGCGGCTGGGCGCCCGGCTGGCCACCACGGGCCAACTCT
Sheep           ------------------------------------------------------------
Human           AGGAAGCAGCCAATGAGTGCCGGCGGCTGGGTGCCCGGCTGGCCACCACGGGCCAGCTCT
Rat             AGGAGGCAGCCAACGAGTGCCGGAGGCTGGGGGCACGGTTGGCCACCACAGGCCAGCTCT

                1261       1271       1281       1291       1301       1311
Cow             ACCTGGCCTGGCAGGGTGGCATGGACATGTGCAGCGCCGGCTGGCTGGCTGACCGCAGCG
Sheep           ------------------------------------------------------------
Human           ACCTGGCCTGGCAGGCTGGCATGGACATGTGCAGCGCCGGCTGGCTGGCCGACCGCAGCG
Rat             ACCTTGCCTGGCAGGGCGGTATGGACATGTGCAGCGCTGGCTGGCTGGCGGACCGCAGCG

                1321       1331       1341       1351       1361       1371
Cow             TGCGATACCCCATCTCCAAGGCCCGGCCTAACTGCGGGGGCAACCTCCTGGGAGTGAGGA
Sheep           ------------------------------------------------------------
Human           TGCGCTACCCCATCTCCAAGGCCCGGCCCAACTGCGGTGGCAACCTCCTGGGCGTGAGGA
Rat             TTCGCTACCCCATCTCCAAGGCTCGGCCCAACTGCGGAGGCAACCTCCTGGGTGTAAGGA
                                                                TGGGAGTGAGGA

                1381       1391       1401       1411       1421       1431
Cow             CCGTCTACCTGCACGCCAACCAGACGGGCTACCCTGACCCTTCATCCCGCTATGACGCCA
Sheep           ----------------------------------------CCTTCATCCCGCTATGACGCCA
Human           CCGTCTACGTGCATGCCAACCAGACGGGCTACCCCGACCCCTCATCCCGCTACGACGCCA
Rat             CTGTCTATCTGCACGCCAACCAGACAGGCTACCCTGATCCCTCATCCCGCTACGACGCCA
                CCGTCTAC

                1441       1451       1461       1471       1481       1491
Cow             TCTGCTACACAGGTGAAGACTTTGTGGACATCCCAGAAAGCTTTTTCGGGGTGGGCGGTG
Sheep           TCTGCTACACAGGTGAAGACTTTGTGGACATCCCAGAAAACTTTTTCGGGGTAGGTGGCG
Human           TCTGCTACACAGGTGAAGACTTTGTGGACATCCCAGAAAACTTCTTTGGAGTGGGGGGTG
Rat             TCTGCTACACAGGTGAAGACTTTGTAGACATCCCAGAAAACTTCTTCGGAGTGGGTGGTG

                1501       1511       1521       1531       1541       1551
Cow             AGGAGGACATCACCATCCAGACGGTGACCTGGCCTGACGTGGAGCTGCCCCTGCCCCGAA
Sheep           AGGAAGACATCACCATCCAGACGGTGACCTGGCCTGATGTGGAGCTGCCCCTGCCCCGAA
Human           AGGAGGACATCACCGTCCAGACAGTGACCTGGCCTGACATGGAGCTGCCACTGCCTCGAA
Rat             AAGAGGACATCACCATCCAGACAGTGACCTGGCCAGATCTGGAGCTGCCCCTGCCCCGTA

                1561       1571       1581       1591       1601       1611
Cow             ATATCACTGAGGGTGAAGCCCGAGGCAGCGTGATCCTCACGGCAAAGCCCGACTTTGAAG
Sheep           ATATCACCGAGGGTGAAGCCCGAGGCAACGTGATCCTCACGGCAAAGCCCGACTTTGAAG
Human           ACATCACTGAGGGTGAAGCCCGAGGCAGCGTGATCCTTACCGTAAAGCCCATCTTCGAGG
Rat             ATATTACGGAGGGAGAAGCCCGGGGCAATGTGATCCTCACTGCAAAGCCCATCTTCGACA
```

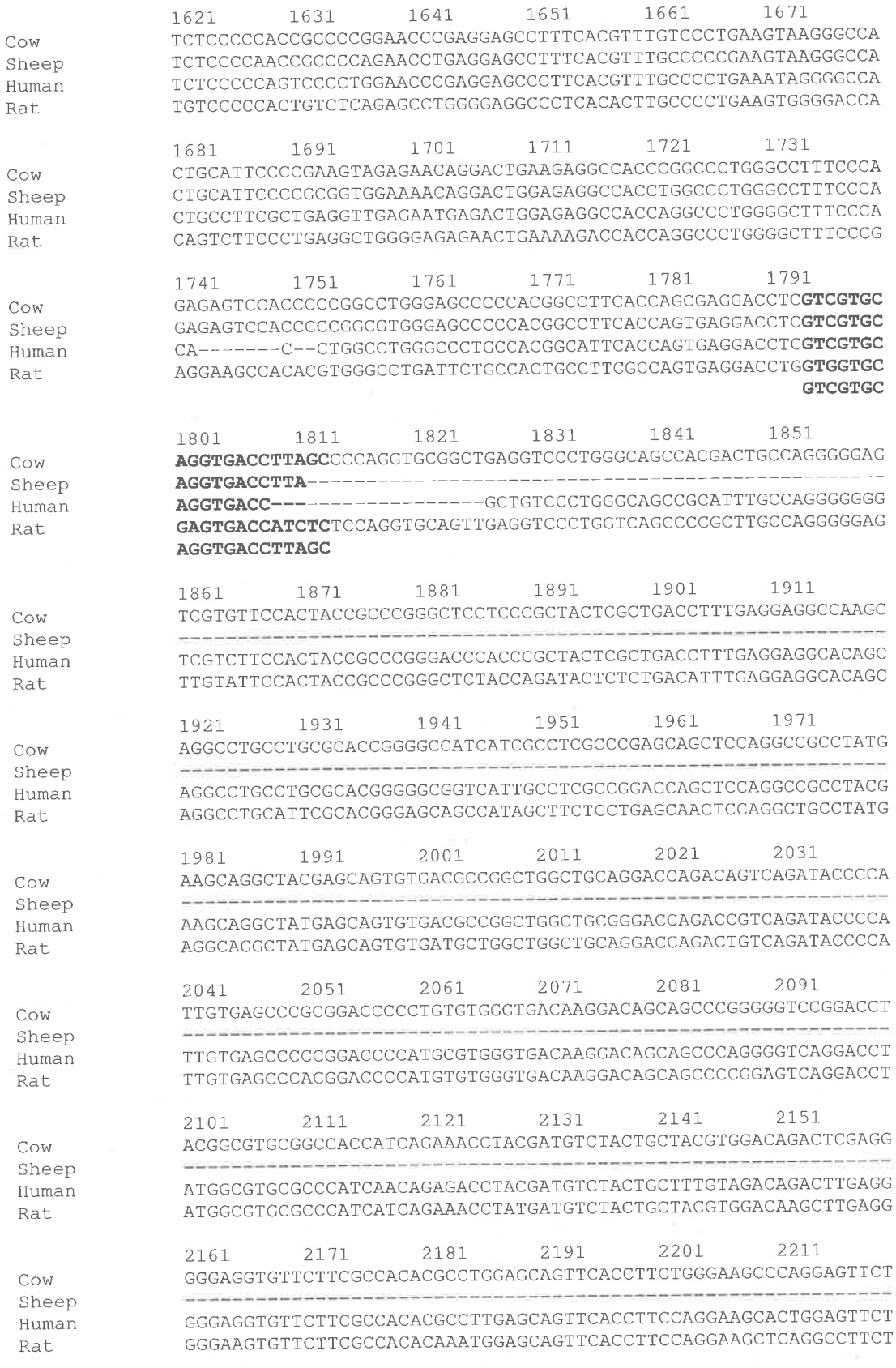
1621 1631 1641 1651 1661 1671
Cow TCTCCCCCACCGCCCCGGAACCCGAGGAGCCTTTCACGTTTGTCCCTGAAGTAAGGGCCA
Sheep TCTCCCCAACCGCCCCAGAACCTGAGGAGCCTTTCACGTTTGCCCCCGAAGTAAGGGCCA
Human TCTCCCCCAGTCCCCTGGAACCCGAGGAGCCCTTCACGTTTGCCCCTGAAATAGGGGCCA
Rat TGTCCCCCACTGTCTCAGAGCCTGGGGAGGCCCTCACACTTGCCCCTGAAGTGGGGACCA
1681 1691 1701 1711 1721 1731
Cow CTGCATTCCCCGAAGTAGAGAACAGGACTGAAGAGGCCACCCGGCCCTGGGCCTTTCCCA
Sheep CTGCATTCCCCGCGGTGGAAAACAGGACTGGAGAGGCCACCTGGCCCTGGGCCTTTCCCA
Human CTGCCTTCGCTGAGGTTGAGAATGAGACTGGAGAGGCCACCAGGCCCTGGGGCTTTCCCA
Rat CAGTCTTCCCTGAGGCTGGGGAGAGAACTGAAAAGACCACCAGGCCCTGGGGCTTTCCCG
1741 1751 1761 1771 1781 1791
Cow GAGAGTCCACCCCCGGCCTGGGAGCCCCCACGGCCTTCACCAGCGAGGACCTCGTCGTGC
Sheep GAGAGTCCACCCCCGGCGTGGGAGCCCCCACGGCCTTCACCAGTGAGGACCTCGTCGTGC
Human CA-------C--CTGGCCTGGGCCCTGCCACGGCATTCACCAGTGAGGACCTCGTCGTGC
Rat AGGAAGCCACACGTGGGCCTGATTCTGCCACTGCCTTCGCCAGTGAGGACCTGGTGGTGC
GTCGTGC
1801 1811 1821 1831 1841 1851
Cow AGGTGACCTTAGCCCCAGGTGCGGCTGAGGTCCCTGGGCAGCCACGACTGCCAGGGGGAG
Sheep AGGTGACCTTA----------
Human AGGTGACC---------- GCTGTCCCTGGGCAGCCGCATTTGCCAGGGGGGG
Rat GAGTGACCATCTCTCCAGGTGCAGTTGAGGTCCCTGGTCAGCCCCGCTTGCCAGGGGGAG
AGGTGACCTTAGC
1861 1871 1881 1891 1901 1911
Cow TCGTGTTCCACTACCGCCCGGGCTCCTCCCGCTACTCGCTGACCTTTGAGGAGGCCAAGC
Sheep ----------
Human TCGTCTTCCACTACCGCCCGGGACCCACCCGCTACTCGCTGACCTTTGAGGAGGCACAGC
Rat TTGTATTCCACTACCGCCCGGGCTCTACCAGATACTCTCTGACATTTGAGGAGGCACAGC
1921 1931 1941 1951 1961 1971
Cow AGGCCTGCCTGCGCACCGGGGCCATCATCGCCTCGCCCGAGCAGCTCCAGGCCGCCTATG
Sheep ----------
Human AGGCCTGCCTGCGCACGGGGGCGGTCATTGCCTCGCCGGAGCAGCTCCAGGCCGCCTACG
Rat AGGCCTGCATTCGCACGGGAGCAGCCATAGCTTCTCCTGAGCAACTCCAGGCTGCCTATG
1981 1991 2001 2011 2021 2031
Cow AAGCAGGCTACGAGCAGTGTGACGCCGGCTGGCTGCAGGACCAGACAGTCAGATACCCCA
Sheep ----------
Human AAGCAGGCTATGAGCAGTGTGACGCCGGCTGGCTGCGGGACCAGACCGTCAGATACCCCA
Rat AGGCAGGCTATGAGCAGTGTGATGCTGGCTGGCTGCAGGACCAGACTGTCAGATACCCCA
2041 2051 2061 2071 2081 2091
Cow TTGTGAGCCCGCGGACCCCCTGTGTGGGTGACAAGGACAGCAGCCCGGGGGTCCGGACCT
Sheep ----------
Human TTGTGAGCCCCCGGACCCCATGCGTGGGTGACAAGGACAGCAGCCCAGGGGTCAGGACCT
Rat TTGTGAGCCCACGGACCCCATGTGTGGGTGACAAGGACAGCAGCCCCGGAGTCAGGACCT
2101 2111 2121 2131 2141 2151
Cow ACGGCGTGCGGCCACCATCAGAAACCTACGATGTCTACTGCTACGTGGACAGACTCGAGG
Sheep ----------
Human ATGGCGTGCGCCCATCAACAGAGACCTACGATGTCTACTGCTTTGTAGACAGACTTGAGG
Rat ATGGCGTGCGCCCATCATCAGAAACCTATGATGTCTACTGCTACGTGGACAAGCTTGAGG
2161 2171 2181 2191 2201 2211
Cow GGGAGGTGTTCTTCGCCACACGCCTGGAGCAGTTCACCTTCTGGGAAGCCCAGGAGTTCT
Sheep ----------
Human GGGAGGTGTTCTTCGCCACACGCCTTGAGCAGTTCACCTTCCAGGAAGCACTGGAGTTCT
Rat GGGAAGTGTTCTTCGCCACACAAATGGAGCAGTTCACCTTCCAGGAAGCTCAGGCCTTCT

Appendix B: Cbfa-1 Multiple Sequence Alignment

Human (NM_004348): 5720 bp
Chicken (AF445419): 1419 bp
Mouse (NM_009820): 5695 bp
Rat (AB025797): 361 bp

The alignment presented here represents a specific region of high homology between several species. The sequence in bold indicates the primers designed for RT-PCR use.

```
                781        791        801        811        821        831
Human           CAACAAGACCCTGCCCGTGGCCTTCAAGGTGGTAGCCCTCGGAGAGGTACCAGATGGGAC
Chicken         CAATAAGACCCTCCCGGTGGCCTTCAAGGTGGTGGCCTTAGGAGAAGTGCCCGATGGGAC
Mouse           CAACAAGACCCTGCCCGTGGCCTTCAAGGTTGTAGCCCTCGGAGAGGTACCAGATGGGAC
Rat             CAACAAGACCCTGCCCGTGGCCTTCAAGGTTGTAGCCCTCGGAGAGGTACCCGATGGGAC

                841        851        861        871        881        891
Human           TGTGGTTACTGTCATGGCGGGTAACGATGAAAATTATTCTGCTGAGCTCCGGAATGCCTC
Chicken         CGTGGTCACCGTGATGGCTGGGAACGACGAGAACTACTCCGCGGAGCTGCGAAATGCTTC
Mouse           TGTGGTTACCGTCATGGCCGGGAATGATGAGAACTACTCCGCCGAGCTCCGAAATGCCTC
Rat             CGTGGTTACCGTCATGGCCGGGAATGATGAGAACTACTCTGCCGAGCTACGAAATGCCTC

                901        911        921        931        941        951
Human           TGCTGTTATGAAAAACCAAGTAGCAAGGTTCAACGATCTGAGATTTGTGGGCCGGAGT**GG**
Chicken         TGCTGTGATGAAGAACCAGGTGGCCAGATTCAATGACCTGCGATTCGTGGGCAGGAGT**GG**
Mouse           CGCTGTTATGAAAAACCAAGTAGCCAGGTTCAACGATCTGAGATTTGTGGGCCGGAGC**GG**
Rat             TGCTGTTATGAAAAACCAAGTGGCCAGGTTCAACGATCTGAGATTTGTAGGCCGGAGC**GG**
                                                                        **GG**

                961        971        981        991        1001       1011
Human           **ACGAGGCAAGAGTTTCAC**CTTGACCATAACCGTCTTCACAAATCCTCCCCAAGTAGCTAC
Chicken         **CAGAGGGAAGAGCTTTAC**TTTGACAATAACTGTCCTGACAAATCCCCCCCCAAGTCGCTAC
Mouse           **ACGAGGCAAGAGTTTCAC**CTTGACCATAACAGTCTTCACAAATCCTCCCCAAGTGGCCAC
Rat             **ACGAGGCAAGAGTTTCAC**TTTGACCATAACGGTCTTCACAAATCCTCCCCAAGTGGCCAC
                **ACGAGGCAAGAGTTTCAC**

                1021       1031       1041       1051       1061       1071
Human           CTATCACAGAGCAATTAAAGTTACAGTAGATGGACCTCGGGAACCCAGAAGGCACAGACA
Chicken         ATACCACAGAGCCATAAAGGTGACGGTGGATGGGCCGAGGGAGCCAAGAAGGCACAGACA
Mouse           TTACCACAGAGCTATTAAAGTGACAGTGGACGGTCCCCGGGAACCAAGAAGGCACAGACA
Rat             TTACCACAGAGCTATTAAAGTGACAGTGGACGGTCCCCGGGAACCAAGAAGGCACAGACA

                1081       1091       1101       1111       1121       1131
Human           GAAGCTTGATGACTCTAAACCTAGTTTGTTCTCTGACCGCCTCAGTGATTTAGGGCGCAT
Chicken         GAAGCTTGATGACTCTAAACCTAGTTTGTTCCCTGAACGCCTCAGTGATTTAGGGCGCAT
Mouse           GAAGCTTGATGACTCTAAACCTAGTTTGTTCTCTGATCGCCTCAGTGATTTAGGGCGCAT
Rat             GAAGCTTGATGACTCTAAACCTAGTTTGTTCTCTGACCGCCTCAGTGATTTAGGGCGCAT

                1141       1151       1161       1171       1181       1191
Human           TCCTCATCCCAGTATGAGAGTAGGTGTCCCGCCTCAGAACCCACGGCCCTCCCTGAACTC
Chicken         TCCTCATCCCAGTATGAGAGTAGGGGTCCCGACCCAGAGCCCACGGCCCTCTCTGAACTC
Mouse           TCCTCATCCCAGTATGAGAGTAGGTGTCCCGCCTCAGAACCCACGGCCCTCCCTGAACTC
Rat             T-----------------------------------------------------------

                1201       1211       1221       1231       1241       1251
Human           TGCACCAAGTCCTTTTAATCCACAAGGACAGAGTCAGATTACAGACCCCAGGCAGGCACA
Chicken         TGCACCAAGTCCTTTTAATCCACAAGGACAGAGTCAGATTACAGACCCCAGGCAGGCGCA
Mouse           TGCACCAAGTCCTTTTAATCCACAAGGACAGAGTCAGATTACAGATCCCAGGCAGGCACA
Rat             -----------------------------------------------------------

                1261       1271       1281       1291       1301       1311
Human           GTCTTCCCCGCCGTGGTCCTATGACCAGTCTTACCCCTCCTACCTGAGCCAGATGACGTC
Chicken         GTCATCCCCGCCGTGGTCCTATGATCAGTCGTACCCGTCCTACTTGAGCCAGATGACTTC
Mouse           GTCTTCCCCACCGTGGTCCTATGACCAGTCTTACCCCTCCTATCTGAGCCAGATGACATC
Rat             -----------------------------------------------------------
```

```
                1321       1331       1341       1351       1361       1371
Human           CCCGTCCATCCACTCTACCACCCCGCTGTCTTCCACACGGGGCACTGGGCTTCCTGCCAT
Chicken         GCCGTCCATTCACTCCACGACTTCCCTGTCCTTCACCCGAGGCACAGGACTTCCAGCCAT
Mouse           CCCATCCATCCACTCCACCACGCCGCTGTCTTCCACACGGGGCACCGGGCTACCTGCCAT
Rat             ------------------------------------------------------------

                1381       1391       1401       1411       1421       1431
Human           CACCGATGTGCCTAGGCGCATTTCAGATGATGACACTGCCACCTCTGACTTCTGCCTCTG
Chicken         CACCGACGTGCC------------------------------CCGAC----GCCTCT-
Mouse           CACTGACGTGCCCAGGCGTATTTCAGATGATGACACTGCCACCTCTGACTTCTGCCTCTG
Rat             ------------------------------------------------------------
                                                CAGATGATGACACTGCCACC

                1441       1451       1461       1471       1481       1491
Human           GCCTTCCACTCTCAGTAAGAAGAGCCAGGCAGGTGCTTCAGAACTGGGCCCTTTTTCAGA
Chicken         ----------------------------CAGGTGCTTCCGAGCTGGGCCCATTTTCAGA
Mouse           GCCTTCCTCTCTCAGTAAGAAGAGCCAGGCAGGTGCTTCAGAACTGGGCCCTTTTTCAGA
Rat             ------------------------------------------------------------

                1501       1511       1521       1531       1541       1551
Human           CCCCAGGCAGTTCCCAAGCATTTCATCCCTCACTGAGAGCCGCTTCTCCAACCCACGAAT
Chicken         TCCCAGGCAGTTCACAAGCATTTCATCCCTCACTGAGAGCCGCTTCTCCAACCCACGAAT
Mouse           CCCCAGGCAGTTCCCAAGCATTTCATCCCTCACTGAGAGCCGCTTCTCCAACCCACGAAT
Rat             ------------------------------------------------------------

                1561       1571       1581       1591       1601       1611
Human           GCACTATCCAGCCACCTTTACTTACACCCCGCCAGTCACCTCAGGCATGTCCCTCGGTAT
Chicken         GCACTATCCAGCCACCTTTACCTATACACCGCCCGTCACCTCAGGCATGTCACTGGGTAT
Mouse           GCACTACCCAGCCACCTTTACCTACACCCCGCCAGTCACGTCAGGCATGTCCCTCGGCAT
Rat             ------------------------------------------------------------

                1621       1631       1641       1651       1661       1671
Human           GTCCGCCACCACTCACTACCACACCTACCTGCCACCACCCTACCCCGGCTCTTCCCAAAG
Chicken         GTCCGCAACCACTCACTACCACACCTACCTGCCACCACCCTACCCCGGCTCCTCCCAAAA
Mouse           GTCCGCCACCACTCACTACCACACGTACCTGCCACCACCCTACCCCGGCTCTTCCCAAAG
Rat             ------------------------------------------------------------

                1681       1691       1701       1711       1721       1731
Human           CCAGAGTGGACCCTTCCAGACCAGCAGCACTCCATATCTCTACTATGGCACTTCGTCAGG
Chicken         CCAAAGTGGACCTTTCCAGACCAGCAGCACTCCATATCTCTACTATGGCACTTCGTCGGG
Mouse           CCAGAGTGGACCCTTCCAGACCAGCAGCACTCCATATCTCTACTATGGTACTTCGTCAGC
Rat             ------------------------------------------------------------

                1741       1751       1761       1771       1781       1791
Human           ATCCTATCAGTTTCCCATGGTGCCGGGGGGAGACCGGTCTCCTTCCAGAATGCTTCCGCC
Chicken         ATCGTACCAGTTCCCCATGGTGCCGGGAGGGGACCGCTCCCCTTCCAGGATGCTTCCTCC
Mouse           ATCCTATCAGTTCCCAATGGTACCCGGGGGAGACCGGTCTCCTTCCAGGATGGTCCCACC
Rat             ------------------------------------------------------------

                1801       1811       1821       1831       1841       1851
Human           ATGCACCACCACCTCGAATGGCAGCACGCTATTAAATCCAAATTTGCCTAACCAGAATGA
Chicken         GTGCACCACCACGTCCAACGGCAGCACGCTGCTAAACCCAAACTTGCCCAACCAGAGTGA
Mouse           ATGCACCACCACCTCGAATGGCAGCACGCTATTAAATCCAAATTTGCCTAACCAGAATGA
Rat             ------------------------------------------------------------

                1861       1871       1881       1891       1901       1911
Human           TGGTGTTGACGCTGATGGAAGCCACAGCAGTTCCCCAACTGTTTTGAATTCTAGTGGCAG
Chicken         CGGTGTGGAGGCGGATGGCAGCCACAGCAGCTCCCCAACTGTTTTGAATTCTAGTGGCAG
Mouse           TGGTGTTGACGCTGACGGAAGCCACAGCAGTTCCCCAACTGTTTTGAATTCTAGCGGCAG
Rat             ------------------------------------------------------------
```

Appendix C: Collagen 2 Multiple Sequence Alignment

Human (BC007252): 1621 bp
Dog (AF023169): 4923 bp
Rat (NM_012929): 4538 bp
Chicken (AY046949): 4837 bp

The alignment presented here represents a specific region of high homology between several species. The sequence in bold indicates the primers designed for RT-PCR use.

```
                3301       3311       3321       3331       3341       3351
Human           ----------------------------------------------------CCAGGGTCCT
Dog             GGTGCACAAGGTCCCATGGGTCCTGCAGGACCGGCTGGAGCCCGGGGAATCCCAGGCCCT
Rat             GGTGCACAAGGTCCTATGGGCCCCTCAGGACCTGCTGGAGCCCGTGGAATTGCTGGCCCT
Chicken         GGTGCACAAGGGCCCATGGGTCCCTCTGGTCCCGCTGGAGCTCGAGGAATGCCGGGTCCC

                3361       3371       3381       3391       3401       3411
Human           CAAGGCCCCAGAGGTGACAAAGGAGAGGCTGGAGAGCCTGGCGAGAGAGGCCTGAAGGGA
Dog             CAAGGTCCCCGAGGTGACAAAGGAGAAGCTGGAGAGGCTGGCGAGAGGGGACTGAAGGGA
Rat             CAAGGCCCCCGAGGTGACAAAGGAGAAGCTGGAGAGCCTGGCGAGAGAGGACTGAAGGGG
Chicken         CAAGGACCTCGTGGTGACAAAGGTGAGACGGGAGAGGCTGGAGAGAGAGGGCTGAAGGGC

                3421       3431       3441       3451       3461       3471
Human           CACCGTGGCTTCACTGGTCTGCAGGGTCTGCCCGGCCCTCCTGGTCCTTCTGGAGACCAA
Dog             CACCGTGGCTTCACTGGTCTGCAGGGACTGCCCGGCCCTCCTGGTCCTTCTGGAGATCAA
Rat             CACCGAGGTTTCACTGGACTGCAGGGTCTGCCTGGCCCCCCGGGTCCTTCTGGAGATCAG
Chicken         CACCGTGGCTTCACCGGTCTGCAGGGTCTGCCCGGACCACCCGGCCCGTCTGGAGACCAA

                3481       3491       3501       3511       3521       3531
Human           GGTGCTTCTGGTCCTGCTGGTCCTTCTGGCCCTAGAGGTCCTCCTGGCCCCGTCGGTCCC
Dog             GGTGCTTCTGGCCCTGCTGGTCCTTCTGGCCCTAGAGGTCCTCCTGGTCCCGTCGGTCCC
Rat             GGTACTTCTGGCCCTGCTGGTCCTTCCGGCCCTAGAGGTCCACCTGGCCCTGTTGGTCCC
Chicken         GGTGCTGCCGGTCCCGCTGGTCCCTCCGGTCCCAGAGGTCCCCCTGGTCCCGTCGGCCCC

                3541       3551       3561       3571       3581       3591
Human           TCTGGCAAAGATGGTGCTAATGGAATCCCTGGCCCCATTGGGCCTCCTGGTCCCCGTGGA
Dog             TCTGGCAAAGATGGTGCTAACGGAATCCCTGGCCCCATCGGACCTCCTGGTCCCCGTGGA
Rat             TCTGGCAAAGATGGCTCTAATGGAATCCCTGGCCCCATCGGGCCTCCAGGTCCCCGTGGA
Chicken         TCTGGCAAAGATGGCTCTAACGGCATGCCCGGCCCCATCGGTCCTCCCGGTCCCCGTGGA

                3601       3611       3621       3631       3641       3651
Human           CGATCAGGCGAAACCGGCC-TGCTGGTCCTCCTGGAAATCCTGGACCCCCTGGTCCTCCA
Dog             CGTTCAGGCGAAACTGGCCCTGCTGGTCCTCCCGGAAACCCCGGACCCCCTGGCCCTCCA
Rat             CGCTCAGGAGAAACTGGCCCTGCTGGTCCTCCTGGAAATCCTGGTCCCCCTGGCCCTCCG
Chicken         CGGAGTGGTGAACCCGGCCCTGCGGGTCCTCCTGGAAACCCCGGTCCTCCCGGTCCTCCT

                3661       3671       3681       3691       3701       3711
Human           GGTCCCCCTGGCCCTGGCATCGACATGTCCGCCTTTGCTGGCTTAGGCCCGAGAGAGAAG
Dog             GGTCCCCCTGGCCCTGGCATCGACATGTCTGCCTTTGCTGGCCTGGGCCAGAGAGAGAAG
Rat             GGTCCTCCTGGTCCTGGCATCGACATGTCAGCCTTTGCTGGCTTAGGACAGAGAGAGAAG
Chicken         GGCCCCCCCCGGCACCGGCATCGACATGTCTGCTTTTGCTGGACTGGGTCAGACGGAGAAG

                3721       3731       3741       3751       3761       3771
Human           GGCCCCGACCCCCTGCAGTACATGCGGGCCGACCAGGCAGCCGGTGGCCTGAGACAGCAT
Dog             GGCCCCGACCCCCTGCAGTACATGCGGGCTGACCAGGCGGCCGGCGACCTGAGACAGCAT
Rat             GGCCCCGATCCCCTGCAGTACATGCGGGCCGACGAGGCAGACAGTACCTTGAGACAGCAT
Chicken         GGCCCCGACCCCATCCGCTACATGAGGGCAGACGAGGCGGCCGGAGGGCTGCGGCAGCAC

                3781       3791       3801       3811       3821       3831
Human           GACGCC GAGGTGGATGCCACACTCAA GTCCCTCAACAACCAGATTGAGAGCATCCGCAGC
Dog             GATGCC GAGGTGGACGCCACGCTCAA GTCCCTCAACAACCAGATTGAGAGCATCCGCAGC
Rat             GACGTC GAGGTGGACGCCACGCTCAA GTCGCTGAACAACCAGATCGAGAGCATCCGCAGC
Chicken         GACGTG GAGGTGGATGCCACCCTCAA ATCCCTCAACAATCAGATTGAGAGCATCCGCAGC
                       GAGGTGGATGCCACGCTCAA

                3841       3851       3861       3871       3881       3891
Human           CCCGAGGGCTCCCGCAAGAACCCTGCTCGCACCTGCAGAGACCTGAAACTCTGCCACCCT
Dog             CCCGAGGGCTCCCGCAAGAACCCCGCTCGTACCTGCCGGGACCTGAAACTCTGCCACCCT
Rat             CCTGATGGCTCCCGCAAGAATCCCGCTCGCACCTGCCAGGACCTGAAACTCTGCCACCCA
Chicken         CCCGAGGGCTCCAAGAAGAACCCTGCCAGGACCTGCCGCGACATCAAACTCTGCCATCCC

                3901       3911       3921       3931       3941       3951
Human           GAGTGGAAGAGTGGAGACTACTGGATTGACCCCAACCAAGGCTGCACCTTGGACGCCATG
```

```
Dog       GAATGGAAGAGCGGAGACTACTGGATTGACCCCAACCAGGGCTGCACCTTGGATGCCATG
Rat       GAGTGGAAGAGCGGAGACTACTGGATTGATCCCAACCAGGGCTGCACCTTGGACGCCATG
Chicken   GAGTGGAAGAGCGGAGATTACTGGATTGACCCGAACCAGGGCTGCACCTTGGACGCCATC

          3961      3971      3981      3991      4001      4011
Human     AAGGTTTTCTGCAACATGGAGACTGGCGAGACTTGCGTCTACCCCAATCCAGCAAACGTT
Dog       AAGGTTTTCTGCAACATGGAGACTGGCGAGACGTGCGTCTACCCCAACCCAGCGAGCGTT
Rat       AAAGTCTTCTGCAACATGGAGACTGGCGAGTCTTGCGTCTACCCCAACCCAGCGACTGTG
Chicken   AAAGTATTCTGCAACATGGAGACGGGCGAGACCTGCGTCTACCCGACCCCCAGCAGCATC

          4021      4031      4041      4051      4061      4071
Human     CCCAAGAAGAACTGGTGGAGCAGCAAGAGCAAGGAGAAGAAACACATCTGGTTTGGAGAA
Dog       CCCAAGAAGAACTGGTGGAGCAGCAAGAGCAAGGACAAGAAACATATCTGGTTTGGAGAA
Rat       CCTCGGAAGAACTGGTGGAGCAGCAAGAGCAAGGAGAAGAAGCACATCTGGTTTGGAGAG
Chicken   CCCAGGAAGAACTGGTGGACCAGCAAGACGAAAGACAAGAAGCACGTCTGGTTTGCAGAG

          4081      4091      4101      4111      4121      4131
Human     ACCATCAATGGTGGCTTCCATTTC**AGCTATGGAGATGACAATCTG**GCTCCCAACACTGCC
Dog       ACCATCAATGGTGGCTTCCACTTC**AGCTACGGTGATGACAACCTG**GCTCCCAACACTGCC
Rat       ACCATGAACGGCGGCTTCCACTTC**AGCTACGGCGACGGCAACCTG**GCTCCCAACACCGCT
Chicken   ACCATCAACGGCGGTTTCCACTTC**AGCTACGGCGATGAGAACCTG**TCCCCCAACACCGCC
                                  **AGCTACGGCGATGAGAACCTG**

          4141      4151      4161      4171      4181      4191
Human     AACGTCCAGATGACCTTCCTACGCCTGCTGTCCACGGAAGGCTCCCAGAACATCACCTAC
Dog       AACGTCCAGATGACCTTCCTCCGCCTGCTGTCCACCGAGGGCTCTCAGAATATCACCTAC
Rat       AACGTCCAGATGACTTTCCTCCGTCTACTGTCCACTGAGGGCTCCCAGAACATCACCTAC
Chicken   AGCATCCAGATGACCTTCCTGCGCCTCCTGTCCACCGAGGGCTCCCAGAACGTCACCTAC

          4201      4211      4221      4231      4241      4251
Human     CACTGCAAGAACAGCATTGCCTATCTGGACGAAGCAGCTGGCAACCTCAAGAAGGCCCTG
Dog       CACTGCAAGAACAGCATTGCCTACCTGGACGAAGCAGCCGGCAACCTCAAGAAGGCCCTG
Rat       CACTGTAAGAACAGCATTGCCTACCTGGACGAAGCAGCCGGCAACCTCAAGAAGGCCTTG
Chicken   CACTGCAAGAACAGCATCGCCTACATGGACGAGGAGACGGGCAACCTGAAGAAAGCCATC

          4261      4271      4281      4291      4301      4311
Human     CTCATCCAGGGCTCCAATGACGTGGAGATCCGGGCAGAGGGCAATAGCAGGTTCACGTAC
Dog       CTCATCCAGGGCTCCAATGATGTGGAGATCCGGGCTGAGGGCAACAGCAGGTTCACATAT
Rat       CTCATCCAGGGCTCCAATGATGTGGAGATGAGGGCCGAGGGCAACAGCAGGTTCACGTAC
Chicken   CTCATCCAGGGATCCAACGACGTGGAGATCAGAGCCGAGGGCAACAGCAGGTTCACCTAC

          4321      4331      4341      4351      4361      4371
Human     ACTGCCCTGAAGGATGGCTGCACGAAACATACCGGTAAGTGGGGCAAGACTGTTATCGAG
Dog       ACTGTTCTGAAGGATGGCTGCACGAAACACACCGGTAAGTGGGGCAAGACTATGATCGAG
Rat       ACTGCCCTGAAGGATGGCTGCACGAAACACACCGGTAAGTGGGGCAAGACCATCATCGAG
Chicken   AGCGTCTTGGAGGACGGCTGCACGAAACACACTGGCAAATGGGGCAAGACGGTGATCGAG

          4381      4391      4401      4411      4421      4431
Human     TACCGGTCACAGAAGACCTCACGCCTCCCCATCATTGACATTGCACCCATGGACATAGGA
Dog       TACCGGTCACAGAAGACCTCGCGCCTCCCCATCATTGACATTGCGCCCATGGACATAGGA
Rat       TACCGATCACAGAAGACCTCACGCCTTCCCATTGTTGACATTGCACCCATGGACATCGGA
Chicken   TACCGGTTGCAGAAGACCTCGCGCCTGTCCATTGTAGATACTGCACCTATGGACATTGGC

          4441      4451      4461      4471      4481      4491
Human     GGGCCCGAGCAGGAATTCGGTGTGGACATAGGGCCGGTCTGCTTCTTGTAAAAACC--TG
Dog       GGGCCCGAGCAGGAATTTGGTGTGGACATCGGGCCTGTCTGCTTCTTGTAAAAACC--CG
Rat       GGGCCTGATCAGGAATTTGGTGTGGACATAGGGCCTGTCTGTTTCTTGTAAAACCC--TC
Chicken   GGAGCCGATCAGGAGTTTGGCGTGGATATTGGCCCAGTCTGCTTCTTGTAAAAAGGGTTG
```

Appendix D: Sox-9 Multiple Sequence Alignment

Mouse (AF42178): 1524 bp
Rat (AB073720): 492 bp
Human (NM_000346): 3935 bp
Cow (AF278703): 557 bp
Chicken (U12533): 1544 bp

The alignment presented here represents a specific region of high homology between several species. The sequence in bold indicates the primers designed for RT-PCR use.

```
                361        371        381        391        401        411
Mouse           TGAATCTCCTGGACCCCTTCATGAAGATGACCGACGAGCAGGAGAAGGGCCTGTCTGGCG
Rat             ----------------------------------------------AAGGGCTTGTCTGGCG
Human           TGAATCTCCTGGACCCCTTCATGAAGATGACCGACGAGCAGGAGAAGGGCCTGTCCGGCG
Cow             TGAATCTCCTGGACCCCTTCATGAAGATGACCGACGAGCAGGAGAAGGGCCTGTCCGCCG
Chicken         TGAATCTCCTAGACCCCTTTATGAAAATGACAGAAGAACAGGATAAAGGCCTCTCCGGCG

                421        431        441        451        461        471
Mouse           CCCCCAGCCCCACCATGTCGGAGGACTCGGCTGGTTCGCCCTGTCCCTCGGGCTCCGGCT
Rat             CCCCCAGCCCCACCATGTCGGAGGACTCGGCTGGTTCGCCCTGCCCCTCGGGCTCAGGCT
Human           CCCCCAGCCCCACCATGTCCGAGGACTCCGCGGGCTCGCCCTGCCCGTCGGGCTCCGGCT
Cow             CCCCCAGCCCCACCATGTCCGAGGACTCTGCGGGCTCGCCCTGCCCTTCGGGCTCCGGCT
Chicken         CCCCCAGCCCCACCATGTCGGATGACTCCGCGGGGTCCCCCTGCCCCTCCGGATCCGGCT

                481        491        501        511        521        531
Mouse           CGGACACGGAGAACACCCGGCCCC---AGGAGAACACCTTCCCCAAGGGCGAGCCGGATC
Rat             CCGACACGGAGAACACACGGCCCC---AGGAGAACACGTTCCCCAAGGGCGAGCCGGATC
Human           CGGACACCGAGAACACGCGGCCCC---AGGAGAACACGTTCCCCAAGGGCGAGCCCGATC
Cow             CCGACACCGAGAACACGCGGCCCC---AGGAGAACACGTTCCCCAAGGGCGAGCCGGACC
Chicken         CGGACACGGAGAACACCCGTCCTCCTCAAGAGAACACCTTCCCCAAAGGCGACCCGGACC

                541        551        561        571        581        591
Mouse           TGAAGAA**GGAGAGCGAGGAAGATAAGTT**CCCCGTGTGCATCCGCGAGGCGGTCAGCCAGG
Rat             TGAAGAA**GGAGAGCGAGGAAGATAAATT**CCCAGTGTGCATCCGCGAGGCGGTCAGCCAGG
Human           TGAAGAA**GGAGAGCGAGGAGGACAAGTT**CCCCGTGTGCATCCGCGAGGCGGTCAGCCAGG
Cow             TGAAGAA**GGAGAGCGAGGAGGACAAGTT**CCCCGTGTGCATCCGCGAGGCCGTCAGCCAGG
Chicken         TGAAGAA**GGAAAGCGACGAGGACAAATT**CCCCGTGTGCATCCGCGAGGCCGTGAGCCAGG
                      **GGAGAGCGAGGAGGACAAGTT**

                601        611        621        631        641        651
Mouse           TGCTGAAGGGCTACGACTGGACGCTGGTGCCCATGCCCGTGCGCGTCAACGGCTCCAGCA
Rat             TGCTGAAGGGCTATGACTGGACCCTGGTGCCCATGCCGGTGCGCGTCAACGGCTCCAGCA
Human           TGCTCAAAGGCTACGACTGGACGCTGGTGCCCATGCCGGTGCGCGTCAACGGCTCCAGCA
Cow             TGCTCAAGGGCTACGACTGGACGCTGGTGCCCATGCCGGTGCGCGTCAACGGCTCGAGCA
Chicken         TGCTCAAGGGCTACGACTGGACCCTGGTGCCCATGCCCGTGCGGGTGAACGGATCCAGCA

                661        671        681        691        701        711
Mouse           AGAACAAGCCACACGTCAAGCGACCCATGAACGCCTTCATGGTGTGGGCGCAGGCTGCGC
Rat             AGAACAAGCCACACGTCAAGCGGCCCATGAACGCCTTCATGGTGTGGGCGCAGGCTGCGC
Human           AGAACAAGCCGCACGTCAAGCGGCCCATGAACGCCTTCATGGTGTGGGCGCAGGCGGCGC
Cow             AGAACAAGCCGCACGTCAAGCGGCCCATGAACGCCTTCATGGTGTGGGCGCAGGCGGCGC
Chicken         AGAACAAACCCCACGTGAAGCGCCCCATGAACGCCTTCATGGTGTGGGCCCAGGCGGCTC

                721        731        741        751        761        771
Mouse           GCAGGAAGCTGGCAGACCAGTACCCGCATCTGCACAACGCGGAGCTCAGCAAGACTCTGG
Rat             GCAGGAAGCTGGCAGACCAGTACCCGCATCTGCACAACGCGGAGCTCAGCAAGACTCTGG
Human           GCAGGAAGCTCGCGGACCAGTACCCGCACTTGCACAACGCCGAGCTCAGCAAGACGCTGG
Cow             GCAGGAAGCTGGCCGACCAGTACCCGCACCTGCACAACGCCGAGCTCAGCAAGACTCTGG
Chicken         GAAGGAAGCTGGCTGACCAGTACCCGCATCTGCACAACGCCGAGCTCAGCAAGACGCTGG

                781        791        801        811        821        831
Mouse           GCAAGCTCTGGAGGCTGCTGAACGAGAGCGAGAAGAGACCCTTCGTGGAGGAGGCGGAGC
Rat             GCAAGCTCTGGAGACTGCTGAACGAGAGCGAGAAGAGACCCTTCGTGGAGGAGGCGGAGC
Human           GCAAGCTCTGGAGACTTCTGAACGAGAGCGAGAAGCGGCCCTTCGTGGAGGAGGCGGAGC
Cow             GCAAGCTCTGGAGACTGCTGAACGAGAGCGAGAAGCGGCCGTTCGTGGAGGAGGCGGAGC
Chicken         GCAAGCTGTGGAGGCTGCTGAATGAGAGCGAGAAGCGTCCCTTCGTGGAGGAGGCCGAGC
```

```
                841        851        861        871        881        891
Mouse           GGCTGCGCGTGCAGCACAAGAAAGACCACCCCGATTACAAGTACCAGCCCCGGCGGAGGA
Rat             GGCTGCGCGTGCAGCACAGGAAAGACCACCCCGATTACAAGTACCAGCCCCGGCGGAGG-
Human           GGCTGCGCGTGCAGCACAAGAAGGACCACCCGGATTACAAGTACCAGCCGCGGCGGAGGA
Cow             GGCTGCGCGTGCAGCACAAGAAGGACCACCCGGACTACAAGTACCAGCCGCGCCGGAGGA
Chicken         GGCTGCGGGTGCAGCACAAGAAGGACCACCCCGACTACAAGTACCAACCACGCAGGAGGA

                901        911        921        931        941        951
Mouse           AGTCGGTGAAGAACGGACAAGCGGAGGCCGAAGAGGCCACGGAACAGACTCACATCTCTC
Rat             ------------------------------------------------------------
Human           AGTCGGTGAAGAACGGGCAGGCGGAGGCAGAGGAGGCCACGGAGCAGACGCACATCTCCC
Cow             AGTCGGTGAAGAACGGGCA------------------------------------------
Chicken         AGACGGTGAAGAACGGGCAGTCGGAGCAGGAGGAGGGCTCCGAGCAGACCCACATCTCCC

                961        971        981        991        1001       1011
Mouse           CTAATGCTATCTTCAAGGCGCTGCAAGCCGACTCCCCACATTCCTCCTCCGGCATGAGTG
Rat             ------------------------------------------------------------
Human           CCAACGCCATCTTCAAGGCGCTGCAGGCCGACTCGCCACACTCCTCCTCCGGCATGAGCG
Cow             ------------------------------------------------------------
Chicken         CCAACGCCATCTTCAAGGCGCTGCAGGCGGACTCCCCGCAGTCATCCTCCAGCATCAGCG
                       ATCTTCAAGGCGCTGCAGG

                1021       1031       1041       1051       1061       1071
Mouse           AGGTGCACTCCCCGGGCGAGCACTCTGGGCAATCTCAGGGTCCGCCGACCCCACCCACCA
Rat             ------------------------------------------------------------
Human           AGGTGCACTCCCCCGGCGAGCACTCGGGGCAATCCCAGGGCCCACCGACCCCACCCACCA
Cow             ------------------------------------------------------------
Chicken         AGGTGCACTCCCCCGGGGAGCACTCAGGGCAGTCGCAGGGCCCCCCCACGCCCCCCACCA

                1081       1091       1101       1111       1121       1131
Mouse           CTCCCAAAACCGACGT---GCAAGCTGGCAAAGTTGATCTGAAGCGAGAGGGGCGCCCTC
Rat             ------------------------------------------------------------
Human           CCCCCAAAACCGACGT---GCAGCCGGGCAAGGCTGACCTGAAGCGAGAGGGGCGCCCCT
Cow             ------------------------------------------------------------
Chicken         CCCCCAAAACGGACGCTCAGCAGCCGGGCAAGCAGGACCTGAAGCGCGAGG---GCCCTT

                1141       1151       1161       1171       1181       1191
Mouse           TGGCAGAGGGGGGCAGACAGCCCCCC---ATCGACTTCCGCGACGTGGACATCGGTGAAC
Rat             ------------------------------------------------------------
Human           TGCCAGAGGGGGGCAGACAGCCCCCT---ATCGACTTCCGCGACGTGGACATCGGCGAGC
Cow             ------------------------------------------------------------
Chicken         TGGCGGAAGGCGGCCGCCAACCTCCCCACATCGATTTCCGAGACGTGGACATCGGCGAGC

                1201       1211       1221       1231       1241       1251
Mouse           TGAGCAGCGACGTCATCTCCAACATTGAGACCTTCGACGTCAATGAGTTTGACCAATACT
Rat             ------------------------------------------------------------
Human           TGAGCAGCGACGTCATCTCCAACATCGAGACCTTCGATGTCAACGAGTTTGACCAGTACC
Cow             ------------------------------------------------------------
Chicken         TCAGCAGCGACGTCATCTCCAACATCGAAACCTTCGACGTCAACGAGTTCGACCAATACC

                1261       1271       1281       1291       1301       1311
Mouse           TGCCACCCAACGGCCACCCAGGGGTTCCGGCCACCCACGGCCAGGTCACC---TACACTG
Rat             ------------------------------------------------------------
Human           TGCCGCCCAACGGCCACCCGGGGGTGCCGGCCACGCACGGCCAGGTCACC---TACACGG
Cow             ------------------------------------------------------------
Chicken         TGCCCCCCAACGGCCACCCGGGGGTCCCGGCCACCCACGGCCAGGTCACCACCTACAGCG

                1321       1331       1341       1351       1361       1371
Mouse           GCAGTTACGGCATCAGCAGCACCGCACCCACCCCTGCGACCGCGGGCCACGTGTGGATGT
Rat             ------------------------------------------------------------
Human           GCAGCTACGGCATCAGCAGCACCGCGGCCACCCCGGCGAGCGCGGGCCACGTGTGGATGT
Cow             ------------------------------------------------------------
Chicken         GTACCTACGGCATCAGCAGCTCGGCCAGCTCTCCGGCGGGCGCCGGGCACGCCTGGATGG
```

BIBLIOGRAPHY

Abad, V., Meyers, J. L., Weise, M., Gafni, R. I., Barnes, K. M., Nilsson, O., Bacher, J. D., and Baron, J. (2002). The role of the resting zone in growth plate chondrogenesis. Endocrinology *143*, 1851-1857.

Abad, V., Uyeda, J. A., Temple, H. T., De Luca, F., and Baron, J. (1999). Determinants of spatial polarity in the growth plate. Endocrinology *140*, 958-962.

Afizah, H., Yang, Z., Hui, J. H., Ouyang, H. W., and Lee, E. H. (2007). A comparison between the chondrogenic potential of human bone marrow stem cells (BMSCs) and adipose-derived stem cells (ADSCs) taken from the same donors. Tissue Eng *13*, 659-666.

Ahn, J. I., Terry Canale, S., Butler, S. D., and Hasty, K. A. (2004). Stem cell repair of physeal cartilage. J Orthop Res *22*, 1215-1221.

Aigner, J., Tegeler, J., Hutzler, P., Campoccia, D., Pavesio, A., Hammer, C., Kastenbauer, E., and Naumann, A. (1998). Cartilage tissue engineering with novel nonwoven structured biomaterial based on hyaluronic acid benzyl ester. J Biomed Mater Res *42*, 172-181.

Allen, T. D., Dexter, T. M., and Simmons, P. J. (1990). Marrow biology and stem cells. Immunol Ser *49*, 1-38.

Alliston, T., Choy, L., Ducy, P., Karsenty, G., and Derynck, R. (2001). TGF-beta-induced repression of CBFA1 by Smad3 decreases cbfa1 and osteocalcin expression and inhibits osteoblast differentiation. Embo J *20*, 2254-2272.

Alvarez, R. H., Kantarjian, H. M., and Cortes, J. E. (2006). Biology of platelet-derived growth factor and its involvement in disease. Mayo Clin Proc *81*, 1241-1257.

Amsel, S., and Dell, E. S. (1971). Response of the preosteoblast and stem cell of rat bone marrow to a lethal dose of x-irradiation or cyclophosphamide. Cell Tissue Kinet *4*, 255-261.

Anderson, D. M., Maraskovsky, E., Billingsley, W. L., Dougall, W. C., Tometsko, M. E., Roux, E. R., Teepe, M. C., DuBose, R. F., Cosman, D., and Galibert, L. (1997). A homologue of the TNF receptor and its ligand enhance T-cell growth and dendritic-cell function. Nature *390*, 175-179.

Anderson, H. C. (1995). Molecular biology of matrix vesicles. Clin Orthop *314*, 266-280.

Anderson, H. C. (2003). Matrix vesicles and calcification. Curr Rheumatol Rep *5*, 222-226.

Anderson, H. C., Hodges, P. T., Aguilera, X. M., Missana, L., and Moylan, P. E. (2000). Bone morphogenetic protein (BMP) localization in developing human and rat growth plate, metaphysis, epiphysis, and articular cartilage. J Histochem Cytochem *48*, 1493-1502.

Angele, P., Kujat, R., Nerlich, M., Yoo, J., Goldberg, V., and Johnstone, B. (1999). Engineering of osteochondral tissue with bone marrow mesenchymal progenitor cells in a derivatized hyaluronan-gelatin composite sponge. Tissue Eng *5*, 545-554.

Aoyagi, Y., Fujita, N., and Tsuruo, T. (2005). Stabilization of integrin-linked kinase by binding to Hsp90. Biochem Biophys Res Commun *331*, 1061-1068.

Aszodi, A., Chan, D., Hunziker, E., Bateman, J. F., and Fassler, R. (1998). Collagen II is essential for the removal of the notochord and the formation of intervertebral discs. J Cell Biol *143*, 1399-1412.

Aubin, J. E., and Turksen, K. (1996). Monoclonal antibodies as tools for studying the osteoblast lineage. Microsc Res Tech *33*, 128-140.

Aung, T., Miyoshi, H., Tun, T., and Ohshima, N. (2002). Chondroinduction of mouse mesenchymal stem cells in three-dimensional highly porous matrix scaffolds. J Biomed Mater Res *61*, 75-82.

Awad, H. A., Butler, D. L., Boivin, G. P., Smith, F. N., Malaviya, P., Huibregtse, B., and Caplan, A. I. (1999). Autologous mesenchymal stem cell-mediated repair of tendon. Tissue Eng *5*, 267-277.

Awad, H. A., Wickham, M. Q., Leddy, H. A., Gimble, J. M., and Guilak, F. (2004). Chondrogenic differentiation of adipose-derived adult stem cells in agarose, alginate, and gelatin scaffolds. Biomaterials *25*, 3211-3222.

Azizi, S. A., Stokes, D., Augelli, B. J., DiGirolamo, C., and Prockop, D. J. (1998). Engraftment and migration of human bone marrow stromal cells implanted in the brains of albino rats--similarities to astrocyte grafts. Proc Natl Acad Sci U S A *95*, 3908-3913.

Baddoo, M., Hill, K., Wilkinson, R., Gaupp, D., Hughes, C., Kopen, G. C., and Phinney, D. G. (2003). Characterization of mesenchymal stem cells isolated from murine bone marrow by negative selection. J Cell Biochem *89*, 1235-1249.

Baker, J., Liu, J. P., Robertson, E. J., and Efstratiadis, A. (1993). Role of insulin-like growth factors in embryonic and postnatal growth. Cell *75*, 73-82.

Balemans, W., and Van Hul, W. (2002). Extracellular regulation of BMP signaling in vertebrates: a cocktail of modulators. Dev Biol *250*, 231-250.

Ball, S. G., Shuttleworth, C. A., and Kielty, C. M. (2007). Mesenchymal stem cells and neovascularization: role of platelet-derived growth factor receptors. J Cell Mol Med *11*, 1012-1030.

Barbero, A., Ploegert, S., Heberer, M., and Martin, I. (2003). Plasticity of clonal populations of dedifferentiated adult human articular chondrocytes. Arthritis Rheum *48*, 1315-1325.

Baron, J., Klein, K. O., Yanovski, J. A., Novosad, J. A., Bacher, J. D., Bolander, M. E., and Cutler, G. B., Jr. (1994). Induction of growth plate cartilage ossification by basic fibroblast growth factor. Endocrinology *135*, 2790-2793.

Barry, F., Boynton, R., Murphy, M., Haynesworth, S., and Zaia, J. (2001a). The SH-3 and SH-4 antibodies recognize distinct epitopes on CD73 from human mesenchymal stem cells. Biochem Biophys Res Commun *289*, 519-524.

Barry, F., Boynton, R. E., Liu, B., and Murphy, J. M. (2001b). Chondrogenic differentiation of mesenchymal stem cells from bone marrow: differentiation-dependent gene expression of matrix components. Exp Cell Res *268*, 189-200.

Barry, F. P., and Murphy, J. M. (2004). Mesenchymal stem cells: clinical applications and biological characterization. Int J Biochem Cell Biol *36*, 568-584.

Baumgart, R., Burklein, D., Hinterwimmer, S., Thaller, P., and Mutschler, W. (2005). The management of leg-length discrepancy in Ollier's disease with a fully implantable lengthening nail. J Bone Joint Surg Br *87*, 1000-1004.

Ben-Ezra, J., Sheibani, K., Hwang, D. L., and Lev-Ran, A. (1990). Megakaryocyte synthesis is the source of epidermal growth factor in human platelets. Am J Pathol *137*, 755-759.

Benya, P. D. (1988). Modulation and reexpression of the chondrocyte phenotype; mediation by cell shape and microfilament modification. Pathol Immunopathol Res *7*, 51-54.

Benya, P. D., Padilla, S. R., and Nimni, M. E. (1978). Independent regulation of collagen types by chondrocytes during the loss of differentiated function in culture. Cell *15*, 1313-1321.

Benya, P. D., and Shaffer, J. D. (1982). Dedifferentiated chondrocytes reexpress the differentiated collagen phenotype when cultured in agarose gels. Cell *30*, 215-224.
Betsholtz, C. (2003). Biology of platelet-derived growth factors in development. Birth Defects Res C Embryo Today *69*, 272-285.

Bi, W., Deng, J. M., Zhang, Z., Behringer, R. R., and de Crombrugghe, B. (1999). Sox9 is required for cartilage formation. Nat Genet *22*, 85-89.

Bi, W., Huang, W., Whitworth, D. J., Deng, J. M., Zhang, Z., Behringer, R. R., and de Crombrugghe, B. (2001). Haploinsufficiency of Sox9 results in defective cartilage primordia and premature skeletal mineralization. Proc Natl Acad Sci U S A *98*, 6698-6703.

Bianchi, G., Banfi, A., Mastrogiacomo, M., Notaro, R., Luzzatto, L., Cancedda, R., and Quarto, R. (2003). Ex vivo enrichment of mesenchymal cell progenitors by fibroblast growth factor 2. Exp Cell Res *287*, 98-105.

Bianco, P., Fisher, L. W., Young, M. F., Termine, J. D., and Robey, P. G. (1991). Expression of bone sialoprotein (BSP) in developing human tissues. Calcif Tissue Int *49*, 421-426.

Bianco, P., Fisher, L. W., Young, M. F., Termine, J. D., and Robey, P. G. (1990). Expression and localization of the two small proteoglycans biglycan and decorin in developing human skeletal and non-skeletal tissues. J Histochem Cytochem *38*, 1549-1563.

Bianco, P., Riminucci, M., Gronthos, S., and Robey, P. G. (2001). Bone marrow stromal stem cells: nature, biology, and potential applications. Stem Cells *19*, 180-192.

Blair, H. C., and Zaidi, M. (2006). Osteoclastic differentiation and function regulated by old and new pathways. Rev Endocr Metab Disord *7*, 23-32.

Bolander, M. E. (1992). Regulation of fracture repair by growth factors. Proc Soc Exp Biol Med *200*, 165-170.

Bosch, P., Musgrave, D. S., Lee, J. Y., Cummins, J., Shuler, T., Ghivizzani, T. C., Evans, T., Robbins, T. D., and Huard (2000). Osteoprogenitor cells within skeletal muscle. J Orthop Res *18*, 933-944.

Boskey, A. L., Gadaleta, S., Gundberg, C., Doty, S. B., Ducy, P., and Karsenty, G. (1998). Fourier transform infrared microspectroscopic analysis of bones of osteocalcin-deficient mice provides insight into the function of osteocalcin. Bone *23*, 187-196.

Boskey, A. L., Maresca, M., Ullrich, W., Doty, S. B., Butler, W. T., and Prince, C. W. (1993). Osteopontin-hydroxyapatite interactions in vitro: inhibition of hydroxyapatite formation and growth in a gelatin-gel. Bone Miner *22*, 147-159.

Bosnakovski, D., Mizuno, M., Kim, G., Takagi, S., Okumura, M., and Fujinaga, T. (2005). Isolation and multilineage differentiation of bovine bone marrow mesenchymal stem cells. Cell Tissue Res *319*, 243-253.

Boudreau, N. J., and Jones, P. L. (1999). Extracellular matrix and integrin signalling: the shape of things to come. Biochem J *339 (Pt 3)*, 481-488.

Brighton, C. T. (1978). Structure and function of the growth plate. Clin Orthop Relat Res, 22-32.

Brighton, C. T. (1987a). Longitudinal bone growth: the growth plate and its dysfunctions. Instr Course Lect *36*, 3-25.

Brighton, C. T. (1987b). Morphology and biochemistry of the growth plate. Rheum Dis Clin North Am *13*, 75-100.

Brighton, C. T., Lorich, D. G., Kupcha, R., Reilly, T. M., Jones, A. R., and Woodbury, R. A., 2nd (1992). The pericyte as a possible osteoblast progenitor cell. Clin Orthop Relat Res, 287-299.

Brittberg, M., Lindahl, A., Nilsson, A., Ohlsson, C., Isaksson, O., and Peterson, L. (1994). Treatment of deep cartilage defects in the knee with autologous chondrocyte transplantation. N Engl J Med *331*, 889-895.

Bruder, S. P., Fink, D. J., and Caplan, A. I. (1994). Mesenchymal stem cells in bone development, bone repair, and skeletal regeneration therapy. J Cell Biochem *56*, 283-294.

Bruder, S. P., Horowitz, M. C., Mosca, J. D., and Haynesworth, S. E. (1997). Monoclonal antibodies reactive with human osteogenic cell surface antigens. Bone *21*, 225-235.

Bruder, S. P., Kraus, K. H., Goldberg, V. M., and Kadiyala, S. (1998a). The effect of implants loaded with autologous mesenchymal stem cells on the healing of canine segmental bone defects. J Bone Joint Surg Am *80*, 985-996.

Bruder, S. P., Ricalton, N. S., Boynton, R. E., Connolly, T. J., Jaiswal, N., Zaia, J., and Barry, F. P. (1998b). Mesenchymal stem cell surface antigen SB-10 corresponds to activated leukocyte cell adhesion molecule and is involved in osteogenic differentiation. J Bone Miner Res *13*, 655-663.

Buckwalter, J. A., Glimcher, M. J., Cooper, R. R., and Recker, R. (1996). Bone biology. I: Structure, blood supply, cells, matrix, and mineralization. Instr Course Lect *45*, 371-386.

Buckwalter, J. A., Mower, D., Schafer, J., Ungar, R., Ginsberg, B., and Moore, K. (1985). Growth-plate-chondrocyte profiles and their orientation. J Bone Joint Surg Am *67*, 942-955.

Buckwalter, J. A., and Rosenberg, L. (1983). Structural changes during development in bovine fetal epiphyseal cartilage. Coll Relat Res *3*, 489-504.

Buckwalter, J. A., and Rosenberg, L. C. (1988). Electron microscopic studies of cartilage proteoglycans. Electron Microsc Rev *1*, 87-112.

Cancedda, R., Dozin, B., Giannoni, P., and Quarto, R. (2003). Tissue engineering and cell therapy of cartilage and bone. Matrix Biol *22*, 81-91.

Cancedda, R., Giannoni, P., and Mastrogiacomo, M. (2007). A tissue engineering approach to bone repair in large animal models and in clinical practice. Biomaterials *28*, 4240-4250.

Carlos, T. M., and Harlan, J. M. (1994). Leukocyte-endothelial adhesion molecules. Blood *84*, 2068-2101.

Carmeliet, P., Ferreira, V., Breier, G., Pollefeyt, S., Kieckens, L., Gertsenstein, M., Fahrig, M., Vandenhoeck, A., Harpal, K., Eberhardt, C., et al. (1996). Abnormal blood vessel development and lethality in embryos lacking a single VEGF allele. Nature *380*, 435-439.

Carrington, J. L., and Reddi, A. H. (1990). Temporal changes in the response of chick limb bud mesodermal cells to transforming growth factor beta-type 1. Exp Cell Res *186*, 368-373.

Castro-Malaspina, H., Gay, R. E., Resnick, G., Kapoor, N., Meyers, P., Chiarieri, D., McKenzie, S., Broxmeyer, H. E., and Moore, M. A. (1980). Characterization of human bone marrow fibroblast colony-forming cells (CFU-F) and their progeny. Blood *56*, 289-301.

Castro-Malaspina, H., Rabellino, E. M., Yen, A., Nachman, R. L., and Moore, M. A. (1981). Human megakaryocyte stimulation of proliferation of bone marrow fibroblasts. Blood *57*, 781-787.

Caterson, E. J., Nesti, L. J., Albert, T., Danielson, K., and Tuan, R. (2001). Application of mesenchymal stem cells in the regeneration of musculoskeletal tissues. MedGenMed, E1.
Chan, D., and Jacenko, O. (1998). Phenotypic and biochemical consequences of collagen X mutations in mice and humans. Matrix Biol *17*, 169-184.

Chang, D. J., Ji, C., Kim, K. K., Casinghino, S., McCarthy, T. L., and Centrella, M. (1998). Reduction in transforming growth factor beta receptor I expression and transcription factor CBFa1 on bone cells by glucocorticoid. J Biol Chem *273*, 4892-4896.

Chang, S. C., Tobias, G., Roy, A. K., Vacanti, C. A., and Bonassar, L. J. (2003). Tissue engineering of autologous cartilage for craniofacial reconstruction by injection molding. Plast Reconstr Surg *112*, 793-799; discussion 800-791.

Cheah, K. S., Stoker, N. G., Griffin, J. R., Grosveld, F. G., and Solomon, E. (1985). Identification and characterization of the human type II collagen gene (COL2A1). Proc Natl Acad Sci U S A *82*, 2555-2559.

Cheifetz, S., Bellon, T., Cales, C., Vera, S., Bernabeu, C., Massague, J., and Letarte, M. (1992). Endoglin is a component of the transforming growth factor-beta receptor system in human endothelial cells. J Biol Chem *267*, 19027-19030.

Chen, F., Hui, J. H., Chan, W. K., and Lee, E. H. (2003a). Cultured mesenchymal stem cell transfers in the treatment of partial growth arrest. J Pediatr Orthop *23*, 425-429.

Chen, G., Liu, D., Tadokoro, M., Hirochika, R., Ohgushi, H., Tanaka, J., and Tateishi, T. (2004). Chondrogenic differentiation of human mesenchymal stem cells cultured in a cobweb-like biodegradable scaffold. Biochem Biophys Res Commun *322*, 50-55.

Chen, G., Sato, T., Ushida, T., Hirochika, R., and Tateishi, T. (2003b). Redifferentiation of dedifferentiated bovine chondrocytes when cultured in vitro in a PLGA-collagen hybrid mesh. FEBS Lett *542*, 95-99.

Chen, J., Wang, C., Lu, S., Wu, J., Guo, X., Duan, C., Dong, L., Song, Y., Zhang, J., Jing, D., et al. (2005). In vivo chondrogenesis of adult bone-marrow-derived autologous mesenchymal stem cells. Cell Tissue Res *319*, 429-438.

Chen, J., Zhang, Q., McCulloch, C. A., and Sodek, J. (1991). Immunohistochemical localization of bone sialoprotein in foetal porcine bone tissues: comparisons with secreted phosphoprotein 1 (SPP-1, osteopontin) and SPARC (osteonectin). Histochem J *23*, 281-289.

Chen, T. L., Shen, W. J., and Kraemer, F. B. (2001). Human BMP-7/OP-1 induces the growth and differentiation of adipocytes and osteoblasts in bone marrow stromal cell cultures. J Cell Biochem *82*, 187-199.

Chiang, H., Kuo, T. F., Tsai, C. C., Lin, M. C., She, B. R., Huang, Y. Y., Lee, H. S., Shieh, C. S., Chen, M. H., Ramshaw, J. A., et al. (2005). Repair of porcine articular cartilage defect with autologous chondrocyte transplantation. J Orthop Res *23*, 584-593.

Chu, C. R., Dounchis, J. S., Yoshioka, M., Sah, R. L., Coutts, R. D., and Amiel, D. (1997). Osteochondral repair using perichondrial cells. A 1-year study in rabbits. Clin Orthop Relat Res, 220-229.

Coffin, J. D., Florkiewicz, R. Z., Neumann, J., Mort-Hopkins, T., Dorn, G. W., 2nd, Lightfoot, P., German, R., Howles, P. N., Kier, A., O'Toole, B. A., and et al. (1995). Abnormal bone growth and selective translational regulation in basic fibroblast growth factor (FGF-2) transgenic mice. Mol Biol Cell *6*, 1861-1873.

Cole, S. R., Ashman, L. K., and Ey, P. L. (1987). Biotinylation: an alternative to radioiodination for the identification of cell surface antigens in immunoprecipitates. Mol Immunol *24*, 699-705.

Colter, D. C., Class, R., DiGirolamo, C. M., and Prockop, D. J. (2000). Rapid expansion of recycling stem cells in cultures of plastic-adherent cells from human bone marrow. Proc Natl Acad Sci U S A *97*, 3213-3218.

Colter, D. C., Sekiya, I., and Prockop, D. J. (2001). Identification of a subpopulation of rapidly self-renewing and multipotential adult stem cells in colonies of human marrow stromal cells. Proc Natl Acad Sci U S A *98*, 7841-7845.

Colvin, J. S., Bohne, B. A., Harding, G. W., McEwen, D. G., and Ornitz, D. M. (1996). Skeletal overgrowth and deafness in mice lacking fibroblast growth factor receptor 3. Nat Genet *12*, 390-397.

Cook, S. D., Patron, L. P., Salkeld, S. L., and Rueger, D. C. (2003). Repair of articular cartilage defects with osteogenic protein-1 (BMP-7) in dogs. J Bone Joint Surg Am *85-A Suppl 3*, 116-123.

Cundy, P. J., Jofe, M., Zaleske, D. J., Ehrlich, M. G., and Mankin, H. J. (1991). Physeal reconstruction using tissue donated from early postnatal limbs in a murine model. J Orthop Res *9*, 360-366.

D'Angelo, M., Billings, P. C., Pacifici, M., Leboy, P. S., and Kirsch, T. (2001). Authentic matrix vesicles contain active metalloproteases (MMP). a role for matrix vesicle-associated MMP-13 in activation of transforming growth factor-beta. J Biol Chem *276*, 11347-11353.

Danielson, K. G., Baribault, H., Holmes, D. F., Graham, H., Kadler, K. E., and Iozzo, R. V. (1997). Targeted disruption of decorin leads to abnormal collagen fibril morphology and skin fragility. J Cell Biol *136*, 729-743.

De Bari, C., Dell'Accio, F., and Luyten, F. P. (2001a). Human periosteum-derived cells maintain phenotypic stability and chondrogenic potential throughout expansion regardless of donor age. Arthritis Rheum *44*, 85-95.

De Bari, C., Dell'Accio, F., and Luyten, F. P. (2004). Failure of in vitro-differentiated mesenchymal stem cells from the synovial membrane to form ectopic stable cartilage in vivo. Arthritis Rheum *50*, 142-150.

De Bari, C., Dell'Accio, F., Tylzanowski, P., and Luyten, F. P. (2001b). Multipotent mesenchymal stem cells from adult human synovial membrane. Arthritis Rheum *44*, 1928-1942.

De Kok, I. J., Peter, S. J., Archambault, M., van den Bos, C., Kadiyala, S., Aukhil, I., and Cooper, L. F. (2003). Investigation of allogeneic mesenchymal stem cell-based alveolar bone formation: preliminary findings. Clin Oral Implants Res *14*, 481-489.

de la Fuente, R., Abad, J. L., Garcia-Castro, J., Fernandez-Miguel, G., Petriz, J., Rubio, D., Vicario-Abejon, C., Guillen, P., Gonzalez, M. A., and Bernad, A. (2004). Dedifferentiated adult

articular chondrocytes: a population of human multipotent primitive cells. Exp Cell Res *297*, 313-328.

Delany, A. M., Amling, M., Priemel, M., Howe, C., Baron, R., and Canalis, E. (2000). Osteopenia and decreased bone formation in osteonectin-deficient mice. J Clin Invest *105*, 1325.

De Luca, F., Barnes, K. M., Uyeda, J. A., De-Levi, S., Abad, V., Palese, T., Mericq, V., and Baron, J. (2001). Regulation of growth plate chondrogenesis by bone morphogenetic protein-2. Endocrinology *142*, 430-436.

De Luca, F., and Baron, J. (1999). Control of Bone Growth by Fibroblast Growth Factors. Trends Endocrinol Metab *10*, 61-65.

de Pablos, J., Villas, C., and Canadell, J. (1986). Bone lengthening by physial distraction. An experimental study. Int Orthop *10*, 163-170.

De Ugarte, D. A., Morizono, K., Elbarbary, A., Alfonso, Z., Zuk, P. A., Zhu, M., Dragoo, J. L., Ashjian, P., Thomas, B., Benhaim, P., et al. (2003). Comparison of multi-lineage cells from human adipose tissue and bone marrow. Cells Tissues Organs *174*, 101-109.

Deans, R. J., and Moseley, A. B. (2000). Mesenchymal stem cells: biology and potential clinical uses. Exp Hematol *28*, 875-884.

Deng, C., Wynshaw-Boris, A., Zhou, F., Kuo, A., and Leder, P. (1996). Fibroblast growth factor receptor 3 is a negative regulator of bone growth. Cell *84*, 911-921.

Denker, A. E., Haas, A. R., Nicoll, S. B., and Tuan, R. S. (1999). Chondrogenic differentiation of murine C3H10T1/2 multipotential mesenchymal cells: I. Stimulation by bone morphogenetic protein-2 in high-density micromass cultures. Differentiation *64*, 67-76.

Deschaseaux, F., Gindraux, F., Saadi, R., Obert, L., Chalmers, D., and Herve, P. (2003). Direct selection of human bone marrow mesenchymal stem cells using an anti-CD49a antibody reveals their CD45med,low phenotype. Br J Haematol *122*, 506-517.

Devine, S. M., Cobbs, C., Jennings, M., Bartholomew, A., and Hoffman, R. (2003). Mesenchymal stem cells distribute to a wide range of tissues following systemic infusion into nonhuman primates. Blood *101*, 2999-3001.

Dexter, T. M., Spooncer, E., Simmons, P., and Allen, T. D. (1984). Long-term marrow culture: an overview of techniques and experience. Kroc Found Ser *18*, 57-96.

Dexter, T. M., Wright, E. G., Krizsa, F., and Lajtha, L. G. (1977). Regulation of haemopoietic stem cell proliferation in long term bone marrow cultures. Biomedicine *27*, 344-349.

Diaz-Romero, J., Gaillard, J. P., Grogan, S. P., Nesic, D., Trub, T., and Mainil-Varlet, P. (2005). Immunophenotypic analysis of human articular chondrocytes: changes in surface markers associated with cell expansion in monolayer culture. J Cell Physiol *202*, 731-742.
Doherty, M. J., Ashton, B. A., Walsh, S., Beresford, J. N., Grant, M. E., and Canfield, A. E. (1998). Vascular pericytes express osteogenic potential in vitro and in vivo. J Bone Miner Res *13*, 828-838.

Dorshkind, K. (1990). Regulation of hemopoiesis by bone marrow stromal cells and their products. Annu Rev Immunol *8*, 111-137.

Drespe, I. H., Polzhofer, G. K., Turner, A. S., and Grauer, J. N. (2005). Animal models for spinal fusion. Spine J *5*, 209S-216S.

Ducy, P., Desbois, C., Boyce, B., Pinero, G., Story, B., Dunstan, C., Smith, E., Bonadio, J., Goldstein, S., Gundberg, C., *et al.* (1996). Increased bone formation in osteocalcin-deficient mice. Nature *382*, 448-452.

Ducy, P., Zhang, R., Geoffroy, V., Ridall, A. L., and Karsenty, G. (1997). Osf2/Cbfa1: a transcriptional activator of osteoblast differentiation. Cell *89*, 747-754.

Dudley, A. T., Lyons, K. M., and Robertson, E. J. (1995). A requirement for bone morphogenetic protein-7 during development of the mammalian kidney and eye. Genes Dev *9*, 2795-2807.

Duhrsen, U., Martinez, T., Vohwinkel, G., Ergun, S., Sun, L., McMahon, G., Durig, J., Hossfeld, D. K., and Fiedler, W. (2001). Effects of vascular endothelial and platelet-derived growth factor receptor inhibitors on long-term cultures from normal human bone marrow. Growth Factors *19*, 1-17.

Erickson, G. R., Gimble, J. M., Franklin, D. M., Rice, H. E., Awad, H., and Guilak, F. (2002). Chondrogenic potential of adipose tissue-derived stromal cells in vitro and in vivo. Biochem Biophys Res Commun *290*, 763-769.

Eustace, B. K., and Jay, D. G. (2004). Extracellular roles for the molecular chaperone, hsp90. Cell Cycle *3*, 1098-1100.

Eustace, B. K., Sakurai, T., Stewart, J. K., Yimlamai, D., Unger, C., Zehetmeier, C., Lain, B., Torella, C., Henning, S. W., Beste, G., et al. (2004). Functional proteomic screens reveal an essential extracellular role for hsp90 alpha in cancer cell invasiveness. Nat Cell Biol *6*, 507-514.

Eyre, D. (2002). Collagen of articular cartilage. Arthritis Res *4*, 30-35.

Falla, N., Van, V., Bierkens, J., Borremans, B., Schoeters, G., and Van Gorp, U. (1993). Characterization of a 5-fluorouracil-enriched osteoprogenitor population of the murine bone marrow. Blood *82*, 3580-3591.

Fan, H., Hu, Y., Zhang, C., Li, X., Lv, R., Qin, L., and Zhu, R. (2006). Cartilage regeneration using mesenchymal stem cells and a PLGA-gelatin/chondroitin/hyaluronate hybrid scaffold. Biomaterials *27*, 4573-4580.

Fang, M. A., Kujubu, D. A., and Hahn, T. J. (1992). The effects of prostaglandin E2, parathyroid hormone, and epidermal growth factor on mitogenesis, signaling, and primary response genes in UMR 106-01 osteoblast-like cells. Endocrinology *131*, 2113-2119.

Ferrara, N., Carver-Moore, K., Chen, H., Dowd, M., Lu, L., O'Shea, K. S., Powell-Braxton, L., Hillan, K. J., and Moore, M. W. (1996). Heterozygous embryonic lethality induced by targeted inactivation of the VEGF gene. Nature *380*, 439-442.

Ferrara, N., and Davis-Smyth, T. (1997). The biology of vascular endothelial growth factor. Endocr Rev *18*, 4-25.

Filshie, R. J., Zannettino, A. C., Makrynikola, V., Gronthos, S., Henniker, A. J., Bendall, L. J., Gottlieb, D. J., Simmons, P. J., and Bradstock, K. F. (1998). MUC18, a member of the immunoglobulin superfamily, is expressed on bone marrow fibroblasts and a subset of hematological malignancies. Leukemia *12*, 414-421.

Fischer, E. M., Layrolle, P., Van Blitterswijk, C. A., and De Bruijn, J. D. (2003). Bone formation by mesenchymal progenitor cells cultured on dense and microporous hydroxyapatite particles. Tissue Eng *9*, 1179-1188.

Fisher, L. W., Termine, J. D., and Young, M. F. (1989). Deduced protein sequence of bone small proteoglycan I (biglycan) shows homology with proteoglycan II (decorin) and several nonconnective tissue proteins in a variety of species. J Biol Chem *264*, 4571-4576.

Fortier, L. A., Mohammed, H. O., Lust, G., and Nixon, A. J. (2002a). Insulin-like growth factor-I enhances cell-based repair of articular cartilage. J Bone Joint Surg Br *84*, 276-288.

Fortier, L. A., Nixon, A. J., and Lust, G. (2002b). Phenotypic expression of equine articular chondrocytes grown in three-dimensional cultures supplemented with supraphysiologic concentrations of insulin-like growth factor-1. Am J Vet Res *63*, 301-305.

Fortier, L. A., Nixon, A. J., Williams, J., and Cable, C. S. (1998). Isolation and chondrocytic differentiation of equine bone marrow-derived mesenchymal stem cells. Am J Vet Res *59*, 1182-1187.

Foster, B. (1989a) Epiphyseal Plate Repair Using Fat Interposition To Reverse Physeal Deformity, Doctor of Medicine, University of Adelaide, Adelaide.

Foster, B. (1989b) Epiphyseal plate repair using fat interposition to reverse physeal deformity. An Experimental study., M.D., The University of Adelaide, Adelaide.

Foster, B. K., Hansen, A. L., Gibson, G. J., Hopwood, J. J., Binns, G. F., and Wiebkin, O. W. (1990). Reimplantation of growth plate chondrocytes into growth plate defects in sheep. J Orthop Res *8*, 555-564.

Foster, B. K., John, B., and Hasler, C. (2000). Free fat interpositional graft in acute physeal injuries. The anticipatory Langenskiold procedure. J Pediat Orthop *20,* 282-285.

Foster, J. W., Dominguez-Steglich, M. A., Guioli, S., Kowk, G., Weller, P. A., Stevanovic, M., Weissenbach, J., Mansour, S., Young, I. D., Goodfellow, P. N., and et al. (1994). Campomelic dysplasia and autosomal sex reversal caused by mutations in an SRY-related gene. Nature *372*, 525-530.

Fragonas, E., Valente, M., Pozzi-Mucelli, M., Toffanin, R., Rizzo, R., Silvestri, F., and Vittur, F. (2000). Articular cartilage repair in rabbits by using suspensions of allogenic chondrocytes in alginate. Biomaterials *21*, 795-801.

Freed, L. E., Marquis, J. C., Nohria, A., Emmanual, J., Mikos, A. G., and Langer, R. (1993). Neocartilage formation in vitro and in vivo using cells cultured on synthetic biodegradable polymers. J Biomed Mater Res *27*, 11-23.

Freed, L. E., Martin, I., and Vunjak-Novakovic, G. (1999). Frontiers in tissue engineering. In vitro modulation of chondrogenesis. Clin Orthop Relat Res, S46-58.

Frenkel, S. R., and Di Cesare, P. E. (2004). Scaffolds for articular cartilage repair. Ann Biomed Eng *32*, 26-34.

Friedenstein, A. J. (1980). Stromal mechanisms of bone marrow: cloning in vitro and retransplantation in vivo. Haematol Blood Transfus *25*, 19-29.

Friedenstein, A. J., Chailakhjan, R. K., and Lalykina, K. S. (1970). The development of fibroblast colonies in monolayer cultures of guinea-pig bone marrow and spleen cells. Cell Tissue Kinet *3*, 393-403.

Friedenstein, A. J., Chailakhyan, R. K., and Gerasimov, U. V. (1987). Bone marrow osteogenic stem cells: in vitro cultivation and transplantation in diffusion chambers. Cell Tissue Kinet *20*, 263-272.

Friedenstein, A. J., Gorskaja, J. F., and Kulagina, N. N. (1976). Fibroblast precursors in normal and irradiated mouse hematopoietic organs. Exp Hematol *4*, 267-274.

Fromigue, O., Marie, P. J., and Lomri, A. (1998). Bone morphogenetic protein-2 and transforming growth factor-beta2 interact to modulate human bone marrow stromal cell proliferation and differentiation. J Cell Biochem *68*, 411-426.

Frosch, K. H., Drengk, A., Krause, P., Viereck, V., Miosge, N., Werner, C., Schild, D., Sturmer, E. K., and Sturmer, K. M. (2006). Stem cell-coated titanium implants for the partial joint resurfacing of the knee. Biomaterials *27*, 2542-2549.

Fujimoto, E., Ochi, M., Kato, Y., Mochizuki, Y., Sumen, Y., and Ikuta, Y. (1999). Beneficial effect of basic fibroblast growth factor on the repair of full-thickness defects in rabbit articular cartilage. Arch Orthop Trauma Surg *119*, 139-145.

Fukumoto, T., Sperling, J. W., Sanyal, A., Fitzsimmons, J. S., Reinholz, G. G., Conover, C. A., and O'Driscoll, S. W. (2003). Combined effects of insulin-like growth factor-1 and transforming growth factor-beta1 on periosteal mesenchymal cells during chondrogenesis in vitro. Osteoarthritis Cartilage *11*, 55-64.

Galmiche, M. C., Koteliansky, V. E., Briere, J., Herve, P., and Charbord, P. (1993). Stromal cells from human long-term marrow cultures are mesenchymal cells that differentiate following a vascular smooth muscle differentiation pathway. Blood *82*, 66-76.

Gao, J., Dennis, J. E., Solchaga, L. A., Goldberg, V. M., and Caplan, A. I. (2002). Repair of osteochondral defect with tissue-engineered two-phase composite material of injectable calcium phosphate and hyaluronan sponge. Tissue Eng *8*, 827-837.

Garces, G. L., Mugica-Garay, I., Lopez-Gonzalez Coviella, N., and Guerado, E. (1994). Growth-plate modifications after drilling. J Pediatr Orthop *14*, 225-228.

Gerber, H. P., Vu, T. H., Ryan, A. M., Kowalski, J., Werb, Z., and Ferrara, N. (1999). VEGF couples hypertrophic cartilage remodeling, ossification and angiogenesis during endochondral bone formation. Nat Med *5*, 623-628.

Gerstenfeld, L. C., Cullinane, D. M., Barnes, G. L., Graves, D. T., and Einhorn, T. A. (2003). Fracture healing as a post-natal developmental process: molecular, spatial, and temporal aspects of its regulation. J Cell Biochem *88*, 873-884.

Gibson, G. (1998). Active role of chondrocyte apoptosis in endochondral ossification. Microsc Res Tech *43*, 191-204.

Gimble, J. M. (1998). Marrow Stromal Adipocytes. In Marrow Stromal Cell Culture, J. N. Beresford, and M. E. Owen, eds. (Cambridge, Cambridge University Press), pp. 67-87.

Goessler, U. R., Bieback, K., Bugert, P., Heller, T., Sadick, H., Hormann, K., and Riedel, F. (2006). In vitro analysis of integrin expression during chondrogenic differentiation of mesenchymal stem cells and chondrocytes upon dedifferentiation in cell culture. Int J Mol Med *17*, 301-307.

Gori, F., Thomas, T., Hicok, K. C., Spelsberg, T. C., and Riggs, B. L. (1999). Differentiation of human marrow stromal precursor cells: bone morphogenetic protein-2 increases OSF2/CBFA1, enhances osteoblast commitment, and inhibits late adipocyte maturation. J Bone Miner Res *14*, 1522-1535.

Gougos, A., and Letarte, M. (1990). Primary structure of endoglin, an RGD-containing glycoprotein of human endothelial cells. J Biol Chem *265*, 8361-8364.

Grande, D. A., Pitman, M. I., Peterson, L., Menche, D., and Klein, M. (1989). The repair of experimentally produced defects in rabbit articular cartilage by autologous chondrocyte transplantation. J Orthop Res *7*, 208-218.

Green, H., Morikawa, M., and Nixon, T. (1985). A dual effector theory of growth-hormone action. Differentiation *29*, 195-198.

Gress, C. J., and Jacenko, O. (2000). Growth plate compressions and altered hematopoiesis in collagen X null mice. J Cell Biol *149*, 983-993.

Grgic, M., Jelic, M., Basic, V., Basic, N., Pecina, M., and Vukicevic, S. (1997). Regeneration of articular cartilage defects in rabbits by osteogenic protein-1 (bone morphogenetic protein-7). Acta Med Croatica *51*, 23-27.

Grigolo, B., Roseti, L., Fiorini, M., Fini, M., Giavaresi, G., Aldini, N. N., Giardino, R., and Facchini, A. (2001). Transplantation of chondrocytes seeded on a hyaluronan derivative (hyaff-11) into cartilage defects in rabbits. Biomaterials *22*, 2417-2424.

Grogan, S. P., Barbero, A., Diaz-Romero, J., Cleton-Jansen, A. M., Soeder, S., Whiteside, R., Hogendoorn, P. C., Farhadi, J., Aigner, T., Martin, I., and Mainil-Varlet, P. (2007). Identification of markers to characterize and sort human articular chondrocytes with enhanced in vitro chondrogenic capacity. Arthritis Rheum *56*, 586-595.

Gronthos, S., Brahim, J., Li, W., Fisher, L. W., Cherman, N., Boyde, A., DenBesten, P., Robey, P. G., and Shi, S. (2002). Stem cell properties of human dental pulp stem cells. J Dent Res *81*, 531-535.

Gronthos, S., Franklin, D. M., Leddy, H. A., Robey, P. G., Storms, R. W., and Gimble, J. M. (2001a). Surface protein characterization of human adipose tissue-derived stromal cells. J Cell Physiol *189*, 54-63.

Gronthos, S., Graves, S. E., Ohta, S., and Simmons, P. J. (1994). The STRO-1+ fraction of adult human bone marrow contains the osteogenic precursors. Blood *84*, 4164-4173.

Gronthos, S., Mankani, M., Brahim, J., Robey, P. G., and Shi, S. (2000). Postnatal human dental pulp stem cells (DPSCs) in vitro and in vivo. Proc Natl Acad Sci U S A *97*, 13625-13630.

Gronthos, S., and Simmons, P. J. (1995). The growth factor requirements of STRO-1-positive human bone marrow stromal precursors under serum-deprived conditions in vitro. Blood *85*, 929-940.

Gronthos, S., Simmons, P. J., Graves, S. E., and Robey, P. G. (2001b). Integrin-mediated interactions between human bone marrow stromal precursor cells and the extracellular matrix. Bone *28*, 174-181.

Gronthos, S., Stewart, K., Graves, S. E., Hay, S., and Simmons, P. J. (1997). Integrin expression and function on human osteoblast-like cells. J Bone Miner Res *12*, 1189-1197.

Gronthos, S., Zannettino, A. C., Hay, S. J., Shi, S., Graves, S. E., Kortesidis, A., and Simmons, P. J. (2003). Molecular and cellular characterisation of highly purified stromal stem cells derived from human bone marrow. J Cell Sci *116*, 1827-1835.

Grundmann, K., Zimmermann, B., Barrach, H. J., and Merker, H. J. (1980). Behaviour of epiphyseal mouse chondrocyte populations in monolayer culture. Morphological and immunohistochemical studies. Virchows Arch Pathol Anat *389*, 167-187.

Gupta, M. C., Theerajunyaporn, T., Maitra, S., Schmidt, M. B., Holy, C. E., Kadiyala, S., and Bruder, S. P. (2007). Efficacy of mesenchymal stem cell enriched grafts in an ovine posterolateral lumbar spine model. Spine *32*, 720-726; discussion 727.

Haaijman, A., Burger, E. H., Goei, S. W., Nelles, L., ten Dijke, P., Huylebroeck, D., and Bronckers, A. L. (2000). Correlation between ALK-6 (BMPR-IB) distribution and responsiveness to osteogenic protein-1 (BMP-7) in embryonic mouse bone rudiments. Growth Factors *17*, 177-192.

Haisch, A., Klaring, S., Groger, A., Gebert, C., and Sittinger, M. (2002). A tissue-engineering model for the manufacture of auricular-shaped cartilage implants. Eur Arch Otorhinolaryngol *259*, 316-321.

Hansen, A. L., Foster, B. K., Gibson, G. J., Binns, G. F., Wiebkin, O. W., and Hopwood, J. J. (1990). Growth-plate chondrocyte cultures for reimplantation into growth-plate defects in sheep. Characterization of cultures. Clin Orthop *256*, 286-298.

Hasler, C. C., and Foster, B. K. (2002). Secondary tethers after physeal bar resection: a common source of failure? Clin Orthop Relat Res, 242-249.

Hata, R., Hori, H., Nagai, Y., Tanaka, S., Kondo, M., Hiramatsu, M., Utsumi, N., and Kumegawa, M. (1984). Selective inhibition of type I collagen synthesis in osteoblastic cells by epidermal growth factor. Endocrinology *115*, 867-876.

Haudenschild, D. R., McPherson, J. M., Tubo, R., and Binette, F. (2001). Differential expression of multiple genes during articular chondrocyte redifferentiation. Anat Rec *263*, 91-98.

Haynesworth, S. E., Baber, M. A., and Caplan, A. I. (1992a). Cell surface antigens on human marrow-derived mesenchymal cells are detected by monoclonal antibodies. Bone *13*, 69-80.

Haynesworth, S. E., Baber, M. A., and Caplan, A. I. (1996). Cytokine expression by human marrow-derived mesenchymal progenitor cells in vitro: effects of dexamethasone and IL-1 alpha. J Cell Physiol *166*, 585-592.

Haynesworth, S. E., Goshima, J., Goldberg, V. M., and Caplan, A. I. (1992b). Characterization of cells with osteogenic potential from human marrow. Bone *13*, 81-88.

Hellstrom, M., Kalen, M., Lindahl, P., Abramsson, A., and Betsholtz, C. (1999). Role of PDGF-B and PDGFR-beta in recruitment of vascular smooth muscle cells and pericytes during embryonic blood vessel formation in the mouse. Development *126*, 3047-3055.

Hendrickson, D. A., Nixon, A. J., Grande, D. A., Todhunter, R. J., Minor, R. M., Erb, H., and Lust, G. (1994). Chondrocyte-fibrin matrix transplants for resurfacing extensive articular cartilage defects. J Orthop Res *12*, 485-497.

Hidaka, C., Goodrich, L. R., Chen, C. T., Warren, R. F., Crystal, R. G., and Nixon, A. J. (2003). Acceleration of cartilage repair by genetically modified chondrocytes over expressing bone morphogenetic protein-7. J Orthop Res *21*, 573-583.

Hildebrand, A., Romaris, M., Rasmussen, L. M., Heinegard, D., Twardzik, D. R., Border, W. A., and Ruoslahti, E. (1994). Interaction of the small interstitial proteoglycans biglycan, decorin and fibromodulin with transforming growth factor beta. Biochem J *302*, 527-534.

Hiraki, Y., Shukunami, C., Iyama, K., and Mizuta, H. (2001). Differentiation of chondrogenic precursor cells during the regeneration of articular cartilage. Osteoarthritis Cartilage *9 Suppl A*, S102-108.

Horner, A., Bishop, N. J., Bord, S., Beeton, C., Kelsall, A. W., Coleman, N., and Compston, J. E. (1999). Immunolocalisation of vascular endothelial growth factor (VEGF) in human neonatal growth plate cartilage. J Anat *194 (Pt 4)*, 519-524.

Hoshi, K., Komori, T., and Ozawa, H. (1999). Morphological characterization of skeletal cells in Cbfa1-deficient mice. Bone *25*, 639-651.

Hoshikawa, A., Nakayama, Y., Matsuda, T., Oda, H., Nakamura, K., and Mabuchi, K. (2006). Encapsulation of chondrocytes in photopolymerizable styrenated gelatin for cartilage tissue engineering. Tissue Eng *12*, 2333-2341.

Hou, L., Cao, H., Wang, D., Wei, G., Bai, C., Zhang, Y., and Pei, X. (2003). Induction of umbilical cord blood mesenchymal stem cells into neuron-like cells in vitro. Int J Hematol *78*, 256-261.

Huang, C. Y., Reuben, P. M., D'Ippolito, G., Schiller, P. C., and Cheung, H. S. (2004). Chondrogenesis of human bone marrow-derived mesenchymal stem cells in agarose culture. Anat Rec A Discov Mol Cell Evol Biol *278*, 428-436.

Huang, J. I., Kazmi, N., Durbhakula, M. M., Hering, T. M., Yoo, J. U., and Johnstone, B. (2005). Chondrogenic potential of progenitor cells derived from human bone marrow and adipose tissue: a patient-matched comparison. J Orthop Res *23*, 1383-1389.

Huang, L., Solursh, M., and Sandra, A. (1996). The role of transforming growth factor alpha in rat craniofacial development and chondrogenesis. J Anat *189 (Pt 1)*, 73-86.

Huang, S., and Terstappen, L. W. (1992). Formation of haematopoietic microenvironment and haematopoietic stem cells from single human bone marrow stem cells. Nature *360*, 745-749.

Huang, W., Chung, U. I., Kronenberg, H. M., and de Crombrugghe, B. (2001). The chondrogenic transcription factor Sox9 is a target of signaling by the parathyroid hormone-related peptide in the growth plate of endochondral bones. Proc Natl Acad Sci U S A *98*, 160-165.

Hui, J. H., Li, L., Teo, Y. H., Ouyang, H. W., and Lee, E. H. (2005). Comparative study of the ability of mesenchymal stem cells derived from bone marrow, periosteum, and adipose tissue in treatment of partial growth arrest in rabbit. Tissue Eng *11*, 904-912.

Hunziker, E. B. (1994). Mechanism of longitudinal bone growth and its regulation by growth plate chondrocytes. Microsc Res Tech *28*, 505-519.

Hunziker, E. B. (2002). Articular cartilage repair: basic science and clinical progress. A review of the current status and prospects. Osteoarthritis Cartilage *10*, 432-463.

Hunziker, E. B., Driesang, I. M., and Morris, E. A. (2001). Chondrogenesis in cartilage repair is induced by members of the transforming growth factor-beta superfamily. Clin Orthop, S171-181.

Hunziker, E. B., Wagner, J., and Zapf, J. (1994). Differential effects of insulin-like growth factor I and growth hormone on developmental stages of rat growth plate chondrocytes in vivo. J Clin Invest *93*, 1078-1086.

Hutmacher, D. W., Ng, K. W., Kaps, C., Sittinger, M., and Klaring, S. (2003). Elastic cartilage engineering using novel scaffold architectures in combination with a biomimetic cell carrier. Biomaterials *24*, 4445-4458.

Hwang, N. S., Varghese, S., Puleo, C., Zhang, Z., and Elisseeff, J. (2007). Morphogenetic signals from chondrocytes promote chondrogenic and osteogenic differentiation of mesenchymal stem cells. J Cell Physiol *212*, 281-284.

Hynes, R. O. (1992). Integrins: versatility, modulation, and signaling in cell adhesion. Cell *69*, 11-25.

Iannotti, J. P. (1990). Growth plate physiology and pathology. Orthop Clin North Am *21*, 1-17.

Iannotti, J. P., Goldstein, S., Kuhn, J., Lipiello, L., and Kaplan, F. S. (1994). Growth Plate and Bone Development. In Orthopaedic Basic Science, S. R. Simon, ed. (American Academy of Orthopaedic Surgeons), pp. 185-217.

Ilizarov, G. A. (1990). Clinical application of the tension-stress effect for limb lengthening. Clin Orthop Relat Res, 8-26.

Ilizarov, G. A., and Frankel, V. H. (1988). The Ilizarov External Fixator, a physiologic method of orthopaedic reconstruction and skeletal correction. A conversation with Prof. G. A. Ilizarov and Victor H. Frankel. Orthop Rev *17*, 1142-1154.

Im, G. I., Kim, D. Y., Shin, J. H., Hyun, C. W., and Cho, W. H. (2001). Repair of cartilage defect in the rabbit with cultured mesenchymal stem cells from bone marrow. J Bone Joint Surg Br *83*, 289-294.

Imabayashi, H., Mori, T., Gojo, S., Kiyono, T., Sugiyama, T., Irie, R., Isogai, T., Hata, J., Toyama, Y., and Umezawa, A. (2003). Redifferentiation of dedifferentiated chondrocytes and chondrogenesis of human bone marrow stromal cells via chondrosphere formation with expression profiling by large-scale cDNA analysis. Exp Cell Res *288*, 35-50.

Inada, M., Yasui, T., Nomura, S., Miyake, S., Deguchi, K., Himeno, M., Sato, M., Yamagiwa, H., Kimura, T., Yasui, N., et al. (1999). Maturational disturbance of chondrocytes in Cbfa1-deficient mice. Dev Dyn *214*, 279-290.

Indrawattana, N., Chen, G., Tadokoro, M., Shann, L. H., Ohgushi, H., Tateishi, T., Tanaka, J., and Bunyaratvej, A. (2004). Growth factor combination for chondrogenic induction from human mesenchymal stem cell. Biochem Biophys Res Commun *320*, 914-919.

Ingram, R. T., Bonde, S. K., Riggs, B. L., and Fitzpatrick, L. A. (1994). Effects of transforming growth factor beta (TGF beta) and 1,25 dihydroxyvitamin D3 on the function, cytochemistry and morphology of normal human osteoblast-like cells. Differentiation *55*, 153-163.

Ishizu, A., Ishikura, H., Nakamaru, Y., Takeuchi, E., Kimura, C., Koike, T., and Yoshiki, T. (1995). Thy-1 induced on rat endothelium regulates vascular permeability at sites of inflammation. Int Immunol *7*, 1939-1947.

Jacenko, O., LuValle, P. A., and Olsen, B. R. (1993). Spondylometaphyseal dysplasia in mice carrying a dominant negative mutation in a matrix protein specific for cartilage-to-bone transition. Nature *365*, 56-61

Jackson, R. L., Busch, S. J., and Cardin, A. D. (1991). Glycosaminoglycans: molecular properties, protein interactions, and role in physiological processes. Physiol Rev *71*, 481-539.

Jaramillo, D., Shapiro, F., Hoffer, F. A., Winalski, C. S., Koskinen, M. F., Frasso, R., and Johnson, A. (1990). Posttraumatic growth-plate abnormalities: MR imaging of bony-bridge formation in rabbits. Radiology *175*, 767-773.

Javazon, E. H., Colter, D. C., Schwarz, E. J., and Prockop, D. J. (2001). Rat marrow stromal cells are more sensitive to plating density and expand more rapidly from single-cell-derived colonies than human marrow stromal cells. Stem Cells *19*, 219-225.

Jelic, M., Pecina, M., Haspl, M., Kos, J., Taylor, K., Maticic, D., McCartney, J., Yin, S., Rueger, D., and Vukicevic, S. (2001). Regeneration of articular cartilage chondral defects by osteogenic protein-1 (bone morphogenetic protein-7) in sheep. Growth Factors *19*, 101-113.

Jessop, H. L., Noble, B. S., and Cryer, A. (1994). The differentiation of a potential mesenchymal stem cell population within ovine bone marrow. Biochem Soc Trans *22*, 248S.

Jiang, X., Cui, P. C., Chen, W. X., and Zhang, Z. P. (2003a). [In vivo chondrogenesis of induced human marrow mesenchymal stem cells in nude mice]. Di Yi Jun Yi Da Xue Xue Bao *23*, 766-769, 773.

Jiang, Y., Henderson, D., Blackstad, M., Chen, A., Miller, R. F., and Verfaillie, C. M. (2003b). Neuroectodermal differentiation from mouse multipotent adult progenitor cells. Proc Natl Acad Sci U S A *100 Suppl 1*, 11854-11860.

Jiang, Y., Vaessen, B., Lenvik, T., Blackstad, M., Reyes, M., and Verfaillie, C. M. (2002). Multipotent progenitor cells can be isolated from postnatal murine bone marrow, muscle, and brain. Exp Hematol *30*, 896-904.

Jin, X. B., Luo, Z. J., and Wang, J. (2006). Treatment of rabbit growth plate injuries with an autologous tissue-engineered composite. An experimental study. Cells Tissues Organs *183*, 62-67.

Jingushi, S., Scully, S. P., Joyce, M. E., Sugioka, Y., and Bolander, M. E. (1995). Transforming growth factor-beta 1 and fibroblast growth factors in rat growth plate. J Orthop Res *13*, 761-768.

Johnson, A., and Dorshkind, K. (1986). Stromal cells in myeloid and lymphoid long-term bone marrow cultures can support multiple hemopoietic lineages and modulate their production of hemopoietic growth factors. Blood *68*, 1348-1354.

Johnstone, B., Hering, T. M., Caplan, A. I., Goldberg, V. M., and Yoo, J. U. (1998). In vitro chondrogenesis of bone marrow-derived mesenchymal progenitor cells. Exp Cell Res *238*, 265-272.

Johnstone, E. W., McArthur, M., Solly, P. B., Higginson, K., Byers, S., and Foster, B. K. (2002). The effect of osteogenic protein-1 in an in vivo physeal injury model. Clin Orthop, 234-240.

Joyner, C. J., Bennett, A., and Triffitt, J. T. (1997). Identification and enrichment of human osteoprogenitor cells by using differentiation stage-specific monoclonal antibodies. Bone *21*, 1-6.

Kadiyala, S., Young, R. G., Thiede, M. A., and Bruder, S. P. (1997). Culture expanded canine mesenchymal stem cells possess osteochondrogenic potential in vivo and in vitro. Cell Transplant *6*, 125-134.

Kaneko, S., Motomura, S., and Ibayashi, H. (1982). Differentiation of human bone marrow-derived fibroblastoid colony forming cells (CFU-F) and their roles in haemopoiesis in vitro. Br J Haematol *51*, 217-225.

Kaplan, F. S., Hayes, W. C., Keaveny, T. M., Boskey, A., Einhorn, T. A., and Iannotti, J. P. (1994). Form and Function of Bone. In Orthopaedic Basic Science, S. R. Simon, ed. (American Academy of Orthopaedic Surgeons), pp. 127-184.

Kaps, C., Frauenschuh, S., Endres, M., Ringe, J., Haisch, A., Lauber, J., Buer, J., Krenn, V., Haupl, T., Burmester, G. R., and Sittinger, M. (2006). Gene expression profiling of human articular cartilage grafts generated by tissue engineering. Biomaterials *27*, 3617-3630.

Karaplis, A. C., Luz, A., Glowacki, J., Bronson, R. T., Tybulewicz, V. L., Kronenberg, H. M., and Mulligan, R. C. (1994). Lethal skeletal dysplasia from targeted disruption of the parathyroid hormone-related peptide gene. Genes Dev *8*, 277-289.

Kavalkovich, K. W., Boynton, R. E., Murphy, J. M., and Barry, F. (2002). Chondrogenic differentiation of human mesenchymal stem cells within an alginate layer culture system. In Vitro Cell Dev Biol Anim *38*, 457-466.

Kayakabe, M., Tsutsumi, S., Watanabe, H., Kato, Y., and Takagishi, K. (2006). Transplantation of autologous rabbit BM-derived mesenchymal stromal cells embedded in hyaluronic acid gel sponge into osteochondral defects of the knee. Cytotherapy *8*, 343-353.

Kerr, J. B. (1999). Atlas of Functional Histology (London, Mosby International).

Kielty, C. M., Kwan, A. P., Holmes, D. F., Schor, S. L., and Grant, M. E. (1985). Type X collagen, a product of hypertrophic chondrocytes. Biochem J *227*, 545-554.

Kim, I. S., Otto, F., Zabel, B., and Mundlos, S. (1999). Regulation of chondrocyte differentiation by Cbfa1. Mech Dev *80*, 159-170.

Kimata, K., Barrach, H. J., Brown, K. S., and Pennypacker, J. P. (1981). Absence of proteoglycan core protein in cartilage from the cmd/cmd (cartilage matrix deficiency) mouse. J Biol Chem *256*, 6961-6968.

Kimura, A., Katoh, O., and Kuramoto, A. (1988). Effects of platelet derived growth factor, epidermal growth factor and transforming growth factor-beta on the growth of human marrow fibroblasts. Br J Haematol *69*, 9-12.

Kirsch, T., and von der Mark, K. (1990). Isolation of bovine type X collagen and immunolocalization in growth-plate cartilage. Biochem J *265*, 453-459.

Knospe, W. H., Blom, J., and Crosby, W. H. (1966). Regeneration of locally irradiated bone marrow. I. Dose dependent, long-term changes in the rat, with particular emphasis upon vascular and stromal reaction. Blood *28*, 398-415.

Knospe, W. H., Gregory, S. A., Husseini, S. G., Fried, W., and Trobaugh, F. E., Jr. (1972). Origin and recovery of colony-forming units in locally curetted bone marrow of mice. Blood *39*, 331-340.

Knudson, C. B., and Knudson, W. (2001). Cartilage proteoglycans. Semin Cell Dev Biol *12*, 69-78.

Komori, T., Yagi, H., Nomura, S., Yamaguchi, A., Sasaki, K., Deguchi, K., Shimizu, Y., Bronson, R. T., Gao, Y. H., Inada, M., et al. (1997). Targeted disruption of Cbfa1 results in a complete lack of bone formation owing to maturational arrest of osteoblasts. Cell *89*, 755-764.

Kon, E., Muraglia, A., Corsi, A., Bianco, P., Marcacci, M., Martin, I., Boyde, A., Ruspantini, I., Chistolini, P., Rocca, M., et al. (2000). Autologous bone marrow stromal cells loaded onto porous hydroxyapatite ceramic accelerate bone repair in critical-size defects of sheep long bones. J Biomed Mater Res *49*, 328-337.

Kopen, G. C., Prockop, D. J., and Phinney, D. G. (1999). Marrow stromal cells migrate throughout forebrain and cerebellum, and they differentiate into astrocytes after injection into neonatal mouse brains. Proc Natl Acad Sci U S A *96*, 10711-10716.

Korbling, M., Robinson, S., Estrov, Z., Champlin, R., and Shpall, E. (2005). Umbilical cord blood-derived cells for tissue repair. Cytotherapy *7*, 258-261.

Krampera, M., Pasini, A., Rigo, A., Scupoli, M. T., Tecchio, C., Malpeli, G., Scarpa, A., Dazzi, F., Pizzolo, G., and Vinante, F. (2005). HB-EGF/HER-1 signaling in bone marrow mesenchymal stem cells: inducing cell expansion and reversibly preventing multilineage differentiation. Blood *106*, 59-66.

Krebsbach, P. H., Mankani, M. H., Satomura, K., Kuznetsov, S. A., and Robey, P. G. (1998). Repair of craniotomy defects using bone marrow stromal cells. Transplantation *66*, 1272-1278.

Kronenberg, H. M. (2003). Developmental regulation of the growth plate. Nature *423*, 332-336.

Kronenberg, H. M., Lanske, B., Kovacs, C. S., Chung, U. I., Lee, K., Segre, G. V., Schipani, E., and Juppner, H. (1998). Functional analysis of the PTH/PTHrP network of ligands and receptors. Recent Prog Horm Res *53*, 283-301; discussion 301-283.

Kumegawa, M., Hiramatsu, M., Hatakeyama, K., Yajima, T., Kodama, H., Osaki, T., and Kurisu, K. (1983). Effects of epidermal growth factor on osteoblastic cells in vitro. Calcif Tissue Int *35*, 542-548.

Kuo, A. C., Rodrigo, J. J., Reddi, A. H., Curtiss, S., Grotkopp, E., and Chiu, M. (2006). Microfracture and bone morphogenetic protein 7 (BMP-7) synergistically stimulate articular cartilage repair. Osteoarthritis Cartilage *14*, 1126-1135.

Kuznetsov, S., and Gehron Robey, P. (1996). Species differences in growth requirements for bone marrow stromal fibroblast colony formation In vitro. Calcif Tissue Int *59*, 265-270.

Kuznetsov, S. A., Krebsbach, P. H., Satomura, K., Kerr, J., Riminucci, M., Benayahu, D., and Robey, P. G. (1997). Single-colony derived strains of human marrow stromal fibroblasts form bone after transplantation in vivo. J Bone Miner Res *12*, 1335-1347.

Kuznetsov, S. A., Mankani, M. H., Gronthos, S., Satomura, K., Bianco, P., and Robey, P. G. (2001). Circulating skeletal stem cells. J Cell Biol *153*, 1133-1140.

Kwan, K. M., Pang, M. K., Zhou, S., Cowan, S. K., Kong, R. Y., Pfordte, T., Olsen, B. R., Sillence, D. O., Tam, P. P., and Cheah, K. S. (1997). Abnormal compartmentalization of cartilage matrix components in mice lacking collagen X: implications for function. J Cell Biol *136*, 459-471.

Lacey, D. L., Timms, E., Tan, H. L., Kelley, M. J., Dunstan, C. R., Burgess, T., Elliott, R., Colombero, A., Elliott, G., Scully, S., et al. (1998). Osteoprotegerin ligand is a cytokine that regulates osteoclast differentiation and activation. Cell *93*, 165-176.

Lane, T. F., and Sage, E. H. (1994). The biology of SPARC, a protein that modulates cell-matrix interactions. Faseb J *8*, 163-173.

Langenskiold, A. (1975). An operation for partial closure of an epiphysial plate in children, and its experimental basis. J Bone Joint Surg Br *57*, 325-330.

Langenskiold, A. (1981). Surgical treatment of partial closure of the growth plate. J Pediatr Orthop *1*, 3-11.

Langenskiold, A., and Osterman, K. (1979). Surgical treatment of partial closure of the epiphysial plate. Reconstr Surg Traumatol *17*, 48-64.

Lansdorp, P. M. (1995). Telomere length and proliferation potential of hematopoietic stem cells. J Cell Sci *108 (Pt 1)*, 1-6.

Leach, R. M., Jr., Sokol, C., and McMurtry, J. P. (1997). Immunolocalization of basic fibroblast growth factor in porcine epiphyseal growth plate. Domest Anim Endocrinol *14*, 129-132.

Lee, B., Thirunavukkarasu, K., Zhou, L., Pastore, L., Baldini, A., Hecht, J., Geoffroy, V., Ducy, P., and Karsenty, G. (1997). Missense mutations abolishing DNA binding of the osteoblast-specific transcription factor OSF2/CBFA1 in cleidocranial dysplasia. Nat Genet *16*, 307-310.

Lee, C. W., Martinek, V., Usas, A., Musgrave, D., Pickvance, E. A., Robbins, P., Moreland, M. S., Fu, F. H., and Huard, J. (2002). Muscle-based gene therapy and tissue engineering for treatment of growth plate injuries. J Pediatr Orthop *22*, 565-572.

Lee, D. C., Rose, T. M., Webb, N. R., and Todaro, G. J. (1985). Cloning and sequence analysis of a cDNA for rat transforming growth factor-alpha. Nature *313*, 489-491.

Lee, E. H., Chen, F., Chan, J., and Bose, K. (1998). Treatment of growth arrest by transfer of cultured chondrocytes into physeal defects. J Pediatr Orthop *18*, 155-160.

Lee, K., Lanske, B., Karaplis, A. C., Deeds, J. D., Kohno, H., Nissenson, R. A., Kronenberg, H. M., and Segre, G. V. (1996). Parathyroid hormone-related peptide delays terminal differentiation of chondrocytes during endochondral bone development. Endocrinology *137*, 5109-5118.

Lee, M. A., Nissen, T. P., and Otsuka, N. Y. (2000). Ultilization of a murine model to investigate the molecular process of transphyseal bone formation. J Pedeatr Orthop *20*, 802-806.

Lefebvre, V., Behringer, R. R., and de Crombrugghe, B. (2001). L-Sox5, Sox6 and Sox9 control essential steps of the chondrocyte differentiation pathway. Osteoarthritis Cartilage *9 Suppl A*, S69-75.

Lennon, D. P., and Caplan, A. I. (2006). Isolation of rat marrow-derived mesenchymal stem cells. Exp Hematol *34*, 1606-1607.

Li, L., Hui, J. H., Goh, J. C., Chen, F., and Lee, E. H. (2004). Chitin as a scaffold for mesenchymal stem cells transfers in the treatment of partial growth arrest. J Pediatr Orthop *24*, 205-210.

Li, S. W., Prockop, D. J., Helminen, H., Fassler, R., Lapvetelainen, T., Kiraly, K., Peltarri, A., Arokoski, J., Lui, H., Arita, M., and et al. (1995). Transgenic mice with targeted inactivation of the Col2 alpha 1 gene for collagen II develop a skeleton with membranous and periosteal bone but no endochondral bone. Genes Dev *9*, 2821-2830.

Li, W. J., Tuli, R., Huang, X., Laquerriere, P., and Tuan, R. S. (2005a). Multilineage differentiation of human mesenchymal stem cells in a three-dimensional nanofibrous scaffold. Biomaterials *26*, 5158-5166.

Li, Z., Yang, Y., Wang, C., Xia, R., Zhang, Y., Zhao, Q., Liao, W., Wang, Y., and Lu, J. (2005b). Repair of sheep metatarsus defects by using tissue-engineering technique. J Huazhong Univ Sci Technolog Med Sci *25*, 62-67.

Lichtman, M. A. (1981). The ultrastructure of the hemopoietic environment of the marrow: a review. Exp Hematol *9*, 391-410.

Lin, Z., Willers, C., Xu, J., and Zheng, M. H. (2006). The chondrocyte: biology and clinical application. Tissue Eng *12*, 1971-1984.

Lisignoli, G., Cristino, S., Piacentini, A., Toneguzzi, S., Grassi, F., Cavallo, C., Zini, N., Solimando, L., Mario Maraldi, N., and Facchini, A. (2005). Cellular and molecular events during chondrogenesis of human mesenchymal stromal cells grown in a three-dimensional hyaluronan based scaffold. Biomaterials *26*, 5677-5686.

Liu, Y., Chen, F., Liu, W., Cui, L., Shang, Q., Xia, W., Wang, J., Cui, Y., Yang, G., Liu, D., et al. (2002). Repairing large porcine full-thickness defects of articular cartilage using autologous chondrocyte-engineered cartilage. Tissue Eng *8*, 709-721.

Liu, Y., Shu, X. Z., and Prestwich, G. D. (2006). Osteochondral defect repair with autologous bone marrow-derived mesenchymal stem cells in an injectable, in situ, cross-linked synthetic extracellular matrix. Tissue Eng *12*, 3405-3416.

Locklin, R. M., Williamson, M. C., Beresford, J. N., Triffitt, J. T., and Owen, M. E. (1995). In vitro effects of growth factors and dexamethasone on rat marrow stromal cells. Clin Orthop Relat Res, 27-35.

Loeser, R. F., Sadiev, S., Tan, L., and Goldring, M. B. (2000). Integrin expression by primary and immortalized human chondrocytes: evidence of a differential role for alpha1beta1 and alpha2beta1 integrins in mediating chondrocyte adhesion to types II and VI collagen. Osteoarthritis Cartilage *8*, 96-105.

Lomri, A., and Marie, P. J. (1990). Effects of transforming growth factor type beta on expression of cytoskeletal proteins in endosteal mouse osteoblastic cells. Bone *11*, 445-451.

Louwerse, R. T., Heyligers, I. C., Klein-Nulend, J., Sugihara, S., van Kampen, G. P., Semeins, C. M., Goei, S. W., de Koning, M. H., Wuisman, P. I., and Burger, E. H. (2000). Use of recombinant human osteogenic protein-1 for the repair of subchondral defects in articular cartilage in goats. J Biomed Mater Res *49*, 506-516.

Lui, V. C., Ng, L. J., Nicholls, J., Tam, P. P., and Cheah, K. S. (1995). Tissue-specific and differential expression of alternatively spliced alpha 1(II) collagen mRNAs in early human embryos. Dev Dyn *203*, 198-211.

Luo, G., Ducy, P., McKee, M. D., Pinero, G. J., Loyer, E., Behringer, R. R., and Karsenty, G. (1997). Spontaneous calcification of arteries and cartilage in mice lacking matrix GLA protein. Nature *385*, 78-81.

Luo, G., Hofmann, C., Bronckers, A. L., Sohocki, M., Bradley, A., and Karsenty, G. (1995). BMP-7 is an inducer of nephrogenesis, and is also required for eye development and skeletal patterning. Genes Dev *9*, 2808-2820.

LuValle, P., Daniels, K., Hay, E. D., and Olsen, B. R. (1992). Type X collagen is transcriptionally activated and specifically localized during sternal cartilage maturation. Matrix *12*, 404-413.

Luyten, F. P., Dell'Accio, F., and De Bari, C. (2001). Skeletal tissue engineering: opportunities and challenges. Best Pract Res Clin Rheumatol *15*, 759-769.

Mackay, A. M., Beck, S. C., Murphy, J. M., Barry, F. P., Chichester, C. O., and Pittenger, M. F. (1998). Chondrogenic differentiation of cultured human mesenchymal stem cells from marrow. Tissue Eng *4*, 415-428.

Majumdar, M. K., Banks, V., Peluso, D. P., and Morris, E. A. (2000). Isolation, characterization, and chondrogenic potential of human bone marrow-derived multipotential stromal cells. J Cell Physiol *185*, 98-106.

Majumdar, M. K., Keane-Moore, M., Buyaner, D., Hardy, W. B., Moorman, M. A., McIntosh, K. R., and Mosca, J. D. (2003). Characterization and functionality of cell surface molecules on human mesenchymal stem cells. J Biomed Sci *10*, 228-241.

Majumdar, M. K., Thiede, M. A., Mosca, J. D., Moorman, M., and Gerson, S. L. (1998). Phenotypic and functional comparison of cultures of marrow-derived mesenchymal stem cells (MSCs) and stromal cells. J Cell Physiol *176*, 57-66.

Majumdar, M. K., Wang, E., and Morris, E. A. (2001). BMP-2 and BMP-9 promotes chondrogenic differentiation of human multipotential mesenchymal cells and overcomes the inhibitory effect of IL-1. J Cell Physiol *189*, 275-284.

Makower, A. M., Wroblewski, J., and Pawlowski, A. (1989). Effects of IGF-I, rGH, FGF, EGF and NCS on DNA-synthesis, cell proliferation and morphology of chondrocytes isolated from rat rib growth cartilage. Cell Biol Int Rep *13*, 259-270.

Malemud, C. J. (2006). Matrix metalloproteinases: role in skeletal development and growth plate disorders. Front Biosci *11*, 1702-1715.

Mancilla, E. E., De Luca, F., Uyeda, J. A., Czerwiec, F. S., and Baron, J. (1998). Effects of fibroblast growth factor-2 on longitudinal bone growth. Endocrinology *139*, 2900-2904.

Mankin, H. J., Mow, V. C., Buckwalter, J. A., Iannotti, J. P., and Ratcliffe, A. (1994). Form and Function of Articular Cartilage. In Orthopaedic Basic Science, S. R. Simon, ed. (American Academy of Orthopaedic Surgeons), pp. 1-44.

Mann, D. C., and Rajmaira, S. (1990). Distribution of physeal and nonphyseal fractures in 2,650 long-bone fractures in children aged 0-16 years. J Pediatr Orthop *10*, 713-716.

Marijnissen, W. J., van Osch, G. J., Aigner, J., van der Veen, S. W., Hollander, A. P., Verwoerd-Verhoef, H. L., and Verhaar, J. A. (2002). Alginate as a chondrocyte-delivery substance in combination with a non-woven scaffold for cartilage tissue engineering. Biomaterials *23*, 1511-1517.

Marijnissen, W. J., van Osch, G. J., Aigner, J., Verwoerd-Verhoef, H. L., and Verhaar, J. A. (2000). Tissue-engineered cartilage using serially passaged articular chondrocytes. Chondrocytes in alginate, combined in vivo with a synthetic (E210) or biologic biodegradable carrier (DBM). Biomaterials *21*, 571-580.

Martin, D. R., Cox, N. R., Hathcock, T. L., Niemeyer, G. P., and Baker, H. J. (2002). Isolation and characterization of multipotential mesenchymal stem cells from feline bone marrow. Exp Hematol *30*, 879-886.

Mason, J. C., Yarwood, H., Tarnok, A., Sugars, K., Harrison, A. A., Robinson, P. J., and Haskard, D. O. (1996). Human Thy-1 is cytokine-inducible on vascular endothelial cells and is a signaling molecule regulated by protein kinase C. J Immunol *157*, 874-883.

Mastrogiacomo, M., Cancedda, R., and Quarto, R. (2001). Effect of different growth factors on the chondrogenic potential of human bone marrow stromal cells. Osteoarthritis Cartilage *9*, S36-40.

Matsunaga, S., Yamamoto, T., and Fukumura, K. (1999). Temporal and spatial expressions of transforming growth factor-betas and their receptors in epiphyseal growth plate. Int J Oncol *14*, 1063-1067.

McKee, M. D., Glimcher, M. J., and Nanci, A. (1992). High-resolution immunolocalization of osteopontin and osteocalcin in bone and cartilage during endochondral ossification in the chicken tibia. Anat Rec *234*, 479-492.

McSheehy, P. M., and Chambers, T. J. (1986a). Osteoblastic cells mediate osteoclastic responsiveness to parathyroid hormone. Endocrinology *118*, 824-828.

McSheehy, P. M., and Chambers, T. J. (1986b). Osteoblast-like cells in the presence of parathyroid hormone release soluble factor that stimulates osteoclastic bone resorption. Endocrinology *119*, 1654-1659.

Middleton, J. F., and Tyler, J. A. (1992). Upregulation of insulin-like growth factor I gene expression in the lesions of osteoarthritic human articular cartilage. Ann Rheum Dis *51*, 440-447.

Migliaccio, A. R., Migliaccio, G., and Adamson, J. W. (1988). Effect of recombinant hematopoietic growth factors on proliferation of human marrow progenitor cells in serum-deprived liquid culture. Blood *72*, 1387-1392.

Minina, E., Kreschel, C., Naski, M. C., Ornitz, D. M., and Vortkamp, A. (2002). Interaction of FGF, Ihh/Pthlh, and BMP signaling integrates chondrocyte proliferation and hypertrophic differentiation. Dev Cell *3*, 439-449.

Minina, E., Wenzel, H. M., Kreschel, C., Karp, S., Gaffield, W., McMahon, A. P., and Vortkamp, A. (2001). BMP and Ihh/PTHrP signaling interact to coordinate chondrocyte proliferation and differentiation. Development *128*, 4523-4534.

Mitlak, B. H., Finkelman, R. D., Hill, E. L., Li, J., Martin, B., Smith, T., D'Andrea, M., Antoniades, H. N., and Lynch, S. E. (1996). The effect of systemically administered PDGF-BB on the rodent skeleton. J Bone Miner Res *11*, 238-247.

Miura, M., Gronthos, S., Zhao, M., Lu, B., Fisher, L. W., Robey, P. G., and Shi, S. (2003). SHED: stem cells from human exfoliated deciduous teeth. Proc Natl Acad Sci U S A *100*, 5807-5812.

Miyazono, K., Maeda, S., and Imamura, T. (2004). Coordinate regulation of cell growth and differentiation by TGF-beta superfamily and Runx proteins. Oncogene *23*, 4232-4237.

Mizuta, T., Benson, W. M., Foster, B. K., Paterson, D. C., and Morris, L. L. (1987). Statistical analysis of the incidence of physeal injuries. J Pediatr Orthop *7*, 518-523.

Moscoso, I., Centeno, A., Lopez, E., Rodriguez-Barbosa, J. I., Santamarina, I., Filgueira, P., Sanchez, M. J., Dominguez-Perles, R., Penuelas-Rivas, G., and Domenech, N. (2005). Differentiation "in vitro" of primary and immortalized porcine mesenchymal stem cells into cardiomyocytes for cell transplantation. Transplant Proc *37*, 481-482.

Moseley, C. F. (1987). Leg length discrepancy. Orthop Clin North Am *18*, 529-535.

Muir, H. (1995). The chondrocyte, architect of cartilage. Biomechanics, structure, function and molecular biology of cartilage matrix macromolecules. Bioessays *17*, 1039-1048.

Mundlos, S., Engel, H., Michel-Behnke, I., and Zabel, B. (1990). Distribution of type I and type II collagen gene expression during the development of human long bones. Bone *11*, 275-279.

Mundlos, S., Otto, F., Mundlos, C., Mulliken, J. B., Aylsworth, A. S., Albright, S., Lindhout, D., Cole, W. G., Henn, W., Knoll, J. H., et al. (1997). Mutations involving the transcription factor CBFA1 cause cleidocranial dysplasia. Cell *89*, 773-779.

Murakami, S., Lefebvre, V., and de Crombrugghe, B. (2000). Potent inhibition of the master chondrogenic factor Sox9 gene by interleukin-1 and tumor necrosis factor-alpha. J Biol Chem *275*, 3687-3692.

Murphy, J. M., Fink, D. J., Hunziker, E. B., and Barry, F. P. (2003). Stem cell therapy in a caprine model of osteoarthritis. Arthritis Rheum *48*, 3464-3474.

Muschler, G. F., Matsukura, Y., Nitto, H., Boehm, C. A., Valdevit, A. D., Kambic, H. E., Davros, W. J., Easley, K. A., and Powell, K. A. (2005). Selective retention of bone marrow-derived cells to enhance spinal fusion. Clin Orthop Relat Res, 242-251.

Mwale, F., Stachura, D., Roughley, P., and Antoniou, J. (2006). Limitations of using aggrecan and type X collagen as markers of chondrogenesis in mesenchymal stem cell differentiation. J Orthop Res *24*, 1791-1798.

Nagai, H., Tsukuda, R., and Mayahara, H. (1995). Effects of basic fibroblast growth factor (bFGF) on bone formation in growing rats. Bone *16*, 367-373.

Nakahara, H., Dennis, J. E., Bruder, S. P., Haynesworth, S. E., Lennon, D. P., and Caplan, A. I. (1991). In vitro differentiation of bone and hypertrophic cartilage from periosteal-derived cells. Exp Cell Res *195*, 492-503.

Naski, M. C., and Ornitz, D. M. (1998). FGF signaling in skeletal development. Front Biosci *3*, d781-794.

Ng, K. W., Partridge, N. C., Niall, M., and Martin, T. J. (1983). Stimulation of DNA synthesis by epidermal growth factor in osteoblast-like cells. Calcif Tissue Int *35*, 624-628.

Niederauer, G. G., Slivka, M. A., Leatherbury, N. C., Korvick, D. L., Harroff, H. H., Ehler, W. C., Dunn, C. J., and Kieswetter, K. (2000). Evaluation of multiphase implants for repair of focal osteochondral defects in goats. Biomaterials *21*, 2561-2574.

Nijweide, P. J., Burger, E. H., Klein Nulend, J., and van der Plas, A. (1996). The Osteocyte. In Principles of Bone Biology, J. P. Bilezikian, L. G. Raisz, and G. A. Rodan, eds. (Sandiego, Academic Press), pp. 115-126.

Nixon, A. J., Fortier, L. A., Williams, J., and Mohammed, H. (1999). Enhanced repair of extensive articular defects by insulin-like growth factor-I-laden fibrin composites. J Orthop Res *17*, 475-487.

Noth, U., Osyczka, A. M., Tuli, R., Hickok, N. J., Danielson, K. G., and Tuan, R. S. (2002). Multilineage mesenchymal differentiation potential of human trabecular bone-derived cells. J Orthop Res *20*, 1060-1069.

Ogden, J. A. (2000). Biology of Repair Of The Immature Skeleton. In Skeletal Injury In The Child (New York, Spring-Verlag), pp. 243-268.

Ohneda, O., Ohneda, K., Arai, F., Lee, J., Miyamoto, T., Fukushima, Y., Dowbenko, D., Lasky, L. A., and Suda, T. (2001). ALCAM (CD166): its role in hematopoietic and endothelial development. Blood *98*, 2134-2142.

Olney, R. C., and Mougey, E. B. (1999). Expression of the components of the insulin-like growth factor axis across the growth-plate. Mol Cell Endocrinol *156*, 63-71.

Olney, R. C., Tsuchiya, K., Wilson, D. M., Mohtai, M., Maloney, W. J., Schurman, D. J., and Smith, R. L. (1996). Chondrocytes from osteoarthritic cartilage have increased expression of insulin-like growth factor I (IGF-I) and IGF-binding protein-3 (IGFBP-3) and -5, but not IGF-II or IGFBP-4. J Clin Endocrinol Metab *81*, 1096-1103.

Olney, R. C., Wang, J., Sylvester, J. E., and Mougey, E. B. (2004). Growth factor regulation of human growth plate chondrocyte proliferation in vitro. Biochem Biophys Res Commun *317*, 1171-1182.

Ong, S. Y., Dai, H., and Leong, K. W. (2006). Hepatic differentiation potential of commercially available human mesenchymal stem cells. Tissue Eng *12*, 3477-3485.

Orlic, D., Kajstura, J., Chimenti, S., Bodine, D. M., Leri, A., and Anversa, P. (2001a). Transplanted adult bone marrow cells repair myocardial infarcts in mice. Ann N Y Acad Sci *938*, 221-229; discussion 229-230.

Orlic, D., Kajstura, J., Chimenti, S., Jakoniuk, I., Anderson, S. M., Li, B., Pickel, J., McKay, R., Nadal-Ginard, B., Bodine, D. M., et al. (2001b). Bone marrow cells regenerate infarcted myocardium. Nature *410*, 701-705.

Osborn, L., Hession, C., Tizard, R., Vassallo, C., Luhowskyj, S., Chi-Rosso, G., and Lobb, R. (1989). Direct expression cloning of vascular cell adhesion molecule 1, a cytokine-induced endothelial protein that binds to lymphocytes. Cell *59*, 1203-1211.

Osterman, K. (1972). Operative elimination of partial premature epiphyseal closure. An experimental study. Acta Orthop Scand Suppl, 3-79.

Osyczka, A. M., Noth, U., Danielson, K. G., and Tuan, R. S. (2002). Different osteochondral potential of clonal cell lines derived from adult human trabecular bone. Ann N Y Acad Sci *961*, 73-77.

Otto, F., Thornell, A. P., Crompton, T., Denzel, A., Gilmour, K. C., Rosewell, I. R., Stamp, G. W., Beddington, R. S., Mundlos, S., Olsen, B. R., et al. (1997). Cbfa1, a candidate gene for cleidocranial dysplasia syndrome, is essential for osteoblast differentiation and bone development. Cell *89*, 765-771.

Otto, W. R., and Rao, J. (2004). Tomorrow's skeleton staff: mesenchymal stem cells and the repair of bone and cartilage. Cell Prolif *37*, 97-110.

Owen, M. (1988). Marrow stromal stem cells. J Cell Sci Suppl *10*, 63-76.

Owen, M., and Friedenstein, A. J. (1988). Stromal stem cells: marrow-derived osteogenic precursors. Ciba Found Symp *136*, 42-60.

Paige, K. T., Cima, L. G., Yaremchuk, M. J., Schloo, B. L., Vacanti, J. P., and Vacanti, C. A. (1996). De novo cartilage generation using calcium alginate-chondrocyte constructs. Plast Reconstr Surg *97*, 168-178.

Park, J. S., Ahn, J. I., and Oh, D. I. (1994). Chondrocyte allograft transplantation for damaged growth plate reconstruction. Yonsei Med J *35*, 378-387.

Park, S. S., Jin, H. R., Chi, D. H., and Taylor, R. S. (2004). Characteristics of tissue-engineered cartilage from human auricular chondrocytes. Biomaterials *25*, 2363-2369.

Paschalis, E. P., Jacenko, O., Olsen, B., deCrombrugghe, B., and Boskey, A. L. (1996). The role of type X collagen in endochondral ossification as deduced by Fourier transform infrared microscopy analysis. Connect Tissue Res *35*, 371-377.

Patt, H. M., and Maloney, M. A. (1975). Bone marrow regeneration after local injury: a review. Exp Hematol *3*, 135-148.

Peltonen, J., Alitalo, I., Karaharju, E., and Helio, H. (1984a). Distraction of the growth plate. Experiments in pigs and sheep. Acta Orthop Scand *55*, 359-362.

Peltonen, J. I., Karaharju, E. O., and Alitalo, I. (1984b). Experimental epiphysial distraction producing and correcting angular deformities. J Bone Joint Surg Br *66*, 598-602.

Pelttari, K., Winter, A., Steck, E., Goetzke, K., Hennig, T., Ochs, B. G., Aigner, T., and Richter, W. (2006). Premature induction of hypertrophy during in vitro chondrogenesis of human mesenchymal stem cells correlates with calcification and vascular invasion after ectopic transplantation in SCID mice. Arthritis Rheum *54*, 3254-3266.

Perka, C., Schultz, O., Spitzer, R. S., and Lindenhayn, K. (2000a). The influence of transforming growth factor beta1 on mesenchymal cell repair of full-thickness cartilage defects. J Biomed Mater Res *52*, 543-552.

Perka, C., Spitzer, R. S., Lindenhayn, K., Sittinger, M., and Schultz, O. (2000b). Matrix-mixed culture: new methodology for chondrocyte culture and preparation of cartilage transplants. J Biomed Mater Res *49*, 305-311.

Perkins, S., and Fleischman, R. A. (1990). Stromal cell progeny of murine bone marrow fibroblast colony-forming units are clonal endothelial-like cells that express collagen IV and laminin. Blood *75*, 620-625.

Perkins, S. J., Nealis, A. S., Dunham, D. G., Hardingham, T. E., and Muir, I. H. (1992). Neutron and X-ray solution-scattering studies of the ternary complex between proteoglycan-binding region, link protein and hyaluronan. Biochem J *285 (Pt 1)*, 263-268.

Peterson, H. (1996). Physeal and apophyseal injuries. In Fractures in children, C. Rockwood, K. Wilkins, and J. Beaty, eds. (Philadelphia, Lippincott-Raven), pp. 103-165.
Peterson, H. A. (1984). Partial growth plate arrest and its treatment. J Pediatr Orthop *4*, 246-258.

Peterson, H. A., Madhok, R., Benson, J. T., Ilstrup, D. M., and Melton, L. J., 3rd (1994). Physeal fractures: Part 1. Epidemiology in Olmsted County, Minnesota, 1979-1988. J Pediatr Orthop *14*, 423-430.

Petite, H., Viateau, V., Bensaid, W., Meunier, A., de Pollak, C., Bourguignon, M., Oudina, K., Sedel, L., and Guillemin, G. (2000). Tissue-engineered bone regeneration. Nat Biotechnol *18*, 959-963.

Phemister, D. B. (1933). Operative arrestment of longitudinal growth of bones in the treatment of deformities. J Bone and Joint Surg *15*, 1-15.

Phieffer, L. S., Meyer, R. A., Jr., Gruber, H. E., Easley, M., and Wattenbarger, J. M. (2000). Effect of interposed periosteum in an animal physeal fracture model. Clin Orthop Relat Res, 15-25.

Phinney, D. G., Kopen, G., Isaacson, R. L., and Prockop, D. J. (1999). Plastic adherent stromal cells from the bone marrow of commonly used strains of inbred mice: variations in yield, growth, and differentiation. J Cell Biochem *72*, 570-585.

Pittenger, M. F., Mackay, A. M., Beck, S. C., Jaiswal, R. K., Douglas, R., Mosca, J. D., Moorman, M. A., Simonetti, D. W., Craig, S., and Marshak, D. R. (1999). Multilineage potential of adult human mesenchymal stem cells. Science *284*, 143-147.

Ponte, A. L., Marais, E., Gallay, N., Langonne, A., Delorme, B., Herault, O., Charbord, P., and Domenech, J. (2007). The in vitro migration capacity of human bone marrow mesenchymal stem cells: comparison of chemokine and growth factor chemotactic activities. Stem Cells *25*, 1737-1745.

Ponticiello, M. S., Schinagl, R. M., Kadiyala, S., and Barry, F. P. (2000). Gelatin-based resorbable sponge as a carrier matrix for human mesenchymal stem cells in cartilage regeneration therapy. J Biomed Mater Res *52*, 246-255.

Price, J. S., Oyajobi, B. O., and Russell, R. G. (1994). The cell biology of bone growth. Eur J Clin Nutr *48 Suppl 1*, S131-149.

Prockop, D. J. (1997). Marrow stromal cells as stem cells for nonhematopoietic tissues. Science *276*, 71-74.

Provot, S., and Schipani, E. (2005). Molecular mechanisms of endochondral bone development. Biochem Biophys Res Commun *328*, 658-665.

Quarto, R., Mastrogiacomo, M., Cancedda, R., Kutepov, S. M., Mukhachev, V., Lavroukov, A., Kon, E., and Marcacci, M. (2001). Repair of large bone defects with the use of autologous bone marrow stromal cells. N Engl J Med *344*, 385-386.

Quintavalla, J., Uziel-Fusi, S., Yin, J., Boehnlein, E., Pastor, G., Blancuzzi, V., Singh, H. N., Kraus, K. H., O'Byrne, E., and Pellas, T. C. (2002). Fluorescently labeled mesenchymal stem cells (MSCs) maintain multilineage potential and can be detected following implantation into articular cartilage defects. Biomaterials *23*, 109-119.

Radice, M., Brun, P., Cortivo, R., Scapinelli, R., Battaliard, C., and Abatangelo, G. (2000). Hyaluronan-based biopolymers as delivery vehicles for bone-marrow-derived mesenchymal progenitors. J Biomed Mater Res *50*, 101-109.

Rahfoth, B., Weisser, J., Sternkopf, F., Aigner, T., von der Mark, K., and Brauer, R. (1998). Transplantation of allograft chondrocytes embedded in agarose gel into cartilage defects of rabbits. Osteoarthritis Cartilage *6*, 50-65.

Recker, R. R. (1992). Embryology, Anatomy, and Microstructure of Bone. In Disorders of Bone and Mineral Metabolism, F. L. Coe, and M. J. Favus, eds. (Raven Press Ltd), pp. 219-240.

Redman, S. N., Oldfield, S. F., and Archer, C. W. (2005). Current strategies for articular cartilage repair. Eur Cell Mater *9*, 23-32; discussion 23-32.

Reilly, T. M., Seldes, R., Luchetti, W., and Brighton, C. T. (1998). Similarities in the phenotypic expression of pericytes and bone cells. Clin Orthop Relat Res, 95-103.

Reinholt, F. P., Hultenby, K., Oldberg, A., and Heinegard, D. (1990). Osteopontin--a possible anchor of osteoclasts to bone. Proc Natl Acad Sci U S A *87*, 4473-4475.

Rhodes, N. P., Srivastava, J. K., Smith, R. F., and Longinotti, C. (2004). Heterogeneity in proliferative potential of ovine mesenchymal stem cell colonies. J Mater Sci Mater Med *15*, 397-402.

Ringe, J., Kaps, C., Schmitt, B., Buscher, K., Bartel, J., Smolian, H., Schultz, O., Burmester, G. R., Haupl, T., and Sittinger, M. (2002). Porcine mesenchymal stem cells. Induction of distinct mesenchymal cell lineages. Cell Tissue Res *307*, 321-327.

Rittenhouse, E., Dunn, L. C., Cookingham, J., Calo, C., Spiegelman, M., Dooher, G. B., and Bennett, D. (1978). Cartilage matrix deficiency (cmd): a new autosomal recessive lethal mutation in the mouse. J Embryol Exp Morphol *43*, 71-84.

Roach, H. I., Aigner, T., and Kouri, J. B. (2004). Chondroptosis: a variant of apoptotic cell death in chondrocytes? Apoptosis *9*, 265-277.

Robey, P. G. (1996). Vertebrate mineralized matrix proteins: structure and function. Connect Tissue Res *35*, 131-136.

Robey, P. G., Young, M. F., Flanders, K. C., Roche, N. S., Kondaiah, P., Reddi, A. H., Termine, J. D., Sporn, M. B., and Roberts, A. B. (1987). Osteoblasts synthesize and respond to transforming growth factor-type beta (TGF-beta) in vitro. J Cell Biol *105*, 457-463.

Robson, H., Siebler, T., Shalet, S. M., and Williams, G. R. (2002). Interactions between GH, IGF-I, glucocorticoids, and thyroid hormones during skeletal growth. Pediatr Res *52*, 137-147.

Roelen, B. A., and Dijke, P. (2003). Controlling mesenchymal stem cell differentiation by TGFBeta family members. J Orthop Sci *8*, 740-748.

Rosado, E., Schwartz, Z., Sylvia, V. L., Dean, D. D., and Boyan, B. D. (2002). Transforming growth factor-beta1 regulation of growth zone chondrocytes is mediated by multiple interacting pathways. Biochim Biophys Acta *1590*, 1-15.

Rosier, R. N., O'Keefe, R. J., Crabb, I. D., and Puzas, J. E. (1989). Transforming growth factor beta: an autocrine regulator of chondrocytes. Connect Tissue Res *20*, 295-301.

Rotter, N., Aigner, J., Naumann, A., Hammer, C., and Sittinger, M. (1999). Behavior of tissue-engineered human cartilage after transplantation into nude mice. J Mater Sci Mater Med *10*, 689-693.

Rotter, N., Aigner, J., Naumann, A., Planck, H., Hammer, C., Burmester, G., and Sittinger, M. (1998). Cartilage reconstruction in head and neck surgery: comparison of resorbable polymer scaffolds for tissue engineering of human septal cartilage. J Biomed Mater Res *42*, 347-356.

Rudert, M., Wilms, U., Hoberg, M., and Wirth, C. J. (2005). Cell-based treatment of osteochondral defects in the rabbit knee with natural and synthetic matrices: cellular seeding determines the outcome. Arch Orthop Trauma Surg *125*, 598-608.

Sakaguchi, Y., Sekiya, I., Yagishita, K., and Muneta, T. (2005). Comparison of human stem cells derived from various mesenchymal tissues: superiority of synovium as a cell source. Arthritis Rheum *52*, 2521-2529.

Salter, D. M., Hughes, D. E., Simpson, R., and Gardner, D. L. (1992). Integrin expression by human articular chondrocytes. Br J Rheumatol *31*, 231-234.

Salter, R. B., and Harris, W. R. (1963). Injuries involving the epiphyseal plate. J Bone and Joint Surg *45A*, 587-622.

Sandberg, M., and Vuorio, E. (1987). Localization of types I, II, and III collagen mRNAs in developing human skeletal tissues by in situ hybridization. J Cell Biol *104*, 1077-1084.

Sandberg, M. M., Aro, H. T., and Vuorio, E. I. (1993). Gene expression during bone repair. Clin Orthop.

Sandell, L. J., Morris, N., Robbins, J. R., and Goldring, M. B. (1991). Alternatively spliced type II procollagen mRNAs define distinct populations of cells during vertebral development: differential expression of the amino-propeptide. J Cell Biol *114*, 1307-1319.

Sandell, L. J., Nalin, A. M., and Reife, R. A. (1994). Alternative splice form of type II procollagen mRNA (IIA) is predominant in skeletal precursors and non-cartilaginous tissues during early mouse development. Dev Dyn *199*, 129-140.

Schilb, A., Riou, V., Schoepfer, J., Ottl, J., Muller, K., Chene, P., Mayr, L. M., and Filipuzzi, I. (2004). Development and implementation of a highly miniaturized confocal 2D-FIDA-based high-throughput screening assay to search for active site modulators of the human heat shock protein 90beta. J Biomol Screen *9*, 569-577.

Schipani, E., Lanske, B., Hunzelman, J., Luz, A., Kovacs, C. S., Lee, K., Pirro, A., Kronenberg, H. M., and Juppner, H. (1997). Targeted expression of constitutively active receptors for parathyroid hormone and parathyroid hormone-related peptide delays endochondral bone formation and rescues mice that lack parathyroid hormone-related peptide. Proc Natl Acad Sci U S A *94*, 13689-13694.

Schipani, E., Ryan, H. E., Didrickson, S., Kobayashi, T., Knight, M., and Johnson, R. S. (2001). Hypoxia in cartilage: HIF-1alpha is essential for chondrocyte growth arrest and survival. Genes Dev *15*, 2865-2876.

Schmid, T. M., and Linsenmayer, T. F. (1985). Immunohistochemical localization of short chain cartilage collagen (type X) in avian tissues. J Cell Biol *100*, 598-605.

Schmid, T. M., Popp, R. G., and Linsenmayer, T. F. (1990). Hypertrophic cartilage matrix. Type X collagen, supramolecular assembly, and calcification. Ann N Y Acad Sci *580*, 64-73.

Schmitt, B., Ringe, J., Haupl, T., Notter, M., Manz, R., Burmester, G. R., Sittinger, M., and Kaps, C. (2003). BMP2 initiates chondrogenic lineage development of adult human mesenchymal stem cells in high-density culture. Differentiation *71*, 567-577.

Schmitt, E., Gehrmann, M., Brunet, M., Multhoff, G., and Garrido, C. (2007). Intracellular and extracellular functions of heat shock proteins: repercussions in cancer therapy. J Leukoc Biol *81*, 15-27.

Schnabel, M., Marlovits, S., Eckhoff, G., Fichtel, I., Gotzen, L., Vecsei, V., and Schlegel, J. (2002). Dedifferentiation-associated changes in morphology and gene expression in primary human articular chondrocytes in cell culture. Osteoarthritis Cartilage *10*, 62-70.

Schonherr, E., Witsch Prehm, P., Harrach, B., Robenek, H., Rauterberg, J., and Kresse, H. (1995). Interaction of biglycan with type I collagen. J Biol Chem *270*, 2776-2783.

Schulze-Tanzil, G., de Souza, P., Villegas Castrejon, H., John, T., Merker, H. J., Scheid, A., and Shakibaei, M. (2002). Redifferentiation of dedifferentiated human chondrocytes in high-density cultures. Cell Tissue Res *308*, 371-379.

Schwartz, Z., Bonewald, L. F., Caulfield, K., Brooks, B., and Boyan, B. D. (1993). Direct effects of transforming growth factor-beta on chondrocytes are modulated by vitamin D metabolites in a cell maturation-specific manner. Endocrinology *132*, 1544-1552.

Sekiya, I., Colter, D. C., and Prockop, D. J. (2001). BMP-6 enhances chondrogenesis in a subpopulation of human marrow stromal cells. Biochem Biophys Res Commun *284*, 411-418.

Sekiya, I., Larson, B. L., Smith, J. R., Pochampally, R., Cui, J. G., and Prockop, D. J. (2002). Expansion of human adult stem cells from bone marrow stroma: conditions that maximize the yields of early progenitors and evaluate their quality. Stem Cells *20*, 530-541.

Sekiya, I., Larson, B. L., Vuoristo, J. T., Reger, R. L., and Prockop, D. J. (2005). Comparison of effect of BMP-2, -4, and -6 on in vitro cartilage formation of human adult stem cells from bone marrow stroma. Cell Tissue Res *320*, 269-276.

Sellers, R. S., Zhang, R., Glasson, S. S., Kim, H. D., Peluso, D., D'Augusta, D. A., Beckwith, K., and Morris, E. A. (2000). Repair of articular cartilage defects one year after treatment with recombinant human bone morphogenetic protein-2 (rhBMP-2). J Bone Joint Surg Am *82*, 151-160.

Semba, I., Nonaka, K., Takahashi, I., Takahashi, K., Dashner, R., Shum, L., Nuckolls, G. H., and Slavkin, H. C. (2000). Positionally-dependent chondrogenesis induced by BMP4 is co-regulated by Sox9 and Msx2. Dev Dyn *217*, 401-414.

Seo, B. M., Miura, M., Gronthos, S., Bartold, P. M., Batouli, S., Brahim, J., Young, M., Robey, P. G., Wang, C. Y., and Shi, S. (2004). Investigation of multipotent postnatal stem cells from human periodontal ligament. Lancet *364*, 149-155.

Serra, R., Karaplis, A., and Sohn, P. (1999). Parathyroid hormone-related peptide (PTHrP)-dependent and -independent effects of transforming growth factor beta (TGF-beta) on endochondral bone formation. J Cell Biol *145*, 783-794.

Sers, C., Riethmuller, G., and Johnson, J. P. (1994). MUC18, a melanoma-progression associated molecule, and its potential role in tumor vascularization and hematogenous spread. Cancer Res *54*, 5689-5694.

Shi, S., and Gronthos, S. (2003). Perivascular niche of postnatal mesenchymal stem cells in human bone marrow and dental pulp. J Bone Miner Res *18*, 696-704.

Shi, S., Gronthos, S., Chen, S., Reddi, A., Counter, C. M., Robey, P. G., and Wang, C. Y. (2002). Bone formation by human postnatal bone marrow stromal stem cells is enhanced by telomerase expression. Nat Biotechnol *20*, 587-591.

Shiang, R., Thompson, L. M., Zhu, Y. Z., Church, D. M., Fielder, T. J., Bocian, M., Winokur, S. T., and Wasmuth, J. J. (1994). Mutations in the transmembrane domain of FGFR3 cause the most common genetic form of dwarfism, achondroplasia. Cell *78*, 335-342.

Shih, I. M., Elder, D. E., Hsu, M. Y., and Herlyn, M. (1994). Regulation of Mel-CAM/MUC18 expression on melanocytes of different stages of tumor progression by normal keratinocytes. Am J Pathol *145*, 837-845.

Shirasawa, S., Sekiya, I., Sakaguchi, Y., Yagishita, K., Ichinose, S., and Muneta, T. (2006). In vitro chondrogenesis of human synovium-derived mesenchymal stem cells: optimal condition and comparison with bone marrow-derived cells. J Cell Biochem *97*, 84-97.

Sibilia, M., Wagner, B., Hoebertz, A., Elliott, C., Marino, S., Jochum, W., and Wagner, E. F. (2003). Mice humanised for the EGF receptor display hypomorphic phenotypes in skin, bone and heart. Development *130*, 4515-4525.

Simmons, D. J., Seitz, P., Kidder, L., Klein, G. L., Waeltz, M., Gundberg, C. M., Tabuchi, C., Yang, C., and Zhang, R. W. (1991). Partial characterization of rat marrow stromal cells. Calcif Tissue Int *48*, 326-334.

Simmons, D. L., Walker, C., Power, C., and Pigott, R. (1990). Molecular cloning of CD31, a putative intercellular adhesion molecule closely related to carcinoembryonic antigen. J Exp Med *171*, 2147-2152.

Simmons, P. J., Przepiorka, D., Thomas, E. D., and Torok-Storb, B. (1987). Host origin of marrow stromal cells following allogeneic bone marrow transplantation. Nature *328*, 429-432.

Simmons, P. J., and Torok-Storb, B. (1991a). CD34 expression by stromal precursors in normal human adult bone marrow. Blood *78*, 2848-2853.

Simmons, P. J., and Torok-Storb, B. (1991b). Identification of stromal cell precursors in human bone marrow by a novel monoclonal antibody, STRO-1. Blood *78*, 55-62.

Simmons, P. J., Zannettino, A., Gronthos, S., and Leavesley, D. (1994). Potential adhesion mechanisms for localisation of haemopoietic progenitors to bone marrow stroma. Leuk Lymphoma *12*, 353-363.

Sims, N. A., Clement-Lacroix, P., Da Ponte, F., Bouali, Y., Binart, N., Moriggl, R., Goffin, V., Coschigano, K., Gaillard-Kelly, M., Kopchick, J., et al. (2000). Bone homeostasis in growth hormone receptor-null mice is restored by IGF-I but independent of Stat5. J Clin Invest *106*, 1095-1103.

Singh, S., Lahiri, A., and Iqbal, M. (2006). The results of limb lengthening by callus distraction using an extending intramedullary nail (Fitbone) in non-traumatic disorders. J Bone Joint Surg Br *88*, 938-942.

Sisson, S. (1975). Sisson and Grossman's The Anatomy of the Domestic Animals (Philadelphia, Saunders).

Sissons, H. A. (1953). Experimental determination of rate of longitudinal bone growth. J Anat *87*, 228-236.

Sjogren, K., Bohlooly, Y. M., Olsson, B., Coschigano, K., Tornell, J., Mohan, S., Isaksson, O. G., Baumann, G., Kopchick, J., and Ohlsson, C. (2000). Disproportional skeletal growth and markedly decreased bone mineral content in growth hormone receptor -/- mice. Biochem Biophys Res Commun *267*, 603-608.

Sledge, C. B., and Noble, J. (1978). Experimental limb lengthening by epiphyseal distraction. Clin Orthop Relat Res, 111-119.

Solchaga, L. A., Gao, J., Dennis, J. E., Awadallah, A., Lundberg, M., Caplan, A. I., and Goldberg, V. M. (2002). Treatment of osteochondral defects with autologous bone marrow in a hyaluronan-based delivery vehicle. Tissue Eng *8*, 333-347.

Solchaga, L. A., Penick, K., Porter, J. D., Goldberg, V. M., Caplan, A. I., and Welter, J. F. (2005). FGF-2 enhances the mitotic and chondrogenic potentials of human adult bone marrow-derived mesenchymal stem cells. J Cell Physiol *203*, 398-409.

Solloway, M. J., Dudley, A. T., Bikoff, E. K., Lyons, K. M., Hogan, B. L., and Robertson, E. J. (1998). Mice lacking Bmp6 function. Dev Genet *22*, 321-339.

Solursh, M. (1991). Formation of cartilage tissue in vitro. J Cell Biochem *45*, 258-260.

Sotiropoulou, P. A., Perez, S. A., Salagianni, M., Baxevanis, C. N., and Papamichail, M. (2006). Characterization of the optimal culture conditions for clinical scale production of human mesenchymal stem cells. Stem Cells *24*, 462-471.

Stadelmaier, D. M., Arnoczky, S. P., Dodds, J., and Ross, H. (1995). The effect of drilling and soft tissue grafting across open growth plates. A histologic study. Am J Sports Med *23*, 431-435.

Stamm, C., Westphal, B., Kleine, H. D., Petzsch, M., Kittner, C., Klinge, H., Schumichen, C., Nienaber, C. A., Freund, M., and Steinhoff, G. (2003). Autologous bone-marrow stem-cell transplantation for myocardial regeneration. Lancet *361*, 45-46.

St-Jacques, B., Hammerschmidt, M., and McMahon, A. P. (1999). Indian hedgehog signaling regulates proliferation and differentiation of chondrocytes and is essential for bone formation. Genes Dev *13*, 2072-2086.

Suda, T., Nakamura, I., Jimi, E., and Takahashi, N. (1997). Regulation of osteoclast function. J Bone Miner Res *12*, 869-879.

Summers, K. L., O'Donnell, J. L., Hoy, M. S., Peart, M., Dekker, J., Rothwell, A., and Hart, D. N. (1995). Monocyte-macrophage antigen expression on chondrocytes. J Rheumatol *22*, 1326-1334.

Switzer, R. C., 3rd, Merril, C. R., and Shifrin, S. (1979). A highly sensitive silver stain for detecting proteins and peptides in polyacrylamide gels. Anal Biochem *98*, 231-237.
Szczesny, G. (2002). Molecular aspects of bone healing and remodeling. Pol J Pathol *53*, 145-153.

Takeda, S., Bonnamy, J. P., Owen, M. J., Ducy, P., and Karsenty, G. (2001). Continuous expression of Cbfa1 in nonhypertrophic chondrocytes uncovers its ability to induce hypertrophic chondrocyte differentiation and partially rescues Cbfa1-deficient mice. Genes Dev *15*, 467-481.

Tallheden, T., Dennis, J. E., Lennon, D. P., Sjogren-Jansson, E., Caplan, A. I., and Lindahl, A. (2003). Phenotypic plasticity of human articular chondrocytes. J Bone Joint Surg Am *85-A Suppl 2*, 93-100.

Talts, J. F., Pfeifer, A., Hofmann, F., Hunziker, E. B., Zhou, X. H., Aszodi, A., and Fassler, R. (1998). Endochondral ossification is dependent on the mechanical properties of cartilage tissue and on intracellular signals in chondrocytes. Ann N Y Acad Sci *857*, 74-85.

Tamama, K., Fan, V. H., Griffith, L. G., Blair, H. C., and Wells, A. (2006). Epidermal growth factor as a candidate for ex vivo expansion of bone marrow-derived mesenchymal stem cells. Stem Cells *24*, 686-695.

Tavassoli, M., and Crosby, W. H. (1968). Transplantation of marrow to extramedullary sites. Science *161*, 54-56.

Tavassoli, M., and Friedenstein, A. (1983). Hemopoietic stromal microenvironment. Am J Hematol *15*, 195-203.

Tavassoli, M., and Khademi, R. (1980). The origin of hemopoietic cells in ectopic implants of spleen and marrow. Experientia *36*, 1126-1127.

Thomas, B. (2004) The Effect of Recombinant Human Osteogenic Protein-1 on Growth Plate Repair in a Sheep Model, Doctor of Philosophy, University of Adelaide, Adelaide.

Thomas, B. J., Byers, S., Johnstone, E. W., and Foster, B. K. (2005). The effect of recombinant human osteogenic protein-1 on growth plate repair in a sheep model. J Orthop Res *23*, 1336-1344.

Thorogood, P. V., and Hinchliffe, J. R. (1975). An analysis of the condensation process during chondrogenesis in the embryonic chick hind limb. J Embryol Exp Morphol *33*, 581-606.

Tobita, M., Ochi, M., Uchio, Y., Mori, R., Iwasa, J., Katsube, K., and Motomura, T. (2002). Treatment of growth plate injury with autogenous chondrocytes: a study in rabbits. Acta Orthop Scand *73*, 352-358.

Toh, W. S., Liu, H., Heng, B. C., Rufaihah, A. J., Ye, C. P., and Cao, T. (2005). Combined effects of TGFbeta1 and BMP2 in serum-free chondrogenic differentiation of mesenchymal stem cells induced hyaline-like cartilage formation. Growth Factors *23*, 313-321.

Trippel, S. B., Whelan, M. C., Klagsburn, M., and Doctrow, S. R. (1992). Interaction of basic fibroblast growth factor with bovine growth plate chondrocytes. J Orthop Res *10*, 638-646.

Trippel, S. B., Wroblewski, J., Makower, A. M., Whelan, M. C., Schoenfeld, D., and Doctrow, S. R. (1993). Regulation of growth-plate chondrocytes by insulin-like growth-factor I and basic fibroblast growth factor. J Bone Joint Surg Am *75*, 177-189.

Tropel, P., Noel, D., Platet, N., Legrand, P., Benabid, A. L., and Berger, F. (2004). Isolation and characterisation of mesenchymal stem cells from adult mouse bone marrow. Exp Cell Res *295*, 395-406.

Trueta, J., and Amato, V. P. (1960). The vascular contribution to osteogenesis. III. Changes in the growth cartilage caused by experimentally induced ischaemia. J Bone Joint Surg Br *42-B*, 571-587.

Trueta, J., and Little, K. (1960). The vascular contribution to osteogenesis II. Studies with the electron microscope. J Bone Joint Surgery *42B*, 367-376.

Tsutsumi, S., Shimazu, A., Miyazaki, K., Pan, H., Koike, C., Yoshida, E., Takagishi, K., and Kato, Y. (2001). Retention of multilineage differentiation potential of mesenchymal cells during proliferation in response to FGF. Biochem Biophys Res Commun *288*, 413-419.

Tuli, R., Tuli, S., Nandi, S., Wang, M. L., Alexander, P. G., Haleem-Smith, H., Hozack, W. J., Manner, P. A., Danielson, K. G., and Tuan, R. S. (2003). Characterization of multipotential mesenchymal progenitor cells derived from human trabecular bone. Stem Cells *21*, 681-693.

Tuncel, M., Halici, M., Canoz, O., Yildirim Turk, C., Oner, M., Ozturk, F., and Kabak, S. (2005). Role of insulin like growth factor-I in repair response in immature cartilage. Knee *12*, 113-119.

Uematsu, K., Hattori, K., Ishimoto, Y., Yamauchi, J., Habata, T., Takakura, Y., Ohgushi, H., Fukuchi, T., and Sato, M. (2005). Cartilage regeneration using mesenchymal stem cells and a three-dimensional poly-lactic-glycolic acid (PLGA) scaffold. Biomaterials *26*, 4273-4279.

Ueta, C., Iwamoto, M., Kanatani, N., Yoshida, C., Liu, Y., Enomoto-Iwamoto, M., Ohmori, T., Enomoto, H., Nakata, K., Takada, K., et al. (2001). Skeletal malformations caused by overexpression of Cbfa1 or its dominant negative form in chondrocytes. J Cell Biol *153*, 87-100.

Urist, M. R. (1965). Bone: formation by autoinduction. Science *150*, 893-899.

Vaananen, K. (1996). Osteoclast Function: Biology and Mechanisms. In Principles of Bone Biology, J. P. Bilezikian, L. G. Raisz, and G. A. Rodan, eds. (San Diego, Academic Press), pp. 103-113.

Vacanti, V., Kong, E., Suzuki, G., Sato, K., Canty, J. M., and Lee, T. (2005). Phenotypic changes of adult porcine mesenchymal stem cells induced by prolonged passaging in culture. J Cell Physiol *205*, 194-201.

van der Eerden, B. C., Karperien, M., and Wit, J. M. (2003). Systemic and local regulation of the growth plate. Endocr Rev *24*, 782-801.

van der Plas, A., Aarden, E. M., Feijen, J. H., de Boer, A. H., Wiltink, A., Alblas, M. J., de Leij, L., and Nijweide, P. J. (1994). Characteristics and properties of osteocytes in culture. J Bone Miner Res *9*, 1697-1704.

van der Plas, A., and Nijweide, P. J. (1992). Isolation and purification of osteocytes. J Bone Miner Res *7*, 389-396.

Van Vlasselaer, P., Falla, N., Snoeck, H., and Mathieu, E. (1994). Characterization and purification of osteogenic cells from murine bone marrow by two-color cell sorting using anti-Sca-1 monoclonal antibody and wheat germ agglutinin. Blood *84*, 753-763.

Veilleux, N., and Spector, M. (2005). Effects of FGF-2 and IGF-1 on adult canine articular chondrocytes in type II collagen-glycosaminoglycan scaffolds in vitro. Osteoarthritis Cartilage *13*, 278-286.

Verfaillie, C. M. (1998). Adhesion receptors as regulators of the hematopoietic process. Blood *92*, 2609-2612.

Verfaillie, C. M., Schwartz, R., Reyes, M., and Jiang, Y. (2003). Unexpected potential of adult stem cells. Ann N Y Acad Sci *996*, 231-234.

Vortkamp, A., Lee, K., Lanske, B., Segre, G. V., Kronenberg, H. M., and Tabin, C. J. (1996). Regulation of rate of cartilage differentiation by Indian hedgehog and PTH-related protein. Science *273*, 613-622.

Wagner, T., Wirth, J., Meyer, J., Zabel, B., Held, M., Zimmer, J., Pasantes, J., Bricarelli, F. D., Keutel, J., Hustert, E., and et al. (1994). Autosomal sex reversal and campomelic dysplasia are caused by mutations in and around the SRY-related gene SOX9. Cell *79*, 1111-1120.

Wai, A. W., Ng, L. J., Watanabe, H., Yamada, Y., Tam, P. P., and Cheah, K. S. (1998). Disrupted expression of matrix genes in the growth plate of the mouse cartilage matrix deficiency (cmd) mutant. Dev Genet *22*, 349-358.

Wakitani, S., Goto, T., Pineda, S. J., Young, R. G., Mansour, J. M., Caplan, A. I., and Goldberg, V. M. (1994). Mesenchymal cell-based repair of large, full-thickness defects of articular cartilage. J Bone Joint Surg Am *76*, 579-592.

Wakitani, S., Goto, T., Young, R. G., Mansour, J. M., Goldberg, V. M., and Caplan, A. I. (1998). Repair of large full-thickness articular cartilage defects with allograft articular chondrocytes embedded in a collagen gel. Tissue Eng *4*, 429-444.

Wakitani, S., Imoto, K., Yamamoto, T., Saito, M., Murata, N., and Yoneda, M. (2002). Human autologous culture expanded bone marrow mesenchymal cell transplantation for repair of cartilage defects in osteoarthritic knees. Osteoarthritis Cartilage *10*, 199-206.

Walker, A. M. (1995). Low power and striking results--a surprise but not a paradox. N Engl J Med *332*, 1091-1092.

Waller, E. K., Huang, S., and Terstappen, L. (1995). Changes in the growth properties of CD34+, CD38- bone marrow progenitors during human fetal development. Blood *86*, 710-718.

Walsh, S., Jefferiss, C. M., Stewart, K., and Beresford, J. N. (2003). IGF-I does not affect the proliferation or early osteogenic differentiation of human marrow stromal cells. Bone *33*, 80-89.

Walthall, B. J., and Ham, R. G. (1981). Multiplication of human diploid fibroblasts in a synthetic medium supplemented with EGF, insulin, and dexamethasone. Exp Cell Res *134*, 303-311.

Wang, J., Zhou, J., Cheng, C. M., Kopchick, J. J., and Bondy, C. A. (2004). Evidence supporting dual, IGF-I-independent and IGF-I-dependent, roles for GH in promoting longitudinal bone growth. J Endocrinol *180*, 247-255.

Wang, Y., Kim, U. J., Blasioli, D. J., Kim, H. J., and Kaplan, D. L. (2005). In vitro cartilage tissue engineering with 3D porous aqueous-derived silk scaffolds and mesenchymal stem cells. Biomaterials *26*, 7082-7094.

Wang, Y., Nishida, S., Sakata, T., Elalieh, H. Z., Chang, W., Halloran, B. P., Doty, S. B., and Bikle, D. D. (2006). Insulin-like growth factor-I is essential for embryonic bone development. Endocrinology *147*, 4753-4761.

Watanabe, H., Cheung, S. C., Itano, N., Kimata, K., and Yamada, Y. (1997). Identification of hyaluronan-binding domains of aggrecan. J Biol Chem *272*, 28057-28065.

Watanabe, H., Kimata, K., Line, S., Strong, D., Gao, L. Y., Kozak, C. A., and Yamada, Y. (1994). Mouse cartilage matrix deficiency (cmd) caused by a 7 bp deletion in the aggrecan gene. Nat Genet *7*, 154-157.

Watanabe, H., Yamada, Y., and Kimata, K. (1998). Roles of aggrecan, a large chondroitin sulfate proteoglycan, in cartilage structure and function. J Biochem (Tokyo) *124*, 687-693.

Weiss, L. (1976). The hematopoietic microenvironment of the bone marrow: an ultrastructural study of the stroma in rats. Anat Rec *186*, 161-184.

Weber, I. T., Harrison, R. W., and Iozzo, R. V. (1996). Model structure of decorin and implications for collagen fibrillogenesis. J Biol Chem *271*, 31767-31770.

Werther, G. A., Haynes, K. M., Barnard, R., and Waters, M. J. (1990). Visual demonstration of growth hormone receptors on human growth plate chondrocytes. J Clin Endocrinol Metab *70*, 1725-1731.

Wetzel, A., Chavakis, T., Preissner, K. T., Sticherling, M., Haustein, U. F., Anderegg, U., and Saalbach, A. (2004). Human Thy-1 (CD90) on activated endothelial cells is a counterreceptor for the leukocyte integrin Mac-1 (CD11b/CD18). J Immunol *172*, 3850-3859.

Whitlock, C. A., and Witte, O. N. (1982). Long-term culture of B lymphocytes and their precursors from murine bone marrow. Proc Natl Acad Sci U S A *79*, 3608-3612.

Wilsman, N. J., Farnum, C. E., Leiferman, E. M., Fry, M., and Barreto, C. (1996). Differential growth by growth plates as a function of multiple parameters of chondrocytic kinetics. J Orthop Res *14*, 927-936.

Winnier, G., Blessing, M., Labosky, P. A., and Hogan, B. L. (1995). Bone morphogenetic protein-4 is required for mesoderm formation and patterning in the mouse. Genes Dev *9*, 2105-2116.

Wirth, T., Byers, S., Byard, R. W., Hopwood, J. J., and Foster, B. K. (1994). The implantation of cartilaginous and periosteal tissue into growth plate defects. Int Orthop *18*, 220-228.

Wong, M., Siegrist, M., Wang, X., and Hunziker, E. (2001). Development of mechanically stable alginate/chondrocyte constructs: effects of guluronic acid content and matrix synthesis. J Orthop Res *19*, 493-499.

Woodbury, D., Schwarz, E. J., Prockop, D. J., and Black, I. B. (2000). Adult rat and human bone marrow stromal cells differentiate into neurons. J Neurosci Res *61*, 364-370.

Worlock, P., Stower, M., and Barbor, P. (1986). Patterns of fractures in accidental and non-accidental injury in children: a comparative study. Br Med J (Clin Res Ed) *293*, 100-102.

Worster, A. A., Brower-Toland, B. D., Fortier, L. A., Bent, S. J., Williams, J., and Nixon, A. J. (2001). Chondrocytic differentiation of mesenchymal stem cells sequentially exposed to transforming growth factor-beta1 in monolayer and insulin-like growth factor-I in a three-dimensional matrix. J Orthop Res *19*, 738-749.

Worster, A. A., Nixon, A. J., Brower-Toland, B. D., and Williams, J. (2000). Effect of transforming growth factor beta1 on chondrogenic differentiation of cultured equine mesenchymal stem cells. Am J Vet Res *61*, 1003-1010.

Wright, E., Hargrave, M. R., Christiansen, J., Cooper, L., Kun, J., Evans, T., Gangadharan, U., Greenfield, A., and Koopman, P. (1995). The Sry-related gene Sox9 is expressed during chondrogenesis in mouse embryos. Nat Genet *9*, 15-20.

Wu, L. N., Sauer, G. R., Genge, B. R., and Wuthier, R. E. (1989). Induction of mineral deposition by primary cultures of chicken growth plate chondrocytes in ascorbate-containing media. Evidence of an association between matrix vesicles and collagen. J Biol Chem *264*, 21346-21355.

Xian, C. J. (2007). Roles of epidermal growth factor family in the regulation of postnatal somatic growth. Endocr Rev *28*, 284-296.

Xian, C. J., and Foster, B. K. (2006a). Biologic Aspects of Children's Fractures. In Fractures In Children, J. Beaty, and J. Kasser, eds. (Philadelphia, Lippincott Williams and Wilkins), pp. 21-50.

Xian, C. J., and Foster, B. K. (2006b). Repair of Injured Articular and Growth Plate Cartilage Using Mesenchymal Stem Cells and Chondrogenic Gene Therapy. Current Stem Cell Research & Therapy, 213-229.

Xian, C. J., Zhou, F. H., McCarty, R. C., and Foster, B. K. (2004). Intramembranous ossification mechanism for bone bridge formation at the growth plate cartilage injury site. J Orthop Res *22*, 417-426.

Xu, T., Bianco, P., Fisher, L. W., Longenecker, G., Smith, E., Goldstein, S., Bonadio, J., Boskey, A., Heegaard, A. M., Sommer, B., *et al.* (1998). Targeted disruption of the biglycan gene leads to an osteoporosis-like phenotype in mice. Nat Genet *20*, 78-82.

Xu, W., Zhang, X., Qian, H., Zhu, W., Sun, X., Hu, J., Zhou, H., and Chen, Y. (2004). Mesenchymal stem cells from adult human bone marrow differentiate into a cardiomyocyte phenotype in vitro. Exp Biol Med (Maywood) *229*, 623-631.

Yamaguchi, Y., Mann, D. M., and Ruoslahti, E. (1990). Negative regulation of transforming growth factor-beta by the proteoglycan decorin. Nature *346*, 281-284.

Yan, H., and Yu, C. (2007). Repair of full-thickness cartilage defects with cells of different origin in a rabbit model. Arthroscopy *23*, 178-187.

Yasuda, H., Shima, N., Nakagawa, N., Yamaguchi, K., Kinosaki, M., Mochizuki, S., Tomoyasu, A., Yano, K., Goto, M., Murakami, A., et al. (1998). Osteoclast differentiation factor is a ligand for osteoprotegerin/osteoclastogenesis-inhibitory factor and is identical to TRANCE/RANKL. Proc Natl Acad Sci U S A *95*, 3597-3602.

Yoo, J. U., Barthel, T. S., Nishimura, K., Solchaga, L., Caplan, A. I., Goldberg, V. M., and Johnstone, B. (1998). The chondrogenic potential of human bone-marrow-derived mesenchymal progenitor cells. J Bone Joint Surg Am *80*, 1745-1757.

Yoon, Y. M., Oh, C. D., Kim, D. Y., Lee, Y. S., Park, J. W., Huh, T. L., Kang, S. S., and Chun, J. S. (2000). Epidermal growth factor negatively regulates chondrogenesis of mesenchymal cells by modulating the protein kinase C-alpha, Erk-1, and p38 MAPK signaling pathways. J Biol Chem *275*, 12353-12359.

Yoshimura, H., Muneta, T., Nimura, A., Yokoyama, A., Koga, H., and Sekiya, I. (2007). Comparison of rat mesenchymal stem cells derived from bone marrow, synovium, periosteum, adipose tissue, and muscle. Cell Tissue Res *327*, 449-462.

Young, H. E., Steele, T. A., Bray, R. A., Hudson, J., Floyd, J. A., Hawkins, K., Thomas, K., Austin, T., Edwards, C., Cuzzourt, J., et al. (2001). Human reserve pluripotent mesenchymal stem cells are present in the connective tissues of skeletal muscle and dermis derived from fetal, adult, and geriatric donors. Anat Rec *264*, 51-62.

Young, M. F., Kerr, J. M., Ibaraki, K., Heegaard, A. M., and Robey, P. G. (1992). Structure, expression, and regulation of the major noncollagenous matrix proteins of bone. Clin Orthop Relat Res, 275-294.

Young, S. J., Barnett, P. L., and Oakley, E. A. (2005). 11. Fractures and minor head injuries: minor injuries in children II. Med J Aust *182*, 644-648.

Zaidi, M., Blair, H. C., Moonga, B. S., Abe, E., and Huang, C. L. (2003). Osteoclastogenesis, bone resorption, and osteoclast-based therapeutics. J Bone Miner Res *18*, 599-609.

Zannettino, A. C., Harrison, K., Joyner, C. J., Triffitt, J. T., and Simmons, P. J. (2003). Molecular cloning of the cell surface antigen identified by the osteoprogenitor-specific monoclonal antibody, HOP-26. J Cell Biochem *89*, 56-66.

Zannettino, A. C., Paton, S., Arthur, A., Khor, F., Itescu, S., Gimble, J. M., and Gronthos, S. (2008). Multipotential human adipose-derived stromal stem cells exhibit a perivascular phenotype in vitro and in vivo. J Cell Physiol *214*, 413-421.

Zannettino, A. C., Paton, S., Kortesidis, A., Khor, F., Itescu, S., and Gronthos, S. (2007). Human mulipotential mesenchymal/stromal stem cells are derived from a discrete subpopulation of STRO-1bright/CD34 /CD45(-)/glycophorin-A-bone marrow cells. Haematologica *92*, 1707-1708.

Zelzer, E., Glotzer, D. J., Hartmann, C., Thomas, D., Fukai, N., Soker, S., and Olsen, B. R. (2001). Tissue specific regulation of VEGF expression during bone development requires Cbfa1/Runx2. Mech Dev *106*, 97-106.

Zenmyo, M., Komiya, S., Kawabata, R., Sasaguri, Y., Inoue, A., and Morimatsu, M. (1996). Morphological and biochemical evidence for apoptosis in the terminal hypertrophic chondrocytes of the growth plate. J Pathol *180*, 430-433.

Zerath, E., Holy, X., Mouillon, J. M., Farbos, B., Machwate, M., Andre, C., Renault, S., and Marie, P. J. (1997). TGF-beta2 prevents the impaired chondrocyte proliferation induced by unloading in growth plates of young rats. Life Sci *61*, 2397-2406.

Zhang, Y., Wang, C., Liao, W., Li, Z., Guo, X., Zhao, Q., Duan, C., and Xia, R. (2004). In vitro chondrogenic phenotype differentiation of bone marrow-derived mesenchymal stem cells. J Huazhong Univ Sci Technolog Med Sci *24*, 275-278.

Zhao, L. R., Duan, W. M., Reyes, M., Keene, C. D., Verfaillie, C. M., and Low, W. C. (2002). Human bone marrow stem cells exhibit neural phenotypes and ameliorate neurological deficits after grafting into the ischemic brain of rats. Exp Neurol *174*, 11-20.

Zhou, Y., Xu, B. C., Maheshwari, H. G., He, L., Reed, M., Lozykowski, M., Okada, S., Cataldo, L., Coschigamo, K., Wagner, T. E., et al. (1997). A mammalian model for Laron syndrome produced by targeted disruption of the mouse growth hormone receptor/binding protein gene (the Laron mouse). Proc Natl Acad Sci U S A *94*, 13215-13220.

Zhou, Y. X., Xu, X., Chen, L., Li, C., Brodie, S. G., and Deng, C. X. (2000). A Pro250Arg substitution in mouse Fgfr1 causes increased expression of Cbfa1 and premature fusion of calvarial sutures. Hum Mol Genet *9*, 2001-2008.

Zuk, P. A., Zhu, M., Mizuno, H., Huang, J., Futrell, J. W., Katz, A. J., Benhaim, P., Lorenz, H. P., and Hedrick, M. H. (2001). Multilineage cells from human adipose tissue: implications for cell-based therapies. Tissue Eng *7*, 211-228.

Zvaifler, N. J., Marinova-Mutafchieva, L., Adams, G., Edwards, C. J., Moss, J., Burger, J. A., and Maini, R. N. (2000). Mesenchymal precursor cells in the blood of normal individuals. Arthritis Res *2*, 477-488.